BioMed Research International

Recent Development in Production and Biotechnological Application of Microbial Enzymes

Guest Editors: Noomen Hmidet, Neelu Nawani, and Sofiane Ghorbel

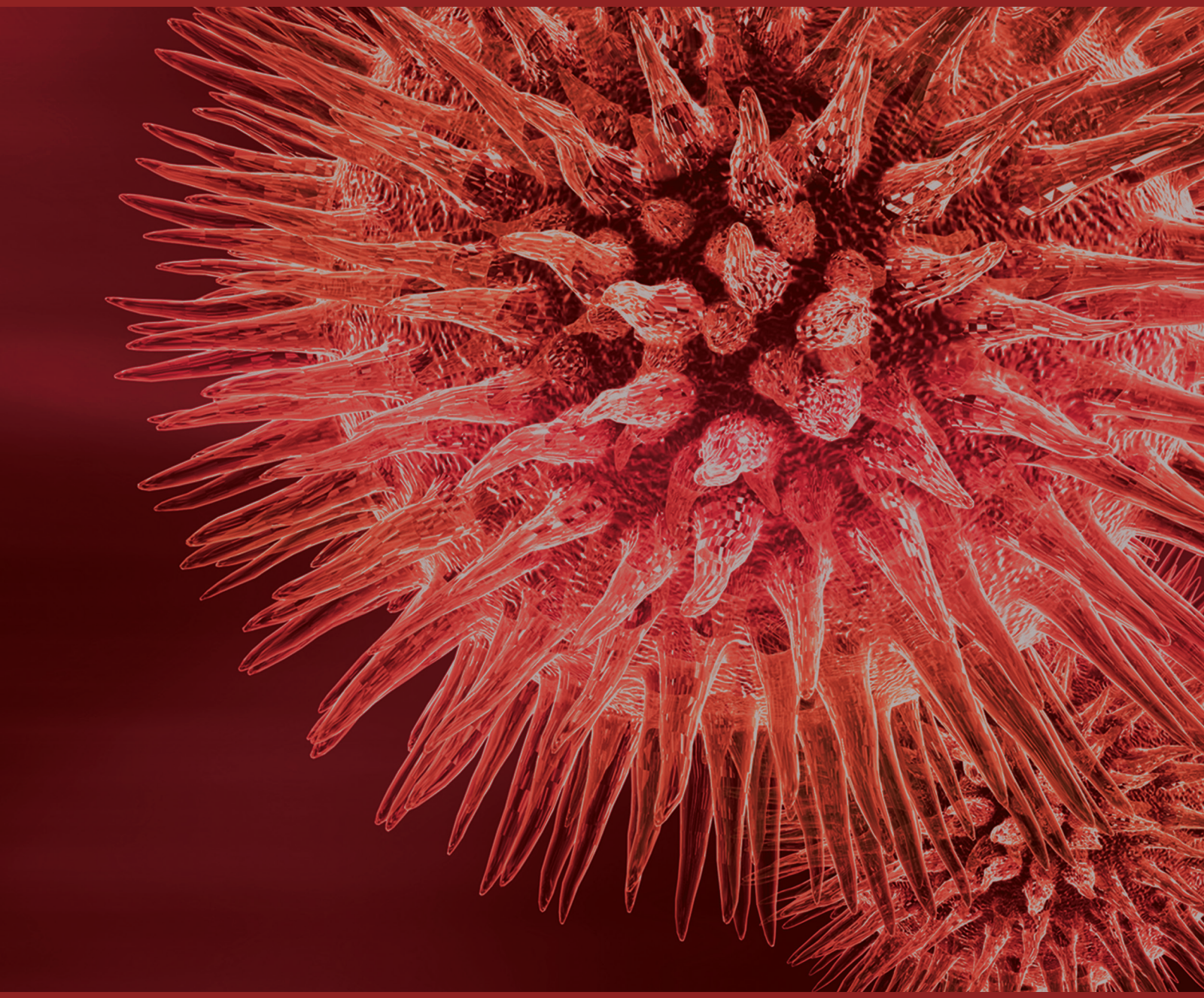

Recent Development in Production and Biotechnological Application of Microbial Enzymes

BioMed Research International

Recent Development in Production and Biotechnological Application of Microbial Enzymes

Guest Editors: Noomen Hmidet, Neelu Nawani, and Sofiane Ghorbel

Contents

Hindawi Publishing Corporation
BioMed Research International
Volume 2015, Article ID 280518, 2 pages
http://dx.doi.org/10.1155/2015/280518

Editorial

Recent Development in Production and Biotechnological Application of Microbial Enzymes

Noomen Hmidet,[1] Neelu Nawani,[2] and Sofiane Ghorbel[1]

[1]*Enzyme Engineering and Microbiology Laboratory, National School of Engineering of Sfax, BP 1173, 3038 Sfax, Tunisia*
[2]*Dr. D. Y. Patil Biotechnology and Bioinformatics Institute, Dr. D. Y. Patil Vidyapeeth, Pune 411033, India*

Correspondence should be addressed to Noomen Hmidet; hmidet_noomen@yahoo.fr

Received 16 December 2014; Accepted 16 December 2014

Microbial enzymes are considered as a potential biocatalyst for several biotechnological applications. They are mainly characterized by their biochemical diversity and susceptibility to gene manipulation. Industries are often interested in new microbial strains producing different enzymes having original activities. The twelve articles published in this special issue balance the investigation of microbial enzymes having potential in several biotechnological and industrial applications.

By their study of the metagenomics of Indian buffalo rumen, K. M. Singh et al. showed the presence of a high potential source for biomass degradation enzymes. Plant cell wall degradation and biomass utilization provide genetic resource for degrading microbial enzymes that could be used in the production of biofuel. They identified potential contigs encoding biomass degrading enzymes including glycoside hydrolases, carbohydrate binding module, glycosyl transferase, carbohydrate esterases, and polysaccharide lyases.

The method of functional protein evaluation was used to identify enzymes for degrading each carbohydrate substrate. K. Yamamoto and Y. Tamaru identified several mannanases from *C. cellulovorans* for degrading LBG using functional protein evaluation and genomic data. In addition, they report that one of the identified mannanases, Man26E, contains a carbohydrate-binding module (CBM) family 59. As a result, four protein bands were classified into GH family 26 (GH26). One of the identified mannanases, Man26E, contains a carbohydrate-binding module (CBM) family 59, which binds to xylan, mannan, and Avicel.

Many papers in this special issue have focused on the optimization of the conditions for enzyme production and activity. In this section, H. Maalej et al. showed the production and biochemical characterization of a high maltotetraose (G4) producing amylase from crude enzyme preparation of *Pseudomonas stutzeri* AS22. The highest α-amylase production was achieved after 24 hours of incubation at 30°C. The formation of very high levels of maltotetraose from starch (98%) in the complete absence of glucose would have a potential application in the manufacturing of maltotetraose syrup.

In addition, S. L. T. Nguyen et al. reported the overexpression of a streptokinase from *Streptococcus pyogenes* DT7 in *Escherichia coli* and its highly effective renaturation and biochemical characterization. The streptokinase (SK) is emerging as an important thrombolytic therapy agent in the treatment of patients suffering from cardiovascular diseases.

Finally, N. Y. Stasyuk et al. reported a novel methylamine-selective amperometric bienzyme biosensor based on recombinant primary amine oxidase isolated from the recombinant yeast strain *Saccharomyces cerevisiae* and commercial horseradish peroxidase is described. The developed biosensor demonstrated good selectivity towards methylamine. The constructed amperometric biosensor was used for MA assay in real samples of fish products in comparison with chemical method.

Protease production and its biotechnological application represent one of the chapters of interest reported in this issue. Therefore, S. Ghorbel et al. characterized the crude extracellular proteases from the newly isolated *Streptomyces flavogriseus* HS1. HS1 strain produced at least five proteases. The crude extracellular proteases showed high stability when used as a detergent additive.

M. Jridi et al. in their paper reported the characterization and potential use of cuttlefish skin gelatin hydrolysates (CSGHs) prepared by different microbial proteases. Composition, functional properties, and *in vitro* antioxidant activities of these gelatin hydrolysates were investigated. The results reveal that CSGHs could be used as food additives possessing both antioxidant activity and functional properties.

R. Saxena and R. Singh in their paper reported the use of MALDI-TOF MS and CD spectral analysis for identification and structure prediction of a purified, novel, organic solvent stable, fibrinolytic metalloprotease from *Bacillus cereus* B80. The biochemical characterization of purified enzyme showed that the enzyme was able to hydrolyze various proteins with the highest affinity towards casein followed by BSA and gelatin. The enzyme exhibited strong fibrinolytic, collagenolytic, and gelatinolytic properties and stability in various organic solvents.

Laccases (*p*-diphenol-dioxygen oxidoreductases, EC 1.10.3.2) represent an interesting class of biocatalysts, being able to oxidize a wide spectrum of aromatic compounds along with reducing molecular oxygen to water. In their paper, C. Pezzella et al. immobilized crude laccase preparation from *Pleurotus ostreatus* on perlite and reported its efficient activity for Remazol Brilliant Blue R (RBBR) decolourisation in a fluidized bed recycle reactor.

G. Macellaro et al. reported the fungal laccases degradation of endocrine disrupting compounds. Over the past decades, water pollution by trace organic compounds has become one of the key environmental issues in developed countries. This is the case of the emerging contaminants called endocrine disrupting compounds (EDCs). EDCs are a new class of environmental pollutants able to mimic or antagonize the effects of endogenous hormones and are recently drawing scientific and public attention. In this study, five different EDCs were treated with four different fungal laccases, also in the presence of both synthetic and natural mediators. Mediators significantly increased the efficiency of the enzymatic treatment, promoting the degradation of substrates recalcitrant to laccase oxidation. Improvement of enzyme performances in nonylphenol degradation rate was achieved through immobilization on glass beads.

C. D. Anobom et al. reported in their review the importance of microbial lipases. These enzymes are highly appreciated as biocatalysts due to their peculiar characteristics such as the ability to utilize a wide range of substrates, high activity and stability in organic solvents, and regio- and/or enantioselectivity. These enzymes are currently being applied in a variety of biotechnological processes, including detergent preparation, cosmetics and paper production, food processing, biodiesel and biopolymer synthesis, and the biocatalytic resolution of pharmaceutical derivatives, esters, and amino acids. This review aims to compile recent advances in the biotechnological application of lipases focusing on various methods of enzyme improvement, such as protein engineering (directed evolution and rational design), as well as the use of structural data for rational modification of lipases in order to create higher active and selective biocatalysts.

B. Sharma et al. described the potential application of L-methionase against many types of cancers. This enzyme is an intracellular enzyme in bacterial species and an extracellular enzyme in fungi and is absent in mammals.

Noomen Hmidet
Neelu Nawani
Sofiane Ghorbel

Hindawi Publishing Corporation
BioMed Research International
Volume 2015, Article ID 527015, 13 pages
http://dx.doi.org/10.1155/2015/527015

Research Article

MALDI-TOF MS and CD Spectral Analysis for Identification and Structure Prediction of a Purified, Novel, Organic Solvent Stable, Fibrinolytic Metalloprotease from *Bacillus cereus* B80

Rajshree Saxena and Rajni Singh

Amity Institute of Microbial Biotechnology, Amity University, Sector 125, Noida, Uttar Pradesh 201303, India

Correspondence should be addressed to Rajni Singh; rsingh3@amity.edu

Received 28 February 2014; Revised 25 August 2014; Accepted 30 September 2014

Academic Editor: Noomen Hmidet

The ability to predict protein function from structure is becoming increasingly important; hence, elucidation and determination of protein structure become the major steps in proteomics. The present study was undertaken for identification of metalloprotease produced by *Bacillus cereus* B80 and recognition of characteristics that can be industrially exploited. The enzyme was purified in three steps combining precipitation and chromatographic methods resulting in 33.5% recovery with 13.1-fold purification of enzyme which was detected as a single band with a molecular mass of 26 kDa approximately in SDS-PAGE and zymogram. The MALDI-TOF MS showed that the enzyme exhibited 70–93% similarity with zinc metalloproteases from various strains *Bacillus* sp. specifically from *Bacillus cereus* group. The sequence alignment revealed the presence of zinc-binding region VVVHEMCHMV in the most conserved C terminus region. Secondary structure of the enzyme was obtained by CD spectra and I-TASSER. The enzyme kinetics revealed a Michaelis constant (K_m) of 0.140 μmol/ml and V_{max} of 2.11 μmol/min. The application studies showed that the enzyme was able to hydrolyze various proteins with highest affinity towards casein followed by BSA and gelatin. The enzyme exhibited strong fibrinolytic, collagenolytic, and gelatinolytic properties and stability in various organic solvents.

1. Introduction

Proteases are recognized by their catalytic type, that is, aspartic, cysteine, metallo, serine, threonine, and the newly identified asparagine peptide lyases [1]. Metalloproteases are the class of hydrolases that cleave peptide bonds by action of a water molecule which is activated by bivalent metal ions like zinc, cobalt, manganese, or nickel. The water molecule serves as a nucleophile in catalysis and also coordinates with the metal ion as a fourth ligand [2]. The catalytic metal ion is usually coordinated by three conserved amino acid side chain ligands that can be His, Asp, Glu, or Lys amino acid and at least one other residue, which may play an electrophilic role [3].

Metalloproteases exhibit deviant physiological and biochemical properties that account for their therapeutical, pathophysiological, and industrial applications. They are implicated in diseases such as arthritis, cancer, cardiovascular diseases, nephritis, central nervous system disorders, and fibrosis [2]. Enzymes with fibrinolytic and collagenolytic properties have been directly employed in clinical therapy, in the regulation of cellular fibrinolysis, prevention, and cure of thrombotic diseases, as antimicrobial agents for removal of necrotic tissue from burns, wound healing, ulcers, treatment of sciatica and herniated intervertebral discs, isolation of pancreatic islets for transplantation, treatment of Dupuytren's disease, and so forth [4, 5].

The study, elucidation, and determination of protein structure have become increasingly vital in proteomics as the structural configuration of the protein significantly contributes towards its functionality. Identification of any enzyme, its active site, and substrate binding region is paramount in finding its application in medicinal and therapeutic fields. In traditional protein chemistry, proteins were identified by de novo sequencing using automated Edman degradation which is based on successive removal of N-terminal amino acids by chemical methods [6]. However since the last decade, this technique has been ousted by

mass spectrometry, which has emerged as the most powerful analytical tool for protein and peptide identification in protein chemistry due to increased sensitivity (femto mole level) and 10-fold increase in speed [7]. Peptide identification using mass spectrometry is based on a simple principle where a peptide is ionized and the peptide bonds are fragmented in an MS-MS spectrometer. Each resulting fragment ion forms a peak in the spectrum at the corresponding mass to charge (m/z) ratio of the ions which are obtained as peptide masses spectra or the peptide mass fingerprint (PMF) that contain sequence information characteristic of its generating peptide [8]. PMF obtained from MS studies is compared with the theoretical peptide masses of proteins stored in databases by means of mass search programs generating a score for each m/z comparison or using fragmentation data [8, 9].

In the present work, metalloprotease produced by *Bacillus cereus* B80 was purified and analyzed using MALDI mass spectrometry and its phylogenetic relationship was explored. The secondary structure of the enzyme was studied by CD spectrometry and predicted by I-TASSER. The enzyme was characterized with respect to its various hydrolytic activities and stability to find a potential industry for its exploitation.

2. Materials and Methods

2.1. Microbial Strain and Enzyme Production. A newly identified *Bacillus cereus* B80 strain (NCBI accession number JQ040533) was selected for the present study. The enzyme was produced in statistically optimized media containing (g/l) sucrose, 5.0; bactopeptone, 50.0; beef extract, 20.0; casein, 20.0; yeast extract, 20.0; and NaCl, 10.0, with 3% inoculum, incubated for 72 h at 180 rpm [10]. The fermented broth was centrifuged at 15,000 rpm for 15 min to remove particulate material. The clear supernatant was used as the crude enzyme.

2.2. Protease and Protein Estimation. Protease production was assayed in terms of protease activity observed using casein as substrate [11]. One unit of protease activity was defined as the amount of enzyme required to liberate 1 μg/mL tyrosine in 1 min under the experimental conditions.

Protein was quantified according to Bradford's method [12]. The experiments were carried out in triplicate and standard error was calculated.

2.3. Enzyme Purification. Chilled ethanol (95%) was added to the enzyme supernatant at 1 : 2 concentrations and kept at −20°C overnight. The mixture was centrifuged at 15,000 rpm for 20 min at 4°C. The supernatant was subjected to freeze drying for ethanol removal and applied on Sephadex-G75 column (50 × 15 mm; Sigma Aldrich) equilibrated with Tris-HCL buffer (pH 7.5) and eluted in the same buffer at a flow rate 1.0 mL/min. The active fractions eluted from the gel filtration column were pooled and subjected to Q Sepharose column (65 × 10 mm; Sigma Aldrich) preequilibrated with glycine NaOH buffer (pH 9). The fractions were eluted with a linear gradient of 0-1 M NaCl in glycine NaOH buffer at a flow rate of 1.0 mL/min.

For all the purification steps, the sample fractions were assayed for protein content and protease activity using casein as substrate. The enzyme recovery and fold purification were calculated in terms of specific activity.

2.4. Effect of Temperature and pH on Enzyme Activity and Stability. The optimum temperature and pH of the enzyme activity were examined by varying the incubation temperature from 30°C to 70°C (at pH 9 for 10 min) and performing the assay with phosphate buffer (pH 6-7) and glycine-NaOH buffer (pH 8–10). To study the thermal stability, the enzyme was incubated at temperatures from 30°C to 70°C for 2 h without the substrate fractions. Enzyme samples were withdrawn at every 30 min and assayed for activity under standard conditions. The stability of the enzyme at different pH values was assessed by incubating the enzyme in different buffers (as above) for 2 h without the substrate fractions and the enzyme activity was assessed at every 30 min under standard conditions.

2.5. Electrophoretic Analysis. In order to determine purity and molecular mass of the purified protein, SDS-PAGE was carried out as described by Laemmli [13] using 12% polyacrylamide resolving gel. The gel was silver stained [14] to visualize the protein bands. Furthermore Casein and gelatin zymography were performed according to the modified method described by Garcia-Carreno et al. [15]. Casein [0.2% (w/v) with sodium salt]/gelatin (0.2%) was copolymerized with 12% resolving gel. After electrophoresis, the gel was washed successively with Tris-HCL buffer (pH 7.5) containing 2.5% triton X-100 and glycine-NaOH buffer (pH 9.0). The gel was then incubated in glycine-NaOH buffer overnight at 37°C and stained with coomassie brilliant blue R-250.

2.6. Identification of Metalloprotease by MALDI Mass Spectrometry. The purified protein bands obtained in SDS-PAGE were excised, subjected to in-gel trypsin digestion. The resulting digests were analyzed by matrix-assisted laser desorption ionization-time of flight mass spectrometry (MALDI-TOF MS; AB SCIEX TOF/TOF 5800 with LC-MALDI). The m/z spectra representing the monoisotopic masses of the digested protein fragments were acquired in the MS and MS/MS modes and analyzed by ProteinPilot Software. These peptide mass values were searched against the published databases (NCBInr, SwissProt) using peptide database search engines as MASCOT, Profound, Sequest, Omssa, and PepFrag to obtain information about the identity of the protein. Searches were performed with a minimum mass accuracy of 50 ppm for the parent ions, an error of 0.3 Da for the fragments, one missed cleavage in the peptide masses, and carbamidomethylation of Cys and oxidation of Met as fixed and variable amino acid modifications, respectively. The confidence threshold for protein identification was set to 95%. The obtained protein sequence was aligned with the similar proteins using "ClustalW" (from EMBL-EBI) for determination of homology or similarity with other reported sequences [16]. Conserved domains and active site in the sequence were identified through NCBI and Prosite from exPASy, respectively.

Table 1: Purification steps for metalloprotease.

	Activity (U)	Protein (mg)	Sp. activity U/mg	Recovery	Fold purification
Crude enzyme	31773.5	117.12	271.29	100	1
EtOH treated	31773.1	87.2	364.76	100	1.34
Sephadex	15682.7	10.4	1507.95	49.35	5.55
Q Sepharose	10668.9	3	3556.3	33.577	13.10

A dendogram was constructed to analyze the phylogenetic relation of the newly identified protein.

2.7. Circular Dichroism of Metalloprotease. To assess the correct conformation of the new metalloprotease UV circular dichroism (CD) spectrum of the protein was acquired. The far-UV CD spectra in a wavelength range of 190–260 nm were recorded on a circular Dichroism spectrometer with Stop Flow (Applied PhotoPhysics Chirascan; AIRF-JNU, Delhi) in a 1-mm path length cuvette. CD spectra were run with a step-resolution of 1 nm, an integration time of 5 sec, and slit width of 0.6 nm, at 37 uC. The spectra were averaged over two scans and corrected by subtraction of the buffer signal. Data are expressed as the mean residue molar ellipticity (MRE) in deg cm^2 $dmol^{-1}$ defined as

$$\text{MRE} = \frac{M\theta_\lambda}{10dcr}, \quad (1)$$

where M is the molecular weight of the protein, θ_λ is CD in millidegree, d is the path length in cm, c is the protein concentration in mg/mL, and r is the number of amino acid residues in the protein. The secondary structure contents were calculated by online software K2D2 (http://k2d2.ogic.ca/) used for analysis of the obtained spectrum to quantify alpha helix, beta sheets, and random coils.

2.8. Structure Prediction of Metalloprotease. Structure of the new enzyme was predicted by submitting the deduced protein sequence to the automated I-TASSER service (http://zhanglab.ccmb.med.umich.edu/I-TASSER/) which uses multiple PDB structures depending on its structural conservation, to model different parts of protein. The best model was selected from output based on C-score.

2.9. Enzyme Kinetics Studies. The effect of incubation time, enzyme concentration, and substrate concentration on casein hydrolysis was studied. The kinetic parameters of the enzyme were determined by measuring the enzyme activity at different substrate concentrations (0–50 mg). The K_m and $V_{\max}$ values were determined using Michaelis-Menten equation and the Lineweaver-Burk double-reciprocal graph was plotted with the calculated values.

2.10. Substrate Specificity Studies. Various soluble protein substrates (gelatin, casein, azocasein, BSA, keratin, and collagen) at 1% concentration were assayed for their activity with the purified enzyme.

2.11. Effect of NaCl on Enzyme Activity at Different pH Values. Aliquots of the enzyme were mixed with NaCl (5 mM and 10 mM) at different pH values (6–10) and the activity was assayed under standard conditions.

2.12. Fibrinolytic Assay and Activity. The fibrinolytic activity of the purified enzyme was performed according to the method of Astrup and Müllertz [17]. Fibrin plates of 1 mm thickness containing agarose 1.2%, fibrinogen 0.4%, and thrombin 20 U/mL were prepared. Sample was loaded in the well made on the plate. Distilled water and plasmin were taken as blank and positive control, respectively. The plates were incubated overnight at 37°C and observed.

Quantitative estimation of the fibrinolytic activity was performed by modified method of Datta et al. [18]. Fibrinolytic activity was quantified in comparison to the standard curve plotted using known concentrations of plasmin against its absorbance at 275 nm. One fibrinolytic unit (FU) was defined as the amount of enzyme required to increase the absorbance by 0.01 per min.

2.13. Collagenolytic and Gelatinolytic Activity. Collagenolytic/gelatinolytic activity was studied on collagen/gelatin plates of 2 mm thickness containing (%) agarose, 1.0 and collagen/gelatin, 1.0. Sample was loaded in the well bored on the plates and the plates were then incubated at 37°C. After 24 h the plates were flooded with coomassie blue R250 staining solution for visualization of the clear zones.

2.14. Stability in Organic Solvents. Purified protease was incubated with 50% (v/v) organic solvents (hexane, acetone, butanol, ethyl benzene, xylene, benzene, chloroform, amyl alcohol, ethanol, acetonitrile, toluene, DMSO, propanol, and glycerol) at 37°C with constant shaking (120 rpm) for 10 days. Samples were removed at every 24 h and the residual activity was estimated. Sample without any solvent served as control and enzyme control activity at day 1 was taken as 100%.

3. Results

3.1. Enzyme Purification. The enzyme was purified to 1.3-fold showing 100% recovery after ethanol treatment. Further purification of the enzyme with Sephadex gel filtration column resulted in 5.55-fold purification and 49.35% recovery. In the final step of purification with Q Sepharose ion exchange column, the enzyme was purified to 13.1-fold with 33.5% recovery (Table 1).

3.2. Effect of Temperature and pH on Enzyme Activity and Stability. The highest enzyme activity was detected at 60°C (Figure 1(a)), while it was stable for 2 h at 30°C. At 40°C and 50°C, the enzyme lost only 16–22% of its activity after 2 h. At 60°C, the enzyme retained 70 and 44% of its activity after

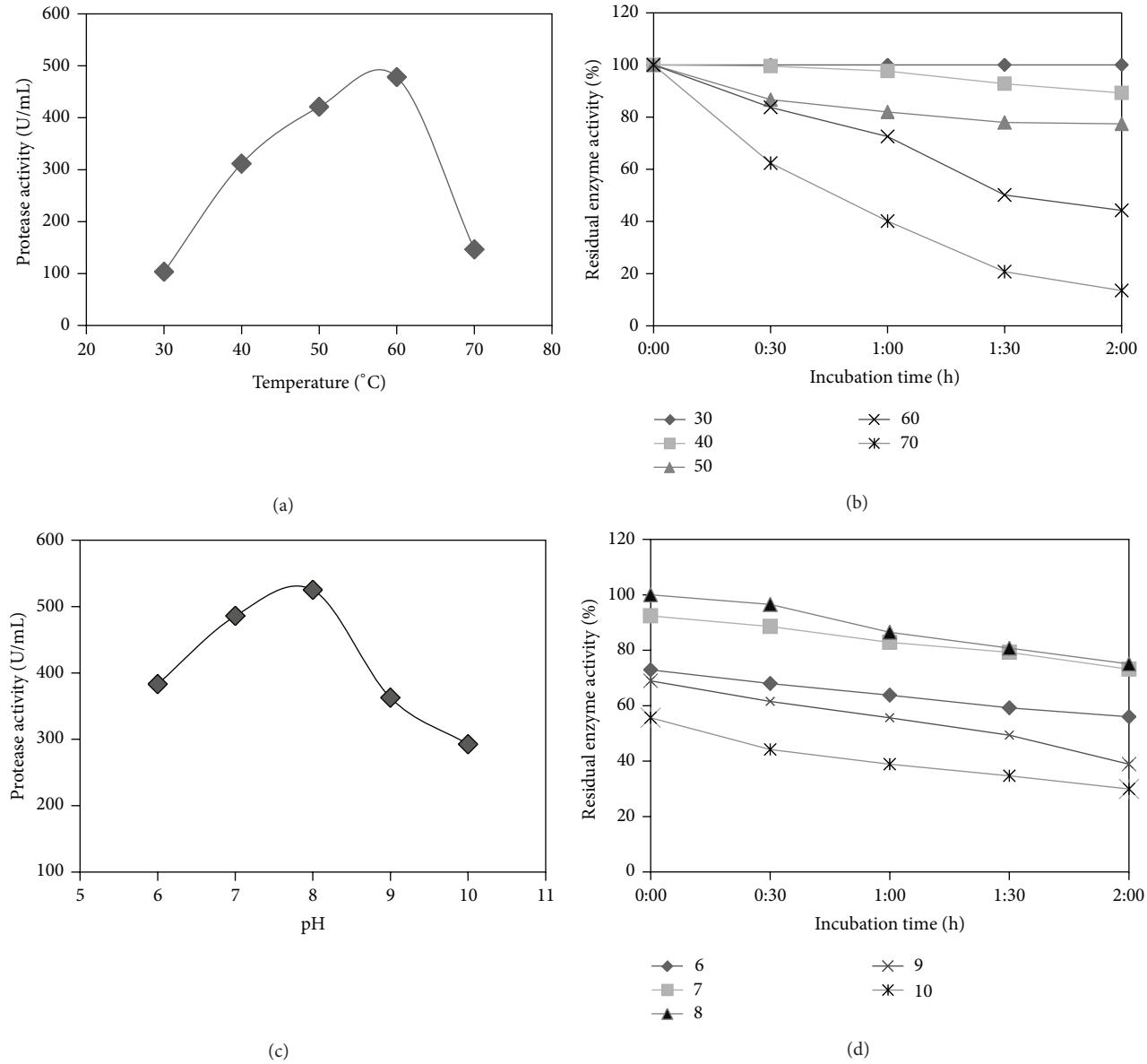

Figure 1: (a) Enzyme activity at different temperatures [30°C to 70°C], (b) stability of enzyme at temperatures from 30°C to 70°C, (c) enzyme activity at different pH values [6 to 10], and (d) stability of enzyme at pH 6–10.

1 h and 2 h, respectively. At 70°C, the enzyme retained 50% of its activity (Figure 1(b)). The enzyme was active between pH 6.0 and pH 9.0 with maximum activity at pH 8.0 when incubated for 10 min at 60°C (Figure 1(c)). Within this range the enzyme retained about 75–80% of the initial activity, while at pH 10 the enzyme retained about 60% of its initial activity (Figure 1(d)).

3.3. SDS-PAGE and Zymography Metalloprotease. The purified protein was detected as a single band with a molecular mass of 26 kDa approximately in SDS-PAGE (Figure 2(a)), which corelated with the clear hydrolytic bands observed in casein and gelatin zymogram (Figures 2(b) and 2(c)).

3.4. Metalloprotease Identification Using MALDI Mass Spectrometry. The MALDI TOF MS analysis of the tryptic digested enzyme generated a spectrum of peaks representing the m/z ratio of each peptide fragment (Figure 3(a)). Automated analysis of the spectra was performed by software Protein Prospector Auto MS-Fit. Five major peptides were further analyzed on nanospray TOFMS/MS which fragmented the peptides into y and b ions, indicating the best matching peptide sequences (Figure 3(b)).

3.5. Database Search. The PMF searches with MASCOT search engine showed matching of six values (1308.69, 2186.07, 1251.66, 862.38, 830.41, 1324.69, and 1641.8) with

Table 2: The peptide matching (12/16 matches) for m/z data of metalloprotease with zinc metalloprotease from *Bacillus cereus* (gi|507041200|ref|WP_016112858.1|).

Spectrum	Prec. m/z	MH+ Matched	Modifications	Missed cleavages	Position	Peptide
1.F2.2.1.5	2704.8679	2761.3123	MSO	0	1–23	MIHTYLGETINFHINCKKKKSVR (I)
1.F2.2.1.7	2383.300	2446.1576	CYS_CAM MSO	0	187–206	(R) VIDYVVVHEMCHMVHLNHDR (S)
1.F2.2.1.9	1638.686	1617.8601	MSO	1	39–51	(K) GTPVEYVLQLLEEK (W)
1.F2.2.1.15	1052.532	979.1244	CYS_CAM MSO	0	129–135	(R) FYYQQCK (A)
1.F2.2.1.12	1350.614	1314.5724		0	61–73	(K) EMKRVLGPQEK (V)
1.F2.2.1.13	1267.53	1260.4618	MSO	0	52–61	(K) WDWIQKTRK (E)
1.F2.2.1.16	868.4659	887.0877	MSO	0	136–143	(K) ALVEKSIK (S)
1.F2.2.1.3	1803.738	1786.1747	CYS_CAM MSO	0	172–186	(K) LQLTFNWKLAMAPPR (V)
1.F2.2.1.4	1707.594	1695.8900		0	24–38	(R) IYIDSYGNVEVQAPK (G)
1.F2.2.1.2	1765.5551	1740.1028		0	204–216	(R) SFWRLVGKIMPDYK (I)
1.F2.2.1.8	1838.717	1757.0606		0	110–123	(K) LHIYVKELEDEKIK (Q)
1.F2.2.1.1	1488.676	1494.6884	MSO	1	221–231	(K) EMEDWLALSSWK (M)

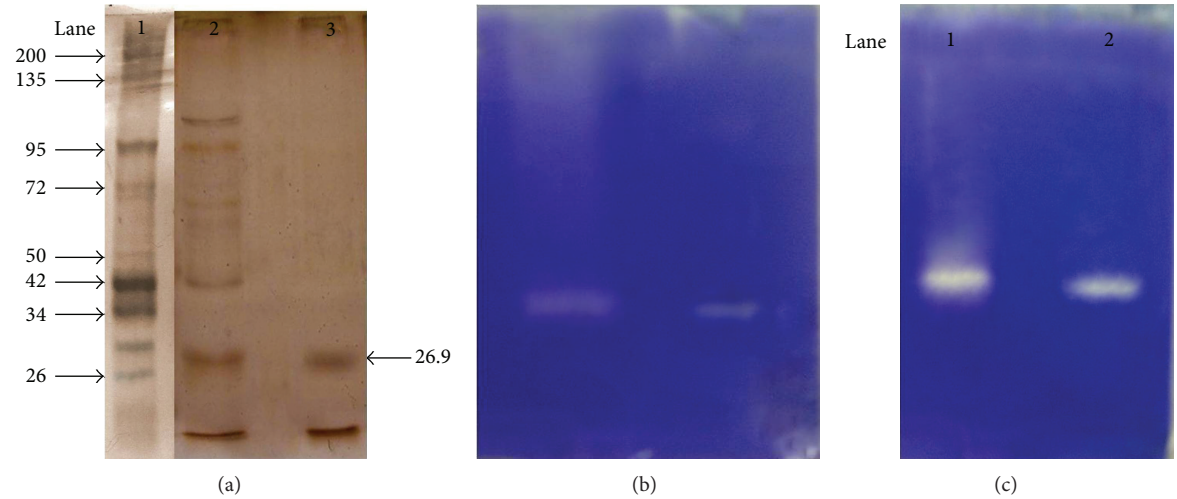

Figure 2: (a) SDS-PAGE of purified metalloprotease. Lane 1: DNA markers of different molecular weights; Lane 2: crude enzyme; Lane 3: purified metalloprotease. (b) Casein zymogram of the purified metalloprotease. Lane 1: Crude enzyme and Lane 2: purified enzyme showing zone of clearance on casein polymerized gel. (c) Gelatin zymogram of the purified metalloprotease. Lane 1: crude enzyme and Lane 2: purified enzyme showing zone of clearance on gelatin polymerized gel.

a statistically significant score of 94 matching hypothetical protein HPHPM1_1713 [*Helicobacter pylori* Hp M1] (gi|393135873) which demonstrated a score of 24.6 with 22–24% identity with bacillolysin [*Bacillus cereus*; gi|401187907] and M6 family metalloprotease domain-containing protein from various *Bacillus cereus* strains [gi|402425459; gi|507050904; gi|507054527; gi|401287019; gi|401220725]. The database search with Profound, however, yielded more significant results exhibiting 1.0 expectation value with zinc metalloprotease from *Bacillus cereus*; gi|507041200 and 0.79 expectation value with *zinc metalloprotease from Bacillus mycoides* Rock3-17 [gi|228995693] and *Bacillus mycoides* Rock1-4 (gi|229003322) with some unmatched peptides though. The matching of the m/z data with zinc metalloprotease from *Bacillus cereus*; gi|507041200 is stated in Table 2 and Figure 4(a). The unmatched peptide masses were further searched in Mascot and Profound. The motif search with Prosite revealed the presence of zinc-binding region VVVHEMCHMV in the most conserved C terminus region (Figure 4(a)).

3.6. Sequence Homology, Alignment, and Phylogenetic Studies. The sequence homology search performed through NCBI protein blast showed that the purified protein held 90–93% similarity with zinc metalloproteases from various *Bacillus* strains that belong to *Bacillus cereus* group. Thus, the protein was identified as zinc metalloprotease. The protein sequence was found to have three conserved domains DUF45, COG1451, and WLM. DUF45 family includes amino acids 190–240, with C terminus being the most conserved region containing three histidines similar to that found in zinc proteases suggesting that this family may also

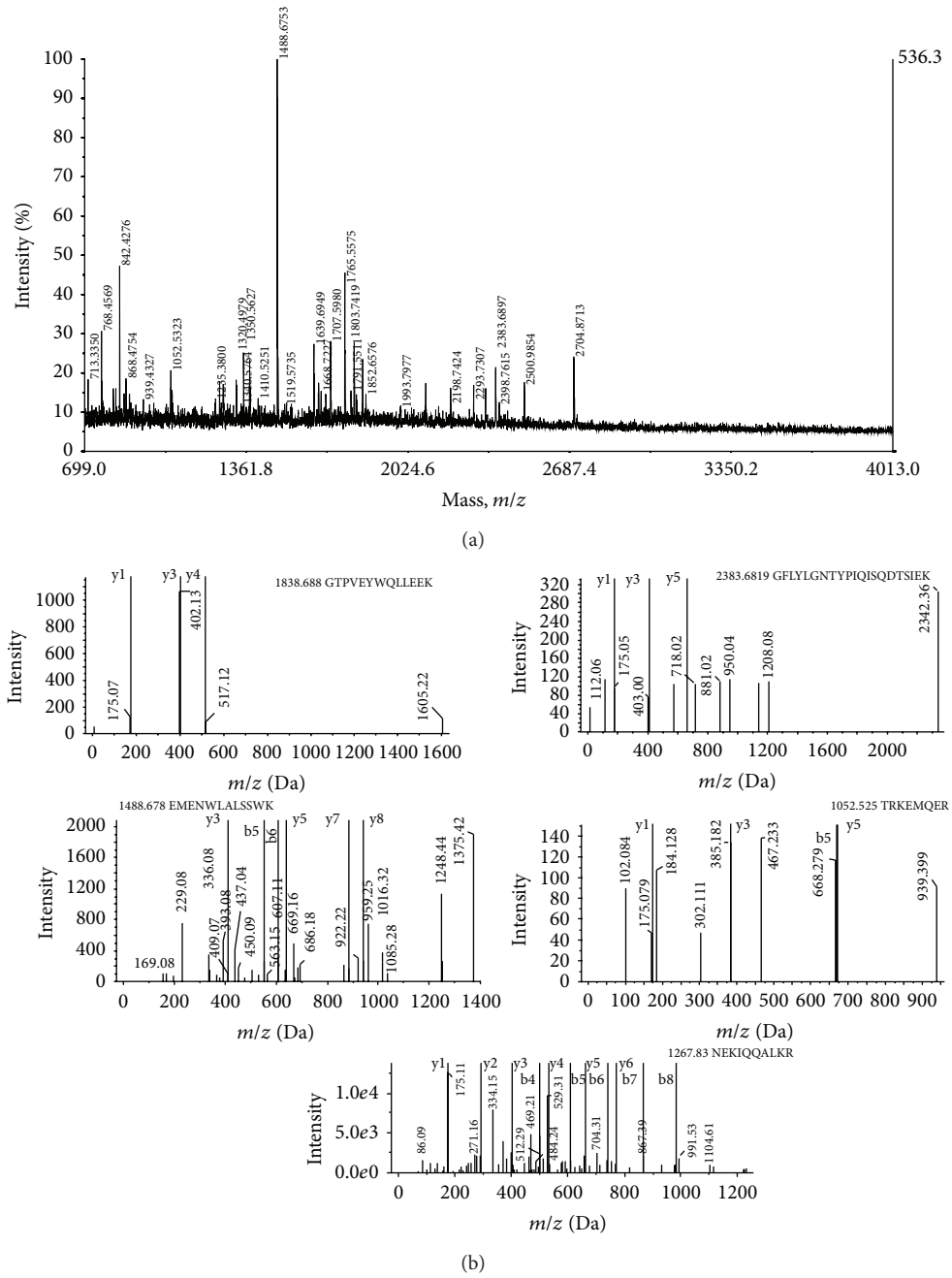

Figure 3: (a) Peptide mass spectra of the tryptic digested peptides as obtained from MALDI TOF mass spectrometry. (b) Annotated MS/MS spectra of fragmentation of 5 peptides in MS/MS that produce mostly y and b ions. The parent m/z values and the sequence of the identified peptides are indicated.

be proteases. COG1451 includes predicted metal-dependent hydrolase and WLM [pfam 08325] is a predicted metallopeptidase domain called WLM (Wss1p-like metalloproteases). The multiple sequence alignment was performed with known sequences of zinc metalloproteases from various strains belonging to the *Bacillus cereus* group, zinc metalloprotease from *Bacillus cereus* [gi|507061435], *Bacillus mycoides* [gi|489287106], *Bacillus mycoides* [gi|489298176], and *Bacillus weihenstephanensis* [gi|501217222]. The alignment demonstrated the similarity of the purified protease with these sequences (Figure 4(b)).

The evolutionary relationship tree (Figure 5) of the new metalloprotease from *Bacillus cereus* B80 showed homology with zinc metalloprotease from various *Bacillus* sp.

3.7. Secondary Structure by CD Spectrometry. The CD spectrum of the metalloprotease is represented in Figure 6(a). The spectrum analysis by K2D2 (Figure 6(b)) showed presence of α helix, 36.26% and β strand, 11.68% with max error more than 0.32. The analysis showed presence of more α helices than β strands.

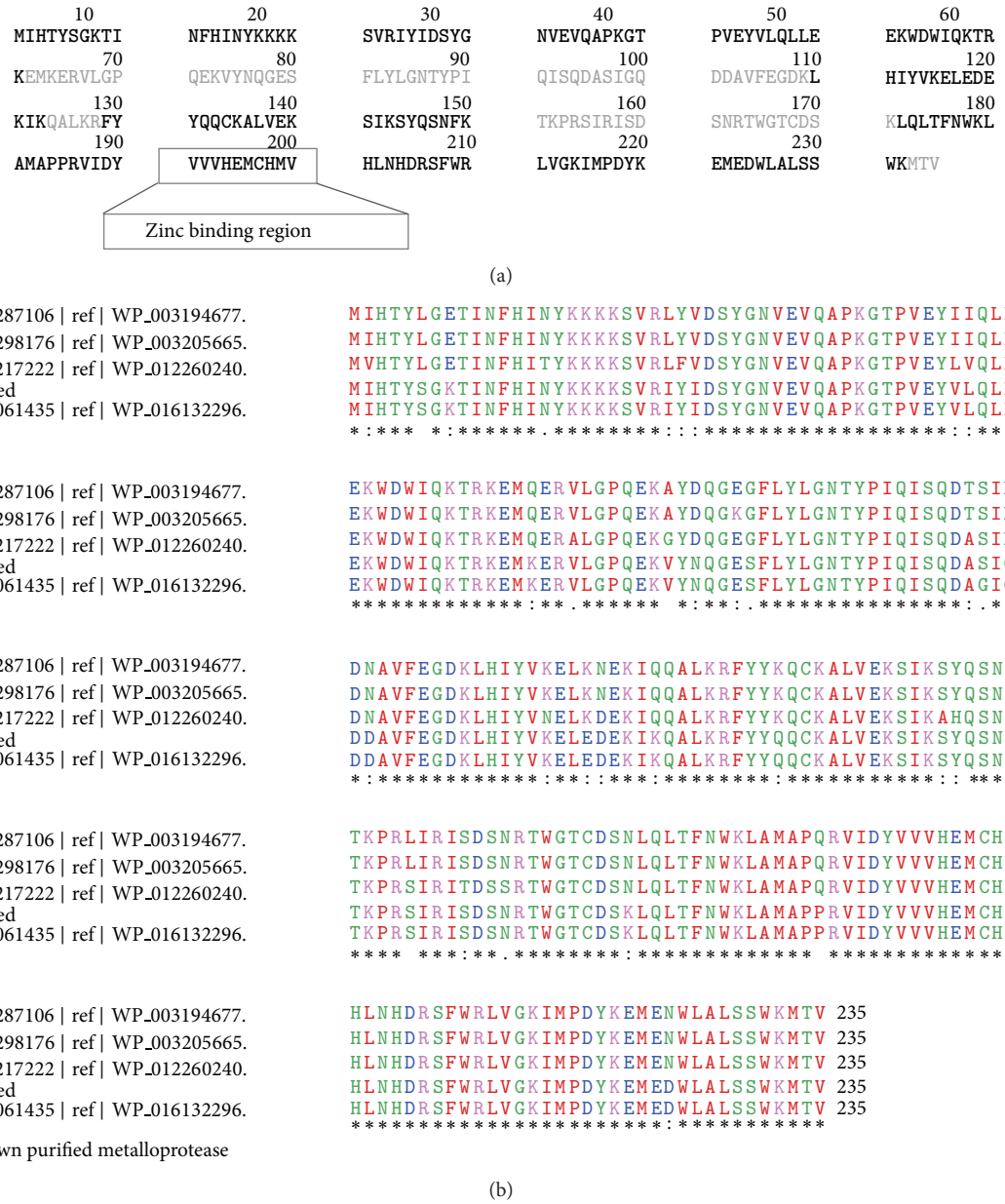

Figure 4: (a) The peptide sequence of zinc metalloprotease from *Bacillus cereus* (gi|507041200) showing matching for m/z data of the new metalloprotease (in bold). (b) Multiple sequence alignment of the purified protease with similar known sequences using ClustalW.

3.8. Elucidation of Protein Structure. Five predicted models for the newly sequenced zinc metalloprotease from *Bacillus cereus* B80 were obtained from I-TASSER (http://zhanglab.ccmb.med.umich.edu/I-TASSER/) [19]. Model 2 with the highest C-score was selected (Figure 6(c)). The estimated accuracy of Model 2 is as follows: C score: −3.26, TM-score: 0.26 + 0.08, and RMSD: 16.5 + 3.0 Å. C-score is a confidence score for estimating the quality of predicted models by I-TASSER, typically in the range from −5 to 2, where higher value signifies a model with high confidence. TM-score is a recently proposed scale for measuring the structural similarity between two structures. A TM-score >0.5 indicates a model of correct topology and a TM-score <0.17 means a random similarity [20]. RMSD is an average distance of all residue pairs in two structures.

3.9. Enzyme Kinetics Studies. The rate of reaction for the enzymatic hydrolysis studied by varying incubation time is represented by a hyperbola, where the rate of reaction increased from 0 to 10 min, and thereafter velocity of the reaction remained constant. The R^2 value of 0.872 validates the study (Figure 7(a)).

The enzyme assay with different aliquots of enzyme (0.02 mL–0.5 mL) is depicted in Figure 7(b). The straight line shows that the reaction velocity increases with the increase in enzyme concentration. R^2 value of 0.9655 validates the study.

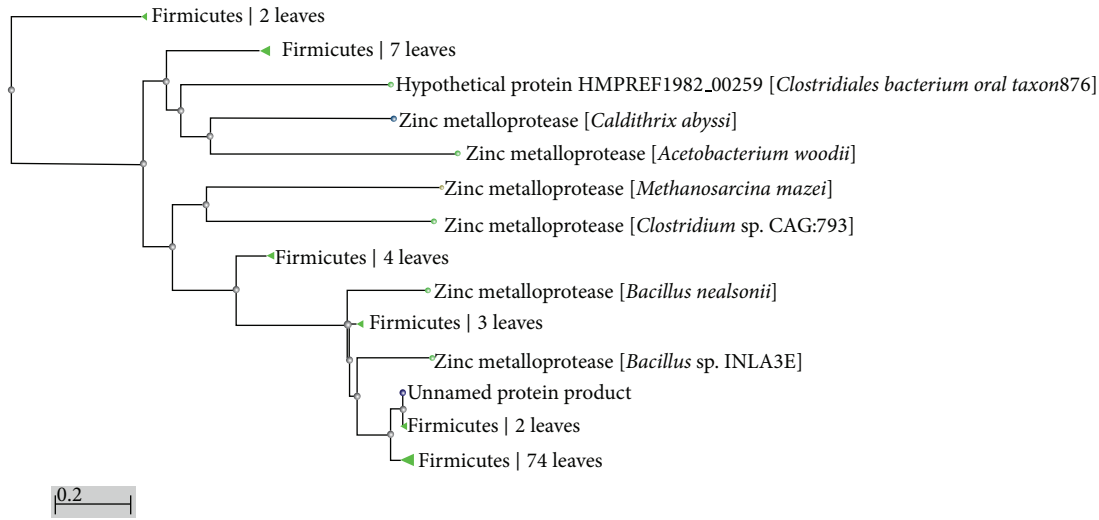

Figure 5: Phylogenetic tree of metallprotease from *Bacillus cereus* B80 with other metalloproteases.

The Michaelis-Menten graph was plotted with reaction velocity (v) as a function of substrate concentration (S) (Figure 7(c)). The kinetic constants values of the purified metalloprotease as obtained from the Michaelis-Menten equation were Michaelis constant (K_m) 0.140 μmol/ml and V_{max} 2.11 μmol/min. The Lineweaver-Burk double-reciprocal plot was prepared with the reciprocal of reaction velocity ($1/v$) as a function of reciprocal of substrate concentration ($1/S$) (Figure 7(d)).

3.10. Substrate Specificity Studies. The enzyme was able to hydrolyze all the soluble proteins as gelatin, casein, azocasein, BSA, keratin hydrolyzed, and collagen, with highest affinity towards casein followed by BSA and gelatin (Figure 8(a)).

3.11. Effect of NaCl on Enzyme Activity. The enzyme activity enhanced in presence of NaCl at 5 and 10 mM concentrations (Figure 8(b)). This shows that the enzyme is a mild halotolerant protease. It was also observed that NaCl had no effect on optimum pH of the enzyme activity as the increase of about 20% was similar at all pH values (6–9) with maximum activity at 7.

3.12. Fibrinolytic Activity. The fibrin plates with the positive (plasmin) and the purified enzyme showed a clear transparent region where fibrin was hydrolyzed, after overnight incubation, indicating fibrinolytic activity of the enzyme (Figure 9(a)). The fibrin plate with the metalloprotease exhibited a bigger zone of hydrolysis than the plasmin plate. Control showed no zone of hydrolysis. The quantitative estimation of the fibrinolytic activity of the purified metalloprotease showed 81FU.

3.13. Collagenolytic and Gelatinolytic Activity. The collagen and gelatin plates exhibited a clear zone of hydrolysis on addition of dye after overnight incubation, while the control plates showed no zone of hydrolysis (Figures 9(b) and 9(c)).

3.14. Stability in Organic Solvents. The enzyme was highly stable in most of the solvents for 4 days retaining 100–74% activity regardless of their log P values (Table 3). The residual activity of enzyme in presence of xylene was 118%, toluene 115%, benzene 83%, ethyl benzene 81%, and amyl alcohol 78% after 10 days. With acetone, the enzyme was stable with 91% activity till day 8, while in presence of DMSO, the enzyme retained 80% activity till the 6th day. The enzyme was less stable with glycerol, chloroform, acetonitrile, ethanol, and propanol retaining only 21, 18, 35, 38, and 28% activity after 10 days and was least stable with butanol retaining only 20% activity after 10 days.

The results also showed that the enzyme activity increased from 100 to 172% in presence of ethyl benzene, 147% with glycerol, 115, 107 and 106% with toluene, chloroform, xylene and DMSO, respectively, on day 1. The activity increased further to 182, 189, 118, 180, 154, 190, 100, 110, and 159% with xylene, toluene, DMSO, amyl alcohol, butanol, acetonitrile, ethanol, acetone, and propanol-2, respectively.

4. Discussion

The three-step purification process of enzyme was followed keeping in view the physicochemical nature of the enzyme and other components present in the media after fermentation. The supernatant obtained after centrifugation appeared to be dense and viscous, which might have been due to the presence of DNA and exopolysaccharides. Protein supernatants are treated with ethanol and isopropanol for reduction in viscosity [21]. Proteins are complex ampholytes that have both positive and negative charges depending upon the proportions of ionizable amino acid residues in its structure. However, in metallo-proteins, an internal metal ion often is coordinated by charged residues and hence the overall charge on the molecule is influenced by the neighboring side-chain groups which give the protein a varying net charge depending on the pH of the solute, which influences its binding and elution in an ion exchange column [22].

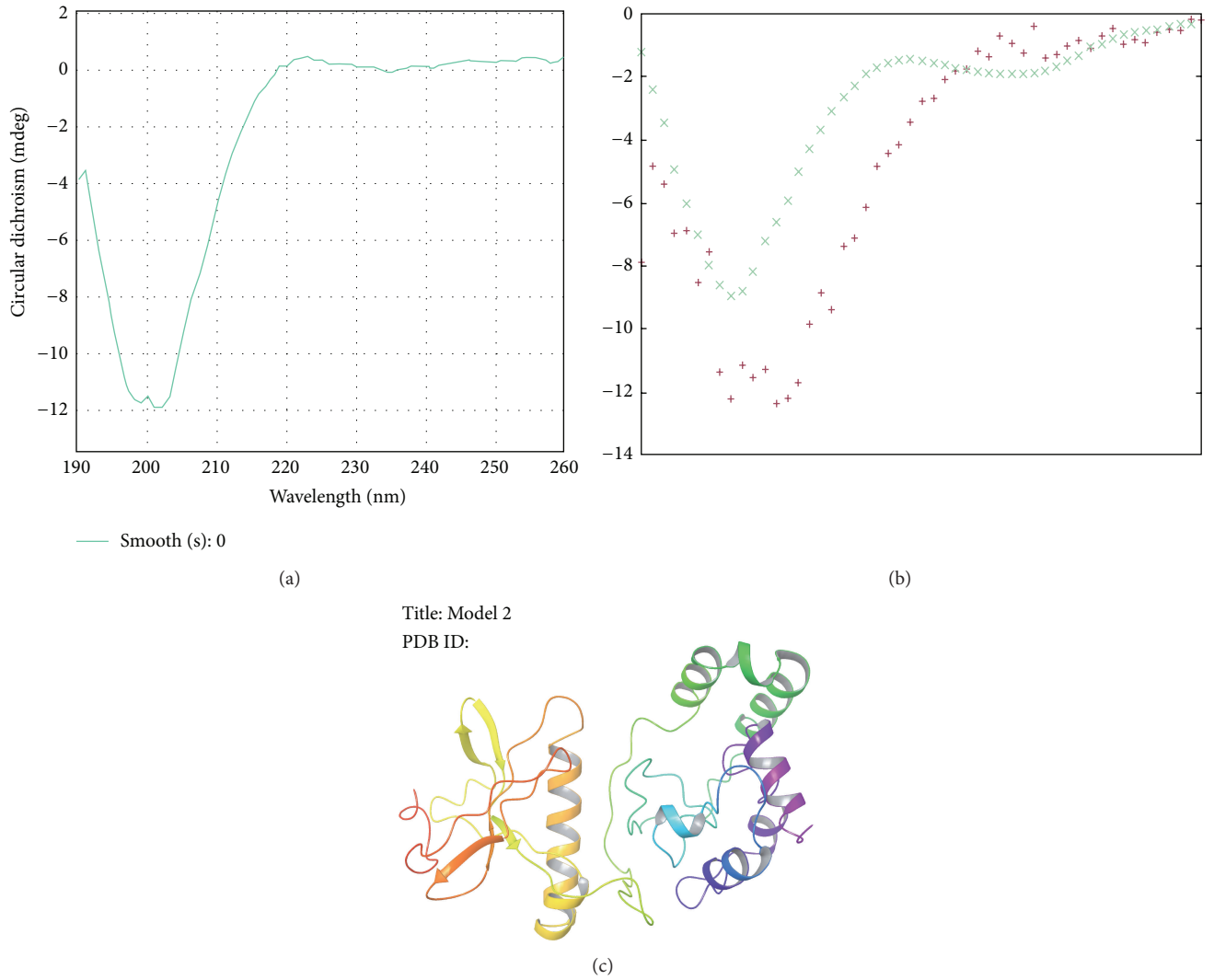

Figure 6: (a) CD spectra of metalloprotease. (b) K2d2 analysis: (+) input spectrum and (×): predicted spectrum of CD spectra. (c) 3D structure (from I-TASSER) of newly identified zinc metalloprotease from *Bacillus cereus* B80.

Table 3: Effects of organic solvents on the stability of the enzyme.

Solvents	log *P* value	Day 1	Day 2	Day 4	Day 6	Day 8	Day 10
None		100	100	98.18	98	96	92
Hexane	3.98	99.26	81.37	96.71	51.29	40.21	38.98
Ethyl benzene	3.15	172.79	139.95	120.32	97.43	85.15	81.48
Xylene	3.15	106.37	182.84	176.40	160.28	132.17	118.39
Toluene	2.73	115.69	189.22	169.01	143.20	126.54	115.94
Benzene	2.13	99.95	95.58	96.95	87.22	86.54	83.1
Chloroform	2	107.6	107.84	84.457	25.94	24.52	18.93
Amyl alcohol	1.2	77.21	180.88	107.00	104.13	94.67	78.67
Butanol	0.88	94.12	154.41	125.35	104.13	14.04	8.41
Propanol 2	0.074	99.50	159.8	74.89	51.29	32.66	28.44
Acetone	−0.21	90.93	110.05	98.42	96.68	91.49	51.72
Ethanol	−0.235	85.29	100.24	88.62	61.53	50.07	38.98
Acetonitrile	−0.394	94.85	190.2	96.71	84.23	54.72	35.74
DMSO	−1.378	106.62	118.63	115.82	80.84	69.77	52.49
Glycerol	−1.93	147.30	95.83	93.77	85.11	76.54	21.58

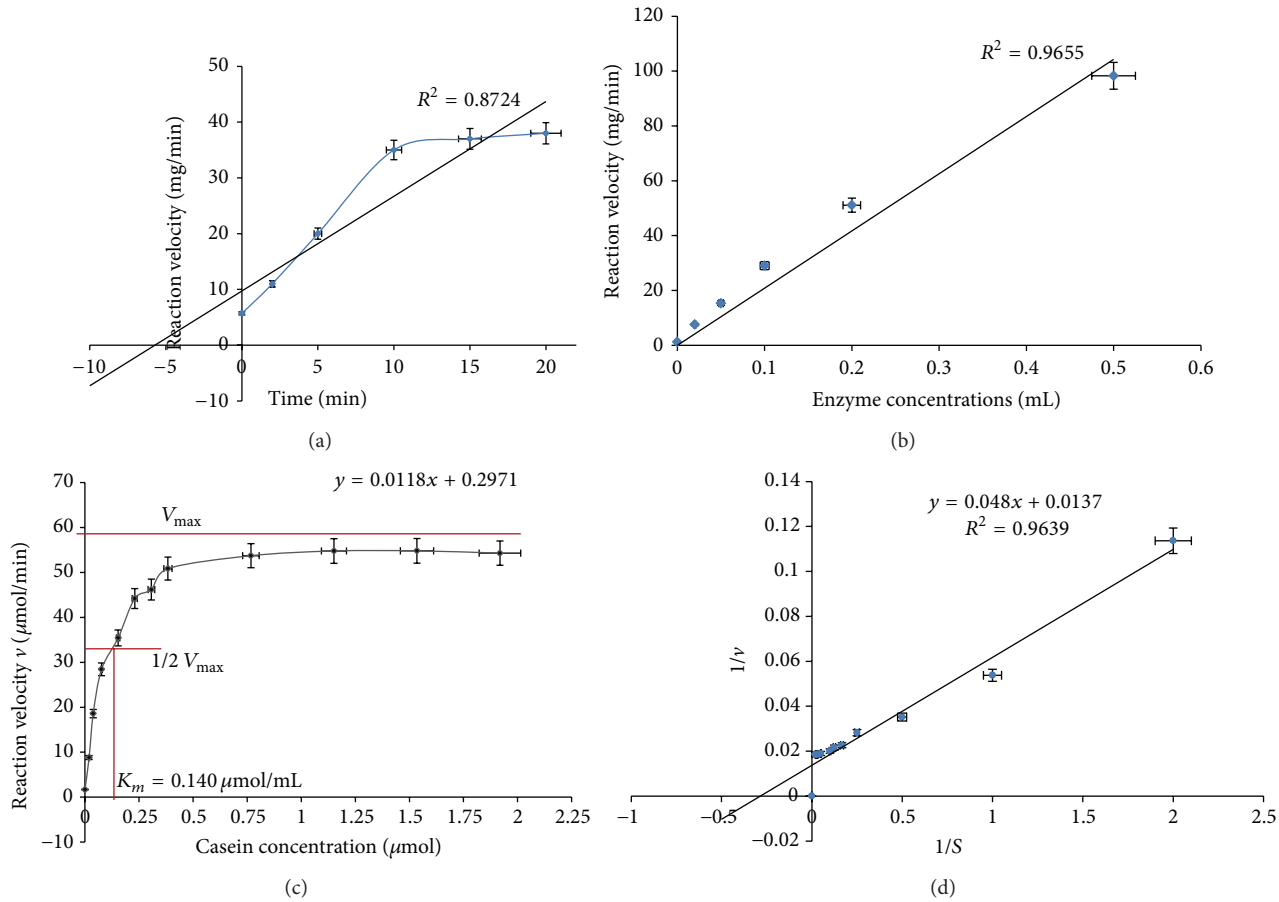

FIGURE 7: (a) Effect of incubation time on Casein hydrolysis. (b) Effect of enzyme concentration on Casein hydrolysis. (c) Enzyme kinetics, Michaelis-Menten Menton graph and (d) Lineweaver-Burk Plot.

The pH and temperature profile of the enzyme demonstrates that the enzyme is pH and thermostable. Proteases with similar thermostability, pH activity, and stability enzymes have been reported by [23–25], where the enzyme retained 100–80% activity only for 30 min in temperatures from 35 to 60°C, while in our study the enzyme retained 100–70% activity after 1 h at 30–70°C demonstrating its unique thermostability at high temperatures.

The masses of the peptide fragments as obtained by MALDI TOF MS were typically constrained between 600 and 3000 Da relating to that the digested protein is of smaller molecular weight [8]. The amino acids modifications alter the residue mass (protein), possibly making the modified peptide more or less readily ionized, hydrophilic, or soluble. Sometimes, a chemical bond that is particularly labile to mass spectrometric fragmentation is introduced into the peptide sequence that makes the fragmentation of the peptide easier. However this results in increased number of false positives (incorrect identifications) and false negatives (missed true identifications), during identification of peptides. The error is minimized by employing Tandem mass spectrometry (MS/MS) that detects the fragmented ions in the spectra, thereby identifying the amino acid modification and peptide identification [26].

Significant m/z matchings were obtained in the database searching; however, some peptides exhibited no significant matching. High quality spectra may show unidentified peptides in a typical data analysis due to several reasons like smaller number of peptides generated due to improper digestion of protein, inaccurate charge state or precursor ion m/z measurement, constrained database search parameters, presence of chemical or posttranslational modifications, and incompleteness of the protein sequence database [27]. The presence of VVVHEMCHMV peptide in the most conserved region identifies the new enzyme as zinc metalloprotease. The majorities of zinc-dependent metallopeptidases share a sequence similarity and common pattern of primary structure in the zinc-binding region and can be grouped together as a superfamily known as the metzincins [3].

Secondary structure analysis by circular dichroism (CD) spectroscopy revealed presence of more α helices and random coils than β sheets. Protein CD spectra result in large part from peptide transitions associated with secondary structural components such as alpha (the alpha-helix is a 3.6_{13} helix), 3_{10} and $4.4_{16}{\cdot}3_{10}$ (other common helical conformations), polyproline-II helices, and parallel and antiparallel b-sheets. These produce characteristic CD spectral features in the ultraviolet (UV) wavelength regions through distinct interactions with the left and right circularly polarized light from

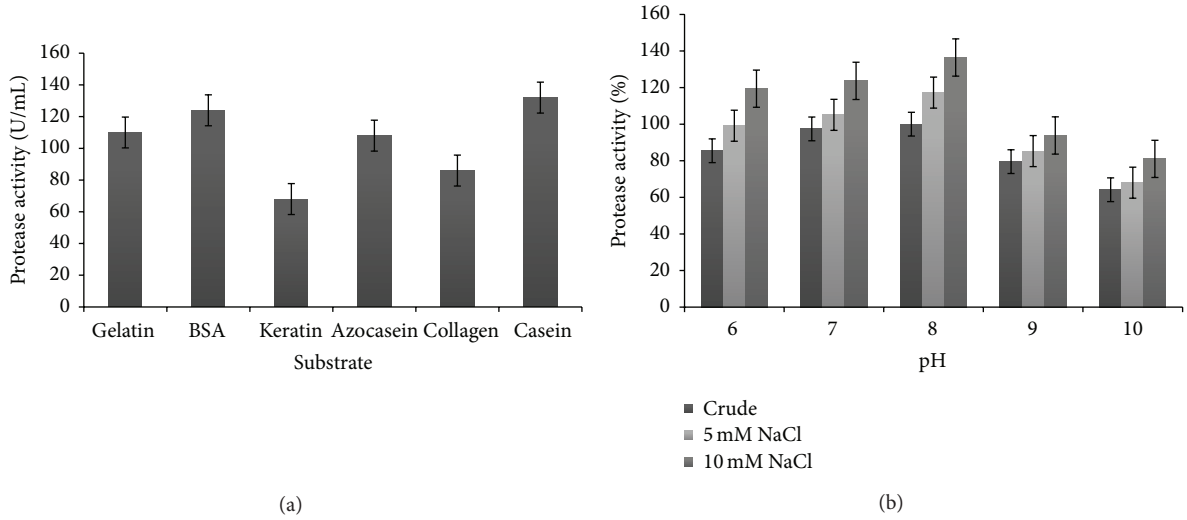

Figure 8: (a) Enzyme activity with different substrates. (b) Protease activity in presence of NaCl at different pH values.

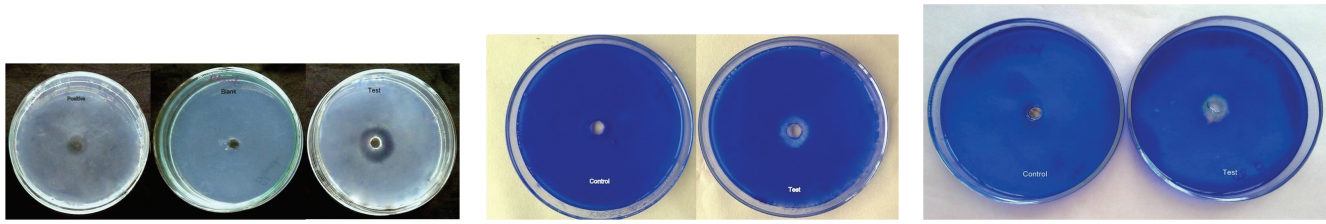

Figure 9: (a) Fibrinolytic activity of the purified metalloprotease against control and positive plates, visible as a clear zone around the well. (b) Collagenolytic activity of purified metalloprotease on collagen plate. (c) Gelatinolytic activity of purified metalloprotease on gelatin plate.

a CD spectrophotometer or a synchrotron radiation circular dichroism (SRCD) beamline [28]. Because the spectra of these molecules in the far UV regions are dominated by the n-π and π-π^* transitions of amide groups and are influenced by the geometries of the polypeptide backbones, their spectra are reflective of the different types of secondary structures present [29]. The alpha helix is the most stable of all the secondary structures, and this explains the extreme stable characteristic of the purified enzyme. α-helical structure has been reported to contribute in stability of enzyme produced by *Pseudomonas aeruginosa* strain K in organic solvents, broad range of temperatures, pHs, and metal ions [30]. Alpha helix proteases have been widely studied and reported to understand the diverse functionality of these enzymes [31, 32].

The results obtained from the CD spectroscopy were validated by the tertiary (3D) structure obtained from I-TASSER which also showed presence of more α helices and random coils than β strands. I-TASSER is an automated pipeline for protein tertiary structure prediction using multiple threading alignments and iterative structure assembly simulations [19].

The enzyme kinetics study revealed that the enzyme exhibited highest affinity towards casein, with a low K_m value suggesting that a minimum amount of enzyme was required for a maximum effect of reaction to occur. Low K_m values also suggest that the enzyme is normally saturated with substrate and will act at a constant rate, regardless of variations in the concentration of substrate within the physiological range [33]. Similar low K_m values have been reported by Gupta et al. [33] (K_m = 2.69 mg/mL, $V_{\max}$ = 3.03 μmol/min) and Tang et al. [25] (K_m = 3.97 mg/mL, $V_{\max}$ = 7.58 μmol/min) towards casein as substrate at 60°C indicating its high affinity and efficient catalytic role.

The salt tolerance of the enzyme shows that it is a mild halotolerant metalloprotease. Inouye et al. [34] have reported that NaCl enhances the catalytic activity and thermal stability of thermolysin. Halotolerant proteases have been reported by Shivanand and Jayaraman [35] and Ningthoujam and Kshetri [36]. Higher salinity may promote binding of a hydrophobic substrate to enzyme or of hydrophobic residues to each other within the enzyme to ensure optimal folding for enzymatic activity. Zinc metalloproteases with fibrinolytic and collagenolytic activity from various *Bacillus cereus* strains have been reported [24, 37].

The enzyme exhibited high stability in various organic solvents. Classical theory suggests that disulfide bonds stabilize proteins by reducing the entropy of the denatured state and hence they have been attributed for the unusual stability properties enzymes [38]. In the light of these findings, we presume that such disulfide bonds existing in the

metalloprotease enzyme make it resistant against various organic solvents. Also the results show an enhanced enzyme activity in presence of some organic solvents. The general explanations offered include disruption of water structure in the vicinity of the active site formation of higher intrinsic activity resulting in as high as tenfold increase, or presence of high concentrations of miscible organic solvents may induce gross changes in substrate specificity and/or more subtle alterations in chiral selectivity [39, 40]. Metalloproteases showing stability in wide range of organic solvents have been reported [24, 31].

5. Conclusion

The enzyme studied in the present work was identified as a zinc metalloprotease as it exhibited 70–93% matching with zinc metalloprotease from various *Bacillus* sp. However, on the basis of its amino acid sequence, phylogenetic relationship and predicted tertiary structure, biochemical characteristics, and stability properties, it is established as a novel zinc metalloprotease.

The enzyme exhibited strong fibrinolytic and collagenolytic activity and thus finds a potential use as a natural agent for oral fibrinolytic therapy or thrombosis prevention, in the clinical therapy and in the wound healing process, and as experimental reagents in laboratory work. The enzyme was observed to be mild salt tolerant, while highly stable, in presence of organic solvents. Enzymes with such stability properties are very important from an industrial perspective. Halo tolerant proteases find application in food fermentation where NaCl is used as preservative. Salt stable collagenases containing ointment are frequently used in clinics to debris wounds. Nonaqueous enzymology has considerably enlarged the use of enzymes for a variety of applications. The unique solvent stability of the enzyme thus establishes it as promising biocatalyst for organic solvent-based enzymatic synthesis.

This enzyme can be exploited for a wide-ranged application in various industries owing to its stability, wide substrate specificity, and fibrinolytic and gelatinolytic properties.

Conflict of Interests

The authors declare that there is no conflict of interests regarding the publication of this paper.

References

[1] N. D. Rawlings, A. J. Barrett, and A. Bateman, "MEROPS: the database of proteolytic enzymes, their substrates and inhibitors," *Nucleic Acids Research*, vol. 40, no. 1, pp. D343–D350, 2012.

[2] J.-W. Wu and X.-L. Chen, "Extracellular metalloproteases from bacteria," *Applied Microbiology and Biotechnology*, vol. 92, no. 2, pp. 253–262, 2011.

[3] K. M. Fukasawa, T. Hata, Y. Ono, and J. Hirose, "Metal preferences of zinc-binding motif on metalloproteases," *Journal of Amino Acids*, vol. 2011, pp. 1–7, 2011.

[4] L. Liu, M. Ma, Z. Cai, X. Yang, and W. Wang, "Purification and properties of a collagenolytic protease produced by *Bacillus cereus* MBL13 strain," *Food Technology and Biotechnology*, vol. 48, no. 2, pp. 151–160, 2010.

[5] A. Jovanovic, R. Ermis, R. Mewaldt, L. Shi, and D. Carson, "The influence of metal salts, surfactants, and wound care products on enzymatic activity of collagenase, the wound debriding enzyme," *Wounds*, vol. 24, no. 9, pp. 242–253, 2012.

[6] R. Deutzmann, "Structural characterization of proteins and peptides," *Methods in Molecular Medicine*, vol. 94, pp. 269–297, 2004.

[7] C. Bechara, G. Bolbach, P. Bazzaco et al., "MALDI-TOF mass spectrometry analysis of amphipol-trapped membrane proteins," *Analytical Chemistry*, vol. 84, no. 14, pp. 6128–6135, 2012.

[8] J. Webster and D. Oxley, "Protein identification by MALDI-TOF mass spectrometry," *Methods in Molecular Biology*, vol. 800, pp. 227–240, 2012.

[9] K. Ning, D. Fermin, and A. I. Nesvizhskii, "Computational analysis of unassigned high-quality MS/MS spectra in proteomic data sets," *Proteomics*, vol. 10, no. 14, pp. 2712–2718, 2010.

[10] R. Saxena and R. Singh, "A modeling study by centre composite design in response surface methodology on production parameters optimization for novel metalloprotease by a newly isolated *Bacillus cereus* b80," *Brazilian Journal of Microbiology*. In press.

[11] R. Saxena and R. Singh, "Statistical optimization of conditions for protease production from *Bacillus* sp," *Acta Biologica Szegediensis*, vol. 54, no. 2, pp. 135–141, 2010.

[12] M. M. Bradford, "A rapid and sensitive method for the quantitation of microgram quantities of protein utilizing the principle of protein dye binding," *Analytical Biochemistry*, vol. 72, no. 1-2, pp. 248–254, 1976.

[13] U. K. Laemmli, "Cleavage of structural proteins during the assembly of the head of bacteriophage T_4," *Nature*, vol. 227, no. 5259, pp. 680–685, 1970.

[14] B. K. Sørensen, P. Højrup, E. Østergård et al., "Silver staining of proteins on electroblotting membranes and intensification of silver staining of proteins separated by polyacrylamide gel electrophoresis," *Analytical Biochemistry*, vol. 304, no. 1, pp. 33–41, 2002.

[15] F. L. Garcia-Carreno, L. E. Dimes, and N. F. Haard, "Substrate-gel electrophoresis for composition and molecular weight of proteinases or proteinaceous proteinase inhibitors," *Analytical Biochemistry*, vol. 214, no. 1, pp. 65–69, 1993.

[16] M. A. Larkin, G. Blackshields, N. P. Brown et al., "Clustal W and Clustal X version 2.0," *Bioinformatics*, vol. 23, no. 21, pp. 2947–2948, 2007.

[17] T. Astrup and S. Müllertz, "The fibrin plate method for estimating fibrinolytic activity," *Archives of Biochemistry and Biophysics*, vol. 40, no. 2, pp. 346–351, 1952.

[18] G. Datta, A. Dong, J. Witt, and A. T. Tu, "Biochemical characterization of basilase, a fibrinolytic enzyme from *Crotalus basiliscus basiliscus*," *Archives of Biochemistry and Biophysics*, vol. 317, no. 2, pp. 365–373, 1995.

[19] A. Roy, A. Kucukural, and Y. Zhang, "I-TASSER: a unified platform for automated protein structure and function prediction," *Nature Protocols*, vol. 5, no. 4, pp. 725–738, 2010.

[20] Y. Zhang and J. Skolnick, "Scoring function for automated assessment of protein structure template quality," *Proteins: Structure, Function and Genetics*, vol. 57, no. 4, pp. 702–710, 2004.

[21] W. W. Ward and G. Swiatek, "Protein purification," in *Current Analytical Chemistry*, vol. 5, Bentham Science, 2009.

[22] M. Hedhammar, A. E. Karlstron, and S. Hober, *Chromatographic Methods for Protein Purification*, Royal Institute of Technology, Stockholm, Sweden, 2006.

[23] R. A. Abusham, R. N. Z. R. A. Rahman, A. Salleh, and M. Basri, "Optimization of physical factors affecting the production of thermo-stable organic solvent-tolerant protease from a newly isolated halo tolerant *Bacillus subtilis* strain Rand," *Microbial Cell Factories*, vol. 8, article 20, 2009.

[24] L. Manni, K. Jellouli, O. Ghorbel-Bellaaj et al., "An oxidant- and solvent-stable protease produced by bacillus cereus SV1: application in the deproteinization of shrimp wastes and as a laundry detergent additive," *Applied Biochemistry and Biotechnology*, vol. 160, no. 8, pp. 2308–2321, 2010.

[25] X.-Y. Tang, B. Wu, H.-J. Ying, and B.-F. He, "Biochemical properties and potential applications of a solvent-stable protease from the high-yield protease producer *Pseudomonas aeruginosa* PT121," *Applied Biochemistry and Biotechnology*, vol. 160, no. 4, pp. 1017–1031, 2010.

[26] S. D. Maleknia and R. Johnson, "Mass spectrometry of amino acids and proteins," in *Amino Acids, Peptides and Proteins in Organic Chemistry: Analysis and Function of Amino Acids and Peptides*, A. B. Hughes, Ed., vol. 5, Wiley-VCH, Weinheim, Germany, 2011.

[27] M. L. Nielsen, M. M. Savitski, and R. A. Zubarev, "Extent of modifications in human proteome samples and their effect on dynamic range of analysis in shotgun proteomics," *Molecular & Cellular Proteomics*, vol. 5, no. 12, pp. 2384–2391, 2006.

[28] D. P. Klose, B. A. Wallace, and R. W. Janes, "DichroMatch: a website for similarity searching of circular dichroism spectra," *Nucleic Acids Research*, vol. 40, no. 1, pp. W547–W552, 2012.

[29] L. Whitmore and B. A. Wallace, "Protein secondary structure analyses from circular dichroism spectroscopy: methods and reference databases," *Biopolymers*, vol. 89, no. 5, pp. 392–400, 2008.

[30] R. N. Z. R. A. Rahman, A. B. Salleh, M. Basri, and C. F. Wong, "Role of α-helical structure in organic solvent-activated homodimer of elastase strain K," *International Journal of Molecular Sciences*, vol. 12, no. 9, pp. 5797–5814, 2011.

[31] A. Ruf, M. Stihle, J. Benz, M. Schmidt, and H. Sobek, "Structure of Gentlyase, the neutral metalloprotease of *Paenibacillus polymyxa*," *Acta Crystallographica Section D: Biological Crystallography*, vol. 69, part 1, pp. 24–31, 2013.

[32] T. Yamaguchi, K. Sahara, H. Bando, and S.-I. Asano, "Intramolecular proteolytic nicking and binding of *Bacillus thuringiensis* Cry8Da toxin in BBMVs of Japanese beetle," *Journal of Invertebrate Pathology*, vol. 105, no. 3, pp. 243–247, 2010.

[33] A. Gupta, I. Roy, S. K. Khare, and M. N. Gupta, "Purification and characterization of a solvent stable protease from *Pseudomonas aeruginosa* PseA," *Journal of Chromatography A*, vol. 1069, no. 2, pp. 155–161, 2005.

[34] K. Inouye, K. Kuzuya, and B. Tonomura, "Sodium chloride enhances markedly the thermal stability of thermolysin as well as its catalytic activity," *Biochimica et Biophysica Acta*, vol. 1388, no. 1, pp. 209–214, 1998.

[35] P. Shivanand and G. Jayaraman, "Production of extracellular protease from halotolerant bacterium, *Bacillus aquimaris* strain VITP4 isolated from Kumta coast," *Process Biochemistry*, vol. 44, no. 10, pp. 1088–1094, 2009.

[36] D. S. Ningthoujam and P. Kshetri, "A thermostable alkaline protease from a moderately halo-alkalithermotolerant *Bacillus Subtilis* strain SH1," *Australian Journal of Basic and Applied Sciences*, vol. 4, no. 10, pp. 5224–5233, 2010.

[37] W. A. Hassanein, E. Kotb, N. M. Awny, and Y. A. El-Zawahry, "Fibrinolysis and anticoagulant potential of a metallo-protease produced by Bacillus subtilis K42," *Journal of Biosciences*, vol. 36, no. 5, pp. 1–7, 2011.

[38] H. Ogino, S. Tsuchiyama, M. Yasuda, and N. Doukyu, "Enhancement of the aspartame precursor synthetic activity of an organic solvent-stable protease," *Protein Engineering, Design and Selection*, vol. 23, no. 3, pp. 147–152, 2010.

[39] Y. L. Khmnelnitsky, A. V. Levashov, N. L. Klyachko, and K. Martinek, "Engineering biocatalytic systems in organic media with low water content," *Enzyme and Microbial Technology*, vol. 10, no. 12, pp. 710–724, 1988.

[40] D. A. Cowan, "Thermophilic proteins: stability and function in aqueous and organic solvents," *Comparative Biochemistry and Physiology A: Physiology*, vol. 118, no. 3, pp. 429–438, 1997.

Hindawi Publishing Corporation
BioMed Research International
Volume 2014, Article ID 506287, 13 pages
http://dx.doi.org/10.1155/2014/506287

Review Article

L-Methionase: A Therapeutic Enzyme to Treat Malignancies

Bhupender Sharma, Sukhdev Singh, and Shamsher S. Kanwar

Department of Biotechnology, Himachal Pradesh University, Summer Hill, Shimla 171 005, India

Correspondence should be addressed to Shamsher S. Kanwar; kanwarss2000@yahoo.com

Received 25 February 2014; Revised 16 July 2014; Accepted 12 August 2014; Published 31 August 2014

Academic Editor: Noomen Hmidet

Cancer is an increasing cause of mortality and morbidity throughout the world. *L*-methionase has potential application against many types of cancers. *L*-Methionase is an intracellular enzyme in bacterial species, an extracellular enzyme in fungi, and absent in mammals. *L*-Methionase producing bacterial strain(s) can be isolated by 5,5′-dithio-*bis*-(2-nitrobenzoic acid) as a screening dye. *L*-Methionine plays an important role in tumour cells. These cells become methionine dependent and eventually follow apoptosis due to methionine limitation in cancer cells. *L*-Methionine also plays an indispensable role in gene activation and inactivation due to hypermethylation and/or hypomethylation. Membrane transporters such as GLUT1 and ion channels like Na^{2+}, Ca^{2+}, K^{+}, and Cl^{-} become overexpressed. Further, the α-subunit of ATP synthase plays a role in cancer cells growth and development by providing them enhanced nutritional requirements. Currently, selenomethionine is also used as a prodrug in cancer therapy along with enzyme methionase that converts prodrug into active toxic chemical(s) that causes death of cancerous cells/tissue. More recently, fusion protein (FP) consisting of *L*-methionase linked to annexin-V has been used in cancer therapy. The fusion proteins have advantage that they have specificity only for cancer cells and do not harm the normal cells.

1. Introduction

L-Methionine-γ-lyase (EC 4.4.1.11; MGL), also known as methionase, methioninase, *L*-methionine-γ-demethiolase, and *L*-methionine methanethiol-lyase (deaminating), is a pyridoxal phosphate (PLP) dependent enzyme. PLP reduces the energy for conversion of amino acids to a zwitterionic carbonion [1] and substantially the apoenzyme catalyzes the cleavage of substrate bond yielding the product [2]. MGL is a cytosolic enzyme inducibly formed by addition of *L*-methionine to the culture medium [3]. MGL has a molecular weight (Mr) of about 149 kDa to 173 kDa and consists of four subunits with identical Mr of about 41 kDa to 45 kDa each except MGL purified to homogeneity from *Pseudomonas putida* (*ovalis*) which was found to consist of two nonidentical subunits of 40 kDa and 48 kDa [4].

L-Methionine must be incorporated into the human diet in order to biosynthesize *L*-cysteine (Figure 1) by *trans*-sulfuration pathway [5]. In yeast, methionine and cysteine supplementation was required in order to biosynthesize cysteine or methionine, respectively. The microorganisms can synthesize the sulphur containing amino acids by utilizing inorganic sulphate via the *de novo* cysteine biosynthesis pathway [6]. *Escherichia coli* and plants utilize the forward *trans*-sulfuration pathway such that methionine is biosynthesized from cysteine or they may utilize inorganic sulphate via *de novo* cysteine biosynthesis [7, 8]. There are different kinds of methionine biosynthesis pathways in different organisms as described in the MetaCyc database. *E. coli* K-12 methionine biosynthesis-I pathway that involves methionine biosynthesis from homoserine, methionine biosynthesis by transsulfuration. *Arabidopsis thaliana*, methionine biosynthesis-II pathway that involves methionine biosynthesis from homoserine-II. *Corynebacterium glutamicum*, *Leptospira meyeri,* and *Saccharomyces cerevisiae* follow methionine biosynthesis-III pathway that performs homoserine methionine biosynthesis and methionine biosynthesis by sufhdrylation. *Arabidopsis thaliana*,

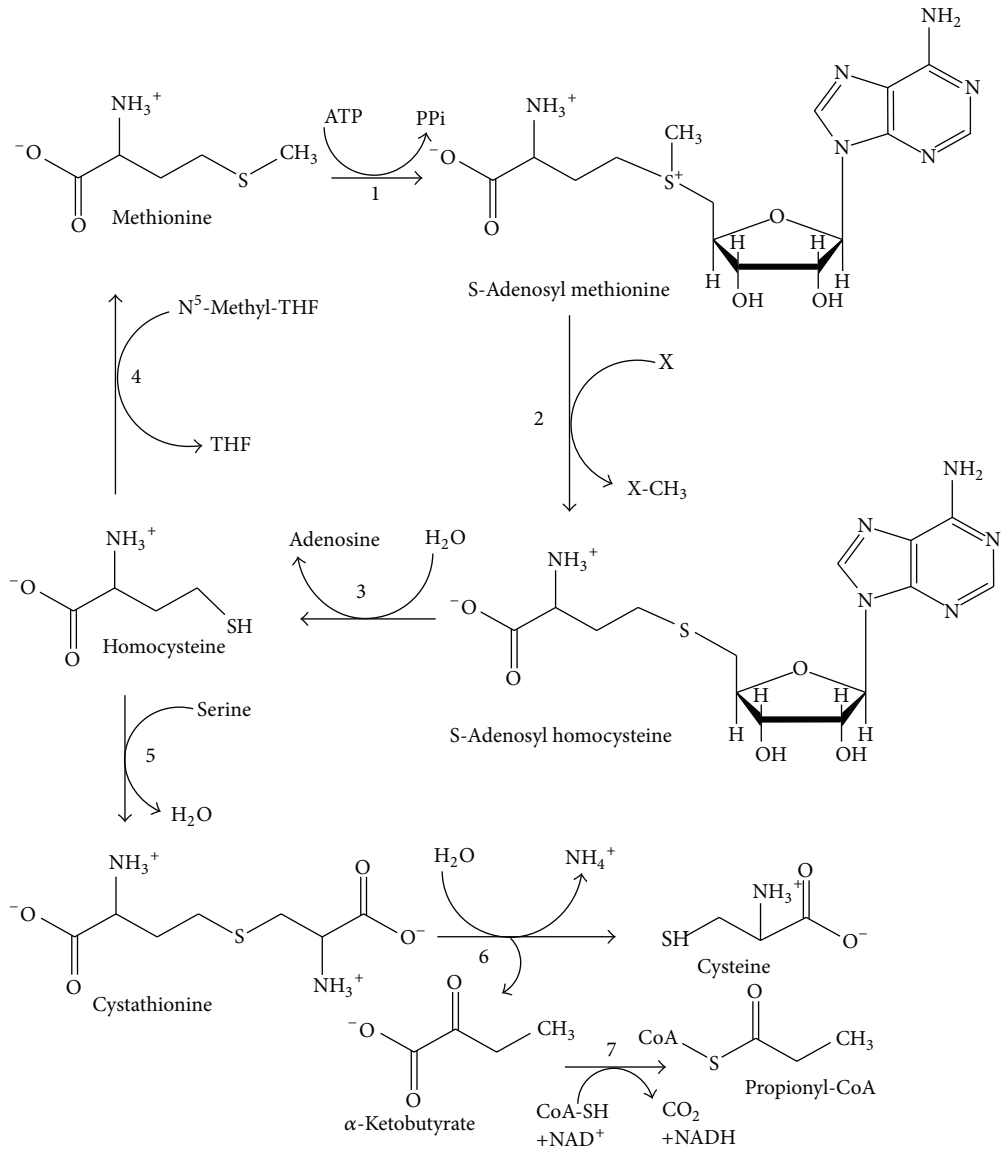

Figure 1: General approach of methionine metabolism (modified from [46]). *L*-Methionine is mainly supplied exogenously from dietary proteins. The enzymes involved in this pathway are (1) methionine adenosyltransferase; (2) S-adenosylmethionine methyltransferases; (3) adenosylhomocysteinase; (4) 5-methyltetrahydrofolate-homocysteine methyltransferase (in mammals betaine-homocysteine methyltransferase or homocysteine methyltransferase); (5) cystathionine-γ-synthase; (6) cystathionine-γ-lyase; (7) α-ketoacid dehydrogenase.

Bacillus subtilis, *Klebsiella oxytoca*, *Klebsiella pneumonia*, *Lupinus luteus,* and *Oryza sativa* follow methionine salvage-I pathway while *Homo sapiens* and *Rattus norvegicus* possess methionine salvage-II system. *Bacillus subtilis*, *Corynebacterium glutamicum*, *Leptospira meyeri*, *Pseudomonas aeruginosa*, *Pseudomonas putida* and *Saccharomyces cerevisiae* possess a unique superpathway of methionine biosynthesis (by sulfhydrylation). On other hand, *Arabidopsis thaliana*, *Lupinus luteus*, *Oryza sativa*, *Plantago major,* and *Solanum lycopersicum* follow Yang cycle/MTA cycle [9]. *E. histolytica* and *T. vaginalis* have a methionine catabolic pathway and elements of a *de novo* sulphide biosynthetic pathway for cysteine biosynthesis in *E. histolytica*. These differences in cysteine metabolism between humans and parasites are of particular interest, especially for the future development of antiparasitic compounds. Currently, *de novo* engineering of a human MGL has been followed for achieving systemic *L*-methionine depletion in cancer therapy [10].

2. Sources of MGL

MGL is widely distributed in bacteria, especially in *Pseudomonas* spp. and is induced by the addition of *L*-methionine to the culture medium. Crystal structures of MGL have been reported from *Pseudomonas putida* (*P. putida*) [17, 18], *Citrobacter freundii* [47], *Trichomonas vaginalis* [3],

Table 1: Potential sources for *L*-methionine γ-lyase isolation.

Source	Examples	Reference(s)
Bacteria	*Brevibacterium linens*	[11]
	Clostridium sporogenes	[12]
	Citrobacter intermedius	[13]
	Citrobacter freundii	[14]
	Porphyromonas gingivalis	[15]
	Pseudomonas ovalis	[16]
	Pseudomonas putida	[17, 18]
	Treponema denticola	[19]
	Micrococcus luteus, Arthrobacter sp., *Corynebacterium glutamicum* and *Staphylococcus equorum*	[20]
Protozoa	*Trichomonas vaginalis*	[3]
	Entamoeba histolytica	[21–23]
Plant	*Arabidopsis thaliana*	[24]
Archaeon	*Ferroplasma acidarmanus*	[25]
Fungus	*Aspergillus* sp. RS-1a	[26]
	Geotrichum candidum	[27]
	Aspergillus flavipes	[28]
	Scopulariopsis brevicaulis	
	A. carneus	
	Penicillium notatum	
	Fusarium solani	

and *Entamoeba histolytica* [21, 22]. The MGL was isolated from different sources such as bacterial, protozoans, fungal, archaeon, and plants (Table 1).

3. MGL Isolation

The bacterial, protozons, archaeal, and plants produce intracellular MGL and fungal sources produce extracellular MGL. Therefore isolation of MGL from microbial sources required cell disruption by chemical, enzymatic, and mechanical methods. Fugal sources produce extracellular MGL; thus, there is no need for cell disruption. Amongst above described MGL sources, *P. putida* is reported to be the best source for MGL production. *P. putida* cell pellets were disrupted by passage through French press. The ammonium sulphate precipitated crude cell lysate was applied on DEAE-cellulose and Sephadex G200 column, respectively. The MGL specific activity (Units/mg protein) from *P. putida* was 14.20 that improved to 3,735 after column chromatography, whereas, in case of *Aspergillus flavipes*, the specific activity (Units/mg protein) was 12.58. *A. flavipes* required 10-day incubation period for growth and 8 days for production time, whereas *P. putida* needed 24–48 h incubation and production time for growth [17, 28]. Microorganisms are most important and convenient sources of commercial enzymes production. Moreover, they have an advantage that they can be cultivated by using inexpensive media and enzyme production occurs in short time.

4. Biochemical Reaction Catalyzed by MGL

MGL catalyzes the conversion of *L*-methionine to α-ketobutyrate, methanethiol, and ammonia by α, γ-elimination reaction (Figure 2).

5. Methionase Assay

The free sulphydryl group in solution could be quantitatively measured [48] by 5,5′-dithio-*bis*-(2-nitrobenzoic acid) (DTNB). The DTNB was used as screening dye in agar media to detect methanethiol, which reduces DTNB to form yellow coloured aryl mercaptan (2-nitro-5-thiobenzoate or TNB) around the bacterial colony that is able to produce MGL enzyme. DTNB has little absorbance, but when it reacts with thiol (SH) groups on proteins under mild alkaline conditions (pH 7-8), the 2-nitro-5-thiobenzoate anion (TNB^{2-}) gives an intense yellow color (Figure 3). Ellman's reagent is useful assay reagent because of its specificity for SH groups [49] at neutral pH, high molar extinction coefficient, and short reaction time. MGL activity was quantitatively assayed by 3-methyl-2-benzothiazolone hydrazone (MBTH) which determines the amount of α-ketobutyrate produced spectrophotometricallY at 320 nm. The 3-(4,5-dimethylthiazol-2-yl)-2,5-dimethyl-tetrazolium bromide (MTT) assay [50] was used to determine the *in vitro* growth inhibition of tumour cells by MGL treatment.

6. Methionine Requirement in Cancer Cell

Tumours cells have uncontrolled rapid growth and proliferation as compared to the normal cells [51]. Many malignant human cell lines have enhanced requirements of methionine for high protein synthesis and regulation of DNA expression in cancer cells [31, 52–57]. Methionine is converted to S-adenosylmethionine and it becomes methyl donor for DNA methylation, an epigenetic phenomenon [58–61] associated with cancer (Figure 4). The high methionine diets were associated with increased prostate cancer risk. The higher availability of *L*-methionine leads to higher bioavailability of S-adenosylmethionine to donate methyl groups to DNA, resulting in DNA hypermethylation of regulatory regions, including tumour suppressors [62, 63].

The CpG is a cytosine-guanosine (CG) dinucleotide DNA sequence, in which the cytosine undergoes chemical modification to contain a methyl group. The methyl binding protein (MBP) primarily was involved in gene regulation of normal cells to exert transcriptional control and also exploited by cancer cells to escape such control [64]. DNA methylation is essential for normal development but in some diseases, such as cancer, gene promoter CpG islands acquire abnormal hypermethylation. The transcriptional silencing due to hypermethylation was inherited by daughter cells following cell division. Alterations of DNA methylation have been recognized to play important role in cancer development. The CpG hypermethylation has been observed in cancer cell lines such as breast, colon, lung, head and neck squamous cell carcinomas, glioblastoma, acute myeloid leukemia,

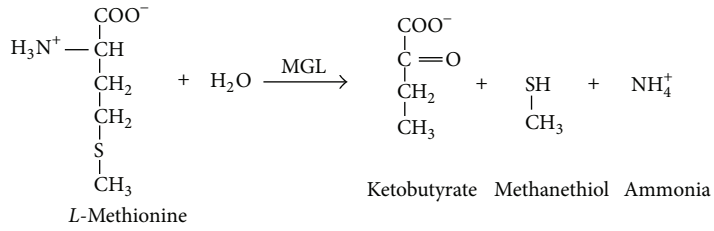

Figure 2: The biochemical reaction catalysed by MGL. MGL catalyses conversion of L-methionine into α-ketobutyrate, methanethiol, and ammonia by α, γ elimination reaction.

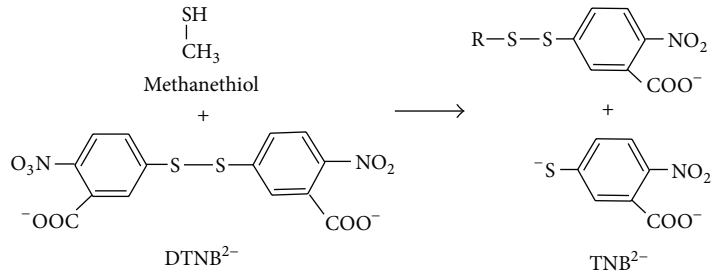

Figure 3: Methionase qualitative detection by DTNB. Methionase catalysis conversion of L-methionine as a substrate in agar plates into α-ketobutyrate, ammonia, and methanethiol. DTNB reagent reacts with SH (thiol) functional group and gives intense yellow coloration around methionase producing bacterial isolates.

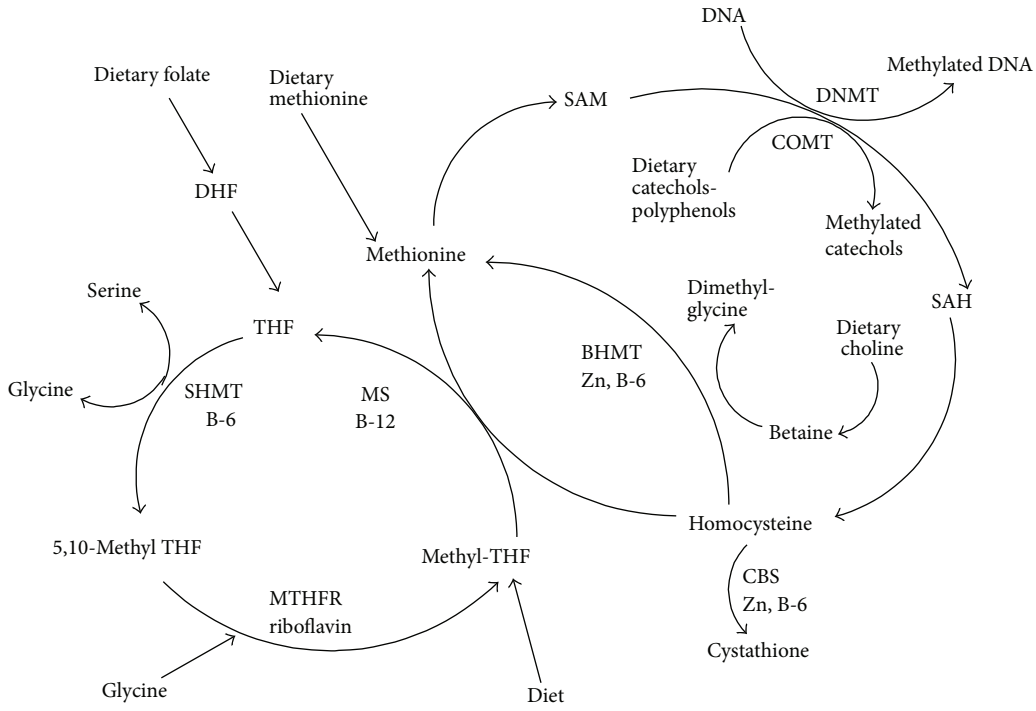

Figure 4: The pathways involved in cellular metabolism and production of S-adenosylmethionine (SAM) for DNA methylation [61]. Dietary factors regulate DNA and histone methylation such as BHMT betaine-homocysteine methyltransferase; CBS cystathionine β-synthase; COMT catechol-O-methyltransferase; DHF dihydrofolate; MS methionine synthase; MTHFR 5, 10-methylenetetrahydrofolate reductase; SAH S-adenosyl homocysteine; SAM S-adenosyl methionine; SHMT serine hydroxymethyltransferase and THF tetrahydrofolate.

medulloblastoma, and testicular germ cells tumours [65]. UHRF1 (also known as ICBP90) and DNA methyltransferases (DNTs) are involved in maintenance of mammalian DNA methylation. UHRF1 (ubiquitin-like, two zinc-finger domains PHD, RING), also known as NP95 in mouse and ICBP90 in human, is required for maintaining DNA methylation. ICBP90 binds to the methylated retinoblastoma gene (RB1) gene promoter in the G1 phase and allows cells to smoothly enter the S phase [66, 67]. DNMT1 was found to be the sole detectable DNA methyltransferase in all murine tissues and cell types examined till date. Pyrosequencing assays were used to measure the DNA methylation of CDKN2A, RASSF1, CYGB, CDH13, DNMT1, DNMT3A, DNMT3B, and UHRF1 promoters [68]. UHRF1 overexpression in zebrafish hepatocytes causes DNA hypomethylation, Tp53-mediated senescence, and hepatocellular carcinoma [69, 70]. Restriction landmark genomic scanning (RLGS) was also used to assess the methylation in human malignancies. *L*-Methionine downregulates the genes belonging to protein kinase families on MCF-7 breast cancer cells and LNCaP prostate cancer cells and showed antiproliferative effect. *L*-Methionine also activates some of the genes involved in cellular redox regulation [71]. *L*-Methionine is required for the biosynthesis of the polyamines spermine and spermidine, which are mainly involved in cell proliferation [72]. The site-specific hypermethylation of cancer-related genes and miRNAs (microRNAs) hypomethylation occur in many cancers. Hypomethylation of miRNAs result in genome instability and activation of protooncogenes. The hypermethylation causes repression of tumour suppressor miRNAs by hypermethylation of their corresponding promoter loci. The miRNAs regulate gene expression within a cell and in the neighboring cells [73–75].

The normal cells have methionine synthase and can form methionine from homocysteine by methyl tetrahydrofolate and betaine as methyl group donors [76]. Methionine-dependent tumour cell lines present no or low levels of methionine synthase [51]. The dependence of tumours on methionine synthase for various cell lines in comparison to the normal cells has been previously reported [77–79]. *L*-Methionine is required for the synthesis of vitamins, antioxidants, DNA stabilizers, epigenetic DNA modulators, coenzymes [61, 80, 81], proteins, polyamines (proper cell development), antioxidative stress defense (glutathione/trypanothione), iron-sulfur cluster biosynthesis (energy metabolism), and methylation reactions and it also regulates the gene expression [5–8, 78]. The *L*-methionine is the first amino acid incorporated into many functional proteins during translation and also serves as a precursor for cysteine biosynthesis. Methionine dependence has been observed in many human cancer cell lines and cancer xenografts in animal models [82–84]. Methionine dependence is a metabolic defect seen only in cancer cells and such malignant cells do not grow in a medium in which methionine is depleted [30, 85]. Thus, *L*-methionase has received appreciable attention as a therapeutic agent against various types of methionine dependent tumours [86]. Dietary factors and epigenetic regulator play essential roles in antitumour activities [87]. Several approaches such as starvation of the tumour cells for methionine using methionine-free diets display a reliable efficacy against various types of tumour cells [88]. When tumour cells were deprived of methionine in a homocysteine containing medium *in vitro*, they were reversibly arrested in the late S/G_2 phase of the cell cycle and finally undergo apoptosis [89–91]. The methionine/valine depleted, tyrosine lowered, and arginine enriched in the diet were the most rationalized form of diet to achieve inhibition of tumour growth [92, 93]. The methionine-free diet is therapeutically not efficient due to economic and technical considerations [88]. A breast cancer cell line MDAMB468 showed methionine dependence and this dependency was due to SAM limitation [94]. There are a few other methionine dependent cell lines (Table 2) reported in the literature.

Table 2: Cancer cells lines that possess methionine dependency.

Methionine dependent cell line(s)	References
PC-3 cell line human prostate	[29]
Prostate cancer PC3; lung carcinoma SKLU-I; fibrosarcoma HT 1080	[30]
Lung adenocarcinoma A-549 and the acute lymphoblastic leukemia CCRF-HSB-2,	[31]
W 256	[32]
D-54, SWB77 (human glioblastomas) and Daoy (human medulloblastoma)	[33]
Human melanoma cell line MeWoLC1	[34]

Cancer cells showed Warburg effect that refers to an increased utilization of glucose via glycolysis and was common in cancerous cells [95]. Glucose transport in cells is rate-limiting step for glucose metabolism mediated by facilitative glucose transporter (GLUT) proteins. The sugar transporters become activated in cancer cells so they incorporate higher amounts of sugar than normal cells. In tumour cells membrane transporter and channel proteins enhance uptake from outer sources and endogenous synthesis increases amongst many transporters glucose transporters (GLUTs) and sodium dependent sugar transporters (SGLT) play main role [96, 97]. The SGLT transporters comprises the sodium-glucose symporter SGLT2 expression was significantly higher in liver and lymph node [98]. The tumour has increased fatty acid synthesis and increased rate(s) of glutamine metabolism. High degree of GLUT1 expression has been reported in human hepatocellular carcinoma, oral cancer [99] and human pancreatic carcinoma (PC) cell line [100–105], and MKN45 (human gastric cancer). The glucose passes through membrane by facilitated diffusion via GLUT or by active transport through a SGLT [106]. Therefore cellular metabolic enzymes such as glucose transporters, hexokinase, pyruvate kinase, lactate dehydrogenase, pyruvate dehydrogenase kinase, fatty acid synthase, and glutaminase targeting enhance the efficacy of common therapeutic agents [95]. GLUT-1 overexpression increased matrix metalloproteinase-2 (MMP-2) promoter activity and was involved in binding of p53 to the MMP-2 promoter [107]. Solute-linked carrier family A1 member 5 (SLC1A5) mediates glutamine transport was overexpressed an associated with squamous lung cancer

[108]. CPT-1 transporter helps in fatty acids transport in the form of acyl CoA and converted acetyl CoA. Acetyl CoA enters the TCA cycle and produces NADH which fuels the cell by oxidative phosphorylation [104]. AKT (protein kinase B PKB), a serine/threonine specific protein kinase activation, promotes cell growth, survival, and upregulation of ER-UDP hydrolysis enzyme as observed in human cancers. The ectonucleoside triphosphate diphosphohydrolase 5 (ENTPD5), an endoplasmic reticulum (ER) enzyme, elevated lactate production under aerobic conditions [109]. ENTPD5 expression and AKT activation is common in both cultured prostate cancer cell lines and primary human prostate carcinoma. Lowered ATP/AMP ratio increases glycolysis, elevates lactate production, and provides glycolytic intermediates for biomass production. The overexpressed α-subunit of ATP synthase, in breast cancer, was involved in the progression and metastasis of breast cancer [110, 111]. Periplocin downregulated the ATP synthase ecto-α-subunit (ATP5A1) and eukaryotic translation initiation factor 5A-1 (eIF5A) by periplocin mediated growth inhibition of A549 cells [112]. ATP synthase was upregulated in cancer cells [113, 114]. Ion channels like Na^{2+}, Ca^{2+}, $K^{+,}$ and Cl^{-} play significant role in cells. The intracellular chloride channel (CLIC) plays an essential role in cellular function, pH, electrogenic balance and maintaining membrane potential in organelles. The chloride channel (CLIC1-5) except CLIC4 became overexpressed in cancer cells. CLIC4 expression reduced in tumour cells [115, 116] and ion channels used to inhibit cancer cell growth [117]. The flow of potassium ions plays important functions, such as cell proliferation, angiogenesis or cell migration, which have also recently been assessed [118, 119]. ABC transporters require energy in the form of adenosine triphosphate (ATP) to translocate substrates across cell membranes. This protein can transport cationic or electrically neutral substrates as well as a broad spectrum of amphiphilic substrates [120]. The ABCG2 (G-subfamily of human ABC) transporter was downregulated in cancer cells [121]. ABC transporters showed multidrug resistance (MDR) in cancer cells by the overexpression of ABC transporters which increased efflux of drugs from cancer cells, thereby decreasing intracellular drug concentration [122, 123].

7. Utilization of MGL in Cancer Therapy

7.1. Combinational Therapy. Therapeutic exploitation of *P. putida* MGL to deplete plasma methionine has been extensively investigated [65, 66]. The MGL was tested as a potent antiproliferative enzyme towards Lewis lung and human colon carcinoma [124], glioblastoma [33], and neuroblastoma [125]. The cancer cell targeted drugs, that is, small molecules, are not fully effective because cancer stem cells are able to expel the drugs before the cancer cells are destroyed and the cancer cells are then able to renew and produce relapse of the disease. A therapeutic approach to deplete methionine from tumours is to treat the cells with recombinant MGL from *P. putida* [PpMGL]. The growth of human tumours *in vivo* and *in vitro* (xenographed in nude mice) is reported to be inhibited upon treatment with recombinant PpMGL when compared to normal cells [126]. Reduction in cell growth is also achieved by integrating PpMGLgene into human lung cancer cells by using a retroviral-based vector. The treatment with exogenous recombinant PpMGL, in order to deplete intracellular and extracellular methionine (Figure 5) levels, has been attempted [38, 127]. MGL alone or in combination with chemotherapeutic agents such as cisplatin, 5-fluorouracil (5-FU), 1-3-bis(2-chloroethyl)-1-nitrosourea (BCNU), and vincristine has shown efficacy and synergy, respectively, in mouse models of colon cancer, lung cancer, and brain cancer [41, 125, 128]. It was also reported that MGL introduced by adenovirus vector inhibited the growth of tumours *in vitro*. MGL, when combined with selenomethionine [SeMET], a suicide prodrug substrate of MGL, inhibited tumour growth in rodents and prolonged their survivals [127].

The effect of prodrug [Selenomethionine] and the toxic product [Methylselenol] synthesized in the tumour cells is presented below:

$$\text{Selenomethionine} + H_2O \xrightarrow{L\text{-Methionase}} \alpha\text{-Ketobutyrate} + \text{Ammonia} + \text{Methylselenol} \quad (1)$$

The MGL gene product, α-methionine-γ-lyase converts nontoxic SeMET to methylselenol that catalyzes oxidation of thiols to generate toxic superoxide. Apoptosis occurs mainly via a mitochondrial pathway [89]. Methylselenol readily diffused to the surrounding nontransduced tumour cells, destroying the mitochondrial membrane by the oxidative stress [39]. Treatment of the transduced cells with exogenous selenomethionine is found to inhibit tumour cell growth [129]. The methylselenol is required in very low concentration to induce cell cycle arrest and apoptosis [130]. Methylselenol promotes the expression of matrix metalloproteinase (MMP) and tissue inhibitor of metalloproteinase (TIMP) that inhibits the migration of tumour cells [131]. Methylselenol induced apoptosis reported in many cancer cells such as murine melanoma B16F10 [132], fibrosarcoma cells HT1080 [130, 131, 133], colon cancer derived HCT-116 [134], andhuman prostate cancer cells LNCaP [135]. Methylselenol inhibits cell proliferation in the cancerous HCT116 cells as compared to normal cells NCM460 [134]. Methylselenol rapidly decreased cellular prostate-specific antigen (PSA) level in LNCaP cells [135]. ROS promote cell proliferation in low concentration, whereas increase of ROS can induce cell death. Therefore balance between generation and elimination of ROS maintains the proper function. Methylselenol catalyzes the oxidation of thiols, generating toxic ROS causing mitochondrial swelling, releasing cytochrome C, activating the caspase cascade, and inducing the cell apoptosis and death [136]. Selenomethionine is relatively nontoxic to the mammalian cells due to their lack of *L*-methionase. The maximum antiprostate cancers activity was observed by selenomethionine methionase treatment [137]. The sensitivity of tumour cells to selenomethionine was increased by 1,000-fold via transduction by adenovirus mediated methionase gene [138]. The combination

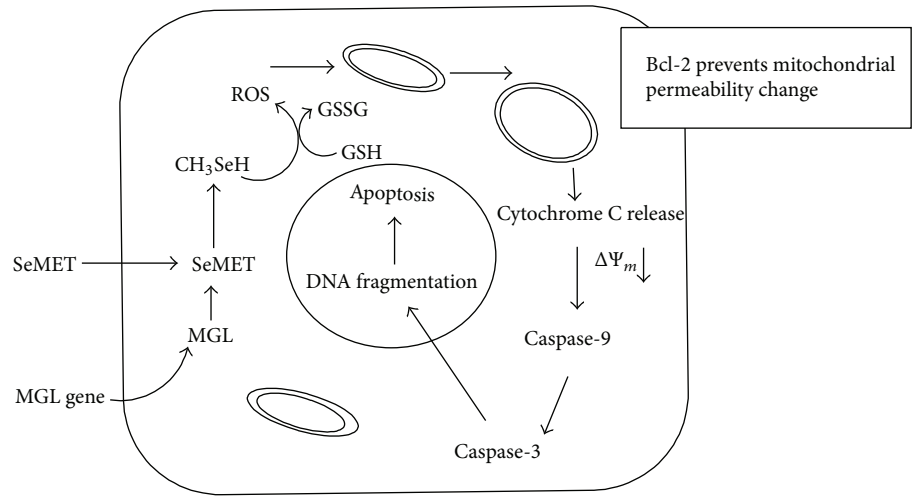

Figure 5: A proposed mechanism of MGL/SeMET-induced apoptosis by combinational therapy method. MGL gene (PpMGL) along with selenomethionine as prodrug was inserted inside the tumour cells. MGL gene product *L*-methionase catalyses the breakdown of methionine from prodrug and synthesizes a toxic molecule "methylselenol" that produces reactive oxygen species (ROS). The ROS thereby causes mitochondrial apoptosis by caspase activation.

of methionase gene, methionase, and selenomethionine are effective against all methionine dependent tumours [39, 127].

7.2. Use of Fusion Proteins in Cancer Cell Targeting. The oxidative stress in tumour cells caused exposure of phosphatidylserine on the surface of the vascular endothelium of blood vessels in tumours but not on normal cells [139]. The fusion protein (FP) consisting of *L*-methionase linked to human annexin-V injected into the bloodstream will bind to the marker on vascular endothelial cells of the tumour only. The FP catalyzed the conversion of nontoxic prodrug selenomethionine into toxic methylselenol and also prevented the methionine supplementation to the tumour cells, thereby killing the tumour and/or inhibiting its growth due to methionine restriction [140–142]. The great advantage of FP is that it does not require to be delivered directly to the tumour cells but only to the bloodstream. ATF-methionase FP (amino-terminal fragment of urokinase) was used to inhibit cancer cell proliferation and migration, which supports targeting *L*-methionase to the surface of the cancer cells. The FP has potential as a selective therapeutic agent for the treatment of various methionine-dependent cancers [143].

8. Modifications of *L*-Methionase to Reduce Its Side Effects

Tumour growth inhibitory effect of rMGL and PEG-MGL on human cancer cells such as human lung, colon, kidney, brain, prostate, and melanoma cancer cells and lung cancer orthotopic model [38, 144]. It was reported that administration of MGL resulted in a steady-state depletion of plasma methionine to less than 2 μM concentration. The only manifested toxicity was a decreased food intake and a slight weight loss. Serum albumin and red cell values declined transiently during treatment, which might be related to extensive blood sampling, although vomiting was frequently observed in macaque monkeys [145]. To overcome this problem, polyethylene glycol-conjugated MGL (PEG-MGL) was prepared. Simultaneous coadministration of pyridoxal 5′-phosphate and oleic acid or dithiothreitol treatment also strengthened effectiveness of PEG-MGL. To improve the MGL therapeutic potential, MGL was coupled to methoxy polyethylene glycol succinimidyl glutarate-5000 (MEGC-PEG-5000). The half-life due to pegylation increased 6 to 19 times while plasma methionine depletion efficacy decreased 8 to 48 times. Protective effect of high-level of pegylation helps to remove PLP dependence. PEG-rMGL demonstrated a significant decrease in antigenicity [146]. The specific activity of PEG-MGL increased with DTT [147]. Although *L*-methionase from bacterial (prokaryotic) origin has immunogenic issues that can be overcome by PEGylation and by other methods such as deimmunization by combinational T-cell epitope removal using neutral drift [148].

9. MGL Cloning

MGL was used for methionine depletion *in vivo* [149]. Bacterial enzymes from various sources have been purified and tested as methionine depleting agents against cancer cell lines. The *P. putida* (pMGL) source was selected for therapeutic applications due to its high catalytic activity, low K_m, and a relatively high k_{cat} value [17]. The reaction mechanism characterized by using site-directed mutagenesis [150, 151]. The gene(s) for MGL was/were cloned into suitable host cells (Table 3).

Table 3: Molecular cloning and functional characterization of MGL gene in various expression systems.

Gene from	Host strain for expression	Selectable marker	References
P. putida	*E. coli* MV1184	Ampicillin	[35]
P. putida	*E. coli* BL21 (DE3)	Ampicillin	[36]
P. putida ICR3460	*E. coli* JM109	Tetracycline	[37]
P. putida	Lung cancer cell line H460	GFP fluorescence, Penicillin, Streptomycin	[38]
P. putida	Human lung adenocarcinoma epithelial cell line (A549 cells)	G418 (Geneticin)	[39]
P. putida ICR3460	*E. coli* JM109	Tetracycline	[40]
P. putida ICR3460	*E. coli* JM109	Tetracycline	[41]
Trichomonas vaginalis	*E. coli* M15pREP4	Ampicillin and Kanamycin	[42]
Trichomonas vaginalis	*E. coli* M15[pREP4]	Ampicillin and Kanamycin	[43]
Treponema denticola ATCC35405	*E. coli* BL21	Ampicillin	[19]
Entamoeba histolytica	*E. coli* BL21	Ampicillin	[22]
Kluyveromyces lactis CLIB 640	*E. coli* DH10B	Ampicillin	[44]
Arabidopsis	*E. coli* BL21	Carbenicillin	[24]
Brevibacterium linens	*E. coli* DH5α	Ampicillin	[45]

10. Future Prospective

The unique catalytic reaction of MGL and its limited distribution in pathogens but not in human make this enzyme a promising target to design novel chemotherapeutic agents. Tumour cells show enhanced methionine dependence/requirement in comparison to the normal cells. The greater requirement of methionine by rapidly growing tumour cells supports high protein synthesis and regulation of DNA expression yet it can be exploited by the use of methionase-based therapy to rapidly deplete the cancerous cells. Thus the forced restriction of methionine may be an important strategy in cancer growth control particularly in malignant/cancers that exhibit dependence on methionine for their survival and proliferation. Currently fusion proteins (consisting of *L*-methionase linked to human annexin-V) may have an advantage in comparison to other approaches as they show application in specifically targeting tumour cells without affecting the normal cells.

Conflict of Interests

The authors declare that there is no conflict of interests regarding the publication of this paper.

Acknowledgments

The authors gratefully acknowledge the financial support provided by Department of Science & Technology, Ministry of Science & Technology, Government of India, New Delhi, for the award of an Inspire Fellowship [IF130378] to one of the authors [BS] as well as Department of Biotechnology for providing liberal funds as well as extending Bioinformatics Facility to the authors.

References

[1] J. P. Richard and T. L. Amyes, "On the importance of being zwitterionic: enzymatic catalysis of decarboxylation and deprotonation of cationic carbon," *Bioorganic Chemistry*, vol. 32, no. 5, pp. 354–366, 2004.

[2] R. Wolfenden, "Benchmark reaction rates, the stability of biological molecules in water, and the evolution of catalytic power in enzymes," *Annual Review of Biochemistry*, vol. 80, pp. 645–667, 2011.

[3] B. C. Lockwood and G. H. Coombs, "Purification and characterization of methionine γ-lyase from *Trichomonas vaginalis*," *Biochemical Journal*, vol. 279, no. 3, pp. 675–682, 1991.

[4] T. Nakayama, N. Esaki, K. Sugie, T. T. Beresov, H. Tanaka, and K. Soda, "Purification of bacterial *L*-methionine γ-lyase," *Analytical Biochemistry*, vol. 138, no. 2, pp. 421–424, 1984.

[5] M. H. Stipanuk, "Metabolism of sulfur-containing amino acids.," *Annual review of nutrition*, vol. 6, pp. 179–209, 1986.

[6] D. Thomas and Y. Surdin-Kerjan, "Metabolism of sulfur amino acids in *Saccharomyces cerevisiae*," *Microbiology and Molecular Biology Reviews*, vol. 61, no. 4, pp. 503–532, 1997.

[7] S. Ravanel, B. Gakière, D. Job, and R. Douce, "The specific features of methionine biosynthesis and metabolism in plants," *Proceedings of the National Academy of Sciences of the United States of America*, vol. 95, no. 13, pp. 7805–7812, 1998.

[8] A. Sekowska, H. Kung, and A. Danchin, "Sulfur metabolism in *Escherichia coli* and related bacteria: facts and fiction," *Journal of Molecular Microbiology and Biotechnology*, vol. 2, no. 2, pp. 145–177, 2000.

[9] R. Caspi, T. Altman, K. Dreher et al., "The MetaCyc database of metabolic pathways and enzymes and the BioCyc collection of pathway/genome databases," *Nucleic Acids Research*, vol. 40, no. 1, pp. D742–D753, 2012.

[10] E. Stone, O. Paley, J. Hu, B. Ekerdt, N. Cheung, and G. Georgiou, "De novo engineering of a human cystathionine-γ-lyase for systemic *L*-methionine depletion cancer therapy," *ACS Chemical Biology*, vol. 7, no. 11, pp. 1822–1829, 2012.

[11] B. Dias and B. Weimer, "Purification and characterization of *L*-methionine γ-lyase from *Brevibacterium linens* BL2," *Applied and Environmental Microbiology*, vol. 64, no. 9, pp. 3327–3331, 1998.

[12] W. Kreis and C. Hession, "Isolation and purification of *L*-methionine-α-deamino-γ-mercapto methane-lyase (*L*-methionase) from *Clostridium sporogenes*," *Cancer Research*, vol. 33, pp. 1862–1865, 1973.

[13] N. G. Faleev, M. V. Troitskaya, E. A. Paskonova, M. B. Saporovskaya, and V. M. Belikov, "*L*-Methionine-γ-lyase in *Citrobacter intermedius* cells: stereochemical requirements with respect to the thiol structure," *Enzyme and Microbial Technology*, vol. 19, no. 8, pp. 590–593, 1996.

[14] I. V. Manukhov, D. V. Mamaeva, E. A. Morozova et al., "*L*-methionine γ-lyase from *Citrobacter freundii*: cloning of the gene and kinetic parameters of the enzyme," *Biochemistry*, vol. 71, no. 4, pp. 361–369, 2006.

[15] M. Yoshimura, Y. Nakano, Y. Yamashita, T. Oho, T. Saito, and T. Koga, "Formation of methyl mercaptan from *L*-methionine by *Porphyromonas gingivalis*," *Infection and Immunity*, vol. 68, no. 12, pp. 6912–6916, 2000.

[16] H. Tanaka, N. Esaki, T. Yamamoto, and K. Soda, "Purification and properties of methioninase from *Pseudomonas ovalis*," *FEBS Letters*, vol. 66, no. 2, pp. 307–311, 1976.

[17] S. Ito, T. Nakamura, and Y. Eguchi, "Purification and characterization of methioninase from *Pseudomonas putida*," *Journal of Biochemistry*, vol. 79, no. 6, pp. 1263–1272, 1976.

[18] D. Kudou, S. Misaki, M. Yamashita et al., "Structure of the antitumour enzyme *L*-methionine γ-lyase from *Pseudomonas putida* at 1.8 Å resolution," *Journal of Biochemistry*, vol. 141, no. 4, pp. 535–544, 2007.

[19] H. Fukamachi, Y. Nakano, S. Okano, Y. Shibata, Y. Abiko, and Y. Yamashita, "High production of methyl mercaptan by *L*-methionine-α-deamino-γ-mercaptomethane lyase from *Treponema denticola*," *Biochemical and Biophysical Research Communications*, vol. 331, no. 1, pp. 127–131, 2005.

[20] P. Bonnarme, L. Psoni, and H. E. Spinnler, "Diversity of *L*-methionine catabolism pathways in cheese-ripening bacteria," *Applied and Environmental Microbiology*, vol. 66, no. 12, pp. 5514–5517, 2000.

[21] D. Sato, W. Yamagata, K. Kamei, T. Nozaki, and S. Harada, "Expression, purification and crystallization of *L*-methionine γ-lyase 2 from *Entamoeba histolytica*," *Acta Crystallographica F: Structural Biology and Crystallization Communications*, vol. 62, no. 10, pp. 1034–1036, 2006.

[22] D. Sato, T. Karaki, A. Shimizu, K. Kamei, S. Harada, and T. Nozaki, "Crystallization and preliminary X-ray analysis of *L*-methionine γ-lyase 1 from *Entamoeba histolytica*," *Acta Crystallographica F: Structural Biology and Crystallization Communications*, vol. 64, no. 8, pp. 697–699, 2008.

[23] M. Tokoro, T. Asai, S. Kobayashi, T. Takeuchi, and T. Nozaki, "Identification and characterization of two isoenzymes of methionine-γ-lyase from *Entamoeba histolytica*: a key enzyme of sulphur amino acid degradation in an anaerobic parasitic protist that lacks forward and reverse trans-sulfuration pathways," *The Journal of Biological Chemistry*, vol. 278, no. 43, pp. 42717–42727, 2003.

[24] F. Rébeillé, S. Jabrin, R. Bligny et al., "Methionine catabolism in *Arabidopsis* cells is initiated by a γ-cleavage process and leads to S-methylcysteine and isoleucine syntheses," *Proceedings of the National Academy of Sciences of the United States of America*, vol. 103, no. 42, pp. 15687–15692, 2006.

[25] D. J. Baumler, K. Hung, K. C. Jeong, and C. W. Kaspar, "Production of methanethiol and volatile sulfur compounds by the archaeon *Ferroplasma acidarmanus*," *Extremophiles*, vol. 11, no. 6, pp. 841–851, 2007.

[26] J. Ruiz-Herrera and R. L. Starkey, "Dissimilation of methionine by a demethiolase of *Aspergillus species*," *Journal of Bacteriology*, vol. 99, no. 3, pp. 764–770, 1969.

[27] P. Bonnarme, C. Lapadatescu, M. Yvon, and H. Spinnler, "*L*-methionine degradation potentialities of cheese-ripening microorganisms," *Journal of Dairy Research*, vol. 68, no. 4, pp. 663–674, 2001.

[28] S. A. Khalaf and A. S. A. El-Sayed, "*L*-Methioninase production by filamentous fungi: I-screening and optimization under submerged conditions," *Current Microbiology*, vol. 58, no. 3, pp. 219–226, 2009.

[29] F. Poirson-Bichat, G. Gonfalone, R. A. Bras-Gonçalves, B. Dutrillaux, and M. F. Poupon, "Growth of methionine-dependent human prostate cancer (PC-3) is inhibited by ethionine combined with methionine starvation," *British Journal of Cancer*, vol. 75, no. 11, pp. 1605–1612, 1997.

[30] H. Guo, H. Herrera, A. Groce, and R. M. Hoffman, "Expression of the biochemical defect of methionine dependence in fresh patient tumors in primary histo-culture," *Cancer Research*, vol. 53, no. 11, pp. 2479–2483, 1993.

[31] W. Kreis and M. Goodenow, "Methionine requirement and replacement by homocysteine in tissue cultures of selected rodent and human malignant and normal cells," *Cancer Research*, vol. 38, no. 8, pp. 2259–2262, 1978.

[32] J. C. Kennelly, J. A. Blair, and A. E. Pheasant, "Metabolism of 5-methyltetrahydrofolate by rats bearing the Walker 256 carcinosarcoma," *British Journal of Cancer*, vol. 46, no. 3, pp. 440–443, 1982.

[33] D. M. Kokkinakis, R. M. Hoffman, E. P. Frenkel et al., "Synergy between methionine stress and chemotherapy in the treatment of brain tumor xenografts in athymic mice," *Cancer Research*, vol. 61, no. 10, pp. 4017–4023, 2001.

[34] D. Watkins, "Cobalamin metabolism in methionine-dependent human tumour and leukemia cell lines," *Clinical and Investigative Medicine*, vol. 21, no. 3, pp. 151–158, 1998.

[35] H. Inoue, K. Inagaki, M. Sugimoto, N. Esaki, K. Soda, and H. Tanaka, "Structural analysis of the *L*-methionine γ-lyase gene from *Pseudomonas putida*," *The Journal of Biochemistry*, vol. 117, no. 5, pp. 1120–1125, 1995.

[36] Y. Tan, M. Xu, X. Tan et al., "Overexpression and large-scale production of recombinant *L*-methionine-α-deamino-γ-mercaptomethane-lyase for novel anticancer therapy," *Protein Expression and Purification*, vol. 9, no. 2, pp. 233–245, 1997.

[37] T. Takakura, T. Ito, S. Yagi et al., "High-level expression and bulk crystallization of recombinant *L*-methionine γ-lyase, an anticancer agent," *Applied Microbiology and Biotechnology*, vol. 70, no. 2, pp. 183–192, 2006.

[38] K. Miki, M. Xu, Z. An et al., "Survival efficacy of the combination of the methioninase gene and methioninase in a lung

cancer orthotopic model," *Cancer Gene Therapy*, vol. 7, no. 2, pp. 332–338, 2000.

[39] N. Yamamoto, A. Gupta, M. Xu et al., "Methioninase gene therapy with selenomethionine induces apoptosis in bcl-2-overproducing lung cancer cells," *Cancer Gene Therapy*, vol. 10, no. 6, pp. 445–450, 2003.

[40] T. Takakura, K. Mitsushima, S. Yagi et al., "Assay method for antitumor *L*-methionine γ- lyase : comprehensive kinetic analysis of the complex reaction with *L* -methionine," *Analytical Biochemistry*, vol. 327, no. 2, pp. 233–240, 2004.

[41] T. Yoshioka, T. Wada, N. Uchida et al., "Anticancer efficacy *in vivo* and *in vitro*, synergy with 5-fluorouracil, and safety of recombinant methioninase," *Cancer Research*, vol. 58, no. 12, pp. 2583–2587, 1998.

[42] A. E. McKie, T. Edlind, J. Walker, J. C. Mottram, and G. H. Coombs, "The primitive protozoon *Trichomonas vaginalis* contains two methionine γ-lyase genes that encode members of the γ-family of pyridoxal 5′-phosphate-dependent enzymes," *The Journal of Biological Chemistry*, vol. 273, no. 10, pp. 5549–5556, 1998.

[43] G. H. Coombs and J. C. Mottram, "Trifluoromethionine, a prodrug designed against methionine γ-lyase-containing pathogens, has efficacy *in vitro* and *in vivo* against *Trichomonas vaginalis*," *Antimicrobial Agents and Chemotherapy*, vol. 45, no. 6, pp. 1743–1745, 2001.

[44] D. Kagkli, P. Bonnarme, C. Neuvéglise, T. M. Cogan, and S. Casaregola, "*L*-methionine degradation pathway in *Kluyveromyces lactis*: identification and functional analysis of the genes encoding *L*-methionine aminotransferase," *Applied and Environmental Microbiology*, vol. 72, no. 5, pp. 3330–3335, 2006.

[45] K. Pavani and S. V. Saradhi, "Cloning and expression of methionine-γ-lyase (MGL) of *Brevibacterium linens*," *International Journal of Current Microbiology and Applied Sciences*, vol. 3, pp. 615–631, 2014.

[46] H. Hori, K. Takabayashi, L. Orvis, D. A. Carson, and T. Nobori, "Gene cloning and characterization of *Pseudomonas putida* L-Methionine-α- deamino-γ-mercaptomethane-lyase," *Cancer Research*, vol. 56, no. 9, pp. 2116–2122, 1996.

[47] D. V. Mamaeva, E. A. Morozova, A. D. Nikulin et al., "Structure of *Citrobacter freundii* L-methionine γ-lyase," *Acta Crystallographica F: Structural Biology and Crystallization Communications*, vol. 61, no. 6, pp. 546–549, 2005.

[48] G. L. Ellman, "Tissue sulfhydryl groups," *Archives of Biochemistry and Biophysics*, vol. 82, no. 1, pp. 70–77, 1959.

[49] A. F. S. A. Habeeb, "Reaction of protein sulphydryl groups with ellmans reagent in enzyme structure," *Methods in Enzymology*, vol. 25, pp. 457–464, 1972.

[50] M. C. Alley, D. A. Scudiero, A. Monks et al., "Feasibility of drug screening with panels of human tumor cell lines using a microculture tetrazolium assay," *Cancer Research*, vol. 48, no. 3, pp. 589–601, 1988.

[51] R. M. Hoffman, "Altered methionine metabolism and transmethylation in cancer," *Anticancer Research*, vol. 5, no. 1, pp. 1–30, 1985.

[52] B. C. Halpern, B. R. Clark, D. N. Hardy, R. M. Halpern, and R. A. Smith, "The effect of replacement of methionine by homocystine on survival of malignant and normal adult mammalian cells in culture," *Proceedings of the National Academy of Sciences of the United States of America*, vol. 71, no. 4, pp. 1133–1136, 1974.

[53] W. Kreis, "Tumor therapy by deprivation of *L*-methionine: rationale and results," *Cancer Treatment Reports*, vol. 63, no. 6, pp. 1069–1072, 1979.

[54] W. Kreis, A. Baker, V. Ryan, and A. Bertasso, "Effect of nutritional and enzymatic methionine deprivation upon human normal and malignant cells in tissue culture," *Cancer Research*, vol. 40, no. 3, pp. 634–641, 1980.

[55] P. H. Stern, C. D. Wallace, and R. M. Hoffman, "Altered methionine metabolism occurs in all members of a set of diverse human tumor cell lines," *Journal of Cellular Physiology*, vol. 119, no. 1, pp. 29–34, 1984.

[56] F. Breillout, E. Antoine, and M. F. Poupon, "Methionine dependency of malignant tumors: a possible approach for therapy," *Journal of the National Cancer Institute*, vol. 82, no. 20, pp. 1628–1632, 1990.

[57] E. M. Swisher, R. M. Gonzalez, T. Taniguchi et al., "Methylation and protein expression of DNA repair genes: association with chemotherapy exposure and survival in sporadic ovarian and peritoneal carcinomas," *Molecular Cancer*, vol. 8, article 48, 2009.

[58] T. M. Geiman and K. Muegge, "DNA methylation in early development," *Molecular Reproduction and Development*, vol. 77, no. 2, pp. 105–113, 2010.

[59] K. Ramani, H. Yang, J. Kuhlenkamp et al., "Changes in the expression of methionine adenosyltransferase genes and S-adenosylmethionine homeostasis during hepatic stellate cell activation," *Hepatology*, vol. 51, no. 3, pp. 986–995, 2010.

[60] G. L. Sen, J. A. Reuter, D. E. Webster, L. Zhu, and P. A. Khavari, "DNMT1 maintains progenitor function in self-renewing somatic tissue," *Nature*, vol. 463, no. 7280, pp. 563–567, 2010.

[61] E. Ho, L. M. Beaver, D. E. Williams, and R. H. Dashwood, "Dietary factors and epigenetic regulation for prostate cancer prevention," *Advances in Nutrition*, vol. 2, no. 6, pp. 497–510, 2011.

[62] A. C. Vidal, D. J. Grant, C. D. Williams et al., "Associations between intake of folate, methionine, and vitamins B-12, B-6 and prostate cancer risk in American veterans," *Journal of Cancer Epidemiology*, vol. 2012, Article ID 957467, 9 pages, 2012.

[63] P. M. Das and R. Singal, "DNA methylation and cancer," *Journal of Clinical Oncology*, vol. 22, no. 22, pp. 4632–4642, 2004.

[64] L. Parry and A. R. Clarke, "The roles of the methyl-CpG binding proteins in cancer," *Genes and Cancer*, vol. 2, no. 6, pp. 618–630, 2011.

[65] D. J. Smiraglia, L. J. Rush, M. C. Frühwald et al., "Excessive CpG island hypermethylation in cancer cell lines versus primary human malignancies," *Human Molecular Genetics*, vol. 10, no. 13, pp. 1413–1419, 2001.

[66] M. Jeanblanc, M. Mousli, R. Hopfner et al., "The retinoblastoma gene and its product are targeted by ICBP90: a key mechanism in the G1/S transition during the cell cycle," *Oncogene*, vol. 24, no. 49, pp. 7337–7345, 2005.

[67] M. Bostick, K. K. Jong, P. Estève, A. Clark, S. Pradhan, and S. E. Jacobsen, "UHRF1 plays a role in maintaining DNA methylation in mammalian cells," *Science*, vol. 317, no. 5845, pp. 1760–1764, 2007.

[68] A. Daskalos, U. Oleksiewicz, A. Filia et al., "UHRF1-mediated tumor suppressor gene inactivation in nonsmall cell lung cancer," *Cancer*, vol. 117, no. 5, pp. 1027–1037, 2011.

[69] D. F. Calvisi, M. M. Simile, S. Ladu et al., "Altered methionine metabolism and global DNA methylation in liver cancer: relationship with genomic instability and prognosis," *International Journal of Cancer*, vol. 121, no. 11, pp. 2410–2420, 2007.

[70] R. Mudbhary, Y. Hoshida, Y. Chemyavskaya et al., "UHRF1 overexpression drives DNA hypomethylation and hepatocellular carcinoma," *Cancer Cell*, vol. 25, pp. 196–209, 2014.

[71] M. A. Benavides, D. Hu, M. K. Baraoidan et al., "*L*-methionine-induced alterations in molecular signatures in MCF-7 and LNCaP cancer cells," *Journal of Cancer Research and Clinical Oncology*, vol. 137, no. 3, pp. 441–453, 2011.

[72] T. Thomas and T. J. Thomas, "Polyamines in cell growth and cell death: molecular mechanisms and therapeutic applications," *Cellular and Molecular Life Sciences*, vol. 58, no. 2, pp. 244–258, 2001.

[73] A. Lujambio, S. Ropero, E. Ballestar et al., "Genetic unmasking of an epigenetically silenced microRNA in human cancer cells," *Cancer Research*, vol. 67, no. 4, pp. 1424–1429, 2007.

[74] G. Mathonnet, M. R. Fabian, Y. V. Svitkin et al., "MicroRNA inhibition of translation initiation *in vitro* by targeting the cap-binding complex eIF4F," *Science*, vol. 317, no. 5845, pp. 1764–1767, 2007.

[75] P. Lopez-Serra and M. Esteller, "DNA methylation-associated silencing of tumor-suppressor microRNAs in cancer," *Oncogene*, vol. 31, no. 13, pp. 1609–1622, 2012.

[76] S. H. Kenyon, C. J. Waterfield, J. A. Timbrell, and A. Nicolaou, "Methionine synthase activity and sulphur amino acid levels in the rat liver tumour cells HTC and Phi-1," *Biochemical Pharmacology*, vol. 63, no. 3, pp. 381–391, 2002.

[77] R. G. Liteplo, S. E. Hipwell, D. S. Rosenblatt, S. Sillaots, and H. Lue-Shing, "Changes in cobalamin metabolism are associated with the altered methionine auxotrophy of highly growth autonomous human melanoma cells," *Journal of Cellular Physiology*, vol. 149, no. 2, pp. 332–338, 1991.

[78] C. D. Davis and E. O. Uthus, "DNA methylation, cancer susceptibility, and nutrient interactions," *Experimental Biology and Medicine*, vol. 229, no. 10, pp. 988–995, 2004.

[79] A. S. A. El-Sayed, "Microbial *L*-methioninase, molecular characterization and therapeutic applications," *Applied Microbiology and Biotechnology*, vol. 86, pp. 445–467, 2010.

[80] E. Cellarier, X. Durando, M. P. Vasson et al., "Methionine dependency and cancer treatment," *Cancer Treatment Reviews*, vol. 29, no. 6, pp. 489–499, 2003.

[81] E. Thivat, X. Durando, A. Demidem et al., "A methionine-free diet associated with nitrosourea treatment down-regulates methylguanine-DNA methyl transferase activity in patients with metastatic cancer," *Anticancer Research*, vol. 27, no. 4, pp. 2779–2783, 2007.

[82] T. Fiskerstrand, B. Christensen, O. B. Tysnes, P. M. Ueland, and H. Refsum, "Development and reversion of methionine dependence in a human glioma cell line: relation to homocysteine remethylation and cobalamin status," *Cancer Research*, vol. 54, no. 18, pp. 4899–4906, 1994.

[83] R. M. Hoffman and R. W. Erbe, "High in vivo rates of methionine biosynthesis in transformed human and malignant rat cells auxotrophic for methionine," *Proceedings of the National Academy of Sciences of the United States of America*, vol. 73, no. 5, pp. 1523–1527, 1976.

[84] J. O. Mecham, D. Rowitch, C. D. Wallace, P. H. Stern, and R. M. Hoffman, "The metabolic defect of methionine dependence occurs frequently in human tumor cell lines," *Biochemical and Biophysical Research Communications*, vol. 117, no. 2, pp. 429–434, 1983.

[85] R. M. Hoffman, "Altered methionine metabolism, DNA methylation and oncogene expression in carcinogenesis: a review and synthesis," *Biochimica et Biophysica Acta*, vol. 738, no. 1-2, pp. 49–87, 1983.

[86] D. M. Kokkinakis, S. C. Schold Jr., H. Hori, and T. Nobori, "Effect of long-term depletion of plasma methionine on the growth and survival of human brain tumor xenografts in athymic mice," *Nutrition and Cancer*, vol. 29, no. 3, pp. 195–204, 1997.

[87] C. Gerhäuser, "Cancer cell metabolism, epigenetics and the potential influence of dietary components—a perspective," *Biomedical Research*, vol. 23, pp. 1–21, 2012.

[88] N. Goseki, S. Yamazaki, M. Endo et al., "Antitumor effect of methionine-depleting total parenteral nutrition with doxorubicin administration on Yoshida sarcoma-bearing rats," *Cancer*, vol. 69, no. 7, pp. 1865–1872, 1992.

[89] H. Guo, V. K. Lishko, H. Herrera, A. Groce, T. Kubota, and R. M. Hoffman, "Therapeutic tumor-specific cell cycle block induced by methionine starvation *in vivo*," *Cancer Research*, vol. 53, no. 23, pp. 5676–5679, 1993.

[90] R. M. Hoffman and S. J. Jacobsen, "Reversible growth arrest in simian virus 40-transformed human fibroblasts," *Proceedings of the National Academy of Sciences of the United States of America*, vol. 77, no. 12, pp. 7306–7310, 1980.

[91] T. Nagahama, N. Goseki, and M. Endo, "Doxorubicin and vincristine with methionine depletion contributed to survival in the Yoshida sarcoma bearing rats," *Anticancer Research*, vol. 18, no. 1, pp. 25–31, 1998.

[92] Y. C. He, Y. H. Wang, J. Cao, J. W. Chen, D. Y. Pan, and Y. K. Zhou, "Effect of complex amino acid imbalance on growth of tumor in tumor-bearing rats," *World Journal of Gastroenterology*, vol. 9, no. 12, pp. 2772–2775, 2003.

[93] Y. He, J. Cao, J. Chen, D. Pan, and Y. Zhou, "Influence of methionine/valine-depleted enteral nutrition on nucleic acid and protein metabolism in tumor-bearing rats," *World Journal of Gastroenterology*, vol. 9, no. 4, pp. 771–774, 2003.

[94] K. Booher, D. Lin, S. L. Borrego, and P. Kaiser, "Downregulation of Cdc6 and pre-replication complexes in response to methionine stress in breast cancer cells," *Cell Cycle*, vol. 11, no. 23, pp. 4414–4423, 2012.

[95] Y. Zhao, E. B. Butler, and M. Tan, "Targeting cellular metabolism to improve cancer therapeutics," *Cell Death and Disease*, vol. 4, no. 3, article e532, 2013.

[96] L. A. Aparicio, M. B. Calvo, A. Figueroa, E. G. Pulido, and R. G. Campelo, "Potential role of sugar transporters in cancer and their relationship with anticancer therapy," *International Journal of Endocrinology*, vol. 2010, Article ID 205357, 14 pages, 2010.

[97] R. Diaz-Ruiz, M. Rigoulet, and A. Devin, "The Warburg and Crabtree effects: On the origin of cancer cell energy metabolism and of yeast glucose repression," *Biochimica et Biophysica Acta*, vol. 1807, no. 6, pp. 568–576, 2011.

[98] N. Ishikawa, T. Oguri, T. Isobe, K. Fujitaka, and N. Kohno, "SGLT gene expression in primary lung cancers and their metastatic lesions," *Japanese Journal of Cancer Research*, vol. 92, no. 8, pp. 874–879, 2001.

[99] R. J. Oliver, R. T. M. Woodwards, P. Sloan, N. S. Thakker, I. J. Stratford, and R. E. Airley, "Prognostic value of facilitative glucose transporter Glut-1 in oral squamous cell carcinomas treated by surgical resection: results of EORTC Translational

Research Fund studies," *European Journal of Cancer*, vol. 40, no. 4, pp. 503–507, 2004.

[100] M. Younes, L. V. Lechago, J. R. Somoano, M. Mosharaf, and J. Lechago, "Wide expression of the human erythrocyte glucose transporter Glut1 in human cancers," *Cancer Research*, vol. 56, no. 5, pp. 1164–1167, 1996.

[101] S. N. Reske, K. G. Grillenberger, G. Glatting et al., "Overexpression of glucose transporter 1 and increased FDG uptake in pancreatic carcinoma," *Journal of Nuclear Medicine*, vol. 38, no. 9, pp. 1344–4348, 1997.

[102] T. Ito, Y. Noguchi, S. Satoh, H. Hayashi, Y. Inayama, and H. Kitamura, "Expression of facilitative glucose transporter isoforms in lung carcinomas: its relation to histologic type, differentiation grade and tumor stage," *Modern Pathology*, vol. 11, pp. 437–443, 1998.

[103] Y. Noguchia, A. Saitoa, Y. Miyagib et al., "Suppression of facilitative glucose transporter-1 mRNA can suppress tumor growth," *Cancer Letters*, vol. 154, pp. 175–182, 2000.

[104] M. L. Macheda, S. Rogers, and J. D. Best, "Molecular and cellular regulation of glucose transporter (GLUT) proteins in cancer," *Journal of Cellular Physiology*, vol. 202, no. 3, pp. 654–662, 2005.

[105] S. Pizzi, A. Porzionato, C. Pasquali et al., "Glucose transporter-1 expression and prognostic significance in pancreatic carcinogenesis," *Histology and Histopathology*, vol. 24, no. 2, pp. 175–185, 2009.

[106] A. N. McCracken and A. L. Edinger, "Nutrient transporters: the Achilles' heel of anabolism," *Trends in Endocrinology and Metabolism*, vol. 24, no. 4, pp. 200–208, 2013.

[107] S. Ito, T. Fukusato, T. Nemoto, H. Sekihara, Y. Seyama, and S. Kubota, "Coexpression of glucose transporter 1 and matrix metalloproteinase-2 in human cancers," *Journal of the National Cancer Institute*, vol. 94, no. 14, pp. 1080–1091, 2002.

[108] M. Hassanein, M. D. Hoeksema, M. Shiota et al., "SLC1A5 mediates glutamine transport required for lung cancer cell growth and survival," *Clinical Cancer Research*, vol. 19, no. 3, pp. 560–570, 2013.

[109] M. Fang, Z. Shen, S. Huang et al., "The ER UDPase ENTPD5 promotes protein N-glycosylation, the Warburg effect, and proliferation in the PTEN pathway," *Cell*, vol. 143, no. 5, pp. 711–724, 2010.

[110] T. C. Huang, H. Y. Chang, C. H. Hsu, W. H. Kuo, K. J. Chang, and H. F. Juan, "Targeting therapy for breast carcinoma by ATP synthase inhibitor aurovertin B," *Journal of Proteome Research*, vol. 7, no. 4, pp. 1433–1444, 2008.

[111] J. Pan, L. Sun, Y. Tao et al., "ATP synthase ecto-α-subunit: a novel therapeutic target for breast cancer," *Journal of Translational Medicine*, vol. 9, no. 1, article 211, 2011.

[112] Z. Lu, Q. Song, J. Yang et al., "Comparative proteomic analysis of anti-cancer mechanism by periplocin treatment in lung cancer cells," *Cellular Physiology and Biochemistry*, vol. 33, pp. 859–868, 2014.

[113] W. J. Israelsen and M. G. V. Heiden, "ATP consumption promotes cancer metabolism," *Cell*, vol. 143, no. 5, pp. 669–671, 2010.

[114] Z. Ma, M. Cao, Y. Liu et al., "Mitochondrial F1Fo-ATP synthase translocates to cell surface in hepatocytes and has high activity in tumor-like acidic and hypoxic environment," *Acta Biochimica et Biophysica Sinica*, vol. 42, no. 8, pp. 530–537, 2010.

[115] K. S. Suh, M. Mutoh, M. Gerdes, and S. H. Yuspa, "CLIC4, an intracellular chloride channel protein, is a novel molecular target for cancer therapy," *Journal of Investigative Dermatology Symposium Proceedings*, vol. 10, pp. 105–109, 2005.

[116] K. S. Suh, J. M. Crutchley, A. Koochek et al., "Reciprocal modifications of CLIC4 in tumor epithelium and stroma mark malignant progression of multiple human cancers," *Clinical Cancer Research*, vol. 13, no. 1, pp. 121–131, 2007.

[117] A. Arcangeli, O. Crociani, E. Lastraioli, A. Masi, S. Pillozzi, and A. Becchetti, "Targeting ion channels in cancer: a novel frontier in antineoplastic therapy," *Current Medicinal Chemistry*, vol. 16, no. 1, pp. 66–93, 2009.

[118] L. A. Pardo and W. Stuhmer, "The roles of K^+ channels in cancer," *Nature Reviews Cancer*, vol. 14, pp. 39–48, 2014.

[119] D. Urrego, A. P. Tomczak, F. Zahed, W. Stuhmer, and L. A. Pardo, "Potassium channels in cell cycle and cell proliferation," *Philosophical Transactions of the Royal Society*, vol. 369, pp. 1–9, 2014.

[120] A. Pohl, P. F. Devaux, and A. Herrmann, "Function of prokaryotic and eukaryotic ABC proteins in lipid transport," *Biochimica et Biophysica Acta*, vol. 1733, no. 1, pp. 29–52, 2005.

[121] T. Ishikawa, H. Nakagawa, Y. Hagiya, N. Nonoguchi, S. Miyatake, and T. Kuroiwa, "Key role of human ABC transporter ABCG2 in photodynamic therapy and photodynamic diagnosis," *Advances in Pharmacological Sciences*, vol. 2010, Article ID 587306, 13 pages, 2010.

[122] I. Hlavata, B. Mohelnikova-Duchonova, R. Vaclavikova et al., "The role of ABC transporters in progression and clinical outcome of colorectal cancer," *Mutagenesis*, vol. 27, no. 2, pp. 187–196, 2012.

[123] Y. Sun, A. Patel, P. Kumar, and Z. Chen, "Role of ABC transporters in cancer chemotherapy," *Chinese Journal of Cancer*, vol. 31, no. 2, pp. 51–57, 2012.

[124] Y. Tan, X. Sun, M. Xu et al., "Polyethylene glycol conjugation of recombinant methioninase for cancer therapy," *Protein Expression and Purification*, vol. 12, no. 1, pp. 45–52, 1998.

[125] J. Hu and N. V. Cheung, "Methionine depletion with recombinant methioninase: In vitro and in vivo efficacy against neuroblastoma and its synergism with chemotherapeutic drugs," *International Journal of Cancer*, vol. 124, no. 7, pp. 1700–1706, 2009.

[126] Y. Tan, J. Zavala Sr., Q. Han et al., "Recombinant methioninase infusion reduces the biochemical endpoint of serum methionine with minimal toxicity in high-stage cancer patients," *Anticancer Research*, vol. 17, no. 5, pp. 3857–3860, 1997.

[127] K. Miki, M. Xu, A. Gupta et al., "Methioninase cancer gene therapy with selenomethionine as suicide prodrug substrate," *Cancer Research*, vol. 61, no. 18, pp. 6805–6810, 2001.

[128] Y. Tan, X. Sun, M. Xu et al., "Efficacy of recombinant methioninase in combination with cisplatin on human colon tumors in nude mice," *Clinical Cancer Research*, vol. 5, no. 8, pp. 2157–2163, 1999.

[129] R. Zhao, F. E. Domann, and W. Zhong, "Apoptosis induced by selenomethionine and methioninase is superoxide mediated and p53 dependent in human prostate cancer cells," *Molecular Cancer Therapeutics*, vol. 5, no. 12, pp. 3275–3284, 2006.

[130] H. Zeng, M. Wu, and J. H. Botnen, "Methylselenol, a selenium metabolite, induces cell cycle arrest in G1 phase and apoptosis via the extracellular-regulated kinase 1/2 pathway and other cancer signaling genes," *Journal of Nutrition*, vol. 139, no. 9, pp. 1613–1618, 2009.

[131] K. Zu, T. Bihani, A. Lin, Y.-. Park, K. Mori, and C. Ip, "Enhanced selenium effect on growth arrest by BiP/GRP78 knockdown in p53-null human prostate cancer cells," *Oncogene*, vol. 25, no. 4, pp. 546–554, 2006.

[132] A. Kim, J. Oh, J. Park, and A. Chung, "Methylselenol generated from selenomethionine by methioninase downregulates integrin expression and induces caspase-mediated apoptosis of B16F10 melanoma cells," *Journal of Cellular Physiology*, vol. 212, no. 2, pp. 386–400, 2007.

[133] H. Zeng, M. Briske-Anderson, J. P. Idso, and C. D. Hunt, "The selenium metabolite methylselenol inhibits the migration and invasion potential of HT1080 tumor cells," *Journal of Nutrition*, vol. 136, no. 6, pp. 1528–1532, 2006.

[134] H. Zeng, M. Briske-Anderson, M. Wu, and M. P. Moyer, "Methylselenol, a selenium metabolite, plays common and different roles in cancerous colon HCT116 cell and noncancerous NCM460 colon cell proliferation," *Nutrition and Cancer*, vol. 64, no. 1, pp. 128–135, 2012.

[135] S. D. Cho, C. Jiang, B. Malewicz et al., "Methyl selenium metabolites decrease prostate-specific antigen expression by inducing protein degradation and suppressing androgen-stimulated transcription," *Molecular Cancer Therapeutics*, vol. 3, no. 5, pp. 605–611, 2004.

[136] D. R. Green and J. C. Reed, "Mitochondria and apoptosis," *Science*, vol. 281, no. 5381, pp. 1309–1312, 1998.

[137] P. Li, D. Nijhawan, I. Budihardjo et al., "Cytochrome c and dATP-dependent formation of Apaf-1/caspase-9 complex initiates an apoptotic protease cascade," *Cell*, vol. 91, no. 4, pp. 479–489, 1997.

[138] K. Miki, W. Al-Refaie, M. Xu et al., "Methioninase gene therapy of human cancer cells is synergistic with recombinant methioninase treatment," *Cancer Research*, vol. 60, no. 10, pp. 2696–2702, 2000.

[139] J. H. Stafford and P. E. Thorpe, "Increased exposure of phosphatidylethanolamine on the surface of tumor vascular endothelium," *Neoplasia*, vol. 13, no. 4, pp. 299–308, 2011.

[140] R. G. Harrison and Norman, "Enzyme prodrug cancer therapy selectively targeted to tumor cells or tumor vasculature and methods of production and use thereof," US/0002978 A1 (patent), 2011.

[141] B. D. V. Rite, J. J. Krais, M. Cherry, V. I. Sikavitsas, C. Kurkjian, and RG. Harrison, "Antitumor activity of an enzyme prodrug therapy targeted to the breast tumor vasculature," *Cancer Investigation*, vol. 31, pp. 505–510, 2013.

[142] B. D. van Rite, Y. A. Lazrak, M. L. Pagnon et al., "Enzyme prodrug therapy designed to target *L*-methioninase to the tumor vasculature," *Cancer Letters*, vol. 301, no. 2, pp. 177–184, 2011.

[143] N. R. Palwai, X. Zang, R. G. Harrison, D. Benbrook, and J. T. Pento, "Selective growth inhibition of cancer cells by L-methioninase-containing fusion protein targeted to the urokinase receptor," *Pharmacology*, vol. 84, no. 5, pp. 271–275, 2009.

[144] Y. Tan, M. Xu, and R. M. Hoffman, "Broad selective efficacy of recombinant methioninase and polyethylene glycol-modified recombinant methioninase on cancer cells *in vitro*," *Anticancer Research*, vol. 30, no. 4, pp. 1041–1046, 2010.

[145] Z. Yang, J. Wang, T. Yoshioka et al., "Pharmacokinetics, methionine depletion and antigenicity of recombinant methioninase in primates," *Clinical Cancer Research*, vol. 10, no. 6, pp. 2131–2138, 2004.

[146] X. Sun, Z. Yang, S. Li et al., "*In vivo* efficacy of recombinant methioninase is enhanced by the combination of polyethylene glycol conjugation and pyridoxal 5′-phosphate supplementation," *Cancer Research*, vol. 63, no. 23, pp. 8377–8383, 2003.

[147] T. Takakura, A. Takimoto, Y. Notsu et al., "Physicochemical and pharmacokinetic characterization of highly potent recombinant *L*-methionine γ-lyase conjugated with polyethylene glycol as an antitumor agent," *Cancer Research*, vol. 66, no. 5, pp. 2807–2814, 2006.

[148] J. R. Cantor, T. H. Yoo, A. Dixit, B. L. Iverson, T. G. Forsthuber, and G. Georgiou, "Therapeutic enzyme deimmunization by combinatorial T-cell epitope removal using neutral drift," *Proceedings of the National Academy of Sciences of the United States of America*, vol. 108, no. 4, pp. 1272–1277, 2011.

[149] V. K. Lishko, O. V. Lishko, and R. M. Hoffman, "Depletion of serum methionine by methioninase in mice," *Anticancer Research*, vol. 13, no. 5, pp. 1465–1468, 1993.

[150] H. Inoue, K. Inagaki, N. Adachi et al., "Role of tyrosine 114 of L-methionine γ-lyase from *Pseudomonas putida*," *Bioscience, Biotechnology and Biochemistry*, vol. 64, no. 11, pp. 2336–2343, 2000.

[151] D. Kudou, S. Misaki, M. Yamashita, T. Tamura, N. Esaki, and K. Inagaki, "The role of cysteine 116 in the active site of the antitumor enzyme *L*-methionine γ-lyase from *Pseudomonas putida*," *Bioscience, Biotechnology and Biochemistry*, vol. 72, no. 7, pp. 1722–1730, 2008.

Hindawi Publishing Corporation
BioMed Research International
Volume 2014, Article ID 267189, 10 pages
http://dx.doi.org/10.1155/2014/267189

Research Article

High Potential Source for Biomass Degradation Enzyme Discovery and Environmental Aspects Revealed through Metagenomics of Indian Buffalo Rumen

K. M. Singh,[1,2] Bhaskar Reddy,[1] Dishita Patel,[1] A. K. Patel,[1] Nidhi Parmar,[1] Anand Patel,[1] J. B. Patel,[3] and C. G. Joshi[1]

[1] *Department of Animal Biotechnology, College of Veterinary Science and Animal Husbandry, Anand Agricultural University, Anand, Gujarat 388001, India*
[2] *Xcelris Genomics Xcelris Labs Ltd, Old Premchandnagar Road, Opp. Satyagrah Chhavani, Bodakdev, Ahmedabad 380054, India*
[3] *Department of Animal Nutrition, Livestock Research Station, Sardarkrushinagar Dantiwada Agricultural University, Gujarat 385506, India*

Correspondence should be addressed to C. G. Joshi; cgjoshi@rediffmail.com

Received 27 February 2014; Revised 4 June 2014; Accepted 5 June 2014; Published 17 July 2014

Academic Editor: Neelu Nawani

The complex microbiomes of the rumen functions as an effective system for plant cell wall degradation, and biomass utilization provide genetic resource for degrading microbial enzymes that could be used in the production of biofuel. Therefore the buffalo rumen microbiota was surveyed using shot gun sequencing. This metagenomic sequencing generated 3.9 GB of sequences and data were assembled into 137270 contiguous sequences (contigs). We identified potential 2614 contigs encoding biomass degrading enzymes including glycoside hydrolases (GH: 1943 contigs), carbohydrate binding module (CBM: 23 contigs), glycosyl transferase (GT: 373 contigs), carbohydrate esterases (CE: 259 contigs), and polysaccharide lyases (PE: 16 contigs). The hierarchical clustering of buffalo metagenomes demonstrated the similarities and dissimilarity in microbial community structures and functional capacity. This demonstrates that buffalo rumen microbiome was considerably enriched in functional genes involved in polysaccharide degradation with great prospects to obtain new molecules that may be applied in the biofuel industry.

1. Introduction

Livestock production in India is subsidiary to plant production. In tropical countries, the ruminants are fed on lignocellulosic agricultural byproducts. Ruminants digest such plant materials by virtue of the extensive microbial community [1, 2], which are found in the rumen and provide the host with nutrients, predominantly in the form of volatile fatty acids and microbial protein [3]. The rumen habitat contains a consortium of microorganisms that harbour the complex lignocellulosic degradation system for the microbial attachment and digestion of plant biomass. However, the complex chemical processes required to break down the plant cell wall are rarely carried out by a single species. Evidence also suggests that the most important organisms and gene sets involved in the most efficient hydrolysis of plant cell wall are associated with the fiber portion of the rumen digesta [4]. Plant cell walls have a basic structure of cellulose surrounded by a complex matrix of hemicellulose, pectin and protein, cell types, and stages of maturity [5]. *Ruminococcus flavefaciens, Ruminococcus albus,* and *Fibrobacter succinogenes* are considered to be the most important cellulose-degrading bacteria in the rumen [6], and they produce a set of cellulolytic enzymes, including endoglucanases, exoglucanases, and glucosidases, as well as hemicellulases. In addition, the predominant ruminal hemicellulose-digesting bacteria such as *Butyrivibrio fibrisolvens* and *Prevotella ruminicola* degrade xylan and pectin and utilize the degraded soluble sugars as substrates [7]. In recent years, rumen metagenomics studies have revealed the vast diversity of fibrolytic enzymes, multiple domain proteins, and the complexity of microbial composition in the ecosystem [8, 9].

The glycoside hydrolases (GHs) are modular enzymes that hydrolyse glycosidic bonds of carbohydrates, with classification based on amino acid sequence and predicted three-dimensional structure. Such enzymes may contain single or multiple catalytic modules (GH) together with single or multiple noncatalytic carbohydrate-binding modules (CBMs) [10]. Conversely, hitting upon the polysaccharide degrading enzyme machineries from metagenomic data is constraint [11, 12]. The microbes present in the rumen are not all culturable; moreover, if cloning is opted, enormous screening of clones will be required for covering the entire metagenome [12, 13]. However, there are limitations to metagenome mining [14], and the number of clones needed to represent the entire metagenome is staggering [15]. It has been reported that the nature of diet is one of the factors that shapes the composition of the gut microbiota [16]. Therefore, in order to improve the digestibility, the modulations of microbial consortia have also been attempted by dietary interventions [17].

Next-generation sequencing technologies have been used to characterize the microbial diversity and functional capacity of a range of microbial communities in the gastrointestinal tracts of humans [18, 19] as well as in several animal species [20–24]. Several groups have succeeded practice in metagenomic gene discovery of biomass-degrading genes from cow rumen and termite gut [9, 25].

The bovine rumen provides a unique genetic resource for the discovery of plant cell wall-degrading microbial enzymes (CAZymes) for use in biofuel production, presumably because of coevolution of microbes and plant cell wall types [9]. Identification of potent cellulolytic and other carbohydrate-active enzymes is of great interest for industrial applications [13]. Shotgun sequencing of the buffalo rumen metagenome was conducted to identify taxonomic diversity, metabolic makeup and discovers putative carbohydrate-active genes in the consortia.

2. Materials and Methods

2.1. Experimental Design and Rumen Sampling. The experimental animals were maintained for feeding experiments at Livestock Research Station, Sardarkrushinagar Dantiwada Agricultural University, Gujarat. Experiment was performed with the approval of the Anand Agricultural University, Institutional Animal Ethics Committee (Permission letter: AAU/GVC/CPCSEA-IAEC/108/2013). Eight 4- to 5-year-old healthy Mehsani breed of water buffaloes (*Bubalus bubalis*) were assigned to two basal diets groups ($n = 4$) based on green and dry roughages. The experimental diets were designed to have an increasing concentration of dry roughage and a decreasing concentration of the concentrate mix. The diets (dry roughage: concentrate and green roughage: concentrate) were M1D (50% dry roughage: 50% concentrate), M2D (75% dry roughage: 25% concentrate), and M3D (100% dry roughage); M1G (50% green roughage: 50% concentrate) and M2G (75% green roughage: 25% concentrate); M3G (100% green roughage). The experimental animals received M1 diet for six weeks followed by M2 for six weeks and then M3 for subsequent six weeks. The animals were maintained on each diet for six weeks to allow for microbial adhesion and adaptation to the new diet. On the last day of each experimental feeding period, rumen samples were collected 3 h after feeding using stomach tube. Each rumen sample was further separated to solid and liquid fractions by squeezing through a four-layered muslin cloth. Samples were immediately placed on ice, transported to the laboratory, and then stored at −80°C prior to metagenome analyses.

2.2. DNA Extraction. For isolation of DNA from liquid samples, the samples were thawed at room temperature and were then centrifuged at 5000 rpm for 5 min. The supernatant obtained thereafter was subjected to DNA isolation using commercially available QIAmp DNA stool mini kit (Qiagen, USA). For DNA extraction from solid samples, the samples were resuspended in phosphate buffer saline and vortexed for one and half hours for dislodging the tightly adhered bacteria from the solid feed particles. The samples were then centrifuged and the supernatant was subjected to DNA isolation using the same kit which was used for liquid sample. DNA samples were measured on a Nanodrop ND-1000 spectrophotometer (Thermo Scientific) to assess DNA quantity.

2.3. Ion Torrent Shotgun Sequencing. The shot gun sequencing on Ion Torrent PGM was performed at the Department of Animal biotechnology, College of Veterinary Science and Animal Husbandry, Anand Agricultural University, Anand, Gujarat, India. In brief, libraries were generated using the Ion Xpress plus fragment library kit (Life Technologies). The quality and quantity of generated libraries was assessed using the Agilent Bioanalyzer (Agilent Technologies) with Agilent High Sensitivity DNA Kit (Agilent Technologies), again quantified with Qubit fluorometer (Life Technologies). Quality check passed libraries were subjected to emulsion PCR using the Ion PGM 200 Xpress Template Kit (Life Technologies). After bead enrichment, beads were loaded onto Ion 316 chips and sequenced using an Ion Torrent PGM.

The data were then analyzed on Metagenome Rapid Annotation using Subsystem Technology (MG-RAST) server. The reads which passed the MG-RAST Quality filters were subjected to M5NR database (M5 nonredundant protein database, http://tools.metagenomics.anl.gov/m5nr/) for functional and diversity analysis. The 5 M's in M5 stand for the intersection of "Metagenomics, Metadata, Meta-analysis, Models, and Meta infrastructure" which target to synthesize the multiple databases with a unified standard and annotation of the metagenomic data in a more comprehensive and effective manner. The M5NR is a single searchable novel nonredundant database containing protein sequences and annotations from multiple sources and associated tools. Furthermore, the functional hierarchical classification was illustrated by using SEED subsystem. The sequences were compared using the BLASTX algorithm with an expected cut off of 1×10^{-5} [26].

2.4. Bioinformatics Analysis. The data analyses were performed with Prinseq and Metagenome Rapid Annotation

using Subsystem Technology (MG-RAST) pipelines. Quality filter reads were subjected to M5NR database for functional and diversity analysis. The M5NR is a single searchable novel nonredundant database containing protein sequences and annotations from multiple sources and associated tools. The functional annotation and classification relied on the SEED subsystem [27]. The maximum E-value of $1e-5$, minimum percent identity of 60, and minimum alignment length of 50 pb were applied as the parameter settings in the analysis. Hierarchal clustering was performed using Ward's minimum variance with unscaled Bay Curtis distances (MGRAST).

Annotations based on the carbohydrate-active enzymes database [10] (http://www.cazy.org/) were performed for all the reads that passed the MG-RAST QC filter at an E value restriction of 1×10^{-6}. Contigs sequences of the metagenomes were screened against PfamA database [28] by Pfam_scan [29] for particular glycoside hydrolase (GH) families and carbohydrate-binding module (CBM). The results were analyzed manually for proportion of different CAZymes. The profile of CAZymes of Buffalo rumen was also compared with cow http://ftp-trace.ncbi.nlm.nih.gov/sra/sra-instant/reads/ByRun/sra/SRR/SRR094/SRR094418/ and termite hindgut (downloaded from: ftp://ftp.metagenom.icsanl.gov/28/4442701.3/raw/2624.fna.gz). All the contigs from cow and termite metagenomes were further processed same as our data and uploaded in CAZy with the same parameters.

3. Results and Discussion

The analysis of the reads yielded a high percentage of species identification in complex and dynamics metagenomes and even higher in less complex samples. Sequence reads from Ion Torrent provided enough specificity that is needed to compare the sequenced reads with the suitable databases and allowed the unambiguous assignment of closely related species. The shot gun sequencing runs of all metagenomics samples together yielded 3914.94 MB data. Prior to further processing, the raw read data were subjected to the MG-RAST online server [27] to remove duplicate and low quality reads. The unique sequence reads that passed the QC filtering step were then subjected to further analysis of taxonomic and functional annotation. The summary of metagenome data is presented in Table 1. In present study, metagenomic sequences were used to characterize genetic and functional capability of rumen microbiota of the buffalo.

3.1. Metabolic Profiles of the Buffalo Rumen Metagenome. Carbohydrate metabolism is the second most abundant functional category, representing 11.45–13.0% of the buffalo rumen metagenomes (Supplementary Table 1; Supplementary Material available online athttp://dx.doi.org/10.1155/2014/267189). Genes associated with amino acid and derivatives, protein metabolism, cofactors (vitamins, prosthetic groups, and pigments), membrane transport, cell wall, and capsule. RNA metabolism and DNA metabolism are also abundant in the cow rumen metagenomes [8] as well as in Surti buffalo rumen [30]. Approximately 15.92–16.97% of the annotated reads from the buffalo rumen metagenomes were categorized within the clustering-based subsystems, most of which have unknown or putative functions. Metabolism-based hierarchical clustering demonstrates that all the buffalo rumen metagenome clustered together. All the samples were similar/dissimilar to each sample to the buffalo rumen (Supplementary Figure 1). The similarity/dissimilarty of function among all buffalo rumen is not surprising, considering the fact that they are all with similar digestive tract structures and functions.

Table 1: Summary of metagenomic data.

Green roughage: dry roughage (diets)	Average read length (bp)	Data (Mb)	Total size (Mb)
50%			
Liquid	146	549.4	1285.4
Solid	149	736	
75%			
Liquid	161	438	1127.85
Solid	149	689.85	
100%			
Liquid	180	800.69	1501.69
Solid	170	701	
Total size			3914.94

3.2. Uncovering CAZymes Form Buffalo Rumen Metagenomes. Rumen fluid is an excellent sample for mining CAZymes due to its apparent selection for evolution as a complex lignocellulosic degradation system [8]. We subjected total contigs to the carbohydrate-active enzymes database (CAZy; http://www.cazy.org), as described by Cantarel et al. [10], to obtain a more in-depth view of the carbohydrate enzymes present. The comparison of the all metagenome reads post-QC processing based on the CAZy database provided 2614 hits at an E value restriction of 1×10^5. Candidate sequences that belong to the glycoside hydrolase GH3 (353) and families GH2 (192), GH92 (135), and GH97 (135) are the most abundant, followed by members of the glycosyl transferase families GT51 (89), families GT35 (88), and families GT2 (84) (Figures 1 and 2). Many genes encoding cellulase have been reported in buffalo rumen [31].

In the category of CBM, sequences that belong to the CE10 (124) are the most abundant (Figures 3 and 4). In addition sequences assigned to family PL are very scanty (Figure 5). Novel carbohydrate-binding module have been identified in a ruminal metagenome [32]. Carbohydrate-binding modules which are one of the structural components of cellulosomes-free enzyme system involved in carbohydrate digestion were also found. Though they were scantly represented (only 19 contigs) their occurrence is in accordance with the finding that microbiome of ruminants render cellulolytic bacteria associated with cellulosome complexes [2, 33].

GHs are a prominent group of enzymes that hydrolyze the glycosidic bond among the carbohydrate molecules. It

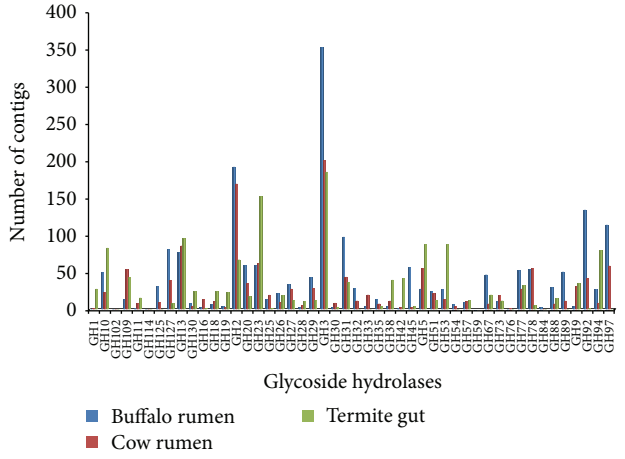

Figure 1: Comparison of predicted carbohydrate-active genes glycoside hydrolase in three cellulosic metagenomes: cow rumen microbiome, termite gut microbiome, and buffalo rumen microbiome.

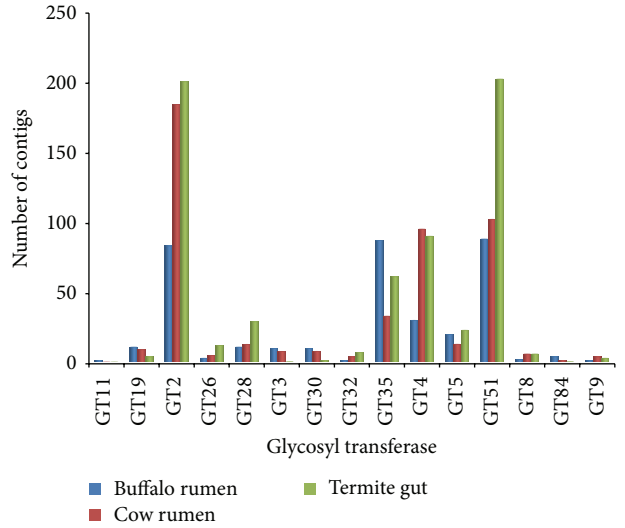

Figure 2: Comparison of predicted carbohydrate-active genes glycosyl transferase (GT) in three cellulosic metagenomes: cow rumen microbiome, termite gut microbiome, and buffalo rumen microbiome.

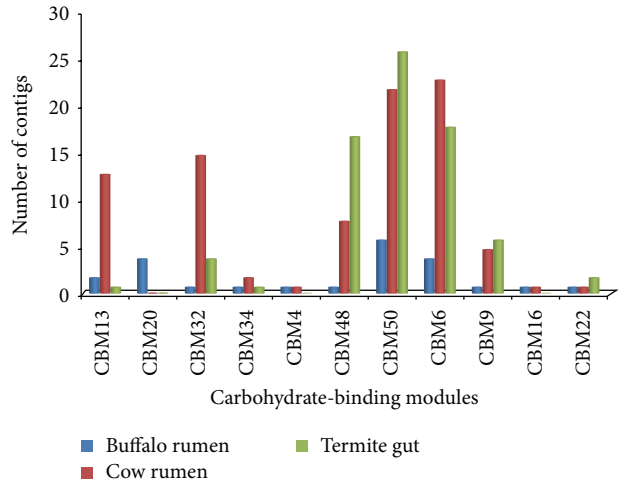

Figure 3: Comparison of predicted carbohydrate-active carbohydrate-binding modules (CBM), in three cellulosic metagenomes: cow rumen microbiome, termite gut microbiome, and buffalo rumen microbiome.

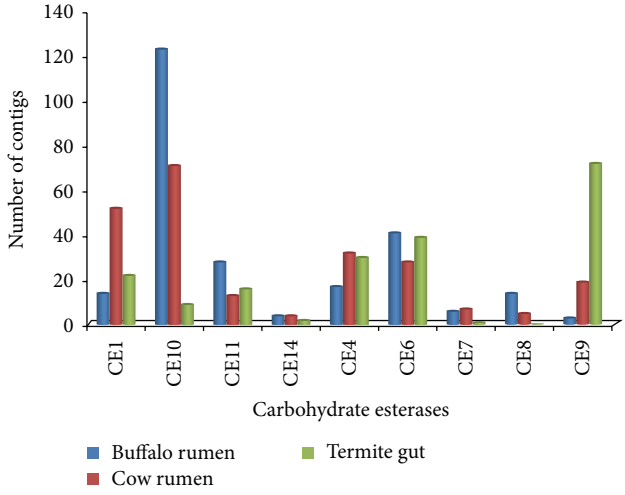

Figure 4: Comparison of predicted carbohydrate-active genes carbohydrate esterases in three cellulosic metagenomes: cow rumen microbiome, termite gut microbiome, and buffalo rumen microbiome.

is interesting to notice that there is a wide diversity of GH catalytic modules in the buffalo rumen microbiome, indicated by the 1943 modules belonging to 48 GH families. The most frequently occurring GH families in the buffalo rumen metagenome were GH3, GH2, and GH92 (Figure 1). Large-scale metagenomic sequencing of hindgut bacteria of a wood-feeding higher termite revealed that GHF5 was predominant in all identified GH families [25]. The most common activities of GH3 include b-D-glucosidases, a-L-arabinofuranosidases, b-D-xylopyranosidases, and N-acetyl-b-D-glucosaminidases [34]. In several cases, the enzymes have dual or broad substrate specificities with respect to monosaccharide residue, linkage position, and chain length of the substrate, such as a-L-arabinofuranosidase and b-D-xylopyranosidase [35]. GH2 components are b-D-galactosidases, b-glucuronidases, b-D-mannosidases, and exo-b-glucosaminidase. GH43 shows b-xylosidase, b-1, 3-xylosidase, a-L-arabinofuranosidase, arabinanase, xylanase, and galactan 1, 3-b-galactosidase activity (http://www.cazy.org/). Recently, Bashir et al. [36] studied the diversity of microbes existing in the guts of arthropods and their roles in biomass degradation and identified 42 unique cellulase-producing microbial strains and major glycosyl hydrolase enzymes.

Many candidate genes that were identified in buffalo rumen metagenome that belong to the glycosyl transferase families GT51, GT2, and GT35 are the most abundant (Figure 2). Glycosyl transferases are ubiquitous enzymes that catalyze the attachment of sugars to a glycone [37]. Amongst

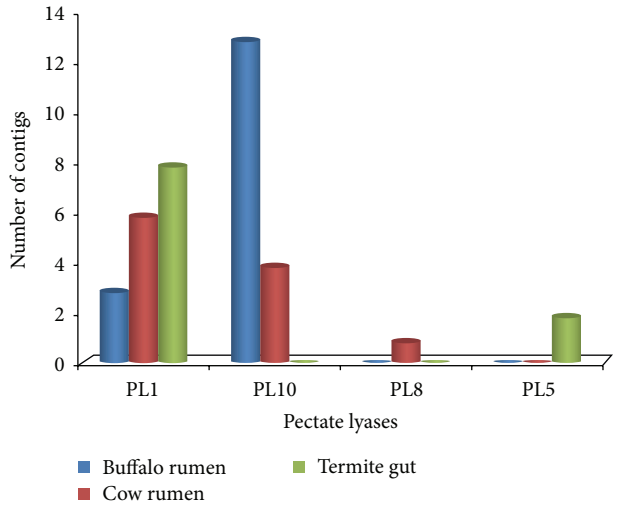

Figure 5: Comparison of predicted carbohydrate-active genes pectate lyases (PL) in three cellulosic metagenomes: cow rumen microbiome, termite gut microbiome, and buffalo rumen microbiome.

hemicellulases, 4 families were found (GHs 10, 11, 26, and 28) which jointly represented a total of 4% of all GHs. Pectin degrading pectin lyases (PL1, 10) was also obtained. Besides, we also identified xylan esterases (CE 1, 4, 6 and 7) and pectin methyl esterase (CE8), which acts on side chains of hemicellulose and pectin, respectively, and render both the large molecules accessible for further breakdown (Figures 4 and 5).

Metagenomes of termite hindgut [25] and cow rumen [9] were chosen for comparison with our data. Analysis indicates that buffalo metagenome had the highest amount of debranching enzymes (5.34%) and oligosaccharide degrading enzymes (25.2%) in which GH3 was predominant accounting for about 18.3% (Table 2). The higher proportion of oligosaccharide degrading enzymes naturally results into rapid formation of simple sugars which means that there will be faster and higher production of VFA (volatile fatty acid). However, the proportion of cellulases (8.91%) and hemicellulases (9.36%) in particular proportion of GH5 (5.71%) and GH10 (5.39%), respectively, was highest in termite. In addition, the proportion of oligosaccharide degrading enzymes GH32 and GH42 was also found to be highest in termite gut metagenome. Since wood has a greater proportion of cellulose and hemicellulose than the forage, the higher proportion of the GH5 and GH10 families in termite hindgut may be ascribed to its feed type. Similar to other metagenomes, buffalo rumen metagenome was also found lacking in enzyme families like GH6, 7, 48, 12, and 62. Furthermore, the contigs showing hits for CAZymes were analyzed to know the taxonomic placement [27]. Phylum Bacteroidetes represented highest percentage of contigs (73.0%) flowed by Firmicutes, Proteobacteria, and Actinobacteria (Figure 6(a)). Among Bacteroidetes, polysaccharide-degrading *Prevotella* genus was most abundant in the rumen of buffalo (Figure 6(b)).

Table 2: Comparison of the carbohydrate active enzymes identified in buffalo rumen metagenome with those of two other metagenomes.

Enzymes	Termite gut (%)	Buffalo rumen (%)	Cow rumen (%)
		Cellulases	
GH5	5.71	1.50	3.85
GH6	0.00	0.00	0.00
GH7	0.00	0.00	0.00
GH9	2.37	0.26	2.20
GH44	0.32	0.00	0.07
GH45	0.51	0.05	0.27
GH48	0.00	0.00	0.00
Total	**8.91**	**1.81**	**6.39**
		Hemicellulases	
GH8	0.834	0.00	0.76
GH10	5.39	2.64	1.65
GH11	1.09	0.15	0.69
GH12	0.00	0.00	0.00
GH26	1.28	1.03	0.76
GH28	0.77	0.21	0.48
Total	**9.36**	**4.04**	**4.34**
		Debranching enzymes	
GH62	0.00	0.00	0.00
GH67	1.34	2.49	0.62
GH78	0.44	2.85	3.85
Total	**1.78**	**5.34**	**4.47**
		Oligosaccharide degrading enzymes	
GH1	1.86	0.05	0.21
GH2	4.36	9.85	11.68
GH3	11.94	18.3	13.87
GH29	0.89	2.28	2.06
GH35	0.38	0.78	0.62
GH38	2.63	0.26	0.89
GH39	0.44	0.00	0.21
GH42	2.76	0.10	0.27
Total	**25.28**	**31.62**	**29.81**

Bacteroidetes has been well reported for their starch, pectin, and xylan digestion [38].

3.3. Taxonomic Analysis of Buffalo Rumen Microbiota. The taxonomic computations provided 89.6–97.6% bacteria, 1.4–9.1% eukaryota, 0.8–1.8% Archea, and 0.20–0.37% viruses (Table 3). In the question metagenomes, Bacteroidetes was the most predominant phylum (30–60%), followed by Firmicutes (20–40%), Proteobacteria (8–10%), and Actinobacteria (3–5%) in all samples (Supplementary Figure 2). This finding is consistent with a previous study [3] in cow rumen metagenome and they characterized the rumen bacterial populations of 16 individual lactating cows and showed 51% similarity in bacterial taxa (Firmicutes,

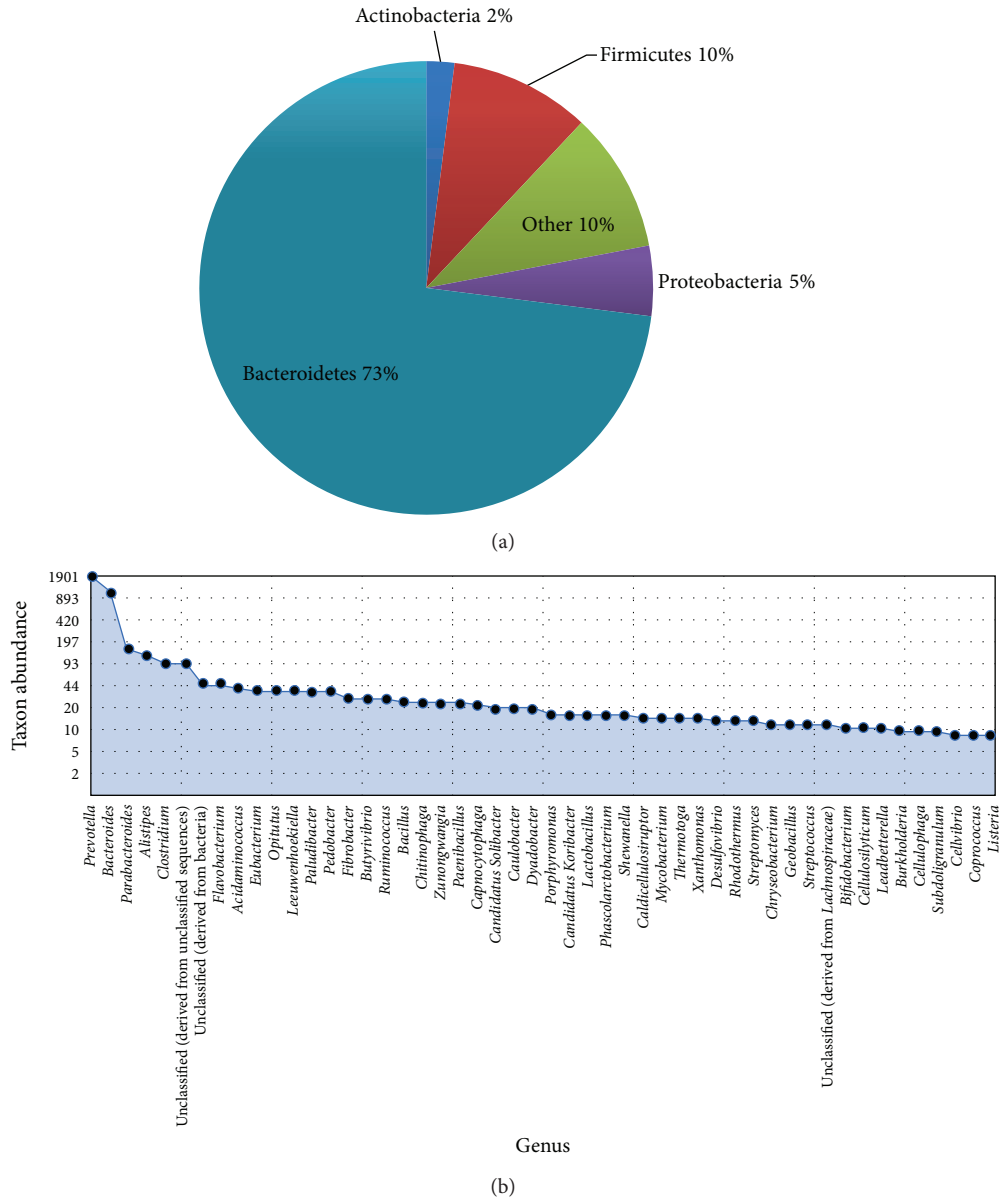

FIGURE 6: Taxonomic classification of putative CAZymes contigs and their microbial origin. (a) The pie chart shows the abundance of phylum and (b) genus abundances ordered from the most abundant to least abundant.

Bacteroidetes, Proteobacteria, and Actinobacteria) across samples. In addition they also identified 32 genera that are shared by all samples, exhibiting high variability in abundance across samples. Jami et al. [39] have also reported predominance of Bacteroidetes, Firmicutes, and Proteobacteria (core microbiota) in lactating cow fed 30% roughage and 70% concentrate. Compared with our previous 16S rRNA gene based data [40], higher percentages of Firmicutes and lower percentages of Bacteroidetes in the Indian Surti buffalo fed green fodder Napier bajra 21 (*Pennisetum purpureum*), mature pasture grass (*Dichanthium annulatum*), and concentrate mixture (20% crude protein, 65% total digestible nutrients) rumen metagenome were observed. These differences may have been caused by the biases associated with the primers, PCR reaction conditions, or selection of clones [41].

Among the Bacteroidetes group, Bacteroidales were the most predominant, among which genera *Prevotella* and *Bacteroides* were consistently overrepresented (Supplementary Figure 3). The genus *Prevotella* was highly represented in shared microbial community; it was the most abundant bacterial genus in buffalo rumen metagenomes. This finding is consistent with a previous study by Li et al. [42] in which several bacterial species were quantified in ruminal samples. The study reported the predominance of *Prevotella* members, which comprised 42 to 60% of the bacterial rRNA gene copies in the samples [38].

Table 3: Phylogenetic classification at domain level.

Domain	50%				75%				100%			
	Green roughage (%)		Dry roughage (%)		Green roughage (%)		Dry roughage (%)		Green roughage (%)		Dry roughage (%)	
	Liquid	Solid	Liquid	Solid	Liquid	Solid	Liquid	Solid	Liquid	Solid	Liquid	Solid
Bacteria	89.6	96.0	95.3	96.3	96.9	97.4	96.5	96.8	97.4	97.4	97.0	97.6
Archea	0.8	1.8	0.8	1.7	0.8	0.8	0.7	1.0	0.6	0.9	0.8	0.8
Eukaryota	9.1	1.9	3.4	1.8	1.7	1.5	2.3	2.0	1.7	1.6	1.7	1.4
Viruses	0.3	0.1	0.3	0.1	0.4	0.1	0.3	0.1	0.2	0.1	0.3	0.1
Unclassified	0.2	0.2	0.2	0.1	0.2	0.1	0.2	0.2	0.2	0.2	0.2	0.2

Firmicutes were the second predominant phylum in the buffalo rumen microbiota with Bacilli and Clostridia as the primary contributor to the Firmicutes populations. The major genus in the Firmicutes phylum is *Clostridium* (Supplementary Figure 3). However, the fiber degrading bacteria, *Ruminococcus albus* and *Ruminococcus flavefaciens,* are less abundant, which is contrast to our previous study [43] in Surti buffalo rumen. Surprisingly, some bacterial taxa were less abundant from the core groups identified by shotgun sequencing and considered crucial for fiber degradation in the rumen. Notably the phylum Fibrobacteres, which includes one of the main cellulolytic bacteria, *Fibrobacter succinogenes* which is of great importance for rumen function, was found in only one-third of the samples. Several studies of the rumen microbiome have suggested that the abundance of this phylum and in particular *F. succinogenes* varies considerably across ruminant and diets. This was evident in a recent metagenomic study in which this phylum was completely absent from the fiber-adherent and total overall rumen microbiome [8].

Phylogenetic level and the metabolic level clustering of forty-eight individual metagenomes were carried out with unscaled Bay Curtis variance distances and presented through a double hierarchical dendrogram (Supplementary Figure 4). In the phylogenetic comparison, the Bacteroidetes, Firmicutes, Proteobacteria, and Actinobacteria were the most abundant with different proportions in all the metagenomes. These phyla are recognized to be omnipresent and dominant in the rumen [8, 26, 44]. The results are corresponding with previous studies, indicating that microbial community composition is similar across animals [3]. The microorganism composition of the animal gastrointestinal tract reflects the constant coevolution of the animal with its host [9]. The bacterial taxa may vary considerably between buffalo rumen; they appear to be phylogenetically related. This suggests that the functional requirement imposed by the rumen ecological niche selects taxa that potentially share similar genetic features. The heat map also demonstrates that the buffalo rumen metagenome contains lower Fibrobacteres, an important phylum of cellulose-degrading bacteria.

In the present study, we have identified cellulose and hemicelluloses encoding contigs from microbial community in buffalo rumen. Cellulose and hemicellulose are the major components of plant cell walls and the most abundant biopolymeric materials [45]. The natural breakdown of plant matter performed by hemicellulases has been exploited by biotechnologists to produce bioethanol [46]. Rubin [44] has identified and characterized 4 highly active beta-glucosidases from fibre-adherent microbial community from the cow rumen. All enzymes were most active at temperatures 45–55°C and exhibited high affinity and activity towards synthetic substrate and natural cello-oligosaccharides. They suggest that beta-glucosidases (animal digestomes) may be of a potential interest for bioethanol production in combination with low dosage of commercial cellulases.

4. Conclusion

The work presented here describes the composition of the overall functional capacity related carbohydrates genes and taxonomic communities of the buffalo rumen ecosystem. Major carbohydrates utilizing genes covering GH, CBM, and GT families were detected in abundance. In addition, results revealed that GH 3 was the most dominant among all the detected GH families. The high magnitude of glycosyl transferase and carbohydrate esterases suggests the development of combined action on biomass degradation process. In the present study four phyla dominated in microbiomes, namely, Bacteroidetes, Firmicutes, Proteobacteria, and Actinobacteria. The information obtained in this research will open new horizons towards a full understanding of the functional genes and metabolic capabilities of the biomass degrading microorganisms, with great prospects to obtain new molecules that may be applied in the biofuel and agricultural industry. In addition, the contigs generated from the buffalo rumen metagenome represent the vital information for isolating the potential enzymes for biofuel and other industrial applications.

Conflict of Interests

The authors declare that there is no conflict of interests regarding the publication of this paper.

Acknowledgments

The work was supported by the Niche Area of Excellence Project funded by Indian Council of Agricultural Research, New Delhi. Authors are thankful to the support staff at Livestock Research Station, S. K. Nagar Agricultural University, for care and handling of buffaloes and assisting in sample collection.

References

[1] J. Miron, D. Ben-Ghedalia, and M. Morrison, "Invited review: adhesion mechanisms of rumen cellulolytic bacteria," *Journal of Dairy Science*, vol. 84, pp. 1294–1309, 2001.

[2] P. B. Pope, A. K. Mackenzie, I. Gregor, W. Smith, M. A. Sundset, and A. C. McHardy, "Metagenomics of the Svalbard reindeer rumen microbiome reveals abundance of polysaccharide utilization loci," *PloS ONE*, vol. 7, Article ID e38571, 2012.

[3] E. Jami and I. Mizrahi, "Composition and similarity of bovine rumen microbiota across individual animals," *PloS One*, vol. 7, article e33306, 2012.

[4] C. W. Forsberg, K. J. Cheng, and B. A. White, "Polysaccharide degradation in the rumen and large intestine," in *Gastrointestinal Microbiology*, R. I. Mackie and B. A. White, Eds., vol. 1, pp. 319–379, Chapman & Hall, New York, NY, USA, 1997.

[5] D. J. Cosgrove, "Growth of the plant cell wall," *Nature Reviews Molecular Cell Biology*, vol. 6, no. 11, pp. 850–861, 2005.

[6] H. J. Flint and E. A. Bayer, "Plant cell wall breakdown by anaerobic microorganisms from the Mammalian digestive tract," *Annals of the New York Academy of Sciences*, vol. 1125, pp. 280–288, 2008.

[7] H. J. Flint, E. A. Bayer, M. T. Rincon, R. Lamed, and B. A. White, "Polysaccharide utilization by gut bacteria: potential for new insights from genomic analysis," *Nature Reviews Microbiology*, vol. 6, pp. 121–131, 2008.

[8] J. M. Brulc, D. A. Antonopoulos, M. E. Miller et al., "Gene-centric metagenomics of the fiber-adherent bovine rumen microbiome reveals forage specific glycoside hydrolases," *Proceedings of the National Academy of Sciences of the United States of America*, vol. 106, pp. 1948–1953, 2009.

[9] M. Hess, A. Sczyrba, R. Egan, T. W. Kim, H. Chokhawala, and G. Schroth, "Metagenomic discovery of biomass-degrading genes and genomes from cow rumen," *Science*, vol. 331, pp. 463–467, 2011.

[10] B. L. Cantarel, P. M. Coutinho, C. Rancurel, T. Bernard, V. Lombard, and B. Henrissat, "The Carbohydrate-Active EnZymes database (CAZy): an expert resource for glycogenomics," *Nucleic Acids Research*, vol. 37, pp. D233–D238, 2009.

[11] C. Bera-Maillet, E. Devillard, M. Cezette, J. P. Jouany, and E. Forano, "Xylanases and carboxymethylcellulases of the rumen protozoa Polyplastron multivesiculatum, Eudiplodinium maggii and Entodinium sp," *FEMS Microbiology Letters*, vol. 244, pp. 149–156, 2005.

[12] M. Qi, P. Wang, N. O'Toole et al., "Snapshot of the eukaryotic gene expression in muskoxen rumen—a metatranscriptomic approach," *PloS ONE*, vol. 6, Article ID e20521, 2011.

[13] D. Tilman, R. Socolow, J. A. Foley et al., "Beneficial biofuels—the food, energy, and environment trilemma," *Science*, vol. 325, no. 5938, pp. 270–271, 2009.

[14] A. Henne, R. Daniel, R. A. Schmitz, and G. Gottschalk, "Construction of environmental DNA libraries in *Escherichia coli* and screening for the presence of genes conferring utilization of 4-hydroxybutyrate," *Applied and Environmental Microbiology*, vol. 65, no. 9, pp. 3901–3907, 1999.

[15] J. Handelsman, M. R. Rondon, S. F. Brady, J. Clardy, and R. M. Goodman, "Molecular biological access to the chemistry of unknown soil microbes: a new frontier for natural products," *Chemistry & Biology*, vol. 5, pp. R245–R249, 1998.

[16] F. Thomas, J. H. Hehemann, E. Rebuffet, M. Czjzek, and G. Michel, "Environmental and gut bacteroidetes: the food connection," *Frontiers in Microbiology*, vol. 2, article 93, 2011.

[17] J. Stiverson, M. Morrison, and Z. Yu, "Populations of select cultured and uncultured bacteria in the rumen of sheep and the effect of diets and ruminal fractions," *International Journal of Microbiology*, vol. 2011, Article ID 750613, 8 pages, 2011.

[18] S. R. Gill, M. Pop, R. T. Deboy et al., "Metagenomic analysis of the human distal gut microbiome," *Science*, vol. 312, pp. 1355–1395, 2006.

[19] P. J. Turnbaugh, M. Hamady, T. Yatsunenko, B. L. Cantarel, A. Duncan, and R. E. Ley, "A core gut microbiome in obese and lean twins," *Nature*, vol. 457, pp. 480–484, 2009.

[20] R. Lamendella, J. W. Domingo, S. Ghosh, J. Martinson, and D. B. Oerther, "Comparative fecal metagenomics unveils unique functional capacity of the swine gut," *BMC Microbiology*, vol. 11, p. 103, 2011.

[21] A. Qu, J. M. Brulc, M. K. Wilson, B. F. Law, and L. A. Theoret Joens Jr., "Comparative metagenomics reveals host specific metavirulomes and horizontal gene transfer elements in the chicken cecum microbiome," *PLoS ONE*, vol. 3, Article ID e2945, 2008.

[22] K. S. Swanson, S. E. Dowd, J. S. Suchodolski et al., "Phylogenetic and gene-centric metagenomics of the canine intestinal microbiome reveals similarities with humans and mice," *The ISME Journal*, vol. 5, pp. 639–49, 2011.

[23] H. M. Tun, M. S. Brar, N. Khin, L. Jun, R. K. Hui, and S. E. Dowd, "Gene-centric metagenomics analysis of feline intestinal microbiome using 454 junior pyrosequencing," *Journal of Microbiological Methods*, vol. 88, pp. 369–376, 2012.

[24] B. Xu, W. Xu, F. Yang et al., "Metagenomic analysis of the pygmy loris fecal microbiome reveals unique functional capacity related to metabolism of aromatic compounds," *PloS One*, vol. 8, article e56565, 2013.

[25] F. Warnecke, P. Luginbuhl, N. Ivanova et al., "Metagenomic and functional analysis of hindgut microbiota of a wood-feeding higher termite," *Nature*, vol. 450, pp. 560–565, 2007.

[26] J. E. Edwards, S. A. Huws, E. J. Kim, and A. H. Kingston-Smith, "Characterization of the dynamics of initial bacterial colonization of nonconserved forage in the bovine rumen," *FEMS Microbiology Ecology*, vol. 62, pp. 323–335, 2007.

[27] F. Meyer, D. Paarmann, M. D'Souza et al., "The metagenomics RAST server—a public resource for the automatic phylogenetic and functional analysis of metagenomes," *BMC Bioinformatics*, vol. 9, p. 386, 2008.

[28] R. D. Finn, J. Mistry, J. Tate, P. Coggill, A. Heger, and J. E. Pollington, "The Pfam protein families database," *Nucleic Acids Research*, vol. 38, pp. D211–D222, 2010.

[29] S. R. Eddy, "Profile hidden Markov models," *Bioinformatics*, vol. 14, pp. 755–763, 1998.

[30] K. M. Singh, V. Ahir, A. K. Tripathi et al., "Metagenomic analysis of Surti buffalo 366 (Bubalus bubalis) rumen: a preliminary study," *Molecular Biology Reports*, vol. 39, no. 4, pp. 4841–4484, 2012.

[31] C. J. Duan, L. Xian, G. C. Zhao et al., "Isolation and partial characterization of novel genes encoding acidic cellulases from metagenomes of buffalo rumens," *Journal of Applied Microbiology*, vol. 107, pp. 245–256, 2009.

[32] C.-J. Duan, J.-J. Liu, X. Wu, J.-L. Tang, and J.-X. Feng, "Novel carbohydrate-binding module identified in a ruminal metagenomic endoglucanase," *Applied and Environmental Microbiology*, vol. 76, no. 14, pp. 4867–4870, 2010.

[33] S. Y. Ding, M. T. Rincon, R. Lamed et al., "Cellulosomal scaffoldin-like proteins from Ruminococcus flavefaciens," *Journal of Bacteriology*, vol. 183, pp. 1945–1953, 2001.

[34] A. J. Harvey, M. Hrmova, R. De Gori, J. N. Varghese, and G. B. Fincher, "Comparative modelling of the three-dimensional structures of family 3 glycoside hydrolases," *Proteins*, vol. 41, pp. 257–269, 2000.

[35] R. C. Lee, M. Hrmova, R. A. Burton, J. Lahnstein, and G. B. Fincher, "Bifunctional family 3 glycoside hydrolases from barley with alpha-L-arabinofuranosidase and beta-D xylosidase activity. Characterization, primary structures, and COOH terminal processing," *Journal of Biological Chemistry*, vol. 278, no. 7, pp. 5377–5387, 2003.

[36] Z. Bashir, V. K. Kondapalli, N. Adlakha et al., "Diversity and functional significance of cellulolytic microbes living in termite, pill-bug and stem-borer guts," *Scientific Reports*, vol. 3, article 2558, 2013.

[37] L. L. Lairson, B. Henrissat, G. J. Davies, and S. G. Withers, "Glycosyltransferases, structures, functions, and mechanisms," *Annual Review of Biochemistry*, vol. 77, pp. 521–255, 2008.

[38] D. M. Stevenson and P. J. Weimer, "Dominance of Prevotella and low abundance of classical ruminal bacterial species in the bovine rumen revealed by relative quantification real- time PCR," *Applied Microbiology and Biotechnology*, vol. 75, pp. 165–174, 2007.

[39] E. Jami, B. A. White, and I. Mizrahi, "Potential role of the bovine rumen microbiome in modulating milk composition and feed efficiency," *PLoS ONE*, vol. 9, no. 1, Article ID e85423, 2014.

[40] P. R. Pandya, K. M. Singh, S. Parnerkar, A. K. Tripathi, H. H. Mehta, and D. N. Rank, "Bacterial diversity in the rumen of Indian Surti buffalo (Bubalus bubalis), assessed by 16S rDNA analysis," *Journal of Applied Genetics*, vol. 51, pp. 395–402, 2010.

[41] D. P. Chandler, J. K. Fredrickson, and F. J. Brockman, "Effect of PCR template concentration on the composition and distribution of total community 16S rDNA clone libraries," *Molecular Ecology*, vol. 6, pp. 475–482, 1997.

[42] M. Li, G. B. Penner, E. Hernandez-Sanabria, M. Oba, and L. L. Guan, "Effects of sampling location and time, and host animal on assessment of bacterial diversity and fermentation parameters in the bovine rumen," *Journal of Applied Microbiology*, vol. 107, pp. 1924–1934, 2009.

[43] K. M. Singh, A. K. Tripathi, P. R. Pandya, S. Parnerkar, D. N. Rank, and R. K. Kothari, "Use of real-time PCR technique in determination of major fibrolytic and non fibrolytic bacteria present in Indian Surti buffaloes (*Bubalus bubalis*)," *Polish Journal of Microbiology*, vol. 62, pp. 195–200, 2013.

[44] E. M. Rubin, "Genomics of cellulosic biofuels," *Nature*, vol. 454, pp. 841–845, 2008.

[45] V. del Pozo Mercedes, L. Fernández-Arrojo, J. Gil-Martínez et al., "Microbial β-glucosidases from cow rumen metagenome enhance the saccharification of lignocellulose in combination with commercial cellulase cocktail," *Biotechnology for Biofuels*, vol. 5, article 73, 2012.

[46] M. Zhang, R. Su, W. Qi, and Z. He, "Enhanced enzymatic hydrolysis of lignocellulose byoptimizing enzyme complexes," *Applied Biochemistry and Biotechnology*, vol. 160, pp. 1407–1414, 2010.

Hindawi Publishing Corporation
BioMed Research International
Volume 2014, Article ID 480498, 8 pages
http://dx.doi.org/10.1155/2014/480498

Research Article

Methylamine-Sensitive Amperometric Biosensor Based on $(His)_6$-Tagged *Hansenula polymorpha* Methylamine Oxidase Immobilized on the Gold Nanoparticles

Nataliya Ye. Stasyuk,[1] Oleh V. Smutok,[1] Andriy E. Zakalskiy,[1] Oksana M. Zakalska,[1] and Mykhailo V. Gonchar[1,2]

[1] *Institute of Cell Biology, NAS of Ukraine, Drahomanov Street 14/16, Lviv 79005, Ukraine*
[2] *Institute of Applied Biotechnology and Basic Sciences, University of Rzeszow, Sokolowska Street 26, 36-100 Kolbuszowa, Poland*

Correspondence should be addressed to Mykhailo V. Gonchar; gonchar@cellbiol.lviv.ua

Received 21 February 2014; Revised 2 June 2014; Accepted 20 June 2014; Published 16 July 2014

Academic Editor: Noomen Hmidet

A novel methylamine-selective amperometric bienzyme biosensor based on recombinant primary amine oxidase isolated from the recombinant yeast strain *Saccharomyces cerevisiae* and commercial horseradish peroxidase is described. Two amine oxidase preparations were used: free enzyme (AMO) and covalently immobilized on the surface of gold nanoparticles (AMO-nAu). Some bioanalytical parameters (sensitivity, selectivity, and storage stability) of the developed biosensors were investigated. The sensitivity for both sensors is high: 1450 ± 113 and $700 \pm 30\ A^{-1} \cdot M^{-1} \cdot m^{-2}$ for AMO-nAu biosensor, respectively. The biosensors exhibit the linear range from 15 μM to 150 μM (AMO-nAu) and from 15 μM to 60 μM (AMO). The developed biosensor demonstrated a good selectivity toward methylamine (MA) (signal for dimethylamine and trimethylamine is less than 5% and for ethylamine 15% compared to MA output) and reveals a satisfactory storage stability. The constructed amperometric biosensor was used for MA assay in real samples of fish products in comparison with chemical method. The values obtained with both approaches different methods demonstrated a high correlation.

1. Introduction

The assay of aliphatic amines in environment and biological samples is important, due to the use of these compounds in industry and their wide distribution in living organisms as a result of natural degradation of proteins, amino acids, and other nitrogen-containing compounds [1]. Methylamine (MA) can be accumulated in some kinds of fish, especially of *Gadoid* species, in very high amounts as a result of enzymatic degradation of the natural osmolyte, trimethylamine *N*-oxide (TMAO). Consuming such fish food in combination with nitrate-containing products could result in the formation of *N*-nitroso derivatives which are very powerful carcinogens [2].

It is also important that MA is widely used in different stages of the preparation of various drug substances; therefore, it may be retained in the drug substance. MA is also controlled by the U.S. Drug Enforcement Administration as a List 1 Regulated Chemical due to its use in production of methamphetamine [3].

It was shown that reactions of trimethylamine (TMA) accumulation are not specific for fish only and may also occur in human organism. This fact has been proven by the discovery of human inherited syndrome of "fish smell," trimethylaminuria [4]. Homozygous carriers of this metabolic disorder produce a specific smell due to continuous TMA excretion with sweat and urea. This disorder is probably caused by defects in flavoenzyme, monooxygenase FMO3, which converts TMA, a compound with a very unpleasant smell, into TMAO, an odourless compound.

Unfortunately, the problem of analysis of fish products quality and biochemical diagnostics of trimethylaminuria is yet to be solved due to the absence of a fast, cheap, and

selective method of analysis of food products and human biological liquids for the presence of primary aliphatic amines, that is, MA, dimethylamine (DMA), and TMA. The majority of the frequently used approaches are time consuming and expensive and require skillful labor techniques, such as the high performance liquid chromatography [5], colorimetry [6], laser spectroscopy [7], fluorometry [8], ion chromatography [9], and enzymatic method [10]. The majority of these methods are marked by poor precision and low sensitivity and selectivity.

The simplest way to detect alkylamines is an enzymatic method based on natural isoforms of amine oxidases with different substrate specificity. The main obstacle for using this method is absence of commercial preparations of primary amine oxidase (AMO; E.C. 1.4.3.21), the key biologically active element of a potential biosensor.

In this paper, we describe the construction of an AMO-based amperometric bioelectrode selective to MA. A ferrocene layer was used as a final electron transfer mediator. The biorecognition membrane includes two enzymes: purified $(His)_6$-tagged AMO from the recombinant yeast *Saccharomyces cerevisiae* [11] and commercial horseradish peroxidase (HRP). The enzymes were dropped on the ferrocene-modified graphite electrode surface and covered with a cathodic polymer GY 83-0270 0005. The principal scheme of MA determination is as follows:

$$\begin{aligned}
&CH_3NH_2 + H_2O + O_2 \xrightarrow{\text{AMO}} CH_2O + NH_3 + H_2O_2,\\
&H_2O_2 + \text{HRP (Fe)} \longrightarrow H_2O + \text{HRP (Fe = O)},\\
&\text{HRP (Fe = O)} + \text{ferrocene}\left(Fe^{2+}\right) + 2H^+ \longrightarrow \text{HRP (Fe)}\\
&\qquad + \text{ferrocene}\left(Fe^{3+}\right) + H_2O,\\
&\text{ferrocene}\left(Fe^{3+}\right) \xrightarrow{\text{Electrode}} \text{ferrocene}\left(Fe^{2+}\right)
\end{aligned} \quad (1)$$

The developed amperometric bienzyme electrode was applied for MA assay in the samples of fish products.

2. Materials and Methods

2.1. Materials. Horseradish peroxidase (HRP) (EC 1.11.1.7, from *Armoracia rusticana*, 500 $U \cdot mg^{-1}$), tetrachloroauric acid trihydrate, sodium salt of ABTS, sodium citrate, *N*-(3-dimethylaminopropyl)-*N′*-ethylcarbodiimide hydrochloride (EDC), pentafluorophenol (PFP), 2-(2-aminoethoxy) ethanol (AEE), dimethylformamide (DMF), *N*,*N*-diisopropylethylamine (DIPEA), 16-mercaptohexadecanoic acid (MHDA), methylamine (MA), dimethylamine (DMA), trimethylamine (TMA), NaCl, KH_2PO_4, Na_2HPO_4, chloroform, and Butvar solution B-98 were purchased from Sigma-Aldrich (ALSI Ltd., Kiev, Ukraine). The cathodic electrodeposition paint "GY 83–0270 0005" was from BASF Farben und Lacke (Munster, Germany). All buffers and standard solutions were prepared using the water purified by the Milli-Q system (Millipore).

2.2. Isolation and Purification of Amine Oxidase (E.C. 1.4.3.21). As a source of $(His)_6$-tagged AMO, the constructed by us recombinant yeast strain *Saccharomyces cerevisiae* C13ABYS86 (*Mat a, leu2-3, ura3, his, pra1-1, prb1-1, prc1-1, cps1-3*) able to overexpress the target enzyme was used. The $(His)_6$-tagged enzyme was purified from the cell-free extract of the recombinant strain by metal-affinity chromatography on Ni-NTA-agarose [11]. Purified AMO with specific activity 13.7 $U \cdot mg^{-1}$ was stored in 20 mM phosphate buffer, pH 7.5 (PB), at 4°C.

2.3. Assay of AMO Activity. The AMO activity was measured according to the method described by Haywood and Large [10]. AMO activity of free and immobilized on nAu enzyme preparations was determined by monitoring ABTS oxidation by H_2O_2 generated during MA cleavage. The millimolar absorption coefficient of the radical-cation product at 405 nm is 18.41 $mM^{-1} \cdot cm^{-1}$. Usually, 100 μL of a substrate mixture (150 mM methylamine hydrochloride, 30 mM Na_2ABTS, and 0.3 $mg \cdot mL^{-1}$ HRP in 75 mM PB, pH 7.5) was preincubated for 5 min at 30°C and added to the test tube containing 10 μL of AMO preparation. The reaction mixture was incubated for 15 min at 30°C followed by radical-cation product assay. The kinetic study was carried out at the same conditions within methylamine concentration range of 0.02 to 5 mM. AMO concentration in the incubation mixture was 40 $ng \cdot mL^{-1}$. One unit of AMO activity was defined as the amount of enzyme required to catalyse the formation of 1 μmole ABTS radical cation per 1 min under standard conditions.

2.4. Synthesis of Gold Nanoparticles (nAu). Gold nanoparticles (nAu) were synthesized by the citrate reduction method [12]. 1.25 mL of 1 mM $HAuCl_4$ and 0.125 mL of 38.8 mM trisodium citrate were mixed at 100°C and stirred for 15 min to obtain a wine-red solution. The nAu were precipitated by centrifugation (6708 g; Hettich Micro-22R centrifuge). The precipitate was washed with water and stored at +4°C before using. Under the described conditions, a colloid solution of nAu in water at concentration of 0.9 mM was obtained for further characterization and enzyme immobilization.

2.5. Immobilization of $(His)_6$-Tagged AMO on nAu. The nAu were incubated overnight in 5 mM MHDA in ethanol at +4°C. After rinsing with DMF, the MHDA-covered nAu were incubated in a DMF solution of 20 mM CMC, 20 mM PFP, and 20 mM DIPEA for 30 min at 25°C. After repeated rinsing with DMF, condensation of the activated Au-linked carboxylic groups with amine groups of the enzyme was carried out. 25 μL of the enzyme solution (0.75 $mg \cdot mL^{-1}$) in 30 mM PB, pH 7.5, was incubated with nAu for 1 h at 25°C. After rinsing with PB, pH 7.5, blocking of unreacted carboxylic groups with 0.1 M solution of AEE in 0.1 M bicarbonate buffer, pH 7.0, was performed. The biofunctionalized nAu were rinsed with PB, pH 7.5, and stored at +4°C until usage. The amount of immobilized enzyme on the nAu was determined as the difference between the initial and unbound protein content in the immobilization medium using the Lowry protein assay method.

2.6. Characterisation of nAu Using Atomic Force Microscopy (AFM). The size and structure of nAu particles (unbound and enzyme-modified) were studied by atomic force microscope Solver P47-PRO (NT-MDT, The Netherlands). An aliquot of the tested sample was spread on the surface of freshly cleaved mica, dried, and analyzed in air using the tapping mode with resonance frequency of 160 kHz, scan rate of 1 Hz/s, and resolution of 256 × 256 pixels.

2.7. Apparatus for Biosensor Analysis. Amperometric biosensors were evaluated using constant potential amperometry in a three-electrode configuration with a Ag/AgCl/KCl (3 M) reference electrode and a Pt-wire counter electrode. Amperometric measurements were carried out using a potentiostat CHI 1200A (IJ Cambria Scientific, Burry Port, UK) connected to a personal computer and performed in batch mode under continuous stirring in a standard 40 mL cell at room temperature.

Graphite rods (type RW001, 3.05 mm diameter, Ringsdorff Werke, Bonn, Germany) were used as working electrodes. They were sealed in glass tubes using epoxy glue thus forming disk electrodes. Before sensor preparation, the graphite electrodes were polished with emery paper.

2.8. Preparation of the Mediator-Modified Graphite Electrodes. Electrodeposition of 5 mM solutions of Mendola blue and methylene blue in 20 mM PB, pH 7.5, on the surface of 3 mm rod graphite electrode was performed using cyclic voltamperometry in the range from −400 to +400 mV with scan rate 50 mV·min^{-1} *versus* Ag/AgCl/3 M KCl reference electrode.

A 5 μL aliquot of 2 mM ferrocene solution in acetone was dropped onto surface of working electrode and air-dried for 10 min.

The mediator-modified electrodes were rinsed with water and equilibrated in 30 mM PB, pH 7.5, before using.

2.9. Immobilization of the Enzymes on the Mediator-Modified Electrode Surface. HRP and AMO were dropped on the mediator-modified electrode and covered by an electrodeposited commercial cathode polymer-GY 83-0270 0005 (*CP*). The immobilization procedure was as follows: 3 μL of HRP solution with activity 200 U·mL^{-1} in 30 mM PB, pH 7.5, was dropped on the top of the mediator-modified carbon electrode. After drying for 2 min at room temperature, the layer of HRP was covered with a 5 μL solution of AMO in FB, pH 7.5, with activity 40 U·mL^{-1} or AMO-nAu, 35.5 U·mL^{-1}, respectively. Dried bienzyme layers were covered with 4 μL of GY 83-0270 0005 for polymer layer formation. The prepared biofunctionalized electrode was rinsed with PB, pH 7.5, and stored at +4°C before application.

2.10. A Colorimetric Method for the Determination of Methylamine in Fish Products. A chemical analysis of MA, based on the use of lactose in alkaline solution [6], was performed using the multiple standard addition method. The absorbance of the reaction product was recorded with a Shimadzu UV-1650 PC spectrophotometer (Shimadzu, Kyoto, Japan) at 545 nm relative to an MA-free control sample. The concentration of MA in the tested samples was determined from a calibration curve.

2.11. Preparation of Fish Products Samples. For assay of MA, the frozen sea fish samples of hake and grouper were used. Muscle tissues (12 g and 60 g) of the frozen fillet were ground in a mortar with a following addition of 50 mL of deionized water. Trichloroacetic acid was added to the samples (to the final concentration of 4%). The protein precipitate was separated by passing the resulting mixture through a folded filter. Before analysis, the obtained filtrates were neutralized to pH value 7.5 by 10 M NaOH. The filtrate was stored before analysis at +4°C.

2.12. Statistic Treatment. All the measurement's results and the level of correlation between results obtained by the different analytical methods were calculated by computer program Origin 8.0 and Microsoft Excel.

3. Results and Discussion

3.1. Evaluation and Optimization of the MA Biosensor. For construction of an MA-selective biosensor, the bienzyme sensor architecture was used which contained $(His)_6$-tagged AMO or AMO-modified nAu and commercial HRP. Using an HRP allows decreasing working potential of the sensor to −50 mV which is important to avoid interfering effects of a sample background.

To improve electron transfer from transducer to the HRP, a number of synthetic mediators were tested. Using cyclic voltamperometry, three mediators (ferrocene, Mendola blue, and methylene blue) were analyzed by their ability to increase the effectiveness of electron transfer from the carbon electrode to HRP. The best results were obtained for ferrocene (data not shown), so all the next experiments were performed using ferrocene as electron transfer mediator. For physical fixation of HRP and AMO on the surface of ferrocene-modified carbon electrodes, entrapment of the enzymes in a polymer layer of a cathodic paint GY 83-0270 0005 (*CP*) was used. The optimized sensor architecture which consisted of *CP*-AMO-HRP-ferrocene was used for chronoamperometric investigation of methylamine oxidation (Figure 1).

The maximal current at substrate saturation (I_{max}) for the *CP*-AMO-HRP-ferrocene-modified carbon electrodes (area 7.3 mm^2) calculated from calibration graph is 1.23 ± 0.02 μA (Figure 1(c)). The value of K_M^{app} to MA derived from the calibration plot for the bienzyme sensor is 0.039 ± 0.003 mM, which is lower compared to K_M^{app} of free AMO in solution (0.22 mM) [11]. The sensitivity of the sensor for methylamine is 1450 ± 113 A·M^{-1}·m^{-2} (Figure 1(b)). The linearity of the bioelectrodes is in the range from 15 μM to 60 μM, and the time of response to the target analyte (corresponds to 90% of the output) was found to be about 10 s.

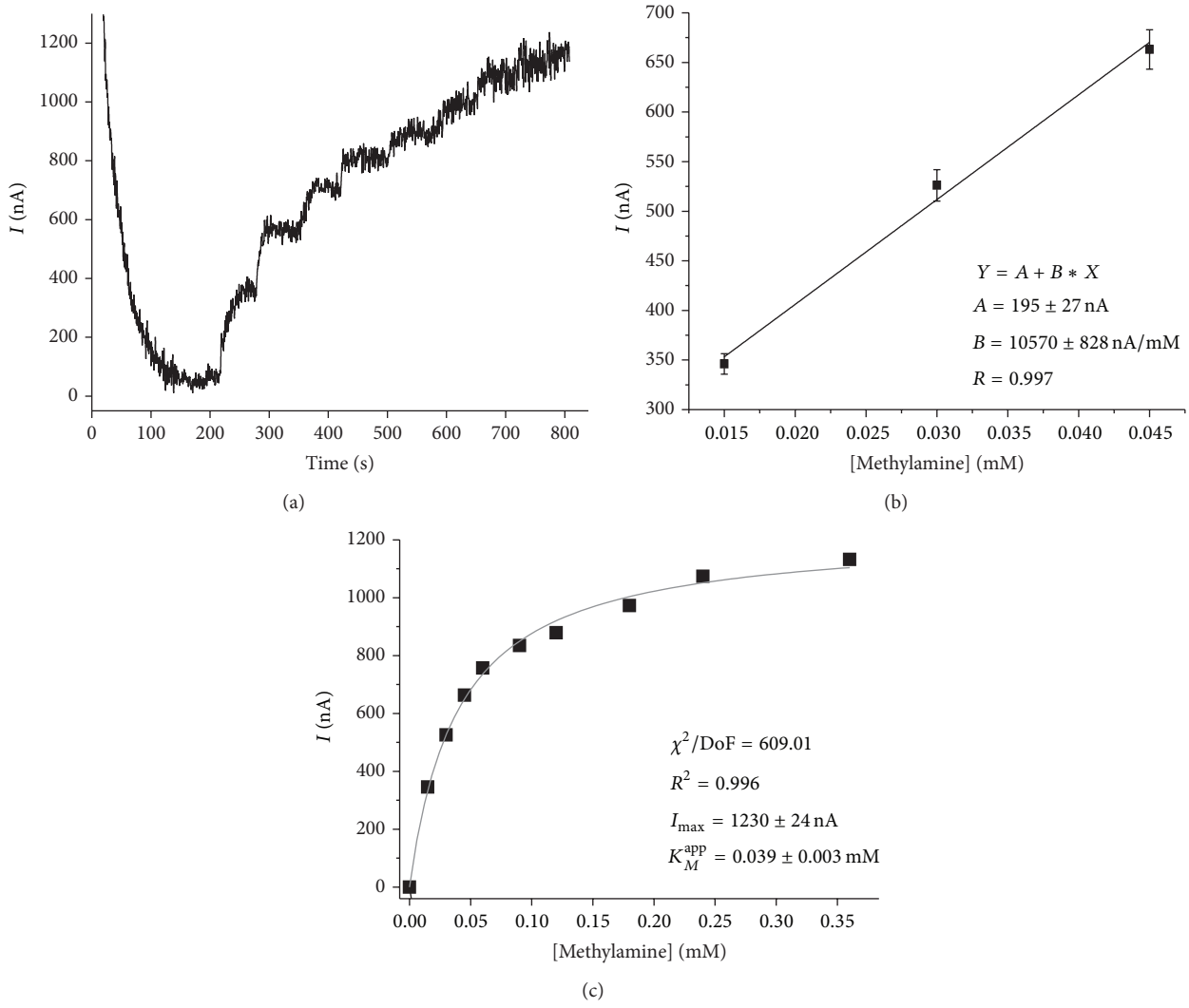

Figure 1: Chronoamperometric current response upon subsequent additions of methylamine (a) and calibration graphs (b), (c) for *CP*-AMO-HRP-ferrocene-modified carbon electrode. Conditions: working potential −50 mV *versus* Ag/AgCl/3 M KCl in 20 mM PB, pH 7.5.

Table 1: The activity of AMO during immobilization on the nAu surfaces.

	Enzyme preparation	Supernatant after enzyme immobilization	Immobilized AMO on nAu
V, mL	0.03	0.015	0.02
$C_{protein}$, mg·mL^{-1}	0.75	0.52	*
Total$_{protein}$, mg	0.02	0.08	*
A, U·mL^{-1}	40.1 ± 1.1	2.55 ± 0.12	35.5 ± 0.2
Total A, U	1.2 ± 0.1	0.04 ± 0.002	0.71 ± 0.01
Yield (%)	=100	3.3 ± 0.1	59.2 ± 1.2

*Under sensitivity.

3.2. Construction of MA-Selective Bioselective Layer Using nAu. It is known that nanomaterials could improve the sensor characteristics [13]. Biofunctionalisation of synthesized nAu was performed by modification of nAu by 16-mercaptohexadecanoic acid and carbodiimide-penta-fluorophenol condensation for covalent binding of the enzyme [14] (see Section 2.5 of Math and Meth.). The activity of AMO during immobilization on the nAu surface is represented in Table 1.

As shown in Table 1, AMO covalently immobilized on the surface of the nAu has kept 59.2 ± 1.2% of the initial enzyme activity.

The Gauss distribution in Figure 2 demonstrates that an average size of the bionanoparticles is close to 17-18 nm.

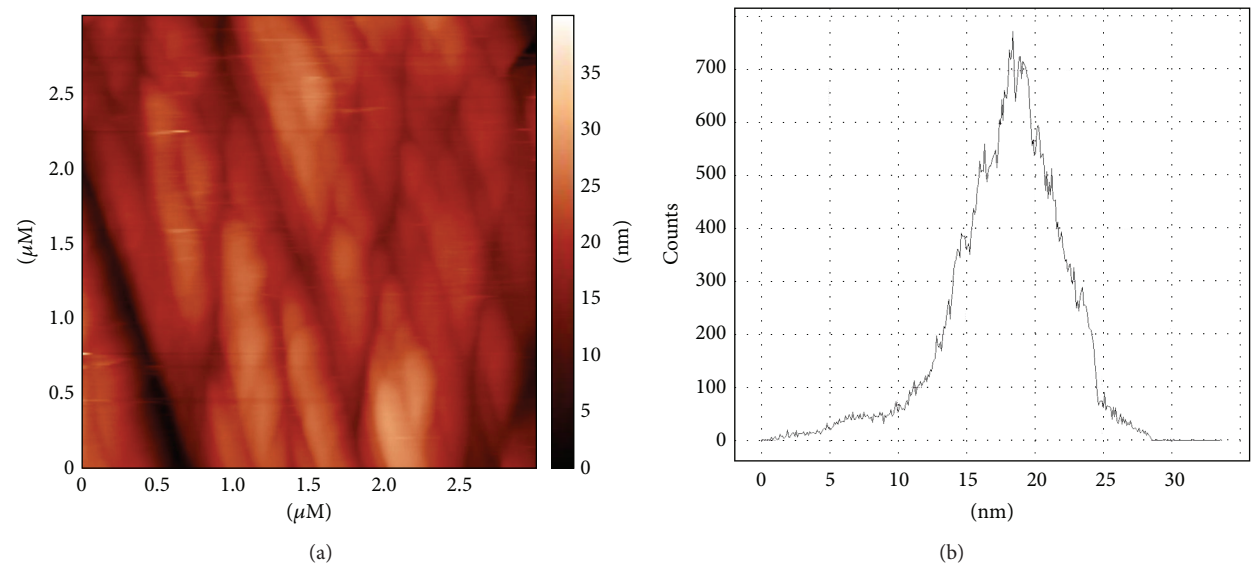

Figure 2: Atomic force microscopy of the AMO-nAu (a) and Gauss distribution of AMO-nAu by size (b).

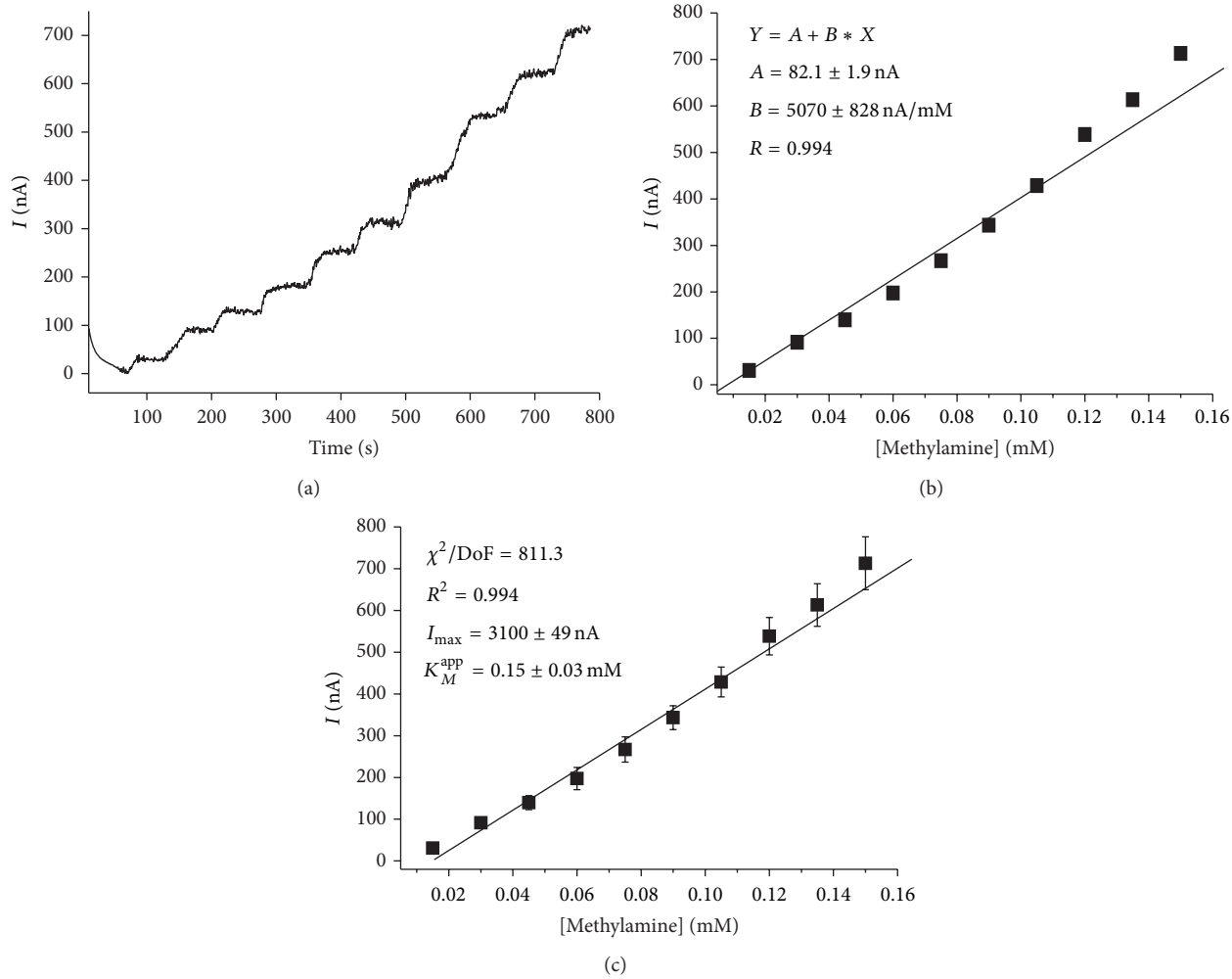

Figure 3: Chronoamperometric current response upon subsequent additions of MA (a) and calibration graphs (b), (c) for *CP*-AMO-nAu-HRP-ferrocene-modified carbon electrode. Conditions: working potential −50 mV *versus* Ag/AgCl/3 M KCl in 20 mM PB, pH 7.5.

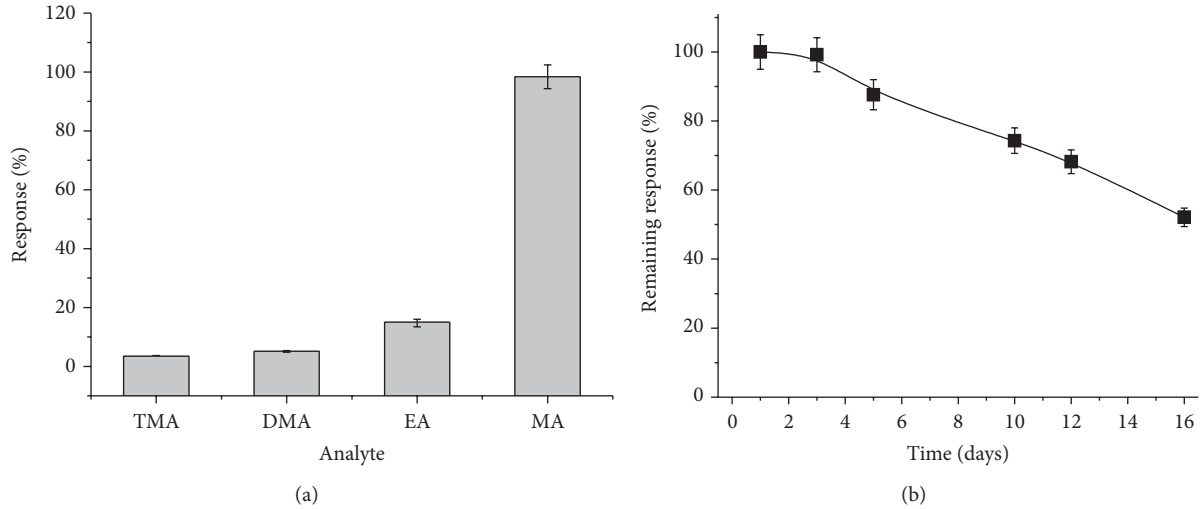

Figure 4: Characteristics of the developed MA biosensor under applied potential of −50 mV at 22°C. The highest current response was chosen as 100% in all experiments. Selectivity test was performed with 0.1 mM solutions of MA, DMA, EA, and TMA in 20 mM PB, pH 7.5 (a); storage stability was checked using 0.05 mM MA in 20 mM PB, pH 7.5, at room temperature during 16 days (b). The bioelectrode was kept at +4°C in 20 mM PB, pH 7.5.

Figure 3 represents chronoamperometric current response and calibration curve for the *CP*-AMO-nAu-HRP-ferrocene-modified carbon electrodes upon subsequent additions of MA.

The calibration was performed by a stepwise addition of a standard analyte solution. The sensitivity of the sensor AMO-nAu-based for MA is 700 ± 30 $A \cdot M^{-1} \cdot m^{-2}$ (Figure 3(b)) which is 2-fold lower compared to biosensor without using nAu. The reason for such phenomenon is not clear. The maximal current response of the bioelectrodes modified by nAu (architecture *CP*-AMO-nAu-HRP-ferrocene) calculated from the calibration graph (Figure 3(c)) is equal to 3.10 ± 0.05 μA which is 2.5 times higher compared to *CP*-AMO-HRP-ferrocene sensor architecture (1.23 ± 0.02 μA). The value of K_M^{app} to methylamine derived from the calibration plot for the sensor is 0.15 ± 0.03 mM, that is, 3.8 times higher compared to *CP*-AMO-HRP-ferrocene sensor (0.039± 0.003 mM). Because of the relatively high affinity of AMO to MA, the observed increased K_M^{app} value for AMO-nAu-based electrode has a positive impact on the biosensor properties due to the wider linear range for MA determination (from 0.015 mM up to 0.15 mM). The 2-fold expanded linearity for *CP*-AMO-nAu-HRP-ferrocene sensor architecture is better adapted to the typical concentration range of MA in the real samples. All the next experiments were performed using bioselective layer *CP*-AMO-nAu-HRP-ferrocene architecture.

3.3. Assay of MA in Fish Samples. For the application of the constructed biosensor for assay of MA in real samples, the selectivity with respect to structurally similar analytes (DMA and TMA) is of great importance. Hence, the amperometric current response of the developed MA-selective sensor was evaluated with respect to the mentioned above compounds (Figure 4(a)). The storage stability of the sensor was also tested (Figure 4(b)).

As shown in Figure 4(a), positive signals to TMA (3.5 ± 0.17%), DMA (5.1 ± 0.25%), and ethanolamine (EA) (15 ± 1.02%) were detected. It is worth to mention that the possible impact of EA on MA assay is negligible, because this compound (in a free form) is present in fish products only in small amounts (less than 0.019 μg per g) [15]. Thus, the impact of these compounds will not be extremely significant for the correct determination of methylamine in the real samples where the mentioned above components can be present.

For analysis of the storage stability of the sensor, the electrodes were stored between exploitation cycles at +4°C. The measurements were performed at room temperature in 20 mM PB, pH 7.5, with addition of 0.05 mM MA. The half-life of the sensor was close to 16 days of the storage (Figure 4(b)).

In order to demonstrate the practical feasibility of the constructed biosensor with architecture *CP*-AMO-nAu-HRP-ferrocene, MA content in frozen fillet of hake and grouper was determined, using standard addition method (Figure 5).

The content of MA in frozen sea fish samples calculated from the calibration curves for standard addition test using MA-selective biosensor was 14.0 ± 0.5 μM for fillet of hake and 15.4 ± 0.2 μM for grouper, respectively.

The results of MA analysis in the real samples by the developed biosensor were compared with the results obtained by chemical method (Table 2).

Only slight differences between the results obtained by biosensor's approach and chemical method were observed (2.1–2.5%). Moreover, the obtained MA contents results are in good correlation with literature data for sea fish samples [16]. These results demonstrate the perspectives for application of the developed *CP*-AMO-nAu-HRP-ferrocene-based electrode for a correct analysis of MA in food technology.

Table 2: MA content in frozen sea fish determined by different methods.

Samples	Methods				Difference, %
	MA-selective biosensor		Chemical method, μM		
	μM (in extract)	μg/g (in wet meat)	μM (in extract)	μg/g (in wet meat)	
Hake	14.0 ± 0.5	2.4 ± 0.1	13.7 ± 1.2	2.3 ± 0.1	2.1
Grouper	15.4 ± 0.2	2.6 ± 0.1	15.8 ± 0.3	2.7 ± 0.2	2.5

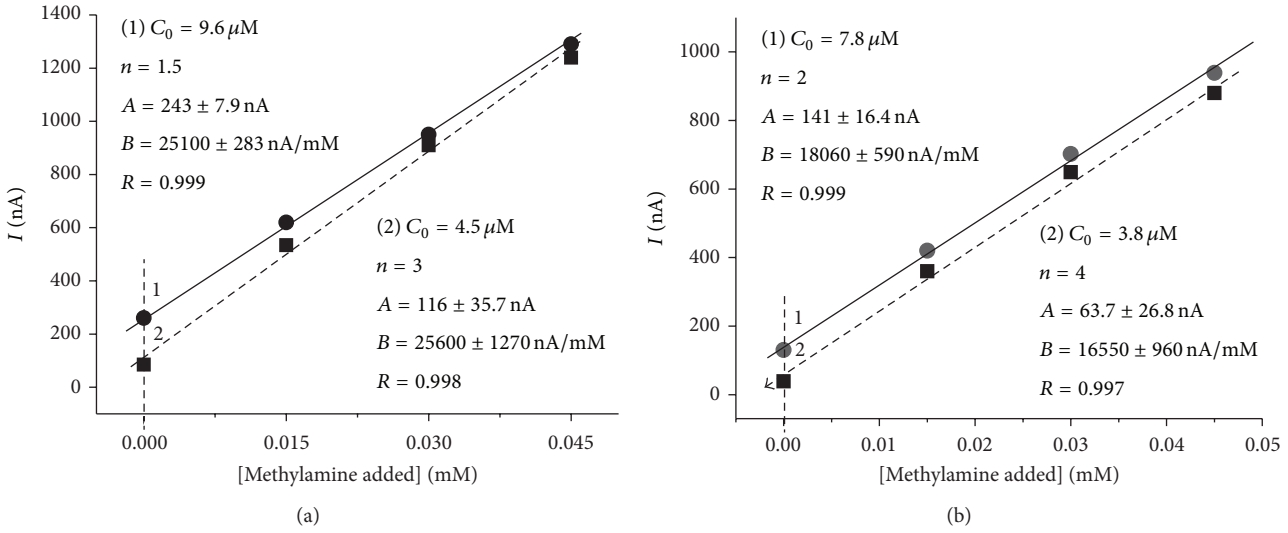

Figure 5: Calibration curves for MA assay in frozen fillet of hake (a) and grouper (b) using standard addition test for biosensor (*CP*-AMO-nAu-HRP-ferrocene). *A*, *B*: parameters for the linear regression line; *n*: dilution factor; C_o: calculated initial concentration; *R*: correlation coefficient.

4. Conclusions

A new methylamine-sensitive bienzyme amperometric biosensor based on the recombinant methylamine oxidase and commercial horseradish peroxidase has been developed. To improve sensor characteristics, covalent immobilization of AMO on the surface of nAu has been performed. The main sensor characteristics (sensitivity, linearity, response time, and K_M value) have been investigated. Testing MA-sensitive laboratory prototype of biosensor on the real samples of sea fish using the multiple standard addition method has been done.

Conflict of Interests

The authors declare that there is no conflict of interests regarding the publication of this paper.

Acknowledgments

This research was supported by Cross-Border Cooperation Programme Poland-Belarus-Ukraine 2007–2013 IPBU. 03.01.00-18-452/11-00, by Ukrainian-Belarussian Project F 54.4/031, and by NATO Project CBP.NUKR.SFP 984173.

References

[1] H. Tseng and D. Graves, "Natural methylamine osmolytes, trimethylamine N-oxide and betaine, increase tau-induced polymerization of microtubules," *Biochemical and Biophysical Research Communication*, vol. 250, pp. 726–730, 1998.

[2] H. Rehbein, D. Eichenauer, P. Feser et al., "Formaldehyde and dimethylamine in frozen fishery products available on the market: an inventory," *Archiv für Lebensmittelhygiene*, vol. 46, no. 5, pp. 122–124, 1995.

[3] "Thermo scientific spplication note 1057: determination of methylamine in drug products," Sunnyvale, Calif, USA, 2008, http://www.dionex.com/en-us/webdocs/114676-AN1057-IC-Methylamine-Drug-Products-AN70523_E.pdf.

[4] A. Q. Zhang, S. C. Mitchell, and R. L. Smith, "Dimethylamine formation in the rat from various related amine precursors," *Food and Chemical Toxicology*, vol. 36, no. 11, pp. 923–927, 1998.

[5] S. Xiao and P. H. Yu, "A fluorometric high-performance liquid chromatography procedure for simultaneous determination of methylamine and aminoacetone in blood and tissues," *Analytical Biochemistry*, vol. 384, pp. 20–26, 2009.

[6] A. A. Ormsby and S. Johnson, "A colorimetric method for the determination of methylamine in urine," *The Journal of Biological Chemistry*, vol. 187, pp. 711–717, 1950.

[7] D. Marinov, J. Rey, and M. W. Sigrist, "Mid-infrared spectroscopic investigation of methylamines by a continuous-wave difference-frequency-generation-based system," *Applied Optics*, vol. 47, pp. 1956–1962, 2008.

[8] H. Gu, H. M. Ma, and S. C. Liang, "A novel water-soluble fluorescent probe for the determination of methylamine," *Journal of Analytical Chemistry*, vol. 371, no. 4, pp. 570–573, 2001.

[9] M. E. Erupe, A. Liberman-Martin, P. J. Silva et al., "Determination of methylamines and trimethylamine-N-oxide in particulate matter by non-suppressed ion chromatography," *Journal of Chromatography A*, vol. 1217, pp. 2070–2073, 2010.

[10] G. W. Haywood and P. J. Large, "Microbial oxidation of amines. Distribution, purification and properties of two primary-amine oxidases from the yeast Candida boidinii grown on amines as sole nitrogen source," *Biochemistry Journal*, vol. 199, pp. 187–201, 1981.

[11] S. Sigawi, M. Nisnevitch, O. Zakalska, A. Zakalskiy, Y. Nitzan, and M. Gonchar, "Bioconversion of airborne methylamine by immobilized recombinant amine oxidase from the thermotolerant yeast *Hansenula polymorpha*," *The Scientific World Journal*, vol. 2014, Article ID 898323, 9 pages, 2014.

[12] X. P. Sun, Z. L. Zhang, B. L. Zhang, X. D. Dong, S. J. Dong, and E. K. Wang, "Preparation of gold nanoparticles protected with polyelectrolyte," *Chinese Chemical Letters*, vol. 14, no. 8, pp. 866–869, 2003.

[13] J. Hong, W. Wang, K. Huang et al., "A highly efficient nanocluster artificial peroxidase and its direct electrochemistry of a nano complex modified glassy carbon electrode," *Analytical Science*, vol. 28, no. 7, pp. 711–716, 2012.

[14] N. Stasyuk, R. Serkiz, S. Mudry et al., "Recombinant human arginase I immobilized on gold and silver nanoparticles: preparation and properties," *Nanotechnology Development*, vol. 1, no. 1, article e3, 2011.

[15] J. B. Knaak, H. W Leung, W. T. Stott, J. Busch, and J. Bilsky, "Toxicology of mono-, di-, and triethanolamine," in *Reviews of Environmental Contamination and Toxicology*, vol. 149, pp. 1–86, Springer, New York, NY, USA, 1997.

[16] J. R. Treberg, J. S. Bystriansky, and W. R. Driedzic, "Temperature effects on trimethylamine oxide accumulation and the relationship between plasma concentration and tissue levels in smelt (Osmerus mordax) Journal of Experimental Zoology A," *Comparative Experimantal Biology*, vol. 303, no. 4, pp. 283–293, 2005.

Hindawi Publishing Corporation
BioMed Research International
Volume 2014, Article ID 461728, 14 pages
http://dx.doi.org/10.1155/2014/461728

Research Article

Characterization and Potential Use of Cuttlefish Skin Gelatin Hydrolysates Prepared by Different Microbial Proteases

Mourad Jridi,[1] Imen Lassoued,[1] Rim Nasri,[1] Mohamed Ali Ayadi,[2] Moncef Nasri,[1] and Nabil Souissi[3]

[1] *Laboratoire de Génie Enzymatique et de Microbiologie, Ecole Nationale d'Ingénieurs de Sfax, Université de Sfax, B.P. 1173, 3038 Sfax, Tunisia*
[2] *Laboratoire d'Analyse Alimentaire, Ecole Nationale d'Ingénieurs de Sfax, Université de Sfax, B.P. 1173, 3038 Sfax, Tunisia*
[3] *Laboratoire de Biodiversité et de Biotechnologie Marine, Centre de Sfax, Institut National des Sciences et Technologies de la Mer, B.P. 1037, 3018 Sfax, Tunisia*

Correspondence should be addressed to Mourad Jridi; jridimourad@gmail.com

Received 27 February 2014; Accepted 23 April 2014; Published 15 June 2014

Academic Editor: Noomen Hmidet

Composition, functional properties, and *in vitro* antioxidant activities of gelatin hydrolysates prepared from cuttlefish skin were investigated. Cuttlefish skin gelatin hydrolysates (CSGHs) were obtained by treatment with crude enzyme preparations from *Bacillus licheniformis* NH1, *Bacillus mojavensis* A21, *Bacillus subtilis* A26, and commercial alcalase. All CSGHs had high protein contents, 74.3–78.3%, and showed excellent solubility (over 90%). CSGH obtained by alcalase demonstrated high antioxidant activities monitored by β-carotene bleaching, DPPH radical scavenging, lipid peroxidation inhibition, and reducing power activity. Its antioxidant activity remained stable or increased in a wide range of pH (1–9), during heating treatment (100°C for 240 min) and after gastrointestinal digestion simulation. In addition, alcalase-CSGH was incorporated into turkey meat sausage to determine its effect on lipid oxidation during 35 days of storage period. At 0.5 mg/g, alcalase-CSGH delayed lipid oxidation monitored by TBARS and conjugated diene up to 10 days compared to vitamin C. The results reveal that CSGHs could be used as food additives possessing both antioxidant activity and functional properties.

1. Introduction

Gelatin is a protein obtained from collagen by heat denaturation. Most commercial gelatins are derived from the skins, hides, and bones of bovine and porcine [1]. Fish skin might be an alternative raw material for gelatin production, because of bovine problems and religions that prohibit the use of porcine. Recently, skin gelatin from various fish species such as grey triggerfish (*Balistes capriscus*) [2], unicorn leatherjacket (*Aluterus monoceros*) [1], brownbanded bamboo shark (*Chiloscylium puntacum*) and blacktip shark (*Carcharhinus limbatus*) [3], and cuttlefish (*Sepia officinalis*) [4] has been extracted and characterized. Gelatin is widely used in food, pharmaceutical, cosmetic, and photographic applications because of its unique chemical and physical characteristics [2]. Furthermore, gelatin may also be used to produce biologically active peptides by protease hydrolysis. Many studies have demonstrated that the enzymatic hydrolysis of proteins improved their functional properties, including solubility, emulsification, and foaming ability, and their biological activities [5]. In this context, fish gelatin hydrolysates having antihypertensive and antioxidant activities have been reported [6].

On the other hand, one of the major problems in food factories is the lipid oxidation which causes food quality deterioration and shortening of shelf life. This unwanted process not only produces offensive odors and flavors but also decreases the nutritional quality and safety of food by forming secondary reaction products, which could reduce the shelf life of food products [7]. Furthermore, consuming oxidative foods is thought to cause serious diseases (heart disease, cancer, stroke, and diabetes). To prevent oxidative

deterioration of foods and to provide protection against serious diseases, it is important to inhibit lipids oxidation and free radicals formation occurring in the food stuff and living body. Antioxidants are used to preserve food products by retarding discoloration and deterioration as a result of oxidation. Synthetic antioxidants such as BHT (butylated hydroxytoluene) and BHA (butylated hydroxyanisole) have a strong antioxidant activity, but their use was restricted because of their potential health hazards. Therefore, there is a growing interest to study antioxidative properties in natural sources including some dietary protein compounds.

Bioactive peptides from collagen and gelatin with antioxidant properties have become a topic of great interest for health food and processing/preservation industries [3, 8]. Further, gelatin hydrolysates from brownstripe red snapper (*Lutjanus vita*) skin [9] and from giant squid (*Dosidicus gigas*) tunics [10] have been reported to exhibit antioxidant activity.

Those works become easier, especially with the recent development of *in vitro* methods for simulating the human digestive tract since they are rapid and safe and do not have the same ethical restrictions as *in vivo* methods [11].

The aim of this investigation was to produce cuttlefish-skin gelatin hydrolysates with different DHs obtained by using several proteases and to study their compositions, antioxidant activities and stability, and water and oil-holding properties. In addition, to test the antioxidant stability of hydrolysates, pH and thermal treatments were also investigated. Then, *in vitro* digestion model system was used to simulate the process of human gastrointestinal digestion (HGID) and to evaluate antioxidant stability using various tests. Furthermore, gelatin hydrolysate showing the strongest antioxidant activities was selected for antioxidant assessment against lipid deterioration in cooked turkey meat sausage during 35 days of storage.

2. Materials and Methods

2.1. Materials. 1,1-Diphenyl-2-picrylhydrazyl (DPPH), bile salt, butylated hydroxyanisole (BHA), β-carotene, α-tocopherol, glycine, ammonium sulphate, and linoleic acid were purchased from Sigma Chemical Co. (St. Louis, MO, USA). Pepsin was purchased from MP Biomedicals (France). Thiobarbituric acid (TBA) was purchased from Suvchem (MH, India). Modified starch (E1422) was provided from Sigma Chemical CO., St Louis, MO. Potassium ferricyanide, trichloroacetic acid (TCA), ferrous chloride, ferrozine, sodium hydroxide, Tween 40, NaCl, $NaNO_2$, and tripolyphosphate (TPP) were of analytical grade.

2.2. Cuttlefish Skin Preparation. Cuttlefish by-products were obtained from marine processing industry "IMPEX" located in Sfax city, Tunisia. The samples were packed in polyethylene bags, placed in ice with a sample/ice ratio of approximately 1 : 3 (w/w). They were washed twice with water to eliminate the dark ink, which consists of a suspension of melanin granules in a viscous colorless medium. Finally, cuttlefish outer skin was collected and then stored in sealed plastic bags at −20°C until used for gelatin extraction and analysis.

2.3. Enzyme Preparation. Alcalase 2.4 L serine-protease from *Bacillus licheniformis* was supplied by Novozymes (Bagsvaerd, Denmark). Crude enzyme preparations from *Bacillus licheniformis* NH1 [12], *Bacillus mojavensis* A21 [13], and *Bacillus subtilis* [14] were prepared in our laboratory. To measure alkaline protease activity, one unit of protease activity was defined as the amount of enzyme required to liberate 1 μg of tyrosine per minute under the experimental conditions used.

2.4. Gelatin Extraction. In order to remove noncollagenous proteins, washed skins were first soaked in 0.05 M NaOH with a skin/solution ratio of 1/10 (w/v) for 2 h at 4°C and the solution was changed every 30 min. The alkaline-treated skins were then washed with cold tap water until neutral pH wash water was obtained. The alkaline-treated skins cuttlefish were soaked in 0.1 M acetic acid with a solid/solvent ratio of 1 : 10 (w/v) and subjected to hydrolysis with pepsine at 15 units/g alkaline-treated skin as described by Jridi et al. [4]. The mixtures were stirred for 48 h at 4°C. To inactivate enzymes, the pH of the mixture was then raised to 7.5 using 10 M NaOH and stirred gently for 1 h at 4°C. Enzymatic-treated skin mixture was then incubated at 40°C for 18 h with continuous stirring to extract the gelatin from the skin.

The mixtures were centrifuged at 10000 g for 30 min using a refrigerated centrifuge to remove insoluble material. The supernatant was collected and freeze-dried (Bioblock Scientific Christ ALPHA 1-2, IllKirch-Cedex, France). The powder obtained referred to as cuttlefish-skin gelatin (CSG) was stored at 4°C until used.

2.5. Production of Gelatin Hydrolysates. The skin gelatin was dissolved in distilled water (1%; w/v) and subjected to enzymatic hydrolysis for 3 h under optimal temperature and pH conditions with an enzyme/substrate ratio of 30/1 (U/mg). The optimal conditions were as follows: alcalase (pH 8.0, 50°C), A21 proteases (pH 8.5, 50°C), A26 proteases (pH 8.0, 45°C), and NH1 proteases (pH 10.0, 50°C). The gelatin solutions were allowed to equilibrate for 30 min before hydrolyses were initiated. Enzymes were used at the same activity levels to compare hydrolytic efficiencies. During the reaction, the pH of the mixture was maintained constant by continuous addition of NaOH 4 N. To inactivate enzymes, the solution was heated for 20 min at 80°C.

Finally, the solutions were then centrifuged at 5000 g for 20 min and soluble fractions were freeze-dried and stored at −20°C for further use. The degree of hydrolysis (DH), defined as the percent ratio of the number of peptide bonds broken to the total number of peptide bonds in the protein substrate, was determined according to Adler-Nissen [15].

2.6. Chemical Analysis. The moisture, ash, and fat contents of CSG and CSGHs powder were determined according to the AOAC methods [16]. The protein content was determined by Kjeldahl method according to the AOAC method. A factor of 5.5 was used to convert the nitrogen value to protein [16]. All measurements were performed in triplicate.

Analyses of calcium (Ca^{2+}), magnesium (Mg^{2+}), sodium (Na^{+}), potassium (K^{+}), chlorure (Cl^{-}), nitrate ($NO_3{}^{-}$), and sulphate ($SO_4{}^{2-}$) contents in freeze-dried hydrolysates were carried out using the inductively coupled plasma optical emission spectrophotometer (ICP-OES) (model 4300 DV, Perkin Elmer, Shelton, CT, USA) according to the method of AOAC [16]. Sample (1 g) was mixed with 1 mL of 70% (v/v) nitric acid. The mixture was heated on the hot plate until digestion was completed. The digested sample was transferred to a volumetric flask and the volume was made up to 10 mL with deionized water. The solution was then subjected to analysis.

In order to determine the amino acid composition, CSG and CSGHs were dissolved in distilled water at 1 mg/mL and 50 μL of each sample was dried and hydrolysed in vacuum-sealed glass tube at 110°C for 24 h in the presence of constant boiling 6 N HCl containing 1% (w/v) phenol and using norleucine as internal standard. After hydrolysis, samples were again vacuum-dried, dissolved in application buffer, and injected into a Beckman 6300 amino acid analyzer (Beckman Instruments Inc., Fullerton, California, USA).

2.7. Functional Properties of CSGHs

2.7.1. Solubility. Solubility of CSG and CSGHs was carried out over a wide range of pH values from 2.0 to 11.0 as described by Tsumura et al. [17], with slight modifications. Briefly, 200 mg of freeze-dried hydrolysates of cuttlefish gelatin was suspended in 20 mL deionized distilled water and the pH of the mixture was adjusted to different values using either 2 N HCl or 2 N NaOH solutions. The mixtures were stirred for 10 min at room temperature (25 ± 1°C) and then centrifuged at 8000 g for 10 min. After appropriate dilution, the nitrogen content in the supernatant was determined by Biuret method. The nitrogen solubility of the CSGHs, defined as the amount of soluble nitrogen from the total nitrogen, was calculated as follows:

$$\text{Nitrogen solubility (\%)} = \frac{\text{Supernatant nitrogen concentration}}{\text{Sample nitrogen concentration}} \times 100. \quad (1)$$

2.7.2. Emulsifying Properties. The emulsifying activity index (EAI) and the emulsion stability index (ESI) of the CSG and CSGHs were determined according to the method of Pearce and Kinsella [18] with a slight modification. Gelatin hydrolysate solutions were prepared by mixing freeze-dried CSGHs in distilled water (pH = 7) for 30 min at 60°C with different concentrations (0.1, 0.5, and 1% (w/v)). Thirty milliliters of each CSGH solutions was homogenized with 10 mL of soybean oil for 1 min at room temperature (25 ± 1°C) using Moulinex R62 homogenizer. Aliquots of the emulsion (50 μL) were pipetted from the bottom of the container at 0 and 10 min after homogenization and diluted 100-fold with 0.1% SDS solution. The absorbance of the diluted solutions was measured at 500 nm. The absorbances measured immediately (A_0) and 10 min (A_{10}) after emulsion formation were used to calculate the emulsifying activity index (EAI) and the emulsion stability index (ESI). All determinations are means of at least three measurements. Consider

$$\text{EAI}\left(\text{m}^2/\text{g}\right) = \frac{2 \times 2.303 \times A_0 \times N}{\varphi \times C \times 10,000}, \quad (2)$$

where N represents a dilution factor, C is the weight of protein per unit volume (g/mL), and φ is the oil volumetric fraction (0.25).

ESI represents the difference of EAI at 0 and 10 min at 500 nm and was calculated using the next formula:

$$\text{ESI (min)} = \frac{A_0 \times \Delta T}{\Delta A}. \quad (3)$$

2.7.3. Foaming Properties. Foam expansion (FE) and foam stability (FS) of CSGHs were determined according to the method of Shahidi et al. [19], with a slight modification. Twenty milliliters (V_0) of protein hydrolysate solution at different concentrations (0.1%, 0.5%, and 1%) (w/v) was homogenized, using a Moulinex R62 homogenizer, to incorporate air for 1 min at room temperature (25 ± 1°C). The whipped sample was then immediately poured into a 50 mL graduated cylinder, and the total volume was measured (V_1). Foam capacity was expressed as foam expansion after homogenization, which was calculated according to the following equation:

$$\text{FE (\%)} = \frac{V_1 - V_0}{V_0} \times 100. \quad (4)$$

Foam stability was calculated as the volume of foam remaining after 30 min at room temperature (V_2). Consider

$$\text{FS (\%)} = \frac{V_2 - V_0}{V_0} \times 100. \quad (5)$$

2.7.4. Fat Absorption and Water Holding Capacity. The ability of the CSGHs to absorb fat was determined as described by Shahidi et al. [19] with a slight modification. A 0.5 g of dried CSGH was mixed with 10 mL of corn oil in a 50 mL centrifuge tube. The mixture was kept for 30 min at room temperature (25 ± 1°C) with mixing every 10 min and then centrifuged for 25 min at 2000 g.

The water holding capacity (WHC) of CSGHs was determined according to the method of Okezie et al. [20] with slight modifications. The sample (1 g) was dispersed in 50 mL of distilled water and mixed for 2 min. The mixture was kept at room temperature for 30 min and then centrifuged for 30 min at 5000 g. The two supernatants were filtered with Whatman N°1 filter paper and the volume recovered was measured. The difference between initial volume of distilled water or oil added to the protein sample and the volume of the supernatant was determined, and results were reported as milliliters of water or fat absorbed per gram of CSGHs.

2.8. Determination of Antioxidative Activities

2.8.1. DPPH Free Radical-Scavenging Assay. The DPPH free radical-scavenging activity of CSGHs was determined as

described by Bersuder et al. [21]. A volume of 500 μL of each sample at different concentrations (0.5 to 5 mg/mL) was mixed with 500 μL of 99.5% ethanol and 125 μL of 0.02 mM DPPH in 99.5% ethanol. The mixtures were then kept for 60 min in dark at room temperature, and the reduction of DPPH radical was measured at 517 nm using a UV-Visible spectrophotometer. The control was conducted in the same condition, except that distilled water was used instead of sample. DPPH radical-scavenging activity was calculated as follows:

$$\text{DPPH free radical-scavenging activity (\%)} = \left(\frac{A_c - A_h}{A_c}\right) \times 100, \quad (6)$$

where A_c is the absorbance of the control reaction and A_h is the absorbance of the hydrolysates. A lower absorbance of the reaction mixture indicated a higher DPPH radical-scavenging activity. Butylated hydroxyanisole (BHA) was used as a standard. The test was carried out in triplicate.

2.8.2. Reducing Power. The sample solution (0.5 mL) at different protein concentrations (0.5 to 5 mg/mL) was mixed with 2.5 mL of 0.2 M phosphate buffer (pH 6.6) and 2.5 mL of 1% potassium ferricyanide. The mixture was incubated at 50°C for 20 min. An aliquot (2.5 mL) of 10% trichloroacetic acid was added to the mixture, followed by centrifugation at 3,000 g for 10 min. The upper layer of solution (2.5 mL) was mixed with 2.5 mL of distilled water and 2.5 mL of 0.1% ferric chloride and the absorbance was read at 700 nm.

2.8.3. DNA Nicking Assay. DNA nicking assay was performed using pCRII TOPO plasmid (invitrogen). A mixture of 10 μL of gelatin hydrolysates at the concentration of 2 mg/mL and plasmid DNA (0.5 μg/well) were incubated for 10 min at room temperature followed by the addition of 10 μL of Fenton's reagent (30 mM H_2O_2, 50 μM L-ascorbic acid, and 80 μM $FeCl_3$). The mixture was then incubated for 5 min at 37°C. The DNA was analysed on 1% (w/v) agarose gel using ethidium bromide staining.

2.9. Determination of Antioxidative Activities in Model Systems

2.9.1. β-Carotene-Linoleate Bleaching Model System. The ability of CSGHs to prevent bleaching of β-carotene was assessed as described by Koleva et al. [22]. In brief, 0.5 mg β-carotene in 1 mL chloroform was mixed with 25 μL of linoleic acid and 200 μL of Tween-40. The chloroform was completely evaporated under vacuum in a rotatory evaporator at 40°C; then, 100 mL of bidistilled water was added, and the resulting mixture was vigorously stirred. The emulsion obtained was freshly prepared before each experiment. Aliquots (2.5 mL) of the β-carotene-linoleic acid emulsion were transferred to test tubes containing 0.5 mL of each CSGH (0.5 to 5 mg/mL). The tubes were immediately placed in water bath and incubated at 50°C for 2 h. The absorbance of each sample was then measured at 470 nm. A control consisted of 0.5 mL of distilled water instead of the sample solution. BHA (butylated hydroxyanisole) was used as positive standard. The antioxidant activity of the hydrolysates was evaluated in terms of bleaching of β-carotene using the following formula:

$$\text{Inhibition (\%)} = \left(1 - \frac{A_{0s} - A_{120s}}{A_{0c} - A_{120c}}\right) \times 100, \quad (7)$$

where A_{0s} and A_{0c} are the absorbances measured at initial time of incubation. A_{120s} and A_{120c} are the absorbances after 120 min of incubation of the sample and the control, respectively.

2.9.2. Inhibition of Linoleate-Autoxidation Model System. Inhibition activity of *in vitro* lipid peroxidation of CSGHs was determined by assessing their ability to inhibit oxidation of linoleic acid in an emulsified model system [23]. Briefly, freeze-dried gelatin hydrolysates at different concentrations (0.5, 1, 2, 3, 4, and 5 mg/mL) were dissolved in 2.5 mL of 50 mM phosphate buffer (pH = 7.0) and added to 2.5 mL of 50 mM linoleic acid in ethanol (95%). The final volume was then adjusted to 6.25 mL with distilled water.

The obtained mixture was incubated in a 10 mL tube with silicone rubber caps at 45°C for 8 days in dark and the degree of oxidation was evaluated by measuring the ferric thiocyanate values. An aliquot of reaction mixture (0.1 mL) was mixed with 4.7 mL of 75% ethanol followed by the addition of 0.1 mL of 30% ammonium thiocyanate and 0.1 mL of 20 mM ferrous chloride solution in 3.5% HCl. After stirring for 3 min, the degree of color development was measured at 500 nm. α-Tocopherol was used as reference and control reaction was conducted without sample. The percentage of oxidation inhibition was expressed as follows:

$$\text{Inhibition (\%)} = \left(1 - \frac{A_{500} \text{ of sample}}{A_{500} \text{ of control}}\right) \times 100. \quad (8)$$

2.10. Stability of Gelatin Hydrolysate

2.10.1. pH Stability. CSGH was dissolved in 10 mL of distilled water at 50 mg/mL of protein concentration; then, the pH was adjusted from 1 to 9 using 1 M HCl or 1 M NaOH and the volume of solution was made up to 25 mL with distilled water. The mixtures were incubated at room temperature (25 ± 2°C) for 1 h. The pH of the mixtures was then adjusted to 7.0 and their volumes were made up to 50 mL with distilled water. The residual antioxidant activities were tested using the β-carotene-linoleate bleaching model, DPPH free radical scavenging, and reducing power assays and expressed as the relative activity (%) to those obtained without pH adjustment.

2.10.2. Thermal Stability. CSGH was dissolved in 10 mL of distilled water at a protein concentration of 50 mg/mL; then, pH of gelatin hydrolysate solution was adjusted to 7 and the volume of solution was made up to 50 mL with distilled water. Ten milliliters of the CSGH solution was transferred to screw-capped test tube and placed in a boiling water bath (100°C) for 0, 15, 30, 60, 120, 180, and 240 min. Then, the tubes were immediately cooled in iced water. The residual antioxidant

activities were tested using the β-carotene-linoleate bleaching model, DPPH free radical scavenging, and reducing power assays and were expressed as relative activity (%) compared to those without heat treatment.

2.10.3. In Vitro Gastrointestinal Digestion (GID). The effect of *in vitro* gastrointestinal digestion of CSGH was evaluated as described by Enari et al. [24] with slight modifications. Briefly, 100 mL of CSGH solution (10 mg/mL) was mixed with 10 mL of phosphate buffer (10 mM, pH = 6.8) and incubated for 2 min at 37°C. Then, 0.5 mL of HCl-KCl buffer (1 M, pH = 1.5) was added to produce an acidic condition, followed by adding 32 U/mL of pepsin solution in 1 M HCl-KCl buffer (pH 1.5) and incubating for 60 min at 37°C (stomach condition). The pH was adjusted to 6.8 with 1 M $NaHCO_3$ (1 mL), and the enzyme mixture of bile and pancreatic juice (1 mL) that contained pancreatin (10 mg/mL), trypsin (14,600 U/mL), and bile extract (13.5 mg/mL) in 10 mM phosphate buffer (pH = 8.2) was added to the solution, followed by incubation at 37°C for 3 h to create duodenal condition. To inactivate duodenal enzymes, the test tubes were kept in boiling water for 10 min. The antioxidant activities were tested using the β-carotene-linoleate bleaching model, DPPH free radical scavenging, and reducing power assays, during the digestion after 0 (control), 30, 60, 120, 180, and 240 min.

2.11. Effect of Gelatin Hydrolysate on Turkey Meat Sausage Lipid Oxidation. Turkey sausage products were formulated using mechanically separated turkey (MST) meat obtained from local processors (Chahia, Sfax, Tunisia). Sausage was prepared as described by Ayadi et al. [25], with slight modification. Dry ingredients such as salt, carrageen, and modified starch were slowly added to the ground MST as powders while processing. Then, cold water was incorporated. The addition of ingredients took less than 5 min at 10°C. The batters were manually stuffed in collagen reconstituted casing and then were heated in a temperature controlled water bath at 90°C until a final internal temperature of 74°C was reached.

After cooling to room temperature, the cooked turkey sausage (placed in polyethylene bag) and the turkey meat sausages were stored at 4°C. The extent of lipid oxidation in each meat sample was determined by the thiobarbituric acid reactive substances (TBARS) assay and the conjugated diene as described by Hogan et al. [26]. The final TBARS value was expressed as mg of malondialdehyde (MDA) equivalents per kg of sample.

2.12. Statistical Analysis. Statistical analyses were performed with SPSS version 2.0, professional edition using ANOVA analysis. All results were given as mean value standard deviation of three separate experiments. Differences were considered significant at $P < 0.05$.

3. Results and Discussion

3.1. Preparation of CSGHs Using Various Proteases. Biological activities of proteins can be increased through hydrolysis with some enzymes, and some peptides or fractions possess stronger activities than others [8]. Thus, gelatin from cuttlefish skin (*Sepia officinalis*), previously extracted [4], was subjected to enzymatic hydrolysis using various proteases: alcalase and crude proteases preparations from *B. mojavensis* A21, *B. subtilis* A26, and *B. licheniformis* NH1.

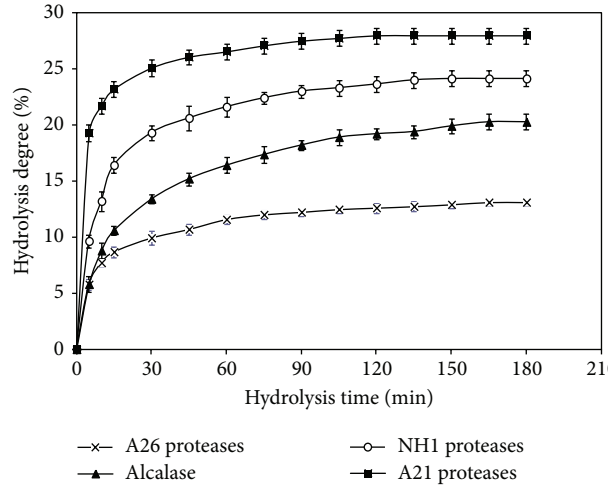

Figure 1: Degree of hydrolysis (DH) of CSGHs during hydrolysis with alcalase, NH1, A21, and A26 proteases at 30 U enzyme/mg substrate. Bars represent standard deviations from triplicate determinations.

After 3 h of hydrolysis, the DHs reached were about 20.3, 26.9, 24.1, and 12.7% with alcalase and crude enzyme preparations from A21, NH1, and A26, respectively. As reported in Figure 1, proteases from *B. mojavensis* A21 showed the highest DH values for cuttlefish gelatin hydrolysis, while crude proteases from *B. subtilis* A26 were the least efficient ($P < 0.05$). The shape of the hydrolysis curves is similar to those previously reported for hydrolysates from muscle of goby [27], sardinelle [28], zebra blenny [29], and gelatin hydrolysates obtained from skin of sole and squid [30].

3.2. Chemical and Amino Acid Composition of CSGHs. As shown in Table 1, ash contents ranged between 9.94% and 14.22%; this may be due to the continual addition of NaOH during hydrolysis step. The analysis of mineral content revealed that Na^+, K^+, and Cl^- were major inorganic matter in CSGHs, while NO_3^-, Ca^{2+}, Mg^{2+}, and SO_4^{2-} were found at a low level. Sathivel et al. [31] reported that K^+, Mg^{2+}, Na^+, and Ca^{2+} were abundant in herring and herring by-product hydrolysates and varied with the substrate used.

Gelatin hydrolysates have a high protein content (NH1-CSGH: 74.3%; A21-CSGH: 75.9%; A26-CSGH: 76.3%; and alcalase-CSGH: 78.3%). The high protein content was a result of the solubilization of proteins during hydrolysis, the removal of insoluble undigested nonprotein substances, and partial removal of lipid after hydrolysis [32]. Generally, alkaline proteases exhibited a greater capability to solubilize fish proteins compared to neutral and acidic proteases, with exception of pepsin. Interestingly, all CSGHs had lower levels of lipid compared with salmon protein hydrolysates [32].

Table 1: Proximate composition (g/100 g dry matter) and mineral content (μg/g) of CSGHs.

	Alcalase-CSGH	NH1-CSGH	A26-CSGH	A21-CSGH
Moisture (%)	9.62 ± 0.002^{b}	8.34 ± 0.32^{c}	10.32 ± 0.076^{a}	7.92 ± 0.81^{d}
Ash (%)	10.22 ± 0.003^{c}	13.87 ± 0.015^{b}	9.94 ± 0.01^{c}	14.22 ± 0.026^{a}
Fat (%)	0.35 ± 0.01^{c}	0.72 ± 0.02^{a}	0.50 ± 0.03^{b}	0.45 ± 0.01^{b}
Protein (%)	78.34 ± 0.12	74.29 ± 0.3	76.33 ± 0.27	75.94 ± 0.22
Mineral content (μg/g)				
Ca^{2+}	74^{d}	84^{b}	96^{a}	77.1^{c}
Na^{+}	360^{b}	384.4^{a}	334.5^{c}	390.7^{a}
K^{+}	827^{d}	1100.2^{a}	990^{c}	1021^{b}
Mg^{2+}	104^{a}	95^{b}	101^{a}	95^{b}
Cl^{-}	168^{b}	170^{c}	169.1^{b}	190.1^{a}
NO_3^{-}	25.5^{d}	33.6^{b}	34.4^{a}	32.4^{c}
SO_4^{2-}	36.5^{a}	24^{d}	31.5^{b}	29.3^{c}

[a,b] Different letters in the same line indicate significant differences ($P \leq 0.05$).

The amino acid composition of CSGHs, expressed as residues per 1000 residues, is shown in Table 2. The amino acid composition of CSGHs was similar to the undigested gelatin. The most abundant amino acids were Gly (>32%), Hyp, Pro, Glx, Ala, Asp, and Arg. Generally, the amino acid composition of gelatin hydrolysates is very similar to the parent proteins, being rich in residues of Gly, Ala, Pro, Hyp, Glx, and Asx but poor in Met, Cys, His, and Tyr [8].

The total number of imino acid (Pro and Hyp) residues (between 185 and 194 residues per 1000 residues) was higher than that of collagen from cold-water fish species (16–18%) [33]. Hyp plays a key role in stabilizing the triple stranded collagen helix through the hydrogen bonding ability of its hydroxyl group. Based on total amino acids, essential amino acids made up 12.96%, 13.64%, 13.06%, and 13.33% of A26, NH1, A21, and alcalase-CSGH, respectively. Therefore, they could serve as an excellent source of useful nutrients. Pro and Ala were the most abundant hydrophobic amino acids in all of the gelatin hydrolysates. The alcalase-CSGH had the highest values of Pro, though the ratio with respect to the total hydrophobic amino acid content was steady. Hydrophobic amino acids have been observed in several antioxidant peptide sequences, and Mendis et al. [34] have suggested that the presence of hydrophobic amino acids in the peptide sequences in jumbo squid skin gelatin contributed greatly to its antioxidant properties.

3.3. Functional Properties. Functional properties influence the usefulness of an ingredient in food and govern the physical behavior during preparation, processing, and storage.

3.3.1. Solubility. All CSGHs presented typical bell-shaped solubility curves with minimum solubility at pH 5, whereas solubility above 95% was noticeable at the other pH values. However, undigested gelatin showed minimum solubility at pH 6 (data not shown). The solubility increases with the increase of the degree of hydrolysis. At pH = 8.0, the solubility of alcalase-CSGH (DH = 20.26%), NH1-CSGH (DH = 24.12%), A21-CSGH (DH = 26.9%), and A26-CSGH (DH = 12.7%) reached about 97.39, 98, 99, and 96.5%, respectively, significantly higher ($P < 0.05$) than that of CSG (94.5%). It has been suggested that an increase in solubility of protein hydrolysates is due to the reduction of the molecular size and also due to the enzymatic release of smaller polypeptide units from the protein. The smaller peptides are expected to have proportionally more polar residues, with the ability to form hydrogen bonds with water and increase solubility [35].

3.3.2. Emulsifying Properties. Emulsifying activity index (EAI) and emulsion stability index (ESI) of CSG and gelatin hydrolysates at various concentrations (0.1%, 0.5%, and 1%) are shown in Table 3. Results show that the EAI of CSGH was remarkably higher than that obtained with nondigested gelatin (CSG). Best results were obtained by A21 proteases. The increase of EAI using CSGH may be due to lower molecular-weight peptides or partially hydrolyzed gelatin. In addition, EAI values of all CSGH significantly decreased with increasing concentration ($P < 0.05$). Furthermore, the ESI of CSGH and CSG was measured. Results show that the emulsion stability was remarkably high with undigested gelatin. Several authors have described the decrease of emulsifying ability with increasing protein concentration for other fish proteins such as soluble collagen from the skin of sole and squid [30].

Although, in general, a positive relationship between peptide length and emulsifying properties has been reported [5], according to Kristinsson and Rasco [32] there is no clear connection between peptide size and emulsification, suggesting that the physicochemical makeup of the peptides may play an important role in the functional properties. Thus, similar values (240 m^2/g protein) were found for EAI in both squid and sole hydrolysates at 0.5% ($P > 0.05$). Finally, a concentration of 0.1% of CSGH can be used to possess a higher index of emulsifying activity and emulsifying stability. Protein hydrolysates are surface-active materials and promote an oil-in-water emulsion because of their hydrophilic and hydrophobic groups and their charge [32, 35].

Table 2: Amino acid composition of CSGHs (number of residues/1000 residues).

Amino acids	CSG	A26-CSGH	NH1-CSGH	A21-CSGH	Alcalase-CSGH
Asx[a]	63	62	61	62.5	60
Thr[b]	23	22	24.6	22.4	22
Ser	49	45	44	42.3	40.7
Glx[a]	92	98	96.4	97.4	89.4
Gly	321	320	316	317	318
Ala	81	87.3	85.4	98.6	97.4
Val[b]	22	12	13.6	13.5	12.1
Met[b]	6	6.3	6.4	6.9	7.1
Ile[b]	22	22.6	23.4	22.1	23.1
Leu[b]	29	19.7	20.4	18.7	20
Try	5	5.9	6.2	6.1	5.8
Phe[b]	10	9.6	9.9	9.3	9.4
His[b]	18	15	14	14	17
Lys[b]	13	32	34	33	32
Arg	51	53.6	52.7	51.2	52
Cys	0	0	0	0	0
Pro	96	92	94	90	98
Hyp	84	97	98	95	96
TAA[c]	1000	1000	1000	1000	1000
THAA[c]	587.0	569.5	569.1	576.1	585.1
TEAA/TAA (%)[c]	14.3	13.92	14.63	13.99	14.27

[a]The aspartic and glutamic acid contents include, respectively, asparagines and glutamine, Asx = Asp + Asn; Glx = Glu + Gln.
[b]Essential amino acids.
[c]TAA = total amino acids; THAA = total hydrophobic amino acids; TEAA = total essential amino acids.

3.3.3. Foaming Properties. Foaming properties are physicochemical characteristics of proteins to form and stabilize foams [36]. Foam expansion (FE) and foam stability (FS) of CSGHs and the control at various concentrations (0.1, 0.5, and 1%) are shown in Table 3.

At the same concentration of hydrolysate used, slight decreases in FE were observed when DH of hydrolysate increased ($P < 0.05$). With the same protein concentration, DH had significant effect ($P > 0.05$) on FE, so the increasing of DH decreases the foaming capacity. At 0.1%, the foaming expansion of alcalase-CSGH (DH = 20.26%), NH1-CSGH (DH = 24.12%), A21-CSGH (DH = 26.9%), and A26-CSGH (DH = 12.7%) reached about 125.1, 126.4, 120, and 131%, respectively. Shahidi et al. [19] reported good foaming properties for capelin protein hydrolysates at low DH (12%). Foam formation is governed by three factors, including transportation, penetration, and reorganization of molecules at the air-water interface [37].

Results show also that the higher foaming stability value was found with A21-CSGHs at different concentrations. The results reveal that when degree of hydrolysis of gelatin increases, the foaming stability decreases. All the CSGHs with a concentration of 1% showed the highest foam stability (Table 3). The stability of foams is a consequence of the well-ordered orientation of the molecules at the interface, where the polar head is located in the aqueous phase and the hydrophobic chain faces the apolar component [38].

3.3.4. Water and Oil-Holding Capacity. Water-holding capacity (WHC) and oil-holding capacity (OHC) are reported in Table 4. OHC and WHC express the quantity of oil and water, respectively, directly bound by the protein and are of great interest, especially in the meat and confectionary industries [35]. As shown in Table 4, A26-CSGH (DH = 12.7%) had significantly higher OHC (4.9 mL oil/g hydrolysate) followed by alcalase-CSGH (DH = 20.26%, 3.1 mL oil/g hydrolysate), NH1-CSGH (DH = 24.12%, 2.6 mL oil/g hydrolysate), and A21-CSGH (DH = 26.9%, 2.4 mL oil/g hydrolysate); this may be attributed to the larger particle sizes in low hydrolyzed proteins.

A decrease in OHC with DH increase has been reported for red salmon head protein hydrolysis [31]. Additionally, WHC increases when the DH increases; for example, A21-CSGH had significantly the highest WHC.

3.4. Antioxidant Activity of Cuttlefish Gelatin Hydrolysates. In order to evaluate the antioxidant activity of the cuttlefish gelatin hydrolysates, various antioxidant tests were conducted, including 1,1-diphenyl-2-picrylhydrazyl (DPPH) free radical-scavenging activity, ferric reducing antioxidant power, and inhibition of supercoiled plasmid DNA scission.

Free radical scavenging is a primary mechanism by which antioxidants inhibit oxidative processes. DPPH is a stable free radical that shows maximum absorbance at 517 nm. When DPPH radicals encounter a proton-donating substrate such as an antioxidant, the radicals would be scavenged

Table 3: Emulsion activity index (EAI), emulsion stability index (ESI), foam expansion (FE), and foam stability (FS) of cuttlefish skin gelatin hydrolysates at various concentrations.

	Concentration % (g/100 mL)	EAI (m^2/g)	ESI (min)	FE (%)	FS (%)
CSG	0.1	15.21 ± 0.2^{dC}	53.29 ± 0.8^{aA}	100.23 ± 0.9^{dC}	49.6 ± 1.2^{dC}
	0.5	17.22 ± 0.2^{dB}	51.28 ± 0.1^{aB}	103.44 ± 0.5^{eB}	83.1 ± 10.0^{aB}
	1	23.67 ± 0.3^{aA}	49.14 ± 0.8^{aB}	113.7 ± 1.53^{dA}	105.3 ± 0.32^{aA}
Alcalase-CSGH	0.1	58.21 ± 1.2^{bA}	25.21 ± 0.9^{cA}	125.1 ± 5.1^{bB}	65.1 ± 5.5^{bB}
	0.5	33.12 ± 0.8^{aB}	18.95 ± 0.75^{bcB}	125 ± 4.7^{cB}	68 ± 4.9^{cB}
	1	10.24 ± 0.2^{bC}	14.01 ± 0.7^{dC}	129.2 ± 3.1^{bA}	84 ± 4.8^{bA}
NH1-CSGH	0.1	48.01 ± 2.1^{cA}	18.14 ± 1.6^{dA}	126.4 ± 4.7^{bB}	60.3 ± 3.7^{cC}
	0.5	13.21 ± 0.9^{eB}	17.01 ± 1.1^{cB}	128 ± 3.5^{bAB}	67 ± 4.2^{cB}
	1	5.47 ± 0.2^{cC}	19.51 ± 0.9^{bA}	130 ± 4.0^{bA}	74 ± 5.9^{cA}
A21-CSGH	0.1	68.24 ± 1.2^{aA}	16.36 ± 2.3^{eA}	120 ± 2.6^{cB}	69.7 ± 1.4^{aC}
	0.5	22.25 ± 1.7^{cB}	14.7 ± 1.9^{dB}	122 ± 3.1^{dAB}	74.4 ± 1.9^{bB}
	1	6.26 ± 0.33^{cC}	13.9 ± 2.0^{dB}	125 ± 2.5^{cA}	88.1 ± 2.7^{bA}
A26-CSGH	0.1	50.76 ± 4.0^{cA}	33.21 ± 1.7^{bA}	131 ± 2.3^{aB}	47.6 ± 0.9^{eC}
	0.5	31.69 ± 2.4^{aB}	19.46 ± 1.9^{bB}	133 ± 3.1^{aAB}	51 ± 1.5^{dB}
	1	9.87 ± 0.7^{bC}	15.94 ± 0.4^{cC}	134.8 ± 4.2^{aA}	59 ± 2.3^{dA}

Values are given as mean ± SD from triplicate determinations.
Different letters in the same column within the same concentration indicate significant differences ($P < 0.05$).
Different capital letters in the same column within the same hydrolysate sample indicate significant differences ($P < 0.05$).

Table 4: Water and oil-holding capacity of CSGHs.

	WHC (mL/g)	OHC (mL/g)
CSG	2.15 ± 0.72^{d}	3.52 ± 0.28^{b}
A26-CSGH	1.9 ± 0.1^{d}	4.9 ± 0.1^{a}
Alcalase-CSGH	2.81 ± 0.2^{c}	3.2 ± 0.1^{c}
NH1-CSGH	3.51 ± 0.1^{b}	2.6 ± 0.2^{d}
A21-CSGH	3.9 ± 0.2^{a}	1.7 ± 0.1^{e}

WHC = water-holding capacity (mL of water absorbed/g of sample); OHC = oil-holding capacity (mL of oil absorbed/g of sample); values are given as mean ± SD from triplicate determinations. [a,b]Different letters indicate significant differences ($P \leq 0.05$).

and the absorbance is reduced [39]. Figure 2(a) shows the results of DPPH radical-scavenging activity of CSGHs at various concentrations. Alcalase-CSGH exhibited the highest antioxidant activity (71% at 5 mg/mL) followed by NH1 and A21-CSGHs with an activity of 69.9% and 64.7%, respectively, while lowest DPPH radical scavenging (26.1%) was obtained with A26-CSGH. However, all hydrolysates showed a lower radical-scavenging activity than BHA at the same concentration.

The results so obtained suggest that the peptides in different hydrolysates, which might be different in terms of chain length and amino acid sequence, contributed to varying degrees of scavenging DPPH radicals. Alcalase and A21 gelatin hydrolysates probably contained more peptides than the other hydrolysates, which are electron donors that could react with free radicals to convert them to more stable products and terminate the radical chain reaction.

Ferric reducing antioxidant power (FRAP) generally measures the reducing ability against ferric ion (Fe^{3+}). This ability indicates the ability of hydrolysates to donate electron to the free radical [9]. As shown in Figure 2(b), the reducing power activities of the different gelatin hydrolysates are concentration dependent. Alcalase-CSGH (DH = 20.26%) and A21-CSGH (DH = 26.9%) have, respectively, a ferric reducing antioxidant power three- and ninefold higher ($P < 0.05$) than that of A26-CSGH (DH = 12.7% at 5 mg/mL). Increases in reducing power of hydrolysate with increasing DH have been reported in blacktip shark (*Carcharhinus limbatus*) skin gelatin hydrolysate prepared using papaya latex enzyme [3], loach (*Chromobotia macracanthus*) protein hydrolysates [40], and gelatin hydrolysate from bigeye snapper (*Lutjanus lutjanus*) during a simulated gastrointestinal digestion [36].

The chemical activity of the hydroxyl radical is the strongest among reactive oxygen species (ROS). It easily reacts with biomolecules, such as amino acids, proteins, and DNA [41]. Therefore, scavenging of the hydroxyl radical is probably one of the most effective defenses of a living body against various diseases.

The hydroxyl radical-scavenging abilities of CSGHs using DNA nicking assay are shown in Figure 2(c). Lane 1 represents the untreated plasmid (native DNA) with its two forms: the upper one is open-circular (nicked) DNA and the faster migrating band is supercoiled (closed circular) plasmid. The incubation of plasmid DNA with Fenton's reagent in the absence of CSGH resulted in the disappearance of both forms, indicating that DNA was completely degraded (lane 2). Interestingly, all gelatin hydrolysates exhibited moderate protection against hydroxyl radical induced DNA breakage (Figure 2(c), lane 3 to lane 6).

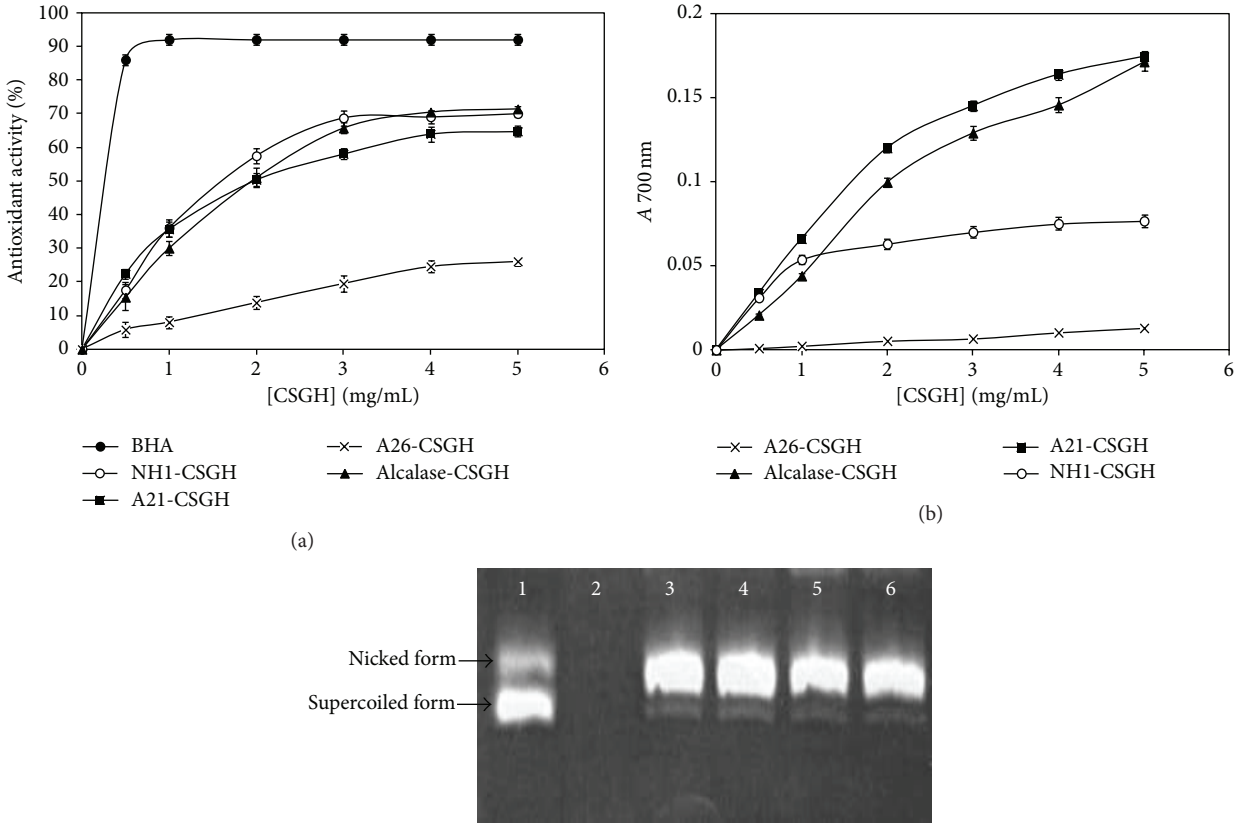

(c) Lane 1: untreated control, native pCRII TOPO DNA (0.5 μg); lane 2: DNA sample incubated with Fenton's reagent; lanes 3, 4, 5, and 6: Fenton's reagent + DNA + 2 mg CSGHs, alcalase-CSGH, NH1-CSGH, A21-CSGH, and A26-CSGH, respectively.

Figure 2: Antioxidant activity using (a) DPPH scavenging, (b) reducing power assay of CSGHs at different concentrations and (c) gel electrophoresis pattern of the plasmid pCRII TOPO incubated with Fenton's reagent in the presence and absence of CSGHs.

3.5. Determination of Antioxidative Activities in Model Systems

3.5.1. β-Carotene-Linoleate Bleaching Model System. The antioxidant assay using the discoloration of β-carotene is widely used to measure the antioxidant activity of bioactive compounds, because β-carotene is extremely susceptible to free radical-mediated oxidation of linoleic acid [42]. The presence of antioxidant in linoleic acid emulsion system hinders β-carotene bleaching, due to the chain-breaking inhibition of lipid peroxidation by neutralizing the linoleic free radical formed. The antioxidant activities of CSGHs as measured by β-carotene bleaching are shown in Figure 3(a). All hydrolysates prevent β-carotene bleaching by donating hydrogen atoms to peroxyl radicals of linoleic acid. As can be seen, the antioxidant activity of CSGHs increased with increasing sample concentration. Alcalase-CSGH which had the lowest reducing power and DPPH radical-scavenging activity showed the highest ability to prevent β-carotene bleaching with 82.1% inhibition at 5 mg/mL and the hydrolysate prepared by NH1 proteases showed the lowest. However, the inhibition of β-carotene bleaching by all hydrolysates was lower than that obtained with BHA (92%).

3.5.2. Inhibition of Linoleic Acid Antioxidant Activity. In vitro lipid peroxidation inhibition activities of CSGHs were determined by assessing their ability to inhibit oxidation of linoleic acid in an emulsified model system.

All hydrolysates could act as significant retarders ($P < 0.05$) of lipid peroxidation and activity increased with increasing concentrations. The comparative study between CSGHs and commercial antioxidant (α-tocopherol) on the inhibition of lipid peroxidation was conducted and illustrated in Figure 3(b). The autoxidation of CSGHs was slightly lower than that of α-tocopherol. This indicates that CSGHs had an effective capacity to inhibit lipid peroxidation. A21-SCGH exhibited the highest inhibition activity (72.1% ± 0.57) followed by alcalase-CSGH (71.5% ± 1.4) at a concentration of 5 mg/mL.

3.6. Stability of Selected Gelatin Hydrolysate and Application. Cuttlefish skin gelatin hydrolysates prepared using alcalase

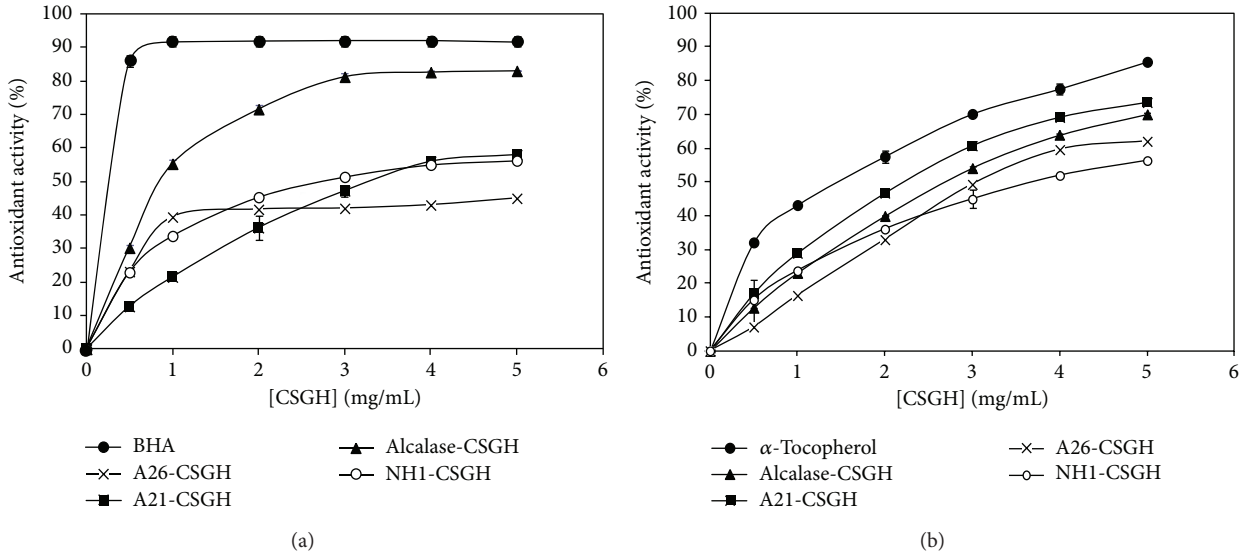

Figure 3: (a) β-Carotene bleaching method and (b) inhibition of lipid peroxidation of CSGHs at different concentrations.

which showed the highest β-carotene bleaching, radical scavenging, lipid peroxidation inhibition, and reducing power activity were selected for stability studies.

3.6.1. pH and Thermal Stability. The relative antioxidant activity (β-carotene-linoleate bleaching model, DPPH free radical scavenging, and reducing power assays) of the CSGH obtained by alcalase proteases at different pH (1 to 9) is presented in Figure 4(a). The antioxidant activity of alcalase-CSGH tested using β-carotene-linoleate bleaching model and DPPH free radical scavenging was stable over the pH range of 1–9 ($P > 0.05$). At pH 7, the ferric reducing activity decreased slightly, compared with that without pH adjustment. Kittiphattanabawon et al. [3] proved that the chelating activity of gelatin hydrolysate increased by 800% after pH adjustment, possibly due to the changes of charges in peptides.

The effect of thermal treatment (0 to 240 min, at 100°C) on antioxidant activity of alcalase-CSGH is shown in Figure 4(b). Radical-scavenging and reducing power activities increased by approximately 140% and 780%, respectively, after 240 min of heating treatment ($P < 0.05$). You et al. [40] also found that heat treatment was beneficial for increasing the antioxidant activity of peanut antioxidant hydrolysate. Thus, it suggests that alcalase-CSGH had a potential for application in any food system over pH range of 1–9 and thermal processed at 100°C for up to 240 min without loss or with increasing of activity.

3.6.2. In Vitro Gastrointestinal Digestion. *In vitro* gastrointestinal enzyme incubation provided an easy process to imitate the fate of this hydrolysate under oral administration. The relative antioxidant activity alcalase-CSGH, as monitored by β-carotene-linoleate bleaching model, DPPH free radical scavenging, and reducing power assays, after different digestion times is presented in Figure 4(c). No change in β-carotene-linoleate bleaching capacity was observed at any digestion times (0–240 min) ($P > 0.05$). It was observed that radical-scavenging activity increased by 163% during the last 15 min of gastrointestinal digestion ($P < 0.05$). Reducing power also increased by 175% during the first hour (stomach condition); then, it increased by 345% at the end of the GID (time = 240 min) ($P < 0.05$). It was observed that antioxidative peptides were modified by enzyme digestion to enhance their radical-scavenging and reducing power activities.

Our results are in accordance with those obtained by You et al. [40] who have proved that digestion of papain-hydrolysed loach peptide with pepsin and pancreatin increases the antioxidant activities. In addition, Nalinanon et al. [43] demonstrated that antioxidant peptides were most likely stable in real digestion system after ingestion in both stomach and intestine, which have high proteolytic activity under acidic and alkaline pH, respectively.

3.6.3. Prevention of Lipid Peroxidation in Meat Sausage System. Protein and gelatin hydrolysates have been shown to effectively inhibit lipid peroxidation in meat products [44], suggesting that food proteins could be utilized to develop specific hydrolysates as natural antioxidants for improving shelf-life of lipid-rich food products. In this study, lipid oxidation in meat sausage containing alcalase-CSGH at levels of 0 (Control), 0.1, 0.25, and 0.5 (g per 100 g of sausage) and vitamin C (0.1%) was monitored during storage at 4°C for 35 days, using TBARS and conjugated diene assays (Figure 5).

Generally, the TBARS of cooked turkey meat sausage increased during storage period and reached the maximum after 15-day storage except for concentrations 0.25% and 0.50% which reached their maximum after 20 and 25 storage days, respectively (Figure 5(a)). Thereafter, the decrease in TBARS was observed until the end of storage ($P < 0.05$). This was probably due to the loss of oxidation products formed, particularly low MW volatile compounds. Malondialdehyde and other short-chain products of lipid oxidation are not

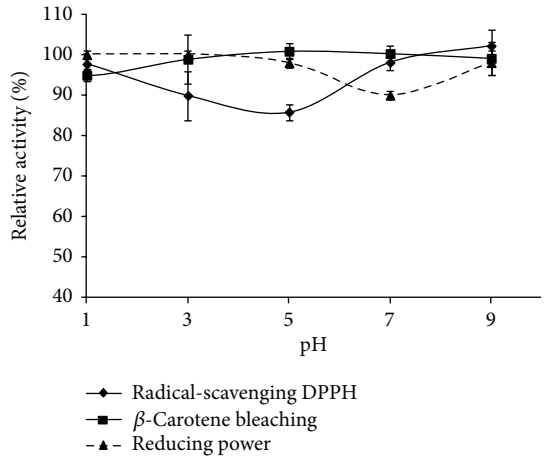

(a)

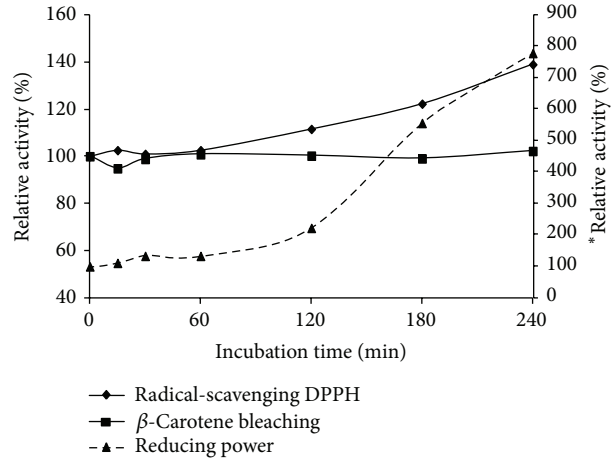

(b) Principal vertical axis indicates relative activity using β-carotene bleaching and radical-scavenging DPPH and secondary vertical axis indicates relative activity using reducing power assay

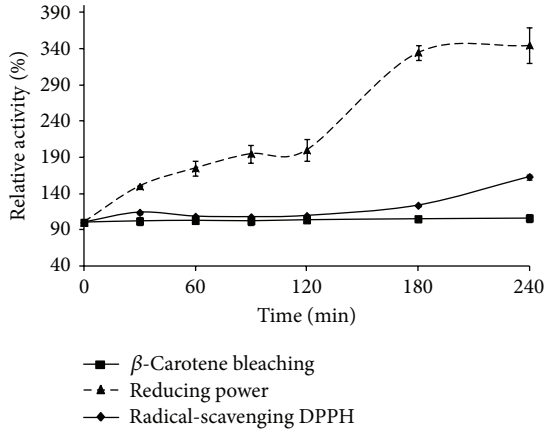

(c) 0 to 60 min: stomach condition; 60 to 240 min: duodenal condition

Figure 4: pH (a), thermal (b), and digestive (c) stabilities of alcalase-CSGH as monitored by β-carotene bleaching, radical-scavenging DPPH, and reducing power assay. Bars represent standard deviation ($n = 3$).

stable and are decomposed to alcohols and acids, which are not determined by the TBARS test [45].

The concentration of conjugated dienes significantly increased in all samples, followed by a decrease (Figure 5(b)). The rate of increase varied with the samples and concentrations used. The formation of conjugated dienes occurs at the early stages of lipid oxidation and hydroperoxides are expected to decompose to create secondary products [45]. The decrease or reaching of a stagnant level in conjugated dienes was generally accompanied by an increase in TBARS [46].

All gelatin hydrolysates could inhibit the early stages of lipid oxidation (formation of conjugated dienes or hydroperoxides) as well as retard propagation of the oxidation process (degradation of hydroperoxide to TBARS) [37]. A concentration of 0.50% of CSGH was generally more effective in inhibiting the lipid oxidation in the meat sausage system than other concentrations of CSGH and vitamin C as shown by the lower conjugated diene formation throughout the incubation. Additionally, an increase in TBARS values was lower than the control and the efficiency in retarding lipid oxidation was concentration dependent.

4. Conclusion

The objective of this work was to investigate some functional properties and the potential antioxidant effect of CSGHs prepared with different microbial enzyme preparations. Cuttlefish skin gelatin hydrolysates obtained with different alkaline proteases resulted in a product with an excellent solubility over a wide pH range. In addition, CSGHs prepared by treatment with different enzyme preparation, which displayed different spectra of substrate specificity, exhibited, to a variable extent, antioxidant activity in various *in vitro* antioxidant systems. The overall antioxidant action of CSGHs is likely attributed to the cooperative effects of several mechanisms, and the differences between functional properties and biological activities of the hydrolysates are

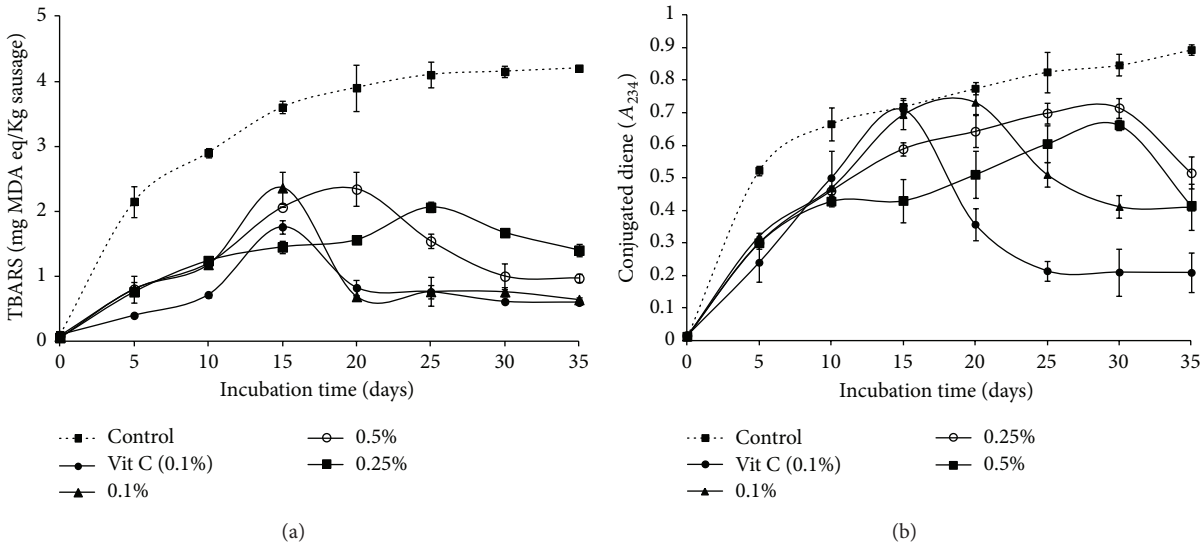

Figure 5: Lipid oxidation of meat sausage added with alcalase-CSGHs at different levels: (a) thiobarbituric acid reactive substances (TBARS) and (b) conjugated dienes. Bars represent the SD from triplicate determinations.

in particular due to diversity of peptides, which might be different in terms of chain length and amino acid sequence. From the results, cuttlefish skin gelatin hydrolysates have also a high nutritional value, based on their amino acid profile. Therefore, alcalase-CSGH exhibits a good antioxidant activity in turkey meat sausage model and can be a promising natural substrate that could be utilized in different food systems.

Conflict of Interests

The authors declare that there is no conflict of interests regarding the publication of this paper.

Acknowledgment

This work was funded by the Ministry of Higher Education and Scientific Research, Tunisia.

References

[1] M. Ahmad and S. Benjakul, "Characteristics of gelatin from the skin of unicorn leatherjacket (*Aluterus monoceros*) as influenced by acid pretreatment and extraction time," *Food Hydrocolloids*, vol. 25, no. 3, pp. 381–388, 2011.

[2] K. Jellouli, R. Balti, A. Bougatef, N. Hmidet, A. Barkia, and M. Nasri, "Chemical composition and characteristics of skin gelatin from grey triggerfish (*Balistes capriscus*)," *LWT*, vol. 44, no. 9, pp. 1965–1970, 2011.

[3] P. Kittiphattanabawon, S. Benjakul, W. Visessanguan, and F. Shahidi, "Gelatin hydrolysate from blacktip shark skin prepared using papaya latex enzyme: antioxidant activity and its potential in model systems," *Food Chemistry*, vol. 135, no. 3, pp. 1118–1126, 2012.

[4] M. Jridi, R. Nasri, I. Lassoued et al., "Chemical and biophysical properties of gelatins extracted from alkali-pretreated skin of cuttlefish (*Sepia officinalis*) using pepsin," *Food Research International*, vol. 54, pp. 1680–1687, 2013.

[5] J. M. Chobert, C. Bertrand-Harb, and M. G. Nicolas, "Solubility and emulsifying properties of caseins and whey proteins modified enzymatically by trypsin," *Journal of Agricultural and Food Chemistry*, vol. 36, no. 5, pp. 883–892, 1988.

[6] S.-K. Kim and E. Mendis, "Bioactive compounds from marine processing byproducts—a review," *Food Research International*, vol. 39, no. 4, pp. 383–393, 2006.

[7] D. J. McClements and E. A. Decker, "Lipid oxidation in oil-in-water emulsions: Impact of molecular environment on chemical reactions in heterogeneous food systems," *Journal of Food Science*, vol. 65, no. 8, pp. 1270–1282, 2000.

[8] M. C. Gomez-Guillen, B. Gimenez, M. E. Lopez-Caballero, and M. P. Montero, "Functional and bioactive properties of collagen and gelatin from alternative sources: a review," *Food Hydrocolloids*, vol. 25, no. 8, pp. 1813–1827, 2011.

[9] S. Khantaphant and S. Benjakul, "Comparative study on the proteases from fish pyloric caeca and the use for production of gelatin hydrolysate with antioxidative activity," *Comparative Biochemistry and Physiology B*, vol. 151, no. 4, pp. 410–419, 2008.

[10] A. Alemán, B. Giménez, P. Montero, and M. C. Gómez-Guillén, "Antioxidant activity of several marine skin gelatins," *LWT*, vol. 44, pp. 407–413, 2011.

[11] C. D. Cinq-Mars, C. Hu, D. D. Kitts, and E. C. Y. Li-Chan, "Investigations into inhibitor type and mode, simulated gastrointestinal digestion, and cell transport of the angiotensin I-converting enzyme-inhibitory peptides in Pacific hake (*Merluccius productus*) fillet hydrolysate," *Journal of Agricultural and Food Chemistry*, vol. 56, no. 2, pp. 410–419, 2008.

[12] N. E. Hadj-Ali, R. Agrebi, B. Ghorbel-Frikha, A. Sellami-Kamoun, S. Kanoun, and M. Nasri, "Biochemical and molecular characterization of a detergent stable alkaline serine-protease from a newly isolated Bacillus licheniformis NH1," *Enzyme and Microbial Technology*, vol. 40, no. 4, pp. 515–523, 2007.

[13] A. Haddar, R. Agrebi, A. Bougatef, N. Hmidet, A. Sellami-Kamoun, and M. Nasri, "Two detergent stable alkaline serine-proteases from Bacillus mojavensis A21: Purification, characterization and potential application as a laundry detergent additive," *Bioresource Technology*, vol. 100, no. 13, pp. 3366–3373, 2009.

[14] R. Agrebi, A. Haddar, N. Hmidet, K. Jellouli, L. Manni, and M. Nasri, "BSF1 fibrinolytic enzyme from a marine bacterium Bacillus subtilis A26: Purification, biochemical and molecular characterization," *Process Biochemistry*, vol. 44, no. 11, pp. 1252–1259, 2009.

[15] J. Adler-Nissen, "Determination of the degree of hydrolysis of food protein hydrolysates by trinitrobenzenesulfonic acid," *Journal of Agricultural and Food Chemistry*, vol. 27, no. 6, pp. 1256–1262, 1979.

[16] AOAC, *Official Methods of Analysis*, Association of Official Analytical Chemists, Washington, DC, USA, 17th edition, 2000.

[17] K. Tsumura, T. Saito, K. Tsuge, H. Ashida, W. Kugimiya, and K. Inouye, "Functional properties of soy protein hydrolysates obtained by selective proteolysis," *LWT*, vol. 38, no. 3, pp. 255–261, 2005.

[18] K. N. Pearce and J. E. Kinsella, "Emulsifying properties of proteins: evaluation of a turbidimetric technique," *Journal of Agricultural and Food Chemistry*, vol. 26, no. 3, pp. 716–723, 1978.

[19] F. Shahidi, X. Q. Han, and J. Synowiecki, "Production and characteristics of protein hydrolysates from capelin (*Mallotus villosus*)," *Food Chemistry*, vol. 53, no. 3, pp. 285–293, 1995.

[20] U. Okezie, C. T. Akanbi, E. T. Otunola, and I. A. Adeyemi, "Effect of addition of ripe bananas on some physico-chemical properties of maize extract," *International Journal of Food Sciences and Nutrition*, vol. 54, no. 6, pp. 437–445, 2003.

[21] P. Bersuder, M. Hole, and G. Smith, "Antioxidants from a heated histidine-glucose model system. I: Investigation of the antioxidant role of histidine and isolation of antioxidants by high-performance liquid chromatography," *Journal of the American Oil Chemists'Society*, vol. 75, no. 2, pp. 181–187, 1998.

[22] I. I. Koleva, T. A. Van Beek, J. P. H. Linssen, A. De Groot, and L. N. Evstatieva, "Screening of plant extracts for antioxidant activity: a comparative study on three testing methods," *Phytochemical Analysis*, vol. 13, no. 1, pp. 8–17, 2002.

[23] T. Osawa and M. Namiki, "Natural antioxidants isolated from Eucalyptus leaf waxes," *Journal of Agricultural and Food Chemistry*, vol. 33, no. 5, pp. 777–780, 1985.

[24] H. Enari, Y. Takahashi, M. Kawarasaki, M. Tada, and K. Tatsuta, "Identification of angiotensin I-converting enzyme inhibitory peptides derived from salmon muscle and their antihypertensive effect," *Fisheries Science*, vol. 74, no. 4, pp. 911–920, 2008.

[25] M. A. Ayadi, A. Kechaou, I. Makni, and H. Attia, "Influence of carrageenan addition on turkey meat sausages properties," *Journal of Food Engineering*, vol. 93, no. 3, pp. 278–283, 2009.

[26] S. Hogan, L. Zhang, J. Li, H. Wang, and K. Zhou, "Development of antioxidant rich peptides from milk protein by microbial proteases and analysis of their effects on lipid peroxidation in cooked beef," *Food Chemistry*, vol. 117, no. 3, pp. 438–443, 2009.

[27] R. Nasri, A. Bougatef, H. Ben Khaled et al., "Antioxidant and free radical-scavenging activities of goby (*Zosterisessor ophiocephalus*) muscle protein hydrolysates obtained by enzymatic treatment," *Food Biotechnology*, vol. 26, no. 3, pp. 266–279, 2012.

[28] H. Ben Khaled, N. Ktari, O. Ghorbel-Bellaaj, M. Jridi, I. Lassoued, and M. Nasri, "Composition, functional properties and in vitro antioxidant activity of protein hydrolysates prepared from sardinelle (*Sardinella aurita*) muscle," *Journal of Food Science and Technology*, vol. 10, pp. 255–263, 2011.

[29] N. Ktari, M. Jridi, I. Bkhairia, N. Sayari, R. Ben Salah, and M. Nasri, "Functionalities and antioxidant properties of protein hydrolysates from muscle of zebra blenny (*Salaria basilisca*) obtained with different crude protease extracts," *Food Research International*, vol. 49, no. 2, pp. 747–756, 2012.

[30] B. Giménez, A. Alemán, P. Montero, and M. C. Gómez-Guillén, "Antioxidant and functional properties of gelatin hydrolysates obtained from skin of sole and squid," *Food Chemistry*, vol. 114, no. 3, pp. 976–983, 2009.

[31] S. Sathivel, P. J. Bechtel, J. K. Babbitt, W. Prinyawiwatkul, and M. Patterson, "Functional, nutritional, and rheological properties of protein powders from arrowtooth flounder and their application in mayonnaise," *LWT*, vol. 70, no. 2, pp. 57–63, 2005.

[32] H. G. Kristinsson and B. A. Rasco, "Fish protein hydrolysates: production, biochemical, and functional properties," *Critical Reviews in Food Science and Nutrition*, vol. 40, no. 1, pp. 43–81, 2000.

[33] L. Wang, X. An, F. Yang, Z. Xin, L. Zhao, and Q. Hu, "Isolation and characterisation of collagens from the skin, scale and bone of deep-sea redfish (*Sebastes mentella*)," *Food Chemistry*, vol. 108, no. 2, pp. 616–623, 2008.

[34] E. Mendis, N. Rajapakse, and S.-K. Kim, "Antioxidant properties of a radical-scavenging peptide purified from enzymatically prepared fish skin gelatin hydrolysate," *Journal of Agricultural and Food Chemistry*, vol. 53, no. 3, pp. 581–587, 2005.

[35] G. A. Gbogouri, M. Linder, J. Fanni, and M. Parmentier, "Influence of hydrolysis degree on the functional properties of salmon byproducts hydrolysates," *Journal of Food Science*, vol. 69, no. 8, pp. 615–619, 2004.

[36] Y. Thiansilakul, S. Benjakul, and F. Shahidi, "Compositions, functional properties and antioxidative activity of protein hydrolysates prepared from round scad (*Decapterus maruadsi*)," *Food Chemistry*, vol. 103, no. 4, pp. 1385–1394, 2007.

[37] V. Klompong, S. Benjakul, D. Kantachote, and F. Shahidi, "Antioxidative activity and functional properties of protein hydrolysate of yellow stripe trevally (*Selaroides leptolepis*) as influenced by the degree of hydrolysis and enzyme type," *Food Chemistry*, vol. 102, no. 4, pp. 1317–1327, 2007.

[38] R. Sánchez-Vioque, C. L. Bagger, C. Rabiller, and J. Guéguen, "Foaming properties of acylated rapeseed (*Brassica napus L.*) hydrolysates," *Journal of Colloid and Interface Science*, vol. 244, no. 2, pp. 386–393, 2001.

[39] K. Shimada, K. Fujikawa, K. Yahara, and T. Nakamura, "Antioxidative properties of xanthan on the autoxidation of soybean oil in cyclodextrin emulsion," *Journal of Agricultural and Food Chemistry*, vol. 40, no. 6, pp. 945–948, 1992.

[40] L. You, M. Zhao, C. Cui, H. Zhao, and B. Yang, "Effect of degree of hydrolysis on the antioxidant activity of loach (*Misgurnus anguillicaudatus*) protein hydrolysates," *Innovative Food Science and Emerging Technologies*, vol. 10, no. 2, pp. 235–240, 2009.

[41] M. A. Cacciuttolo, L. Trinh, J. A. Lumpkin, and G. Rao, "Hyperoxia induces DNA damage in mammalian cells," *Free Radical Biology and Medicine*, vol. 14, no. 3, pp. 267–276, 1993.

[42] S. Kumazawa, M. Taniguchi, Y. Suzuki, M. Shimura, M.-S. Kwon, and T. Nakayama, "Antioxidant activity of polyphenols in carob pods," *Journal of Agricultural and Food Chemistry*, vol. 50, no. 2, pp. 373–377, 2002.

[43] S. Nalinanon, S. Benjakul, H. Kishimura, and F. Shahidi, "Functionalities and antioxidant properties of protein hydrolysates from the muscle of ornate threadfin bream treated with pepsin from skipjack tuna," *Food Chemistry*, vol. 124, no. 4, pp. 1354–1362, 2011.

[44] B. Kong and Y. L. Xiong, "Antioxidant activity of zein hydrolysates in a liposome system and the possible mode of action," *Journal of Agricultural and Food Chemistry*, vol. 54, no. 16, pp. 6059–6068, 2006.

[45] J. Fernández, J. A. Perez-Alvarez, and J. A. Fernández –Lopez, "Thiobarbituric acid test for monitoring lipid oxidation in meat," *Food Chemistry*, vol. 59, pp. 345–353, 1997.

[46] E. A. Peña-Ramos and Y. L. Xiong, "Antioxidant activity of soy protein hydrolysates in a liposomal system," *Journal of Food Science*, vol. 67, no. 8, pp. 2952–2956, 2002.

Hindawi Publishing Corporation
BioMed Research International
Volume 2014, Article ID 156438, 11 pages
http://dx.doi.org/10.1155/2014/156438

Research Article

Production and Biochemical Characterization of a High Maltotetraose (G4) Producing Amylase from *Pseudomonas stutzeri* AS22

Hana Maalej, Hanen Ben Ayed, Olfa Ghorbel-Bellaaj, Moncef Nasri, and Noomen Hmidet

Laboratoire de Génie Enzymatique et de Microbiologie, Ecole Nationale d'Ingénieurs de Sfax, BP 1173, 3038 Sfax, Tunisia

Correspondence should be addressed to Noomen Hmidet; hmidet_noomen@yahoo.fr

Received 24 February 2014; Accepted 22 April 2014; Published 26 May 2014

Academic Editor: Sofiane Ghorbel

Amylase production and biochemical characterization of the crude enzyme preparation from *Pseudomonas stutzeri* AS22 were evaluated. The highest α-amylase production was achieved after 24 hours of incubation in a culture medium containing 10 g/L potato starch and 5 g/L yeast extract, with initial pH 8.0 at 30°C under continuous agitation at 200 rpm. The optimum temperature and pH for the crude α-amylase activity were 60°C and 8.0, respectively. The effect of different salts was evaluated and it was found that both α-amylase production and activity were Ca^{2+}-dependent. The amylolytic preparation was found to catalyze exceptionally the formation of very high levels of maltotetraose from starch (98%, w/w) in the complete absence of glucose since the initial stages of starch hydrolysis (15 min) and hence would have a potential application in the manufacturing of maltotetraose syrups.

1. Introduction

Maltotetraose, known as G4, is an oligosaccharide of 4 units of α-D-glucopyranose linked by α-(1–4) bond. This compound has a considerable specific interest like its use as a substrate of amylases to study their mode of action and as a highly sensitive substrate for detection of specific α-amylase activity when coupled with a chromogenic compound [1]; it also finds potential applications in the food industries due to its properties [2, 3]. In fact, it can be used in baking due to its high moisture retention power which serves to prevent retrogradation of starch ingredient [4]. Maltotetraose is also being tested for its use as a food additive to improve the texture or to reduce the sweetness of foods without affecting their inherent taste and flavor [5, 6].

Besides the above properties, G4 syrup, considered as a partially undigested and unabsorbed substrate in the small intestine, has shown a prebiotic effect by selectively promoting the growth and/or activity of beneficial bacteria, once it reaches the colon. In fact it has been demonstrated through *in vitro* and *in vivo* experiments that oligosaccharides were utilized by bifidobacteria classified as beneficial intestinal bacteria, but they were not utilized by *Escherichia coli* or the *Clostridium* species which were unfavourable for their producing putrefactive substances (protein degrading) in the digestive tract. Consequently, the ingestion of G4 syrup could improve intestinal flora and suppress the formation of putrefactive products [7].

However, the preparation of maltooligosaccharides with a specific degree of polymerisation (DP) in larger amounts is so expensive. Therefore, the discovery of microbial enzymes that produce from starch maltooligosaccharides of a specific length has made it possible to produce with good yield various maltooligosaccharides [8].

Microbial amylases are produced mainly from cultures of *Aspergillus*, *Bacillus*, *Streptomyces*, and *Pseudomonas* species [9]. Amylolytic activity is one of phenotypic characteristics of *Pseudomonas stutzeri* species [10], especially G4-α-amylases that have been subject of intense biochemical research such as purification and biochemical characterization [11].

In the view of advantages offered by the use of the amylolytic preparation instead of the purified enzyme, such as to avoid enzyme purification procedures that are expensive and time-consuming, we report in the present study

the isolation and characterization of a novel G4-α-amylase producing bacteria *Pseudomonas stutzeri* AS22 from Tunisian soil samples. Conditions of α-amylase production were optimized to achieve high enzyme production and the amylolytic preparation was characterized.

2. Materials and Methods

2.1. Strain Isolation and Identification. Various soil samples were collected in the region of Sfax (Tunisia) and different microorganisms were screened for their amylolytic activity using nutrient agar plates containing soluble starch (1% w/v) (Figure 1(a)). The strain, having the highest activity, was identified as *Pseudomonas stutzeri* by using the phylogenetic analysis based on the 16S rDNA sequence analysis. Genomic DNA, for the PCR template, was isolated from bacterial cells grown in Luria-Bertani (LB) media overnight by the *Wizard Genomic DNA Purification Kit* from Promega and amplified using the universal oligonucleotide primers (Bio Basic Inc.) 16SF (5′GCTAACTAACGTGCCAGCAG) and 16SR (5′CCCGGGATCCAAGCTTAAGGAGGTGATCCAGCC). Nucleotide sequence of the amplified 16S rDNA gene region was compared with those available in the GenBank database by using the BLAST method. The BLAST result showed that the 16S rDNA sequence of the isolated strain AS22 has 99% sequence similarity with the strain *Pseudomonas stutzeri*.

2.2. Medium Composition and Culture Condition. Inocula were routinely grown in Luria-Bertani (LB) broth medium composed of (g/L) peptone 10.0, yeast extract 5.0, and NaCl 5.0 [12], and the initial pH was adjusted to 7.0.

The basal liquid culture medium used for α-amylase production by the *P. stutzeri* AS22 strain was composed of (g/L) carbon source 10, ammonium sulphate as nitrogen source 1, $MgSO_4$ (7 H_2O) 0.1, K_2HPO_4 1.4, KH_2PO_4 0.7, and NaCl 0.5. The medium was adjusted to pH 8.0. Media were autoclaved at 121°C for 20 min.

The strain was cultivated in 250 mL conical flasks containing 25 mL medium inoculated at initial OD of 0.016 and maintained for 24 h at 37°C and 200 rpm. The cultures were centrifuged at 13.000 rpm for 15 min, and the cell-free supernatants were evaluated for their amylolytic activity.

2.3. α-Amylase Activity Assay. α-Amylase activity was measured by the determination of reducing sugars released during starch hydrolysis, by the dinitrosalicylic acid (DNS) method [13]. The reaction mixture, containing 0.5 mL of appropriately diluted enzyme and 0.5 mL of 1.0% (w/v) soluble potato starch (Sigma) in 100 mM Tris-HCl buffer (pH 8.0), was incubated at 60°C for 10 min. After that, 3 mL of DNS reagent was added to the reaction volume, boiled for 10 min, and mixed with 20 mL distilled water. To determine the activity, the absorbance was measured at 550 nm and one unit (U) of α-amylase activity was defined as the amount of enzyme that released 1 μmol of reducing end groups per minute under the assay conditions.

2.4. α-Amylase Localization. The 24 h culture broth (25 mL) of *P. stutzeri* AS22 was centrifuged at 13.000 ×g for 10 min, and the supernatant was considered as the extracellular fraction. The cell pellet was washed twice with distilled water and suspended in 5 mL of Sodium Chloride-Tris-EDTA (STE) buffer containing 10 mM Tris-HCl (pH 8.0), 100 mM NaCl, and 1 mM EDTA. Then, lysozyme was added to a final concentration of 200 μg/mL and the mixture was incubated at 0°C for 1 h. After centrifugation at 8.000 ×g for 25 min, the supernatant was considered as the periplasmic fraction and 5 mL of Tris-HCl buffer (100 mM, pH 8.0) was added. The obtained mixture was sonicated twice for 3 min each time to disrupt cells. The homogenate was finally centrifuged, and its supernatant was considered as the intracellular fraction. Finally, the obtained three fractions were tested for their amylolytic activity.

2.5. Optimization of α-Amylase Production

2.5.1. Effects of Different Carbon Sources. The effects of different carbon sources (glucose, lactose, maltose, potato starch, wheat starch, and maize starch) on α-amylase production by the *P. stutzeri* strain were examined at a concentration of 1%, keeping constant the rest of the media composition. The best of these carbon sources was further optimized in the range of 0.25–2% (w/v).

2.5.2. Effects of Different Nitrogen Sources. To investigate the effects of different nitrogen sources on α-amylase production, ammonium sulphate in the basal medium, containing 10 g/L potato starch, was replaced with different organic (yeast extract, casein, pastone, and soya peptone) and inorganic (ammonium sulphate and ammonium chloride) compounds as nitrogen source at a concentration of 0.1% (w/v), keeping constant the rest of the media composition. The concentration of the selected nitrogen source was further optimized in the range of 0.1–1% (w/v).

2.5.3. Effects of Temperature, Agitation, Initial pH, Salts, and Incubation Time on α-Amylase Production. The effect of incubation temperature on α-amylase production was investigated by incubating the media for 24 h at different temperatures (25, 30, 37, and 45°C) in an automatic incubator.

The effect of agitation on enzyme production was also determined by incubating the inoculated culture flasks in an automatic mechanical shaker for 24 hours at 150, 200, and 250 rpm and then checking for extracellular α-amylase production.

To investigate the effect of pH on enzyme production, the initial pH of the medium was adjusted from 6.0 to 12.0.

KH_2PO_4 (0.7 g/L), K_2HPO_4 (1.4 g/L), NaCl (0.5 g/L), $MgSO_4$, and $CaCl_2$ were incorporated into growth medium to study the effects of mineral sources on α-amylase production. The basal medium containing 10 and 5 g/L potato starch and yeast extract, respectively, was used as control. To study the effect of $CaCl_2$ and $MgSO_4$, these chemicals were added to the medium so that their final concentration ranged from 0.1 to

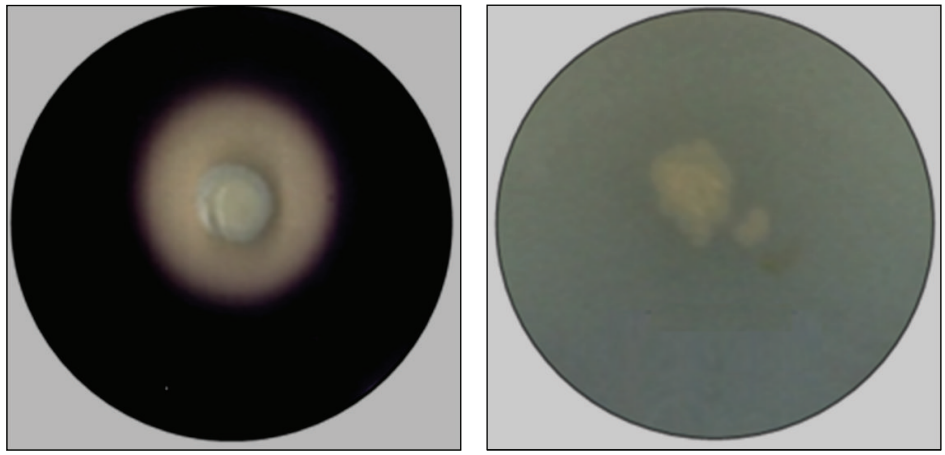

(a) (b)

Figure 1: Amylolytic (a) and proteolytic (b) activities of the isolated strain AS22. The amylolytic and proteolytic activities of the strain AS22 were evaluated by puncture inoculation of the strain inside nutrient agar medium containing soluble starch (1% w/v) (a) and casein (b), respectively. After incubation at 37°C for 24 h, to detect the amylolytic activity, the plates were flooded with iodine solution at room temperature.

0.8 g/L. Amylolytic activity was determined after incubation for 24 h at 30°C and 200 rpm agitation speed.

For maximal α-amylase production, fermentation period (0–240 h) was also optimized under the optimized fermentation conditions. Fermentation was performed at 30°C in an automatic incubator and samples were prepared at different intervals (continuously for 10 days) for enzyme assay.

2.6. Biochemical Properties of the Crude α-Amylase Preparation

2.6.1. Effect of Temperature on Activity and Stability. The effect of temperature on α-amylase activity was studied from 20 to 90°C. Thermal stability was examined by incubating the enzyme preparation for 60 min at different temperatures ranging from 30 to 70°C. Aliquots were withdrawn at desired time intervals and the remaining activity was measured under enzyme assay conditions. The nonheated enzyme was taken as 100%.

2.6.2. Effect of pH on Activity and Stability. The effect of pH on α-amylase activity was evaluated for the pH range of 3.0–13.0 at 60°C. For pH stability measurement, the enzyme was incubated at 30°C for 1 h in different buffers and the residual activity was determined under the enzyme assay conditions. The following buffer systems were used: 100 mM glycine-HCl buffer, pH 3.0-4.0; 100 mM acetate buffer, pH 4.0–6.0; 100 mM Tris-HCl buffer, pH 7.0-8.0; 100 mM glycine-NaOH buffer, pH 9.0–11.0; and 100 mM Na_2HPO_4-NaOH buffer, pH 12.0 and 13.0.

2.6.3. Effect of Metal Ions, Surfactants, and Enzyme Inhibitors. The influence of various metal ions (5 mM) on α-amylase activity was investigated using $CaCl_2$, $ZnCl_2$, $FeCl_2$, $HgCl_2$, $BaCl_2$, $MnCl_2$, $MgCl_2$, $CuCl_2$, $CdCl_2$, NaCl, and KCl. Activity in the absence of any additives was taken as 100%.

The effects of some surfactants (Triton X-100, Tween 20, Tween 80, and SDS) and enzyme inhibitors (phenylmethylsulfonyl fluoride (PMSF), β-mercaptoethanol, and ethylenediaminetetraacetic acid (EDTA)) on α-amylase stability were studied by preincubating the amylolytic preparation for 30 min at room temperature. The remaining enzyme activity was measured under enzyme assay conditions. The activity of enzyme incubated under similar conditions without any additive was taken as 100%.

2.7. Analysis of End Products Starch Hydrolysis. Starch solution (1% w/v, 50 mL) was prepared using Tris-HCl buffer (100 mM, pH 8.0). The *P. stutzeri* AS22 crude α-amylase (0.6 U) was added into 50 mL of starch solution. Reaction mixture was incubated at 60°C. Aliquots were withdrawn at various time intervals and boiled for 10 min to stop the reaction and samples were then centrifuged at 13.000 g for 10 min and passed through 0.22 μm filter. Samples thus obtained were analyzed by thin-layer chromatography (TLC) and gel permeation chromatography (GPC) on Bio-Gel P2.

TLC was performed on silica gel 60 (20 × 20 cm, Merck, Germany) with a mobile phase composed of chloroform/acetic acid/water (60 : 70 : 10, v/v/v). The spots were visualized by spraying TLC plates with H_2SO_4/ethanol (5 : 95, v/v) followed by heating at 120°C for 10 min.

GPC was performed on a Bio-Gel P2 column (1.5 × 200 cm) eluted with water at a rate of 30 mL/h. The different oligosaccharides in the range of G1 to G7 were fractionated and the percentages of different products were determined.

2.8. Visualisation of α-Amylase Activity by Zymography. α-Amylase activity staining was done by layering the SDS-PAGE gel on a thin 2% agarose-1% soluble potato starch gel

incubated as a sandwich for 60 min at 50°C. Upon staining the agarose gel with iodine solution at room temperature, protein bands with amylolytic activity became visible as a white band against a dark blue background.

3. Results and Discussion

3.1. α-Amylase Production by P. stutzeri AS22. The production of amylases enzymes by microorganisms is significantly affected by physical and chemical parameters of the medium [14, 15]. In this regard, appropriate media components and suitable conditions must be attained for optimal production of the required products.

3.1.1. Effects of Different Carbon Sources on α-Amylase Production. Because amylase synthesis is known to be induced by starch or its hydrolytic products [16–18], *P. stutzeri* AS22 was grown in the basal medium supplemented with starch from various natural sources (potato, wheat, and maize starch) and other carbohydrates including lactose, maltose, and glucose, for assessing their effects on the production of amylase (Table 1).

The highest amylase activity (0.8 U/mL) was produced on potato starch followed by maltose (0.5 U/mL). However, amylase production was significantly low when the strain was grown on lactose (0.055 U/mL) and glucose (0.1 U/mL). This study falls in line with previous studies on *P. stutzeri* amylase production, in which enzyme was induced using starch, amylodextrin or maltose, while glucose was found to inhibit amylase production [1, 19–21]. In contrast to our results, glucose was found to be the best carbon source for amylase production by *Pseudomonas* sp. IMD 353 (13 U/mL), while the amylolytic activity decreased to 2 and 3 U/mL, when maltose and starch were used, respectively, as sole carbon sources in the same conditions [22].

Since potato starch was the best carbon source for amylase synthesis, the effect of its concentration (0.25–2%) on the amylase production was studied in media containing 0.1% ammonium sulphate as nitrogen source. It was observed that the increase in concentration of potato starch increases amylase production and maximum activity (0.75 U/mL) was obtained in the presence of 1% substrate (data not shown). However, further increase (1.5 and 2%) of potato starch concentration resulted in rapid decrease of enzyme production although biomass remained nearly constant (decreased slightly). This may be explained by the degradation, during the fermentation, of starch by α-amylases, resulting in the accumulation of high quantities of reducing sugar, which led to an enhancement of sugar concentration and therefore to catabolite repression of α-amylase synthesis [17].

3.1.2. Effects of Various Nitrogen Sources on α-Amylase Production. In general, both organic and inorganic nitrogen sources were used efficiently in the growth medium for the biosynthesis of α-amylase.

In the present study, various nitrogen sources at a concentration of 0.1% were evaluated using an optimum potato starch concentration of 1% (Table 2). Maximum activity was obtained when yeast extract was used (2.5 U/mL). Addition of yeast extract to the medium increased the production of α-amylase activity by more than three times over medium with ammonium sulphate as nitrogen source. Compared to the organic nitrogen sources which support good growth and extracellular α-amylase production, inorganic nitrogen sources like ammonium sulphate and ammonium chloride are not efficient for amylase production. These results corroborate well with previous studies showing that organic nitrogen sources were preferred for the α-amylase production. The stimulatory effect of these complex compounds may be attributed to their carbohydrate and protein compositions, as well as to the trace of minerals and ions that could be present and which enhance the enzyme secretion [18]. Yeast extract has been also used as nitrogen source in the culture medium for amylase production, alone in the case of *P. stutzeri* NRRL B-3389 [19], or in combination with other nitrogen sources such as polypeptone in the case of *Pseudomonas* strain MS300 [23] and yeatex for *Pseudomonas* sp. IMD 353 [22]. Other organic nitrogen sources have been also reported to support α-amylase production by *P. stutzeri* MO-19 such as corn steep liquor and peptone [20] and polypeptone in the case of *P. saccharophila* IAM 1504 [24].

To investigate the best concentration on α-amylase production, yeast extract (range 1–10 g/L) was added to basal

Table 1: Effects of different carbon sources on the production of α-amylase by *P. stutzeri* AS22.

Carbon sources	Final pH value	Biomass (OD_{600})	α-Amylase activity (U/mL)
Lactose	7.49	0.1	0.055
Glucose	5.69	0.8	0.1
Maltose	6.62	1.0	0.5
Potato starch	6.52	0. 8	0.8
Wheat starch	6.69	1.04	0.1
Maize starch	6.59	0.5	0.17

Cultivation was performed for 24 h at 37°C with shaking at 200 rpm in media that consisted of (g/L) carbon source 10, ammonium sulphate 1, K_2HPO_4 1.4, KH_2PO_4 0.7, $MgSO_4$ 0.1, and NaCl 0.5 and that were inoculated at initial OD of 0.016 and adjusted to pH 8.0.

Table 2: Effects of different nitrogen sources supplemented to the potato starch on the production of α-amylase by *P. stutzeri* AS22.

Nitrogen sources	Final pH value	Biomass (OD_{600})	α-Amylase activity (U/mL)
NH_4Cl	6.6	0.94	0.5
$(NH_4)_2SO_4$	6.5	0.9	0.7
Soya peptone	7.9	3.21	0.97
Casein	7.85	1.61	1.0
Pastone	7.78	3.08	1.5
Yeast extract	7.87	3.56	2.5

Cultivation was performed for 24 h at 37°C with shaking at 200 rpm in media that consisted of (g/L) potato starch 10, K_2HPO_4 1.4, KH_2PO_4 0.7, $MgSO_4$ 0.1, NaCl 0.5, and different nitrogen sources (1 g/L) and were adjusted to pH 8.0.

Table 3: Effect of different initial pH values of fermentation medium on the production of α-amylase by *P. stutzeri* AS22.

Initial pH value	Final pH value	Biomass (OD_{600})	α-Amylase activity (U/mL)
6.0	4.73	3.9	0
7.0	7.2	4.9	3.8
8.0	8.0	5.6	5.9
9.0	8.55	5.5	5.85
10.0	8.9	5.5	5.8
11.0	9.22	5.6	5.6
12.0	9.32	5.4	5.4

Cultivation was performed for 24 h at 30°C with shaking at 200 rpm in media that consisted of (g/L) potato starch 10, yeast extract 5, K_2HPO_4 1.4, KH_2PO_4 0.7, $MgSO_4$ 0.1, and NaCl 0.5 and were adjusted to different initial pH values.

medium containing potato starch (10 g/L). Maximum amylase production by *P. stutzeri* AS22 was obtained with 5 g/L yeast extract, reaching 3.95 U/mL and further addition of yeast extract decreased the level of amylase (data not shown).

3.1.3. Effects of Temperature, Agitation, Initial pH Values, and Salts on α-Amylase Production. The effects of temperature (25 to 45°C), agitation (150, 200 and 250 rpm) and initial pH (6.0 to 12.0) on α-amylase production by *P. stutzeri* AS22 were studied in optimized medium containing 10 g/L potato starch and 5 g/L yeast extract.

Optimum level of α-amylase production (6 U/mL) was achieved at 30°C (data not shown). This result falls in line with previous studies on *Pseudomonas* α-amylases, in which most of them are reported to be produced at 25 [23] and 30°C [20, 24]. Amylase production seems to be very sensitive to higher temperatures. Indeed, at 37°C, the amylolytic activity was 40% lower than that at 30°C and at 45°C; no α-amylase activity was detected.

Among the tested agitation speeds, the maximum amylase activity (6.1 U/mL) was found at 200 rpm (data not shown).

The pH of the production medium strongly affects many enzymatic processes and transport of compounds across the cell membrane [18, 25]. In this study, the effect of pH on α-amylase production by *P. stutzeri* AS22 was investigated with varying pHs (6.0–12.0). The results revealed that the pH of the medium influences the α-amylase production as well as the strain growth (Table 3), which were more favorable at alkaline pH 8.0–12.0 than the neutral one. In contrast, acidic conditions (pH 6.0) seem to affect the α-amylase production, even when the stain might be able to grow. From this result, it has been understood that amylase production may occur at pH 6.0, but since the final pH was lowered to 4.5, no amylase activity was detected after 24 h of incubation because of the instability of the enzyme toward acidic conditions. Most of the earlier studies revealed neutral or alkaline initial pH for α-amylase production by *Pseudomonas* species [20, 22, 24]. On the other hand, Lalucat et al. [10] reported that none of the *Pseudomonas stutzeri* strains tolerate acidic conditions and they do not grow at pH 4.5.

In an attempt to increase the α-amylase production by *P. stutzeri*, the effect of some salts including K_2HPO_4 (1.4 g/L), KH_2PO_4 (0.7 g/L), NaCl (0.5 g/L), $MgSO_4$ (0.1 g/L), and $CaCl_2$ (0.1 g/L) was investigated. Results (Table 4) revealed that even though the growth rate was lower in medium supplemented with phosphate ions (as K_2HPO_4 and KH_2PO_4), production of α-amylase was enhanced as compared to the medium without salts addition (none). It is also interesting to note that while amylase production was slightly affected by the addition in the culture medium of the monovalent cation Na^+ (in the form of NaCl), divalent cations (0.1 g/L) seem to enhance moderately or effectively the amylase production by *P. stutzeri* AS22, in the case of Mg^{2+} and Ca^{2+}, respectively. As mentioned by Gupta et al. [18], differences in the mineral requirements of amylase producing bacteria have been reported and whereas most of previous studies indicated that addition of $CaCl_2$ to the fermentation medium is known to be essential for amylase production [9, 26, 27], Ca-independent amylase production has also been reported [28, 29]. In comparison with the control medium, when $CaCl_2$ (0.4 g/L) was added individually as a mineral source to the medium, amylase production was enhanced from 5.9 to 6.6 U/mL. However, by increasing the $CaCl_2$ concentration from 0.8 to 1.2 g/L, decline in enzyme production by approximately 30% was observed. This finding is in accordance with previous studies showing inhibition of amylase production by the excess of some minerals such Ca^{2+} [30] and Mg^{2+} ions [31].

Maximum amylase production (6.8 U/mL) occurred when $CaCl_2$ (0.4 g/L) was supplemented to the control medium containing potato starch 10 g/L, yeast extract 5 g/L, $MgSO_4$ (7 H_2O) 0.1 g/L, K_2HPO_4 1.4 g/L, KH_2PO_4 0.7 g/L, and NaCl 0.5 g/L.

3.1.4. Pattern of α-Amylase Production by P. stutzeri AS22. *P. stutzeri* AS22 was grown aerobically in the optimized medium (potato starch 10 g/L, yeast extract 5 g/L, $MgSO_4$ (7 H_2O) 0.1 g/L, K_2HPO_4 1.4 g/L, KH_2PO_4 0.7 g/L, and NaCl 0.5 and $CaCl_2$ 0.4 g/L) for 240 h at 30°C. The pattern of α-amylase production and bacterial growth was followed with time (Figure 2). Amylase production was initiated during the exponential growth phase of the strain, reached 6.75 U/mL during the stationary phase at 24 h, and remained constant till 72 h, suggesting that the enzyme production is growth associated and induced by the presence of starch hydrolysis products in the medium. These results are in agreement with the reports of Nakada et al. [20] and Fogarty et al. [22] on the relationship between pattern of cell growth and α-amylase production.

However, the level of α-amylase increased slightly from 72 h to 96 h, and thereafter it increased more rapidly from 192 to 216 h, as the bacterial cells approached their death phase. Since the increase of α-amylase activity was concomitant with the cell optical density decrease, the amylase activity increase may be the result of bacterial cell dying and release of intracellular or periplasmic α-amylases in the culture medium. Therefore, attempts to confirm this statement resulted in the localization of α-amylase activity after 24 h of incubation. It was found that *P. Stutzeri* AS22 produced

Table 4: Effect of supplementation of the culture medium with various salts on the production of α-amylase by *P. stutzeri* AS22.

Chemicals	Concentration (g/L)	Final pH value	Biomass (OD_{600})	α-Amylase activity (U/mL)
None		7.2	4.77	3.5
Control		7.8	5.45	5.9
NaCl	0.5	7.32	4.9	3.8
K_2HPO_4	1.4	7.6	2.57	5.19
KH_2PO_4	0.7	7.7	2.01	5.9
$MgSO_4$	0.1	7.08	5.43	4.13
	0.4	7.0	6.35	4.42
	0.8	7.3	5.73	3.24
$CaCl_2$	0.1	6.9	7.15	6.01
	0.4	6.7	6.3	6.6
	0.8	6.5	6.19	6.5
	1.2	6.3	6.2	4.6
Control + $CaCl_2$ (0.4 g/L)		7.2	6.2	6.8

Cultivation was performed for 24 h at 30°C with shaking at 200 rpm in media that consisted of (g/L) potato starch 10, yeast extract 5, and different salts and were adjusted to pH 8.0. Control: potato starch 10, yeast extract 5, K_2HPO_4 1.4, KH_2PO_4 0.7, $MgSO_4$ 0.1, and NaCl 0.5 g/L.

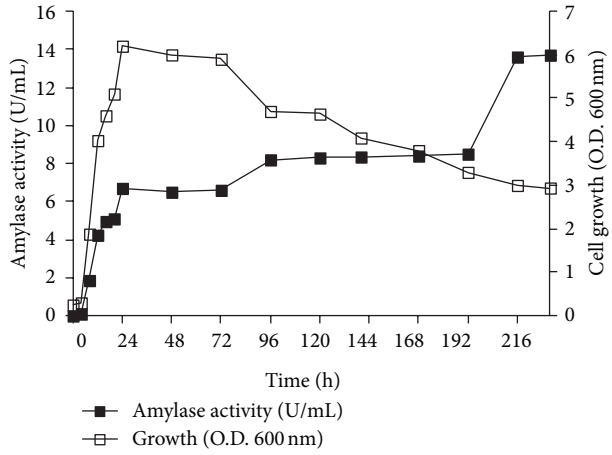

Figure 2: Pattern of growth and α-amylase production of *P. stutzeri* AS22 strain. Culture was conducted in media consisting of (g/L) potato starch 10, yeast extract 5, $MgSO_4$ 0.1, K_2HPO_4 1.4, KH_2PO_4 0.7, $CaCl_2$ 0.4 g/L, and NaCl 0.5 g/L. Incubation was carried out at 30°C, in a rotary shaker, with stirring at 200 rpm.

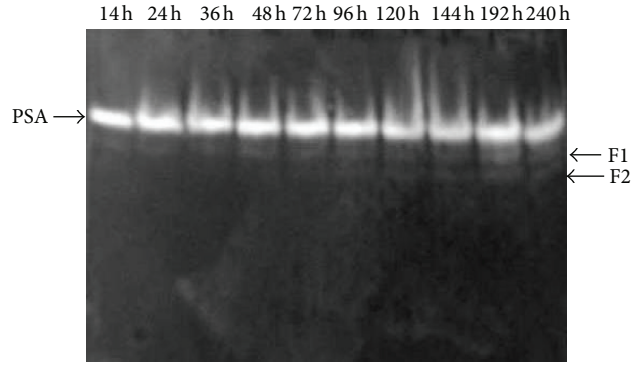

Figure 3: Changes in zymogram pattern for *P. stutzeri* α-amylases during cultivation.

a dominant extracellular α-amylase as well as intracellular and periplasmic α-amylases, which constitute approximately 10% and 3% of the extracellular fraction, respectively.

A zymogram prepared using the cell-free culture supernatant at various time intervals (Figure 3) showed only one dominant protein band (PSA) in all the culture supernatants. Two minor amylases were also observed; one active form (F1) was detected in 14–240 hr culture supernatants and the other form (F2) was observed in 48–240 hr culture supernatants. The change of PAGE pattern led us to suspect that F1 and F2 are either produced from proteolytic degradation of PSA, or later secreted in the extracellular medium. However, since *P. stutzeri* AS22 lacks proteolytic activity (Figure 1(b)) and the intensity of the PSA band remains constant from beginning to 240 h, this clearly indicates that F1 and F2 are not derived from PSA proteolysis but are later secreted in the extracellular medium.

Multiple forms of G4-amylase from *Pseudomonas stutzeri* strains have been reported. Robyt and Ackerman [19] reported that *P. stutzeri* NRRL B-3389 produced seven G4-amylases which differed in molecular mass and isoelectric point. Strain MS300 was found to produce two major G4-amylases (amylases A and B) and two minor amylases (amylases C and D) [23]. However, the G4-amylase of *P. stutzeri* MO-19 has been found to exist in two forms. One of these is a 57 kDa protein (G4-1); the other is a 46 kDa protein (G4-2) which was derived by the limited proteolysis of G4-1 [20].

3.2. Biochemical Characterization of Crude α-Amylase Preparation

3.2.1. Effect of Temperature on α-Amylase Activity and Stability. The temperature activity profile shows that the crude α-amylase was active at temperatures ranging from 20 to 70°C with an optimum activity at 60°C (Figure 4(a)).

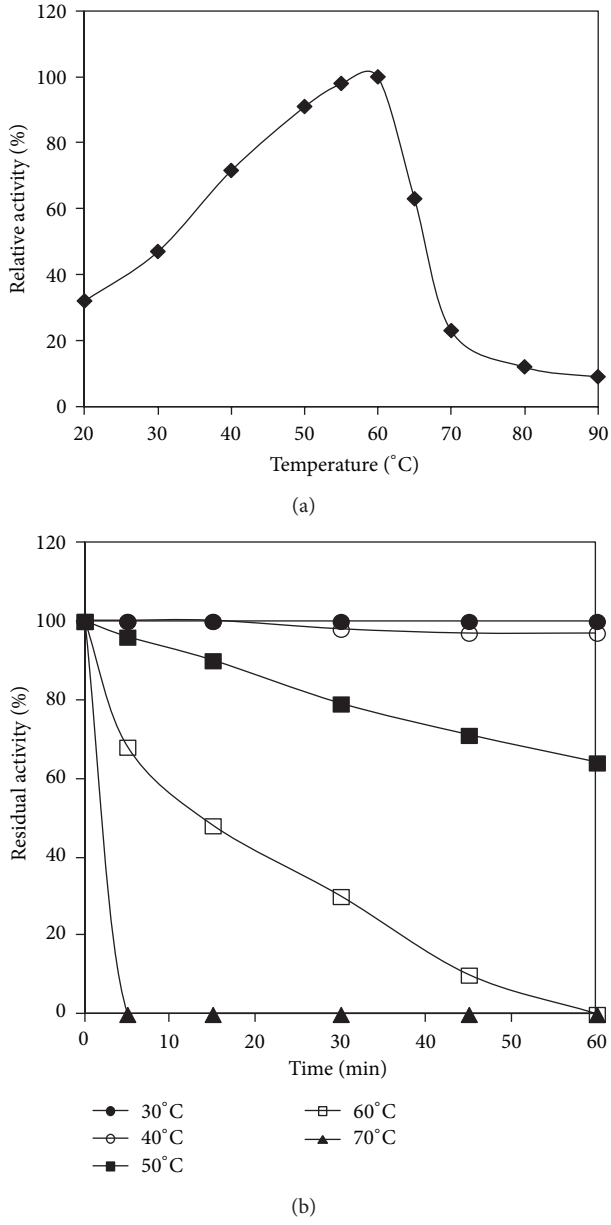

Figure 4: Temperature profile (a) and thermal stability (b) of *P. stutzeri* crude enzyme. Amylolytic activity was assayed at different temperatures ranging from 20 to 90°C at pH 8.0. The activity of the enzyme at 60°C was taken as 100%. To assess the thermostability, the *P. stutzeri* crude enzyme was heated at the indicated temperatures. The residual activity was assayed at pH 8.0 and 60°C. The nonheated crude enzyme was considered as the control (100%).

The relative activities at 65 and 70°C were about 63% and 23%, respectively. At 80°C, only 12% of the optimum activity was detected. While the optimum activity temperature of the crude α-amylase from *P. stutzeri* is comparable to that of the G4-α-amylase amyl I from *Bacillus* GM8901 [32], it was higher than that of previously reported maltotetraose-forming amylases from *Pseudomonas* species such as *Pseudomonas* MS300 [23] and *Pseudomonas stutzeri* NRRL B-3389 [33], which were reported to have optima temperatures of 40 and 45°C, respectively.

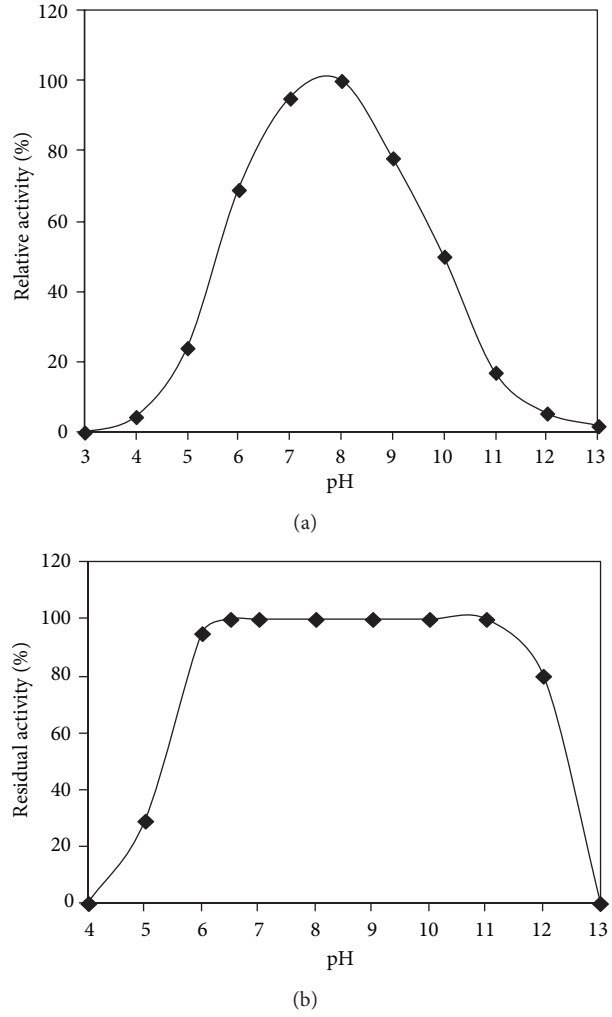

Figure 5: pH activity (a) and pH stability (b) of *P. stutzeri* crude enzyme. Amylolytic activity was assayed in the pH range of 3.0 to 13.0 at 60°C. The maximum activity obtained at pH 8.0 was considered as 100% activity. To assess the pH stability, the *P. stutzeri* crude enzyme was preincubated at the indicated pH at 30°C for 60 min and the residual enzyme activity was determined at pH 8.0 and 60°C. The activity of the crude enzyme before incubation was taken as 100%. Buffer solutions used for pH activity and stability are presented in Materials and Methods.

The effect of temperature on α-amylase stability was determined by incubating the enzyme preparation at different temperatures ranging from 30 to 70°C (Figure 4(b)). The crude amylase of the AS22 strain was stable at temperatures below 40°C. However, the activity decreased above 40°C and retained about 64% of its initial activity after 1 hour of incubation at 50°C. After 30 min of preincubation at 60°C, AS22 amylolytic preparation retained only 30% of its initial activity, showing therefore better thermostability than G4-amylases A and B from *Pseudomonas* MS300, which were reported to loose completely their activities after heating at 60°C for 30 min [23].

3.2.2. Effect of pH on α-Amylase Activity and Stability. The pH activity profile reported in Figure 5(a) showed that the

Table 5: Stability of the crude α-amylase in the presence of various additives.

Additives	Concentration	Remaining activity (%)
None	—	100
Inhibitors		
PMSF	5 mM	90
β-Mercaptoethanol	5 mM	66
EDTA	5 mM	70
Surfactants		
Tween 20	5% (v/v)	81
Tween 80	5% (v/v)	90
Triton X-100	5% (v/v)	82
SDS	0.1% (w/v)	100
	1% (w/v)	49

Enzyme activity measured in the absence of any additive was taken as 100%. The remaining α-amylase activity was measured after preincubation of the crude α-amylase with each additive at room temperature for 30 min.

crude enzyme was active between pH 5.0 and pH 11.0 with an optimum at around pH 8.0. The relative activities at pH 6.0 and pH 10.0 were approximately 69% and 50% of that at pH 8.0, respectively. However, the activity decreased significantly to 20% at pH 5.0 and pH 11.0. Most of the earlier studies on *Pseudomonas* maltotetraose-forming amylases revealed an optimum pH range between 6.0 and 7.0 [20, 22, 33].

The crude α-amylase was completely stable in the pH range 6.0–11.0 since it retained its full activity after 1 hour of incubation at 30°C (Figure 5(b)) and retained up to 80% of its original activity at pH 12.0. However, at pH 5.0 the amylase activity decreased by 80% of the maximum activity at pH 8.0 and was completely lost at pH 4.0. According to previous studies, the crude α-amylase from *P. stutzeri* AS22 was found to be as stable as the purified G4-amylase from *P. stutzeri* NRRLB-3389 towards the same pH range but interestingly higher than G4-amylases from *Pseudomonas* sp. MS300 and *P. stutzeri* MO-19 which were stable in the pH range of 7.0~9.0 and 6.5~9.5, respectively [20, 23, 33].

3.2.3. Effect of Metal Ions, Surfactants, and Enzyme Inhibitors. Because most of α-amylases are known to be metal ion-dependent enzymes [9], the effect of metal ions on the crude α-amylase activity was measured in the presence of various metal ions at a concentration of 5 mM. The enzyme activities were stimulated in the presence of Ca^{2+} and Ba^{2+} ions by 123% and 110%, respectively (data not shown). On the other hand, a strong inhibitory effect was observed in the presence of Hg^{2+}, Zn^{2+}, Mn^{2+}, and Cd^{2+} and more than 90% of the amylolytic activity was lost. Results suggest that AS22 amylolytic preparation did not require any metal ions for catalytic activity except Ca^{2+} and Ba^{2+}. According to Gupta et al. [18] and Sharma and Satyanarayana [34], α-amylase contains at least one Ca^{2+} ion and affinity of Ca is much stronger than that of other metal ions.

The stability of the AS22 crude α-amylase was also studied by incubating the amylolytic preparation in the presence of some enzyme inhibitors and surfactants for 30 min at room

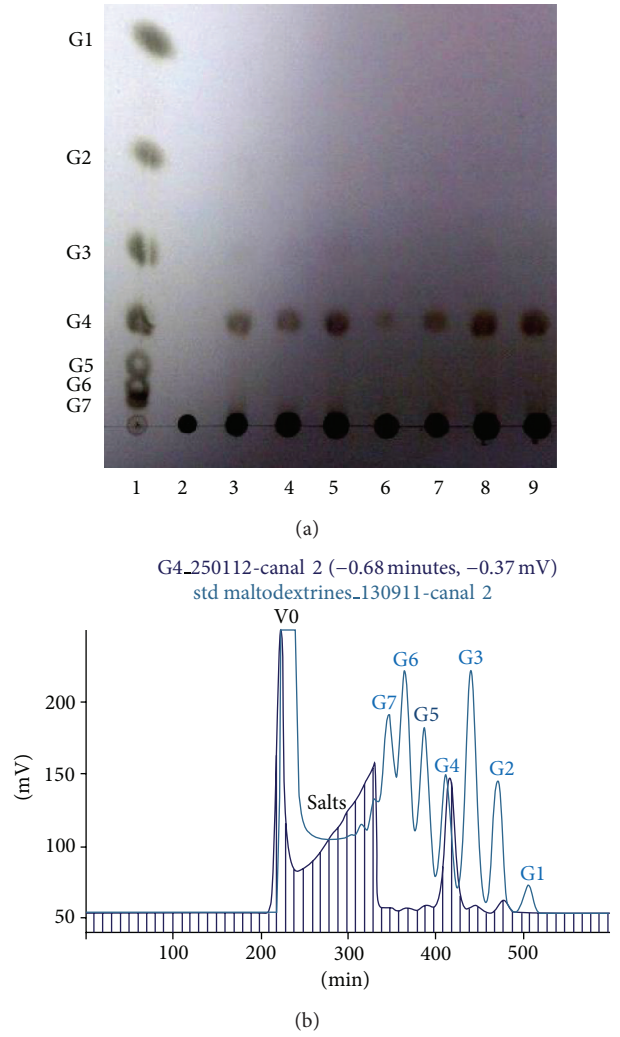

Figure 6: Thin-layer chromatography (a) and GPC (b) analysis of the soluble starch hydrolysates by crude α-amylases of *P. stutzeri* AS22. The reaction mixture containing 0.2 U of α-amylase activity and 1% substrate in 0.1 M Tris-HCl buffer (pH 8.0) was incubated at 60°C. (a) Lane 1: standard maltooligosaccharides (G1–G7), lane 2: starch used as substrate, and lanes 3–9: soluble starch hydrolyzed by *P. stutzeri* AS22 after 2 min, 10 min, 30 min, 1 h, 2 h, 4 h, and 6 h. (b) End products analysis after 6 h hydrolysis of soluble starch. GPC analysis was performed on a Bio-Gel P2 column (1.5 × 200 cm) eluted with water at a rate of 30 mL/h. The different oligosaccharides released after starch hydrolysis were fractionated and quantified in comparison with standard oligosaccharides ranging from G1 to G7. G1: glucose, G2: maltose, G3: maltotriose, G4: maltotetraose, G5: maltopentaose, G6: maltohexaose, and G7: maltoheptaose. V0: the void volume.

temperature (Table 5). Among all inhibitors tested, the chelating agent EDTA and the reducing agent β-mercaptoethanol inactivated the amylolytic activity where it could retain 70% and 66% of its initial activity, respectively. However, the serine proteinase inhibitor PMSF showed no significant inhibition (10%).

The amylolytic preparation revealed a high stability in the presence of 5% of the nonionic surfactants (Tween 20, Tween

Table 6: Time course of maltooligosaccharides production from 1% soluble starch by *P. stutzeri* crude enzyme.

Hydrolysis time	Oligosaccharides concentration (g/L) and **percentage (%)**					
	G1	G2	G3	G4	G5	G6
0 min	0	0	0	0	0	0
5 min	0	0	0	2.68 (**100**)	0	0
15 min	0	0.06 (**1.1**)	0.03 (**0.5**)	5.31 (**98**)	0.02 (**0.4**)	0
30 min	0	0.08 (**1.6**)	0.05 (**0.95**)	5.1 (**97**)	0.023 (**0.45**)	0
1 h	0	0.04 (**0.8**)	0.03 (**0.8**)	4.9 (**98**)	0.02 (**0.4**)	0.01 (**0.2**)
2 h	0	0.058 (**1.2**)	0.03 (**0.6**)	4.75 (**97.5**)	0.02 (**0.41**)	0.014 (**0.29**)
6 h	0	0.07 (**1.4**)	0.05 (**1**)	4.92 (**97**)	0.04 (**0.8**)	0.02 (**0.4**)

0.1 unit of the α-amylase activity was reacted with 1% of soluble starch at 60°C and pH 8.0 and reaction products were analyzed at different time intervals.

80, and Triton X-100) retaining more than 80% residual activity and was fully stable in the presence of 0.1% SDS. However, with further increase in SDS concentration to 1%, around 50% loss of amylolytic activity was observed.

3.2.4. Action Pattern of the Amylolytic Preparation. To examine the mode of action of *P. stutzeri* AS22 crude enzyme on starch hydrolysis, starch was treated with the culture supernatant and the reaction products of samples taken at different time intervals were analysed by TLC. As shown in Figure 6(a), at an early stage of hydrolysis (2 min of reaction), maltotetraose (G4) was released without any intermediate as the specific end product.

On the basis of its mode of action, *P. stutzeri* amylolytic preparation consists in a maltotetraose-forming-α-amylase activity. Previously, maltotetraose-forming-amylases were mainly discovered in *Pseudomonas* strains such as *Pseudomonas stutzeri* [19, 20, 33, 35] *Pseudomonas saccharophila* [24], *Pseudomonas* sp. IMD 353 [22], and *Pseudomonas* MS300 [23] and also in *Bacillus* strains such as *Bacillus* sp. GM8901 [32] and *Bacillus halodurans* MS-2-5 [36].

3.3. Course of Hydrolysis of Starch with the Amylolytic Preparation. To quantify the amounts of the products generated from starch hydrolysis by *P. stutzeri* AS22 crude enzyme, the hydrolysates were analyzed at function of time by gel permeation chromatography (GPC) which was carried out as written in Materials and Methods.

Table 6 and Figure 6(b) summarize the GPC analysis of maltooligosaccharides formed at various time periods of hydrolysis reaction. It is very clear that maltotetraose (G4) is the specific product formed with a high degree of purity in the hydrolysates even from the early stage of the reaction (5 min). While traces of contaminating maltose, maltotriose, maltopentaose and maltohexaose could be produced, glucose was not detectable. Moreover, maltotetraose concentration remains constant at 97–100% from 5 min to 6 h of hydrolysis reaction. This clearly indicates that initially formed maltotetraose was not hydrolyzed and therefore the *P. stutzeri* amylolytic preparation consists principally of a maltotetraose-forming amylase.

Interestingly, the maltotetraose production reached its maximum of 5.3 g/L after 15 min of hydrolysis with negligible amounts of maltose (0.06 g/L), maltotriose (0.03 g/L), and maltopentaose (0.02 g/L). In addition, more than half (55%) of the starch hydrolysis was achieved in 15 min without optimization. Therefore, optimization of reaction conditions especially starch concentration and amylase amount may further increase its yield.

Despite the fact that the starch hydrolysis reaction by *P. stutzeri* crude enzyme occurred without optimization, the level of maltotetraose produced was higher as compared with that of the known maltotetraose-forming amylases. Interestingly, *P. stutzeri* AS22 amylase preparation produced maltotetraose representing up to 97% as compared with the yield of maltotetraose released by the action of *P. stutzeri* [37] purified amylase which was estimated to be only 55%. The isolated amylase from *Bacillus circulans* MG-4 [38] yields 64.9% of maltotetraose with amounts of contaminating glucose, maltose, and maltotriose. Therefore, besides the cost effectiveness offered by its use, the amylolytic preparation of *P. stutzeri* AS22 seems to be quite different, with respect to its efficiency, from the other G4-amylases from *Pseudomonas* species.

4. Conclusion

The nature of culture conditions and composition of media for optimal production of α-amylase by *P. stutzeri* AS22, as well as its crude enzyme biochemical characterization, have been developed in this study.

Incubation period of 24 h, initial pH of 8.0, 30°C incubation temperature, and an agitation speed of 200 rpm were found to be optimum for the production of α-amylase. Amylase production reached 6.8 U/mL by supplementing the fermentation media with starch (1%), yeast extract (0.5%), $MgSO_4$ (0.01%), NaCl (0.05%), K_2HPO_4 (0.14%), KH_2PO_4 (0.07%), and $CaCl_2$ (0.04%).

Temperature 60°C and pH 8.0 were found to be the best for amylase activity. The crude α-amylase was highly stable at the pH ranging from 6.0 to 12.0 and amylase activity was enhanced in presence of Ba^{2+} and Ca^{2+} ions.

The production of high yields of a specific maltooligosaccharide on degradation of starch by α-amylases is of considerable commercial interest. An important characteristic of the *P. stutzeri* AS22 amylase preparation is that it hydrolyses potato starch (1%) into high amount of maltotetraose (5.3 g/L) without synchronous glucose production. Interestingly, this

amylase preparation, producing maltotetraose on a higher yield (98%) as compared with that of previously reported G4-amylases, seems to be promising in the manufacture of high maltotetraose syrups from starch.

Conflict of Interests

The authors declare that there is no conflict of interests regarding the publication of this paper.

Acknowledgments

The authors wish to thank Alain Heyraud and Laurine Buon (CERMAV, CNRS, Grenoble, FR) for providing us with the GPC analysis.

References

[1] M. Fujita, K. Torigoe, T. Nakada et al., "Cloning and nucleotide sequence of the gene (*amy*P) for maltotetraose-forming amylase from *Pseudomonas stutzeri* MO-19," *Journal of Bacteriology*, vol. 171, no. 3, pp. 1333–1339, 1989.

[2] H. Barreteau, C. Delattre, and P. Michaud, "Production of oligosaccharides as promising new food additive generation," *Food Technology and Biotechnology*, vol. 44, no. 3, pp. 323–333, 2006.

[3] T. Nakakuki, "Present status and future of functional oligosaccharide development in Japan," *Pure and Applied Chemistry*, vol. 74, no. 7, pp. 1245–1251, 2002.

[4] H. R. Palacios, P. B. Schwarz, and B. L. D'Appolonia, "Effect of α-amylases from different sources on the retrogradation and recrystallization of concentrated wheat starch gels: relationship to bread staling," *Journal of Agricultural and Food Chemistry*, vol. 52, no. 19, pp. 5978–5986, 2004.

[5] M. Rivero-Urgell and A. Santamaria-Orleans, "Oligosaccharides: application in infant food," *Early Human Development*, vol. 65, no. 2, pp. S43–S52, 2001.

[6] P. V. Aiyer, "Amylases and their applications," *African Journal of Biotechnology*, vol. 4, no. 13, pp. 1525–1529, 2005.

[7] J. Malabendu, M. Chiranjit, S. Saptadip et al., "Salt-independent thermophilic α-amylase from *Bacillus megaterium* VUMB109: an efficacy testing for preparation of maltooligosaccharides," *Industrial Crops and Products*, vol. 41, pp. 386–390, 2013.

[8] L. Duedahl-Olesen, K. Matthias Kragh, and W. Zimmermann, "Purification and characterisation of a malto-oligosaccharide-forming amylase active at high pH from *Bacillus clausii* BT-21," *Carbohydrate Research*, vol. 329, no. 1, pp. 97–107, 2000.

[9] A. Pandey, P. Nigam, C. R. Soccol, V. T. Soccol, D. Singh, and R. Mohan, "Advances in microbial amylases," *Biotechnology and Applied Biochemistry*, vol. 31, no. 2, pp. 135–152, 2000.

[10] J. Lalucat, A. Bennasar, R. Bosch, E. García-Valdés, and N. J. Palleroni, "Biology of *Pseudomonas stutzeri*," *Microbiology and Molecular Biology Reviews*, vol. 70, no. 2, pp. 510–547, 2006.

[11] H. Maalej, N. Hmidet, O. Ghorbel-Bellaaj, and M. Nasri, "Purification and biochemical characterization of a detergent stable α-amylase from *Pseudomonas stutzeri* AS22," *Biotechnology and Bioprocess Engineering*, vol. 18, no. 5, pp. 878–887, 2013.

[12] J. H. Miller, *Experiments in Molecular Genetics*, Cold spring Harbor Laboratory, Cold Spring Harbor, NY, USA, 3rd edition, 1972.

[13] G. L. Miller, "Use of dinitrosalicyIic acid reagent for determination of reducing sugar," *Analytical Chemistry*, vol. 31, no. 3, pp. 426–428, 1959.

[14] A. Sharma and T. Satyanarayana, "Optimization of medium components and cultural variables for enhanced production of acidic high maltose-forming and Ca^{2+}-independent α-amylase by *Bacillus acidicola*," *Journal of Bioscience and Bioengineering*, vol. 111, no. 5, pp. 550–553, 2011.

[15] K. R. Babu and T. Satyanarayana, "Parametric optimization of extracellular α-amylase production by thermophilic *Bacillus coagulans*," *Folia Microbiologica*, vol. 38, no. 1, pp. 77–80, 1993.

[16] K. Tonomura, H. Suzuki, N. Nakamura, K. Kuraya, and O. Tanabe, "On the inducers of α-amylase formation in *Aspergillus oryzae*," *Agricultural and Biological Chemistry*, vol. 25, no. 1, pp. 1–6, 1961.

[17] R. Morkeberg, M. Carlsen, and J. Nielsen, "Induction and repression of α-amylase production in batch and continuous cultures of *Aspergillus oryrae*," *Microbiology*, vol. 141, no. 10, pp. 2449–2454, 1995.

[18] R. Gupta, P. Gigras, H. Mohapatra, V. K. Goswami, and B. Chauhan, "Microbial α-amylases: a biotechnological perspective," *Process Biochemistry*, vol. 38, no. 11, pp. 1599–1616, 2003.

[19] J. F. Robyt and R. J. Ackerman, "Isolation, purification, and characterization of a maltotetraose-producing amylase from *Pseudomonas stutzeri*," *Archives of Biochemistry and Biophysics*, vol. 145, no. 1, pp. 105–114, 1971.

[20] T. Nakada, M. Kubota, S. Sakai, and Y. Tsujisaka, "Purification and characterization of two forms of maltotetraose-forming amylase from *Pseudomonas stutzeri*," *Agricultural and biological chemistry*, vol. 54, no. 3, pp. 737–743, 1990.

[21] W. M. Fogarty and C. T. Kelly, *Industrial Enzymes and Biotechnology*, Elsevier Applied Science, New York, NY, USA, 2nd edition, 1990, W. M. Fogarty, C. T. Kelly, Eds.

[22] W. M. Fogarty, C. T. Kelly, A. C. Bourke, and E. M. Doyle, "Extracellular maltotetraose-forming amylase of *Pseudomonas* sp. IMD 353," *Biotechnology Letters*, vol. 16, no. 5, pp. 473–478, 1994.

[23] H. Kobayashi, Y. Takaki, K. Kobata, H. Takami, and A. Inoue, "Characterization of α-maltotetraohydrolase produced by *Pseudomonas* sp. MS300 isolated from the deepest site of the Mariana trench," *JAMSTEC Journal of Deep Sea Research*, vol. 16, pp. 109–116, 2000.

[24] S. Kobayashi, H. Okemoto, K. Hara, H. Hashimoto, and K. Yamasato, "Preparation and some properties of a novel maltotetraose-forming enzyme of *Pseudomonas saccharophila*," *Journal of the Japanese Society of Starch Science*, vol. 38, no. 1, pp. 27–36, 1991.

[25] K. Kathiresan and S. Manivannan, "α-Amylase production by *Penicillium fellutanum* isolated from mangrove rhizosphere soil," *African Journal of Biotechnology*, vol. 5, no. 10, pp. 829–832, 2006.

[26] A. Rameshkumar and T. Sivasudha, "Optimization of nutritional constitute for enhanced alpha amylase production using by solid state fermentation technology," *International Journal of Microbiological Research*, vol. 2, no. 2, pp. 143–148, 2011.

[27] S. Sivaramakrishnan, D. Gangadharan, K. M. Nampoothiri, C. R. Soccol, and A. Pandey, "α-amylases from microbial sources—an overview on recent developments," *Food Technology and Biotechnology*, vol. 44, no. 2, pp. 173–184, 2006.

[28] R. Malhotra, S. M. Noorwez, and T. Satyanarayana, "Production and partial characterization of thermostable and calcium-independent α-amylase of an extreme thermophile *Bacillus*

thermooleovorans NP54," *Letters in Applied Microbiology*, vol. 31, no. 5, pp. 378–384, 2000.

[29] G. Subramanian, S. Ayyadurai, T. Sharma, S. A. Singh, M. Rele, and L. S. Kumar, "Studies on maltoheaose (G6) producing alkaline amylase from a novel alkalophilic *Streptomyces* species," *The IIOAB Journal*, vol. 3, no. 3, pp. 15–30, 2012.

[30] Z. Konsoula and M. Liakopoulou-Kyriakides, "Co-production of α-amylase and β-galactosidase by *Bacillus subtilis* in complex organic substrates," *Bioresource Technology*, vol. 98, no. 1, pp. 150–157, 2007.

[31] Sudha, "Effect of different concentrations of metal ions on alpha amylase production by *Bacillus amyloliquefaciens*," *Research in Biotechnology*, vol. 3, pp. 67–71, 2012.

[32] T. U. Kim, B. G. Gu, J. Y. Jeong, S. M. Byun, and Y. C. Shin, "Purification and characterization of a maltotetraose-forming alkaline α- amylase from an alkalophilic *Bacillus* strain, GM8901," *Applied and Environmental Microbiology*, vol. 61, no. 8, pp. 3105–3112, 1995.

[33] Y. Sakano, Y. Kashiwagi, and T. Kobayashi, "Purification and properties of an exo-α-amylase from *Pseudomonas stutzeri*," *Agricultural and Biological Chemistry*, vol. 46, no. 3, pp. 639–646, 1982.

[34] A. Sharma and T. Satyanarayana, "Microbial acid-stable α-amylases: characteristics, genetic engineering and applications," *Process Biochemistry*, vol. 48, no. 2, pp. 201–211, 2013.

[35] M. J. Lee and M. J. Chung, "Studies on the exo-maltotetraohydrolase of *Pseudomonas stutzeri* IAM 12097—part II: characteristics of exo-maltotetraohydrolase," *Journal of the Korean Chemical Society*, vol. 27, pp. 271–273, 1984.

[36] S. Murakami, K. Nagasaki, H. Nishimoto et al., "Purification and characterization of five alkaline, thermotolerant, and maltotetraose-producing α-amylases from *Bacillus halodurans* MS-2-5, and production of recombinant enzymes in *Escherichia coli*," *Enzyme and Microbial Technology*, vol. 43, no. 4-5, pp. 321–328, 2008.

[37] J. Schmidt and M. John, "Starch metabolism in *Pseudomonas stutzeri*. I. Studies on maltotetraose-forming amylase," *Biochimica et Biophysica Acta*, vol. 566, no. 1, pp. 88–99, 1979.

[38] Y. Takasaki, H. Shinohara, M. Tsuruhisa, S. Hayashi, and K. Imada, "Maltotetraose-producing amylase from *Bacillus* sp. MG-4," *Agricultural and Biological Chemistry*, vol. 55, no. 7, pp. 1715–1720, 1991.

Hindawi Publishing Corporation
BioMed Research International
Volume 2014, Article ID 308613, 11 pages
http://dx.doi.org/10.1155/2014/308613

Research Article

Immobilization of a *Pleurotus ostreatus* Laccase Mixture on Perlite and Its Application to Dye Decolourisation

Cinzia Pezzella,[1] Maria Elena Russo,[2] Antonio Marzocchella,[3] Piero Salatino,[3] and Giovanni Sannia[1]

[1] *Dipartimento di Scienze Chimiche, Università di Napoli Federico II, via Cynthia 4, 80126 Napoli, Italy*
[2] *Istituto di Ricerche sulla Combustione, Consiglio Nazionale delle Ricerche, Piazzale V. Tecchio 80, 80125 Napoli, Italy*
[3] *Dipartimento di Ingegneria Chimica, dei Materiali e della Produzione Industriale, Università degli Studi di Napoli Federico II, Piazzale V. Tecchio 80, 80125 Napoli, Italy*

Correspondence should be addressed to Cinzia Pezzella; cpezzella@unina.it

Received 13 January 2014; Revised 3 April 2014; Accepted 24 April 2014; Published 8 May 2014

Academic Editor: Neelu Nawani

In the present study, a crude laccase preparation from *Pleurotus ostreatus* was successfully immobilized on perlite, a cheap porous silica material, and tested for Remazol Brilliant Blue R (RBBR) decolourisation in a fluidized bed recycle reactor. Results showed that RBBR decolourisation is mainly due to enzyme action despite the occurrence of dye adsorption-related enzyme inhibition. Fine tuning of immobilization conditions allowed balancing the immobilization yield and the resulting rate of decolourisation, with the adsorption capacity of the solid biocatalyst. In the continuous lab scale reactor, a maximum conversion degree of 56.1% was achieved at reactor space-time of 4.2 h. Stability and catalytic parameters of the immobilized laccases were also assessed in comparison with the soluble counterparts, revealing an increase in stability, despite a reduction of the catalytic performances. Both effects are most likely ascribable to the occurrence of multipoint attachment phenomena.

1. Introduction

The ever-increasing attention towards the design of industrial processes with low environmental impact and high sustainability has encouraged the search for new biocatalysts to be employed as green tools for several industrial applications. In this "greener" perspective, laccases (*p*-diphenol-dioxygen oxidoreductases; EC 1.10.3.2) represent an interesting class of biocatalyst, being able to oxidize a wide spectrum of aromatic compounds along with reducing molecular oxygen to water [1]. Besides the exploitation in several applicative fields, such as in food sector, paper and pulp industry, biosensing, polymer functionalization, and textile industries [2], laccases have attracted growing interest for their successful use in bioremediation processes [3], particularly for the treatment of dye-containing wastewaters [4, 5], thanks to the structural similarity of many textile dyes with laccase natural substrates. In particular, laccases from the white rot fungus *Pleurotus ostreatus* have been extensively studied for their decolourisation ability towards several classes of dyes and wastewater models [6–8]. Reported data indicated that the extent of decolourisation depends on the laccase isoform used [6] and on the chemical class of the dye [8].

Even though laccase efficacy in dye conversion has been extensively demonstrated [9], there are still many constraints to their application for real wastewater treatment, due to the hard conditions characterizing real wastewaters (extreme pH values, very high ionic strength, presence of surfactants, cheating agents, etc.) and the huge volume of polluted waters demanding remediation. Both constraints clearly highlight the need for the choice of very robust catalyst for the process. Enzyme immobilization has widened the scope of laccase application allowing not only reusing of the biocatalyst, with a benefit in terms of costs, but especially improving enzyme

performances, leading to higher activity and stability at extreme pHs, elevated temperatures, or in organic solvents and improved thermostability. Such enhanced features have encouraged the use of immobilized laccases in several applications, as recently reviewed by Fernández-Fernández [10]. Different methodologies have been reported for laccase immobilization, such as adsorption, entrapment, encapsulation, covalent binding, and self-immobilization. The choice of the most suited method clearly depends on application that laccase is devoted to. Particularly, covalent binding is the most widely applied method for exploitation of immobilized laccases in industrial applications [11–13].

Covalent immobilization represents an attractive option to obtain enzymatic catalyst for wastewater treatment. This technique provides different advantages: (i) it prevents enzyme leakage even under harsh conditions; (ii) it facilitates enzyme use in continuous, packed bed, stirred tank, and fluidized bed reactors; (iii) it causes stabilization of the enzyme tertiary structure, usually as a consequence of multipoint attachment of the enzyme to the support, providing enzyme rigidity. The stabilization provided by covalent bonding is usually counterbalanced by partial enzyme deactivation. This negative effect can be mitigated by carefully optimizing the immobilization conditions in order to maximize the ratio between immobilized enzyme activity and activity of the primary enzyme solution.

Decolourisation of several dyes has been achieved by means of laccase covalently bound to different supports, such as alumina oxide pellets [14], controlled porosity-carrier beads [15], and epoxy-activated supports [13]. Effective dye removal was also carried out by *C. unicolor* laccase covalently immobilized on mesostructured siliceous cellular foams (MCGs) [16] or on supports functionalized with epoxy groups [2]. In the latter case, the degradation of different classes of dyes was reported, along with an improvement of stability toward pH, temperature, and storage of the immobilized enzyme. Entrapment of laccase has also been used as an immobilization approach for environmental applications. Chitosan-coated alginate beads have been packed in a fixed bed reactor and employed in RBBR decolourisation, achieving up to 70% decolourisation [6]. Alginate beads differently modified with chitosan or polyethylene glycol (PEG) have also shown to effectively decolourise several different dyes [17–19]. Entrapment in hydrogel structures has also been applied, for example, in the immobilization of a *T. versicolor* laccase, resulting in low substrate affinity but improvement in storage stability and in the decolourisation of Acid Orange 52 [20].

An important aspect to be considered in the design of an ideal immobilized biocatalyst is the cost related to the support and to the enzyme to be linked to it. In this study, a low-cost laccase mixture was obtained from *P. ostreatus* culture broth after optimization of laccase production conditions and one-step protein enrichment, as described by Palmieri et al. [6]. On the other hand, the search for a cheap solid support has oriented our study toward the choice of a siliceous material, perlite. Perlite is an amorphous aluminium silicate with more than 70% content of silica. Besides exhibiting the advantages of an inorganic carrier with respect to organic ones, such as a greater mechanical stability and resistance toward microbial attack and organic solvents, perlite turns out to be a cheaper alternative in comparison with other reported inorganic supports such as silica gels, alumina, and zeolites [21]. The choice of such an inert support implies that its surface has to be properly modified in order to offer functional groups for protein binding. Surface modification of these materials can be easily achieved and their reactivity may be finely tuned in the derivatization steps [22].

In this work, covalent immobilization of laccase on activated siliceous support, perlite, was investigated and the immobilized biosystem was tested for its potential exploitation in dye decolourisation using the reactive dye RBBR as model substrate. The immobilization process was properly optimized with reference to the immobilization yield and to the dye adsorption capacity of the solid biocatalyst. Stability and catalytic parameters of immobilized laccases were also assessed in comparison with the soluble counterpart.

2. Materials and Methods

2.1. Fungal Culture and Crude Laccase Extraction. *Pleurotus ostreatus* (type: Florida ATCC number MYA-2306) was maintained through periodic transfer every 3 weeks, at 4° on agar plates containing 24 g/L potato dextrose and 5 g/L yeast extract. Medium components were supplied by Difco Laboratories (Detroit, MI). Mycelium growth and crude laccase mixture extraction were carried out following the procedures described by Faraco et al. [7].

The crude laccase mixture extract is characterized by four isoforms (POXA1b, POXA3a, POXA3b, and POXC). The activity of the POXC isoform accounts for about 99% of the total mixture activity [7]. The laccase mixture used in the immobilization trials displays a specific activity of 70 U/mg.

2.2. Dye. The anthraquinonic dye Remazol Brilliant Blue R (RBBR) was purchased from Sigma-Aldrich. Powder purity was 50%. Dye concentration was measured by recording optical absorbance at 592 nm. The extinction coefficient (ε_{592} = 9,000 M^{-1} cm^{-1}), referred to total powder concentration, was corrected taking into account the purity. All other reagents were purchased from Sigma-Aldrich with a ≥98% purity.

Laccase Activity Assay. Laccase activity was assayed at 25°C by monitoring the oxidation of ABTS at 420 nm (ε_{420} = 36 × 10^3 M^{-1} cm^{-1}) [6]. The assay mixture contained 2 mM ABTS in 0.1 M sodium citrate buffer (pH 3.0).

K_M values were estimated using the software GraphPad Prism (GraphPad Software, La Jolla, CA, USA; http://www.graphpad.com/) on a wide range of substrate concentrations (0.05–3 mM). Enzyme activity was expressed in international units (IU).

2.3. Protein Determination and Electrophoresis. Protein concentration was determined using the BioRad Protein Assay (Bio-Rad Laboratories, Segrate (MI), Italy), with bovine Serum albumin (BSA) as standard.

2.4. Perlite Pretreatment and Derivatization. Perlite (SIPERNAT 22©) was supplied by Degussa (Hanau, Germany). Solids (density about 1,026 kg/m^3) were sieved in the range of 90–150 μm. Perlite was pretreated with 1.2 M HNO_3 at 60°C for 4 hours and then extensively washed with water and dried at 60°C. Solids were vigorously fluidized with water to remove fines. The minimum fluidization velocity estimated according to Fan [23] for the liquid-solids system is about $4{\cdot}10^{-6}$ m/s.

Silanization is a crucial step with regard to subsequent reproducibility of the chemical functionalization. However, the surface coverage, orientation, and organization of reactive groups are still a subject of controversy [24]. Despite resulting in a lower surface concentration of amino groups in comparison with reaction in organic solvents, aqueous silanization with APTS (aminopropyltrimethoxysilane) has been selected for this study, since it was demonstrated to result in a more stable and uniform immobilized enzyme layer [25].

Glutaraldehyde is a bifunctional molecule which has been extensively used as an enzyme immobilizing agent. Although there are many discussions on the composition of the glutaraldehyde solution (monomeric and polymeric forms) and on the structures responsible for its properties, it is generally accepted that it is capable of reacting with surface amine groups of enzyme and carriers, through the formation of Schiff's bases and Michael's adducts [26].

Carrier activation was carried out as follows: (i) 0.2 g of dry pretreated perlite was mixed with APTS at a concentration from 0.4% to 4% in 5 mL distilled water and incubated at 80°C for 2 h under constant mixing; (ii) the suspension was washed thoroughly with 50 mM sodium phosphate (NaP) buffer, pH 6.5, and treated with glutaraldehyde solutions and dissolved at different concentrations, in the same buffer, for 2 h at room temperature; (iii) the activated perlite was extensively washed with the overcited buffer and finally incubated for 1 h with 5 mL of a solution of laccase mixture (22 U/mL) in 50 mM NaP buffer, pH 6.5, at room temperature. Residual active glutaraldehyde was inactivated by 1 h incubation with 100 mM glycine at room temperature.

2.5. Adsorption Experiments. Dye adsorption on unreacted particles was determined by incubating 0.2 g of particles in a RBBR solution at preset concentrations. All the experiments were performed in the conditions usually adopted during dye conversion tests, 20 mM sodium acetate (NaA) pH 4.5 at room temperature. Dye concentration in the liquid phase was measured as optical absorbance at 592 nm. The dye adsorption was highlighted by the decrease of the optical absorbance in the liquid phase as well as by an increase of particles colouration. The procedure adopted for each experiment was (i) dispersion of particles in dye solution; (ii) as the dye concentration in the liquid did not changed anymore (achievement of equilibrium between solids and liquid), the liquid was replaced with fresh dye solution. The cyclic operation was repeated until no change in the initial concentration of dye was observed. The overall amount of adsorbed dye during each cycle was calculated from the mass balance referred to the dye.

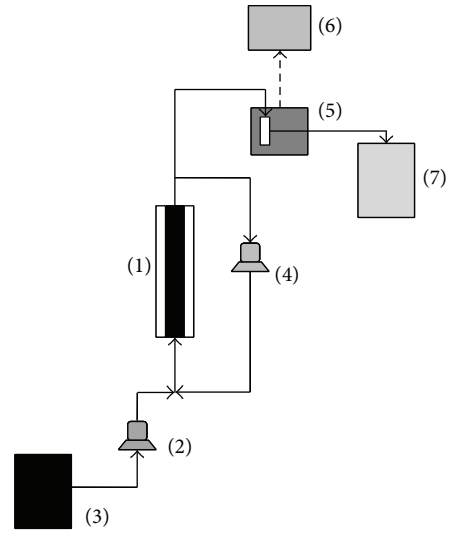

Figure 1: Apparatus equipped with fluidized bed reactor adopted for RBBR conversion by means of immobilized laccases. (1) Fluidized bed reactor; (2) peristaltic pump; (3) feed tank; (4) recirculation gear pump; (5) flow-cell and spectrophotometer; (6) data acquisition unit; (7) waste tank.

2.6. Assay of Immobilized Enzyme Activity. The activity of laccase immobilized on perlite was estimated by measuring the oxidation rate of 2,2′-azino-bis (3-ethylbenzothiazoline-6-sulphonic acid) (ABTS) in a recirculating fixed bed reactor previously designed for the assessment of activity of enzymes immobilized on granular solids [13]. The device was equipped with a fixed bed reactor, loaded with biocatalyst particles. It was operated by circulating the liquid phase containing the substrate between the fixed bed and a mixed tank according to the procedure reported by Russo et al. [13]. The increase of optical absorbance at 420 nm was assessed by online measurements on the circulating liquid phase in the mixed tank. The operating conditions were purposely selected in order to prevent mass transfer limitations during the enzymatic conversion: the assay was carried out under kinetic controlled regime. The operating conditions were total reaction volume (tank, tubes, fittings, and inert fixed bed) 72 mL, tubular reactor packed with 0.18 mL solid biocatalyst and liquid circulation rate at volumetric flow rate 20 mL/min.

2.7. Fluidized Bed Reactor for RBBR Conversion. Conversion of RBBR by immobilized laccases was investigated in a fluidized bed reactor continuously operated with respect to the liquid phase. A sketch of the apparatus is shown in Figure 1. Biocatalyst particles were loaded in a cylindrical vessel (2.5 cm ID, 30 cm long). Solid particles were fluidized with the liquid stream delivered by a gear pump (VG 1000 digit, Verder). The dye-bearing liquid solution was fed at the reactor by means of a peristaltic pump. The liquid was recirculated through the reactor at volumetric flow rate (Q_r) by means of a peristaltic pump (Miniplus, Gilson). Dye concentration in the outlet stream was measured continuously by means of a spectrophotometer (Cary 50, Varian Inc.) equipped with

a flow-cell. Optical absorbance was measured at 592 nm. Dye conversion was carried out in conditions assessed as optimal for RBBR decolourisation, 20 mM sodium acetate buffer pH 4.5 at room temperature [6]. The minimum liquid flow rate required for the solid fluidization, estimated assuming the crude solid density, for example, without any adsorbed species, was about 0.10 mL/min.

Total liquid volume was set at 71 mL. The test procedure was as follows:

(i) saturation of the catalyst with the dye. The reactor was fed with dye bearing liquid stream at 12.4 mL/min (more than 100 times the expected minimum fluidization rate) without stream recycling. The liquid flow rate was enough to fluidized particles. The reactor space-time ($\tau \cong 4$ min) was set to saturate the solids with dye at a negligible enzymatic conversion; solid saturation was accomplished within 2 hours;

(ii) as the solid was saturated, the feeding flow rate Q was decreased to the set value and the liquid was recycled ($Q_r = 13$ mL/min). A series of steady state regimes was investigated by setting Q in the interval 0.3–13 mL/min. The reactor was operated at the preset Q until dye concentration in the reactor approached a steady value. The dye conversion was assessed under steady state conditions.

3. Results and Discussion

3.1. Optimization of Immobilization Process on Activated Perlite. Functionalization of perlite surface has been achieved by two main steps: (i) silanization with a trifunctional organosilane agent APTS that provides the reactive amino groups susceptible to the following activation; (ii) reaction with a crosslinking reagent, glutaraldehyde.

In this section, results on the optimization of immobilization of crude laccase preparation on perlite are reported.

Activity of laccase immobilized on perlite was measured adopting a specifically designed device as described in Section 2. Immobilization yield (Y) is the objective parameter assessed to optimize the immobilization protocol. Y was defined as the ratio between laccase activity expressed by the solid biocatalyst and total activity in the liquid solution at the beginning of the immobilization processes.

Process optimization has been carried out assessing the effect of the following operating conditions on the immobilization yield: glutaraldehyde concentration, pH and buffer composition of immobilization solution, time and temperature of incubation, total activity, and total protein contents. Table 1 reports the results in terms of immobilized activity and yield for each run. The operating conditions of each run are also reported.

3.1.1. Effect of Glutaraldehyde Concentration. The effect of the results reported in Table 1 indicates that, at 1% and 2.5% glutaraldehyde concentrations, immobilization yield is higher when incubation is performed at RT for shorter time (R1, R3), with respect to overnight incubation at 4°C (R2, R4). No laccase activity or proteins were detected in the recovered supernatant at the end of incubation, indicating that 100% of the initial protein content was bounded to the carrier. The lower immobilization yield found in R2 and R4 could be ascribed to further interaction of enzymes with glutaraldehyde molecules for prolonged incubation time, causing laccase inactivation. When glutaraldehyde concentration is raised up to 5%, immobilization yields are almost comparable at RT for 4 h or overnight at 4°C (see R5 and R6). It is conceivable that, at higher concentration, glutaraldehyde-glutaraldehyde interactions prevail on glutaraldehyde-protein ones, thus reducing the negative effect on the enzyme observable at longer incubation times. Taken together, these results indicate that the reactive groups, made available by using glutaraldehyde concentrations in the range 1% to 5%, are sufficient to bind to all proteins present in the crude mixture, resulting in a maximum immobilization yield of about 34%. When immobilization experiments were carried out further lowering glutaraldehyde concentration down to 0.5%, a comparable yield (32%) was achieved (see R10). Thus, glutaraldehyde concentration was set at 0.5% for further immobilization experiments.

3.1.2. Effect of pH and Buffer Composition. One of the factors that can affect enzyme immobilization is the pH value of the coupling mixture. The optimal pH value should be the compromise between conditions favoring enzyme stability and those promoting the nucleophilic attack of protein reactive groups to the glutaraldehyde functionalized support. The results obtained performing laccase immobilization at pH values 5.5, 6.5, and 7.5 are listed in Table 1 (R17–R22). The immobilization yield was almost constant in the neutral pH range (~50%) and decreased at 19% at low pH. Except for test carried out at low pH, no laccase activity or proteins were found in the recovered supernatant at high pH (6.5 and 7.5). At low pH, about 25% of the initial laccase activity was detected in the supernatant.

As reported in Table 1, immobilization at pH 5.5 was carried out in a buffer containing a different counterion, sodium citrate instead of sodium phosphate buffer at the same molarity. To complete the scenario of the combined pH buffer effects, tests were also performed at the three investigated pH values adopting citrate-based buffer, the McIlvaine buffer. Under these conditions (R20 through R22), a significant reduction of immobilization yield was observed at all the tested pH, with up to 28% of the initial laccase activity recovered in the supernatants.

These findings could be a consequence of the heterofunctional nature of the activated matrix: after glutaraldehyde activation, the support may expose unreacted amino groups which confer some ionic exchanger features to the support [22]. In such heterofunctional matrices, a first ionic adsorption of the protein on the amino groups of the support was found to occur before the covalent reaction between glutaraldehyde activated sites and the enzymes occurs. A different counterion selectivity (citrate > phosphate) towards the unreacted amino groups of the support could explain the observed effect, by assuming that most of the positively charged groups on the support are shielded by citrate (whose

Table 1: Effects of experimental parameters on laccase immobilization yield on perlite. NaC: 50 mM sodium citrate buffer; McI: McIlvaine's buffer. *Incubations were performed in 50 mM sodium phosphate buffer, unless otherwise is indicated. Reported data are the mean values of three independent experiments. The standard deviation of tests carried out at a given set of operating conditions was less than ±10%.

Run	Initial activity (IU/g)	Initial protein (mg/g)	Glutaraldehyde % vol	pH*	Incubation time and temperature	Immobilized activity (IU/g)	Immobilization yield (%)
R1	550	4.5	1	6.5	4 h RT	200	36
R2	550	4.5	1	6.5	Overnight 4°C	128	23
R3	550	4.5	2.5	6.5	4 h RT	206	37
R4	550	4.5	2.5	6.5	Overnight 4°C	151	27
R5	550	4.5	5	6.5	4 h RT	206	37
R6	550	4.5	5	6.5	Overnight 4°C	207	38
R7	550	7.75	1	6.5	1 h RT	160	29
R8	550	7.75	1	6.5	4 h RT	161	29
R9	550	7.75	0.5	6.5	1 h RT	186	34
R10	550	7.75	0.5	6.5	4 h RT	178	32
R11	80	1.3	0.5	6.5	1 h RT	56	70
R12	285	4.75	0.5	6.5	1 h RT	136	48
R13	800	11.25	0.5	6.5	1 h RT	199	25
R14	500	4.25	0.5	6.5	1 h RT	173	35
R15	500	12	0.5	6.5	1 h RT	173	35
R16	500	22.5	0.5	6.5	1 h RT	184	37
R17	275	2.25	0.5	NaC 5.5	1 h RT	52	19
R18	275	2.25	0.5	6.5	1 h RT	137	50
R19	275	2.25	0.5	7.5	1 h RT	120	43
R20	275	2.25	0.5	McI 5.5	1 h RT	32	12
R21	275	2.25	0.5	McI 7.5	1 h RT	66	24
R22	275	2.25	0.5	McI 6.5	1 h RT	42	15

concentration increases lowering pH in McIlvaine buffer composition). Such charge-shielding effect would hinder the first ionic interchange of the protein on the amino groups of the supports, thus impairing immobilization yield.

3.1.3. Temperature and Time of Incubation. The effect of temperature on the immobilization yield was assessed comparing the runs R1–R10. The immobilization yield assessed for tests carried out at incubation temperature as low as 4°C did not changed with respect to that assessed at room temperature. In addition, extending the incubation time to overnight incubation (at 4°C) caused a decrease in immobilization yield (compare R1–R3 with R2–R4) or resulted in almost comparable yields (compare R5 to R6) with respect to 4 hours room-temperature incubation. When laccase activity and total protein content were determined in the liquid supernatant as a function of the incubation time, both measured values became negligible after 15 minutes incubation, indicating the immobilization of almost the entire protein content of the crude mixture occurred. Hence, further experiments were carried out at incubation time set at 1 h without temperature control.

3.1.4. Effect of Total Activity and Total Protein Contents. Some immobilization tests were carried out at the ratio between initial laccase activity and mass of dry support set in the range of 80–800 IU/g (experiments R11–R13). For a given amount of dry support, results showed that the immobilization yield decreased with the amount of initial laccase activity while the immobilized activity (IU/g) approached a constant value (Figure 2). This observation could be interpreted taking into account protein overcrowding on the carrier surface that

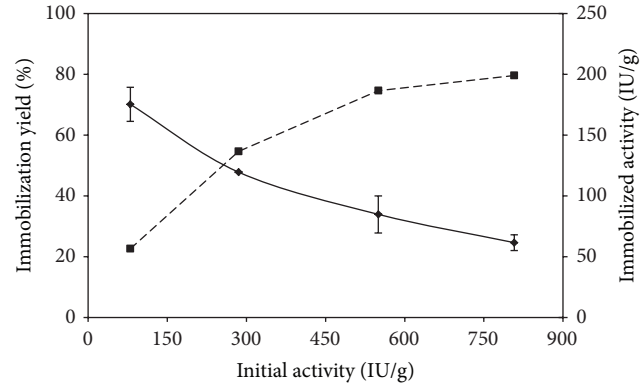

Figure 2: Immobilization yield (solid line) and immobilized activity (dashed line) versus laccase initial activity.

may reduce substrate accessibility to the active site. However, results of the test series of tests R14 through R16 enabled us to rule out this hypothesis. As a matter of fact, tests carried out at a given activity (IU/g) and at protein content increased by adding BSA were characterized by absence of immobilization yield, as it would have been expected if the above interpretation was verified. Moreover, it is worth noting that proteins were completely bounded to the support even at the highest concentration investigated. Both series of data (R11 through 13 and R14 through R16) can be accounted for considering that access of substrate to immobilized enzyme was restricted by the irreversible sealing of carrier micropores by polymeric components contained in the crude mixture (i.e., ferulic acid polymer) or other contaminants, whose amount increases when a more concentrated laccase mixture is used. On the basis of the abovementioned results, the optimal parameters selected are (i) solids activation with 0.5% glutaraldehyde; (ii) 1 h incubation with laccase mixture (50 mM sodium phosphate buffer, pH 6.5, and 80 IU/g support) at room temperature. In these conditions, a maximum immobilization yield of about 70% was achieved.

As expected, there is a difference between the actual laccase activity expressed by the biocatalyst and the activity loss in the liquid supernatant. This effect may be due to the modifications of the enzyme structures occurring during covalent immobilization.

The analysis of POXC primary sequence coupled to the examination of protein 3D model reveals the presence of six Lys residues, all of them localized on the protein surface and potentially available for the covalent bonding with glutaraldehyde. As shown in Figure 3, all Lys residues are mapped on the opposite side with respect to the active site; thus enzyme binding in nonproductive orientation is less probable. On the other hand, multipoint attachment of protein to support seems to be favored since two couples of lysine residues very close to each other are identifiable on the protein surface (Lys 504 and Lys 70 in Figure 3(a); Lys 51 and Lys 20 in Figure 3(b)). Such kind of interaction with the support may be responsible for distortion of enzymatic conformation, causing a decrease in its activity [10].

3.2. Assessment of Immobilized Biosystem Performances. The performances of the immobilized biosystem have been tested by assessing its stability and catalytic parameters.

3.2.1. Stability Parameters. In order to have a suitable amount of immobilized activity on an easily handling amount of solid support, an enzyme to support ratio of about 290 IU/g was used, obtaining, with the aforesaid optimized conditions, an immobilization yield of about 45%. Storage stability of the immobilized laccase mixture has been monitored both at room temperature and at 4°C and was compared with that observed for free laccase mixture. Residual activity was calculated and expressed as percentages of residual activity at different time intervals. As showed in Figure 4, the immobilized mixture, stored at room temperature, displays about 7-fold increased stability with respect to the free laccase mixture ($t_{1/2}$ free enzyme = 1.6 days; $t_{1/2}$ immobilized enzyme = 11.6 days). On the contrary, stability at 4°C shows a 3-fold increase of $t_{1/2}$ ($t_{1/2}$ free enzyme = 18.5 days; $t_{1/2}$ immobilized enzyme = 61 days).

The enhanced stability of immobilized laccase may be due to the prevention of structural rearrangement and the lower flexibility of the immobilized form, both caused by multipoint attachment to the support [28]. These results are consistent with those described in other reports of covalent laccase immobilization on silica-based supports such as kaolinite or mesoporous silica nanoparticles [15, 29–32]. In most cases in which glutaraldehyde was used as crosslinking agent, immobilization process exhibits low laccase recovery but improvements in the operational stability and stability against denaturing agents are evident [16]. Liu et al, for example, reported an improvement of both thermal and operational stability of laccase, when silanized and glutaraldehyde activated silica nanoparticles were used as supports, as illustrated by the retention of 61% of the residual activity after 4 h at 60°C and the retention of 55% of the activity after 10 cycles of operation.

Immobilization can provide an artificial microenvironment surrounding the enzyme that can alter surface-exposed hydrophilic and/or charged groups and their electrostatic interactions and thus influencing protein structure and function. In particular, in the immobilized system described in this study, enzymes could be doubly protected by thermal inactivation thanks to the higher number of positive charges on the surface and to the increased hydrophobicity, both provided by silanization [33].

3.2.2. Catalytic Parameters. In order to perform a kinetic characterization of the immobilized biocatalyst, purified laccase POXC from *P. ostreatus* has been used rather than the crude mixture. The purified enzyme has been immobilized in the following conditions: 0.2 g of activated perlite was incubated for 1 h with purified POXC solution (50 mM NaP buffer, pH 6.5, and 250 IU/g of support as initial activity) at room temperature, resulting in about 40% immobilization yield (100 IU/g support). Kinetics of immobilized POXC against ABTS has been assessed by means of the circulating fixed bed reactor commonly employed for activity measurements. Results provided $K_M = 0.44$ mM and $K_{cat} = 1.2 \cdot 10^4$ min^{-1}. Comparing these parameters with those characteristics of POXC in liquid phase ($K_M = 0.03$ mM, $K_{cat} = 6.2 \cdot 10^5$ min^{-1}), both a decreased value for K_{cat} and a higher value for K_M were found. These differences could be a consequence of either the loss of conformational integrity of the immobilized enzyme due to multipoint attachment, as also reported for different immobilized biocatalyst [10], or of lower accessibility of substrate to the active sites of the immobilized enzyme, caused by enzyme overcrowding on support surface.

3.3. Dye Adsorption. The immobilized enzyme mixture was tested for its decolourisation potential against the model anthraquinonic dye Remazol Brilliant Blue R (RBBR). A first series of tests was addressed to assess the extension of dye

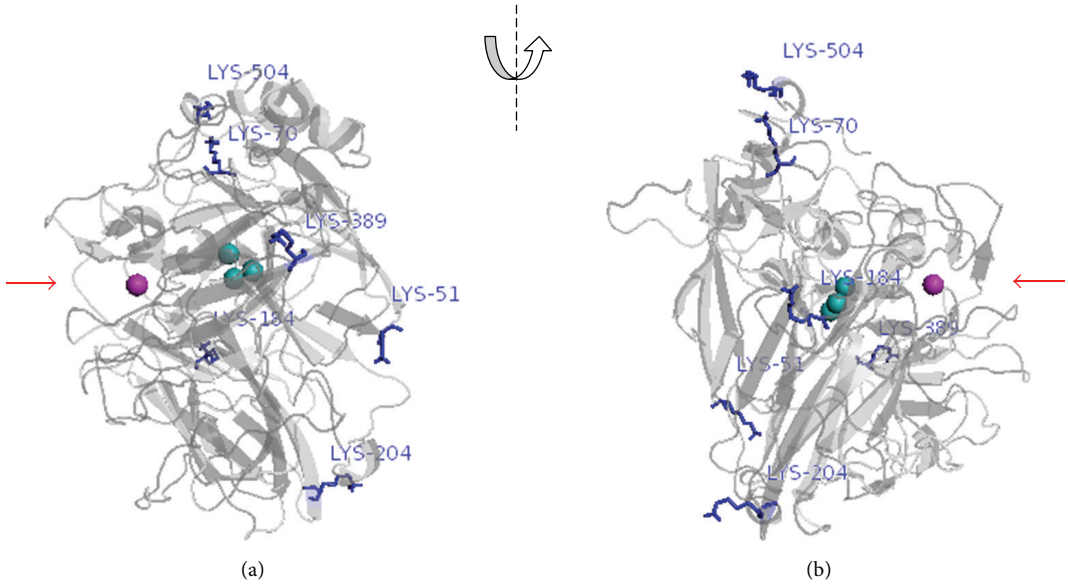

FIGURE 3: Three-dimensional model of POXC, elaborated with Pymol [27], with accessible lysine residues shown as stick. The protein is showed in two opposite orientations, wherein the access to the active site is indicated by a red arrow. T1 copper is shown as a magenta sphere. Copper atoms of the trinuclear cluster are displayed as cyano spheres.

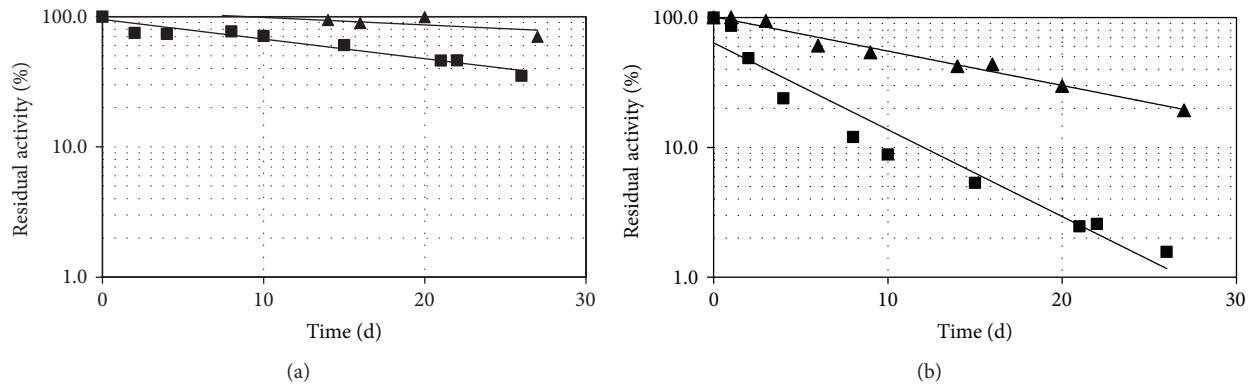

FIGURE 4: Stability of immobilized and free laccase mixture monitored at 4°C (a) and at room temperature (b). Black squares and free enzyme; black triangles and immobilized enzyme.

adsorption on solids surface. This characterization was carried out to discriminate between dye conversion by immobilized enzyme and dye adsorption: the enzymatic conversion could be masked by a rapid adsorption kinetics and/or large adsorption capacity of the solid support. Moreover, the adsorption of dyes as well as adsorption of their oxidized products on the immobilization support could inactivate/inhibit the enzyme [34]. The assessment of the RBBR on the activated carrier could allow adopting strategies to minimize any adverse effect on dye conversion.

Tests were carried out with both untreated particles and activated particles. No adsorption of RBBR was observed on the inert particles. Tests carried out with samples prepared adopting the optimal conditions defined in the previous section reported an adsorption of about 71 $mg_{RBBR}/g_{perlite}$. Therefore, the adsorption phenomenon is related to the functional groups from silanization or glutaraldehyde activation process. Enzymatic assays performed after dye saturation showed that immobilized laccase activity was completely inhibited.

The reported findings inspired modifications of the immobilization protocol to limit dye adsorption to a negligible value. The effect of several parameters on adsorption capacity and immobilization yield was investigated. In particular, the parameters affecting the surface properties of the support (i.e., APTS concentration and pH, temperature, and concentration for glutaraldehyde crosslinking) were tuned. Results are summarized in Table 2. The adsorption capacity of the silanized perlite rises up to 96.1 $mg_{RBBR}/g_{perlite}$ (A2 in Table 2). As a matter of fact, by reducing the APTS concentration from 4 to 0.4% volume, keeping the other conditions constant, the adsorption capacity was approximately halved and an undesired drop of immobilization yield was observed. The extent of perlite silanization determined

Table 2: Adsorption capacity of treated perlite samples obtained in different experimental conditions. Data are average values of three independent experiments. The standard deviation of each series of results was less than ±10%.

Perlite sample	APTS (%)	Glutaraldehyde activation	Adsorption capacity (mg RBBR/g solid)	Immobilization yield (%)
A1	4	0.5% (pH 6.5)	71	45
A2	4	—	96	—
A3	0.4	0.5% (pH 6.5)	28	29
A4	4	0.5% (pH 6.5, 2X)	64	—
A5	0.4	0.5% (pH 8)	31	16
A6	4	0.5% (pH 8)	64	38
A7	0.4	1% (pH 8 60°C)	33	51

Table 3: Immobilized enzyme samples employed in decolourisation experiments. Initial and final activity refer to laccase activity measured on solid carrier at the beginning and at the end of the decolourisation experiment.

Perlite sample	Immobilization conditions	Adsorption capacity (mg_{RBBR}/g_{solid})	Initial activity (IU/mL)	Immobilization yield (%)	Final activity (IU/mL)
C1	0.4% APTS, 0.5% Glut pH 6.5	27.5	10	23	3
C2	0.4% APTS, 1% Glut pH 8.5 60°C	33	28	51	9

the concentration of active amino groups on the carrier surface; this parameter likely plays a key role in the adsorption of the dye. Thus, the improvement of the condition for glutaraldehyde activation would provide a reliable solution to saturate the free amino groups available for the interaction with the anionic dye. In run A4, two consecutive activation steps with glutaraldehyde were assessed. However, adsorption was not significantly affected by this treatment. Rising of the pH from 6.5 up to 8 during glutaraldehyde reaction provided a further decrease of the immobilization yield down to 16.4%, together with a negligible effect on adsorption capacity (compare A5 with A3). This effect was assessed on carrier silanized with 4 or 0.4% APTS solutions (A5-A6).

An effective reduction of RBBR loading (32.9 mg/g), coupled with a satisfying immobilization yield (51.2%), was achieved by incubating the solid silanized with 0.4% APTS with 1% glutaraldehyde at pH 8 and 60°C [25]. The latter operating conditions were selected for further investigation of dye degradation by laccase immobilized on perlite.

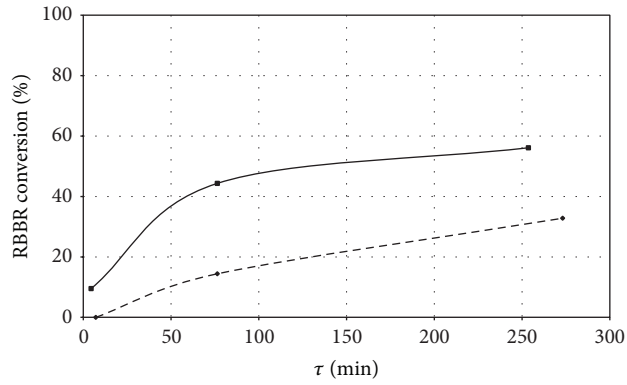

Figure 5: RBBR conversion degrees versus reactor space-time (τ). Data refer to decolourisation experiments carried out in fluidized bed reactor operated with immobilized laccases: sample C1 (dashed line); sample C2 (solid line).

3.4. Decolourisation Experiments. Preliminary tests carried out in fixed beds filled with of enzyme-immobilized particles pointed out that this reactor system does not fit with the features of the coated particles. As a matter of fact, the bed made of inert particles was successfully operated even though a high pressure drop was measured. However, clogging phenomena were recorded when particles with immobilized enzymes were adopted: liquid stream flowed very slowly notwithstanding the high pressure drop adopted across the bed.

The fluidized bed was chosen to get round the fixed bed constraint [35, 36]. Liquid flow rate required for particles fluidization was supplied by the recirculating stream while the stream containing the dye was continuously supplied at the flow rate related to the residence time suitable for dye conversion.

Preliminary decolourisation experiments were carried out adopting two batches of immobilized enzyme: samples C1 and C2 reported in Table 3 with the operating conditions adopted for the immobilization and samples C1 and C2 area characterized by comparable dye adsorption capacities and different amount of immobilized laccase activity. The initial activity of sample C1 was 10 IU/mL and that of sample C2 was 28 IU/mL. Table 4 reports the dye conversion degrees measured under steady state conditions as a function of the reactor space-time τ. Dye conversion degrees versus the reactor space-time are plotted in Figure 5.

Table 4: Decolourisation experiments with laccase immobilized on perlite.

Perlite sample	Inlet RBBR concentration (mg/L)	Recirculation flow rate, Q_r (mL/min)	Total volume (mL)	Dye-feeding rate, Q (mL/min)	Recirculation ratio	τ (min)	Outlet RBBR concentration (mg/L)	Dye conversion (%)
C1	41.5	13	71	10	—	7.1	41.5	—
				0.9	14	76	35.5	14
				0.3	50	273	27.9	33
C2	39.1	13	71	16	—	4.4	35.4	9.5
				0.9	14	76	21.8	44
				0.28	46	253	17.2	56

The maximum conversion degree was measured for tests carried out with sample C1: 33% at $\tau = 4.6$ h. Performance measured with the C2 sample were definitively satisfactory: 56.1% conversion at $\tau = 4.2$ h. Decolourisation runs with both samples C1 and C2 lasted about 80 and 160 h with a total volume of treated RBBR solution of 3.5 and 4.5 L, respectively. Comparing the results of the decolourisation tests carried out with samples C1 and C2, it could be inferred that the better performance achieved by sample C2 was due to its higher activity per volume unit of carrier. It is remarkable to note that (i) in both decolourisation experiments residual enzyme activity was about 30% of the initial activity; (ii) both samples are characterized by almost the same dye adsorption capacity (about 30 mg/g carrier). These results suggest that the biocatalyst deactivation is mainly related to adsorption phenomena occurring at the same extent for both samples. Twofold reason suggests ruling out the effect of the extent of conversion on biocatalyst deactivation within the operation time investigated (about 160 h): (a) the same deactivation extent has been measured even though different conversions have been measured; (b) constant conversion was observed under steady state conditions for long time.

The analysis of reported results suggests that the procedure adopted for the preparation of sample C2 (Table 3) produced a catalyst characterized by satisfactory values of immobilization yield, for example, satisfactory rate of decolourisation, and low adsorption capacity of RBBR. The latter feature provides the minimum deactivation extent related to the fast dye adsorption phenomenon that initially competes with the dye conversion during decolourisation tests.

4. Conclusions

In the present study, a crude laccase preparation from *P. ostreatus* was successfully immobilized on perlite, a cheap porous silica material. Optimization of process experimental parameters was performed. Stability and catalytic parameters of the immobilized laccases were compared with those of free enzyme. Remarkable results show that the stability increases as a consequence of enzyme immobilization but a reduction of the catalytic performances in terms of ABTS conversion kinetics was also observed. These results are in agreement with those expected phenomena occurring as consequences of enzyme immobilization on solid supports [37], for example, reduced catalytic activity and/or increased stability with respect to the soluble counterpart as results of electrostatic and partitioning effects in the immobilized enzyme microenvironment, of conformational losses inside the pores of the support, and external and internal mass transfer phenomena. Moreover, decreased protein flexibility resulting from multipoint attachment and/or enzyme overcrowding on the surface of the support [38] are also responsible for impaired catalytic performances of the immobilized system. Concerning the optimization of immobilization protocol, it can be concluded that the large achieved yield of immobilization, the enhanced stability of the immobilized biocatalyst together with the relatively low cost of both the crude enzyme extract, and the support encourage the exploitation of such biosystem in different industrial application demanding laccases.

Part of the study was devoted to the assessment of the performances of the immobilized laccase in terms of continuous conversion of a reference dye. Accordingly, the immobilized system was tested for RBBR conversion in a fluidized bed recycle reactor. Results obtained in this work showed that the observed RBBR decolourisation by immobilized laccase is mainly due to enzyme action despite the occurrence of dye adsorption-related enzyme inhibition. In this regard, fine tuning of immobilization conditions has allowed balancing the immobilization yield and the resulting rate of decolourisation, with the adsorption capacity of the solid biocatalyst. In the continuous lab scale reactor, a maximum conversion degree of 56.1% was achieved at reactor space-time of 4.2 h.

In conclusion, the reported data may inspire further work concerning the applicability of such immobilized biocatalyst to the treatment of wastewaters containing dyes. Kinetic parameters of dye conversion as well as of deactivation processes (adsorption-related and long-term deactivation) may be inferred, in order to provide tools for the rational design of continuous decolourisation processes with immobilized biocatalysts.

Conflict of Interests

The authors declare that there is no conflict of interests regarding the publication of this paper.

Acknowledgments

This work was supported by grants from the Italian MIUR (Ministero dell'Università e della Ricerca Scientifica Progetti di Rilevante Interesse Nazionale) PRIN 2009STNWX3. The authors are grateful to Mrs. Serena Fiorenzano for her precious assistance in the experimental work.

References

[1] P. Giardina, V. Faraco, C. Pezzella, A. Piscitelli, S. Vanhulle, and G. Sannia, "Laccases: a never-ending story," *Cellular and Molecular Life Sciences*, vol. 67, no. 3, pp. 369–385, 2010.

[2] A. Kunamneni, I. Ghazi, S. Camarero, A. Ballesteros, F. J. Plou, and M. Alcalde, "Decolorization of synthetic dyes by laccase immobilized on epoxy-activated carriers," *Process Biochemistry*, vol. 43, no. 2, pp. 169–178, 2008.

[3] J.-A. Majeau, S. K. Brar, and R. D. Tyagi, "Laccases for removal of recalcitrant and emerging pollutants," *Bioresource Technology*, vol. 101, no. 7, pp. 2331–2350, 2010.

[4] A. Piscitelli, C. Pezzella, V. Lettera, P. Giardina, V. Faraco, and G. Sannia, "Fungal laccases: structure, function and application," in *Fungal Enzymes: Progress and Prospects*, T. M. P. Maria de Lourdes and M. Rai, Eds., pp. 113–151, 2013.

[5] D. Wesenberg, I. Kyriakides, and S. N. Agathos, "White-rot fungi and their enzymes for the treatment of industrial dye effluents," *Biotechnology Advances*, vol. 22, no. 1-2, pp. 161–187, 2003.

[6] G. Palmieri, G. Cennamo, and G. Sannia, "Remazol Brilliant Blue R decolourisation by the fungus *Pleurotus ostreatus* and its oxidative enzymatic system," *Enzyme and Microbial Technology*, vol. 36, no. 1, pp. 17–24, 2005.

[7] V. Faraco, C. Pezzella, A. Miele, P. Giardina, and G. Sannia, "Bioremediation of colored industrial wastewaters by the white-rot fungi *Phanerochaete chrysosporium* and *Pleurotus ostreatus* and their enzymes," *Biodegradation*, vol. 20, no. 2, pp. 209–220, 2009.

[8] V. Faraco, C. Pezzella, P. Giardina, A. Piscitelli, S. Vanhulle, and G. Sannia, "Decolourization of textile dyes by the white-rot fungi *Phanerochaete chrysosporium* and *Pleurotus ostreatus*," *Journal of Chemical Technology and Biotechnology*, vol. 84, no. 3, pp. 414–419, 2009.

[9] S. Rodríguez Couto and J. L. Toca Herrera, "Industrial and biotechnological applications of laccases: a review," *Biotechnology Advances*, vol. 24, no. 5, pp. 500–513, 2006.

[10] M. Fernández-Fernández, M. A. Sanromán, and D. Molde, "Recent developments and applications of immobilized laccase," *Biotechnology Advances*, vol. 31, no. 8, pp. 1808–1825, 2013.

[11] M. Arroyo, "Inmovilización de enzimas fundamentos, métodos y aplicaciones," *Ars Pharmaceutica*, vol. 39, no. 2, pp. 23–29, 1998.

[12] D. Brady and J. Jordaan, "Advances in enzyme immobilisation," *Biotechnology Letters*, vol. 31, no. 11, pp. 1639–1650, 2009.

[13] M. E. Russo, P. Giardina, A. Marzocchella, P. Salatino, and G. Sannia, "Assessment of anthraquinone-dye conversion by free and immobilized crude laccase mixtures," *Enzyme and Microbial Technology*, vol. 42, no. 6, pp. 521–530, 2008.

[14] S. Rodríguez Couto, J. F. Osma, V. Saravia, G. M. Gübitz, and J. L. Toca Herrera, "Coating of immobilised laccase for stability enhancement: a novel approach," *Applied Catalysis A: General*, vol. 329, pp. 156–160, 2007.

[15] P.-P. Champagne and J. A. Ramsay, "Reactive blue 19 decolouration by laccase immobilized on silica beads," *Applied Microbiology and Biotechnology*, vol. 77, no. 4, pp. 819–823, 2007.

[16] A. Rekuć, B. Jastrzembska, J. Liesiene, and J. Bryjak, "Comparative studies on immobilized laccase behaviour in packed-bed and batch reactors," *Journal of Molecular Catalysis B: Enzymatic*, vol. 57, no. 1–4, pp. 216–223, 2009.

[17] L. Lu, M. Zhao, and Y. Wang, "Immobilization of laccase by alginate-chitosan microcapsules and its use in dye decolorization," *World Journal of Microbiology and Biotechnology*, vol. 23, no. 2, pp. 159–166, 2007.

[18] P. WANG, X. FAN, L. CUI, Q. WANG, and A. ZHOU, "Decolorization of reactive dyes by laccase immobilized in alginate/gelatin blent with PEG," *Journal of Environmental Sciences*, vol. 20, no. 12, pp. 1519–1522, 2008.

[19] J. Phetsom, S. Khammuang, P. Suwannawong, and R. Sarnthima, "Copper-alginate encapsulation of crude laccase from *Lentinus polychrous* lev. and their effectiveness in synthetic dyes decolorizations," *Journal of Biological Sciences*, vol. 9, no. 6, pp. 573–583, 2009.

[20] O. Yamak, N. A. Kalkan, S. Aksoy, H. Altinok, and N. Hasirci, "Semi-interpenetrating polymer networks (semi-IPNs) for entrapment of laccase and their use in Acid Orange 52 decolorization," *Process Biochemistry*, vol. 44, no. 4, pp. 440–445, 2009.

[21] S.-F. Torabi, K. Khajeh, S. Ghasempur, N. Ghaemi, and S.-O. R. Siadat, "Covalent attachment of cholesterol oxidase and horseradish peroxidase on perlite through silanization: activity, stability and co-immobilization," *Journal of Biotechnology*, vol. 131, no. 2, pp. 111–120, 2007.

[22] L. Betancor, F. López-Gallego, A. Hidalgo et al., "Different mechanisms of protein immobilization on glutaraldehyde activated supports: effect of support activation and immobilization conditions," *Enzyme and Microbial Technology*, vol. 39, no. 4, pp. 877–882, 2006.

[23] L. S. Fan, *Gas-Liquid-Solid Fluidization Engineering*, Butterworths, Boston, Mass, USA, 1989.

[24] A. K. Singh, A. W. Flounders, J. V. Volponi, C. S. Ashley, K. Wally, and J. S. Schoeniger, "Development of sensors for direct detection of organophosphates—part I: immobilization, characterization and stabilization of acetylcholinesterase and organophosphate hydrolase on silica supports," *Biosensors and Bioelectronics*, vol. 14, no. 8-9, pp. 703–713, 1999.

[25] S. W. Park, Y. I. Kim, K. H. Chung, S. I. Hong, and S. W. Kim, "Covalent immobilization of GL-7-ACA acylase on silica gel through silanization," *Reactive and Functional Polymers*, vol. 51, no. 2-3, pp. 79–92, 2002.

[26] I. Migneault, C. Dartiguenave, M. J. Bertrand, and K. C. Waldron, "Glutaraldehyde: behavior in aqueous solution, reaction with proteins, and application to enzyme crosslinking," *BioTechniques*, vol. 37, no. 5, pp. 790–802, 2004.

[27] W. L. DeLano, *The PyMOL Molecular Graphics System*, DeLano Scientific, San Carlos, Calif, USA, 2002.

[28] P. Brandi, A. D'Annibale, C. Galli, P. Gentili, and A. S. N. Pontes, "In search for practical advantages from the immobilisation of an enzyme: the case of laccase," *Journal of Molecular Catalysis B: Enzymatic*, vol. 41, no. 1-2, pp. 61–69, 2006.

[29] D. E. Dodor, H.-M. Hwang, and S. I. N. Ekunwe, "Oxidation of anthracene and benzo[a]pyrene by immobilized laccase from *Trametes versicolor*," *Enzyme and Microbial Technology*, vol. 35, no. 2-3, pp. 210–217, 2004.

[30] X. Hu, X. Zhao, and H.-M. Hwang, "Comparative study of immobilized *Trametes versicolor* laccase on nanoparticles and kaolinite," *Chemosphere*, vol. 66, no. 9, pp. 1618–1626, 2007.

[31] Y. Liu, C. Guo, F. Wang, C.-Z. Liu, and H.-Z. Liu, "Preparation of magnetic silica nanoparticles and their application in laccase immobilization," *The Chinese Journal of Process Engineering*, vol. 8, no. 3, pp. 583–588, 2008.

[32] A. Salis, M. Pisano, M. Monduzzi, V. Solinas, and E. Sanjust, "Laccase from *Pleurotus sajor-caju* on functionalised SBA-15 mesoporous silica: immobilisation and use for the oxidation of phenolic compounds," *Journal of Molecular Catalysis B: Enzymatic*, vol. 58, no. 1–4, pp. 175–180, 2009.

[33] V. R. Sarath Babu, M. A. Kumar, N. G. Karanth, and M. S. Thakur, "Stabilization of immobilized glucose oxidase against thermal inactivation by silanization for biosensor applications," *Biosensors and Bioelectronics*, vol. 19, no. 10, pp. 1337–1341, 2004.

[34] N. Durán, M. A. Rosa, A. D'Annibale, and L. Gianfreda, "Applications of laccases and tyrosinases (phenoloxidases) immobilized on different supports: a review," *Enzyme and Microbial Technology*, vol. 31, no. 7, pp. 907–931, 2002.

[35] G. Olivieri, A. Marzocchella, and P. Salatino, "Hydrodynamics and mass transfer in a lab-scale three-phase internal loop airlift," *Chemical Engineering Journal*, vol. 96, no. 1–3, pp. 45–54, 2003.

[36] G. Olivieri, A. Marzocchella, and P. Salatino, "A novel three-phase airlift reactor without circulation of solids," *Canadian Journal of Chemical Engineering*, vol. 88, no. 4, pp. 574–578, 2010.

[37] P. W. Tardioli, G. M. Zanin, and F. F. de Moraes, "Characterization of *Thermoanaerobacter* cyclomaltodextrin glucanotransferase immobilized on glyoxyl-agarose," *Enzyme and Microbial Technology*, vol. 39, no. 6, pp. 1270–1278, 2006.

[38] D. S. Clark, "I Can immobilization be exploited to modify enzyme activity?" *Trends in Biotechnology*, vol. 12, no. 11, pp. 439–443, 1994.

Hindawi Publishing Corporation
BioMed Research International
Volume 2014, Article ID 324705, 9 pages
http://dx.doi.org/10.1155/2014/324705

Research Article

Highly Effective Renaturation of a Streptokinase from *Streptococcus pyogenes* DT7 as Inclusion Bodies Overexpressed in *Escherichia coli*

Sy Le Thanh Nguyen,[1] Dinh Thi Quyen,[1,2] and Hong Diep Vu[1]

[1] *Institute of Biotechnology, Vietnam Academy of Science and Technology, 18 Hoang Quoc Viet Road, District of Cau Giay, Hanoi 10600, Vietnam*
[2] *Department of Biotechnology and Pharmacology, University of Science and Technology of Hanoi, 18 Hoang Quoc Viet Road, District of Cau Giay, Hanoi 10600, Vietnam*

Correspondence should be addressed to Dinh Thi Quyen; quyen@ibt.ac.vn

Received 12 November 2013; Revised 28 February 2014; Accepted 31 March 2014; Published 5 May 2014

Academic Editor: Noomen Hmidet

The streptokinase (SK) is emerging as an important thrombolytic therapy agent in the treatment of patients suffering from cardiovascular diseases. We reported highly effective renaturation of a SK from *S. pyogeness* DT7 overexpressed in *E. coli*, purification, and biochemical characterization. A gene coding for the SK was cloned from *S. pyogeness* DT7. Because accumulation of active SK is toxic to the host cells, we have expressed it in the form of inclusion bodies. The mature protein was overexpressed in *E. coli* BL21 DE3/pESK under the control of the strong promoter *tac* induced by IPTG with a level of 60% of the total cell proteins. The activity of the rSK, renatured in phosphate buffer supplemented with Triton X-100 and glycerol, was covered with up to 41 folds of its initial activity. The purified of protein was identified with MALDI-TOF mass spectrometry through four peptide fragments, which showed 100% identification to the corresponding peptides of the putative SK from GenBank. Due to overexpression and highly effective renaturation of large amounts of inclusion bodies, the recombinant *E. coli* BL21 DE3/pESK system could be potentially applied for large-scale production of SK used in the therapy of acute myocardial infarction.

1. Introduction

Streptokinase (EC 3.4.99.22) (SK), a commercially important nonprotease, binds stoichiometrically to both circulating and thrombus-bound plasminogen (Plg) to generate SK-plasminogen activator complex. Cleavage of plasminogen in zymogen form at an Arg-Val bond generates plasmin, an active enzyme that degrades fibrin component of thrombin [1]. Due to this property, the streptokinase has been widely used in the therapy of acute myocardial infarction for its strong activity in dissolving blood clots [2].

Most group A, C, and G β-hemolytic streptococci isolated from human hosts secrete streptokinase with molecular mass of 47 kDa, which convert the plasminogen to the serine protease plasmin. However, due to low SK production yields from natural host and its pathogenicity, so research interest has shifted to cloning and expression of SK in hyperproductive and safe heterologous host systems. Therefore, *sk* genes have been cloned and expressed in different expression systems including *Bacillus subtilis* [3], *Streptococcus sanguis* [4], *Streptomyces lividans* [5, 6], *Schizosaccharomyces pombe* [7], *Pichia pastoris* [1, 8], *Lactococcus lactis* [9], and *Escherichia coli* [10, 11]. However, there are some disadvantages of producing recombinant proteins in *Pichia pastoris* due to high glycosylation level [12] or in *Lactococcus lactis* due to low cell density [9].

Escherichia coli is the most commonly used host for the production of recombinant proteins, both in research and industry [13]. High-level expression of recombinant proteins in the form of a soluble intracellular product, secretory product, or as insoluble inclusion bodies depends on promoter system, host-vector interactions, sequence, and

characteristics of recombinant products and the effect of the expressed foreign protein on host cell physiology [14].

The expression of SK as inclusion bodies by *E. coli* systems is shown to be useful for obtaining large amounts of protein, provided that renaturation is effective and recovery of active protein is high. Thus, the purpose of this study was firstly to overproduce the recombinant streptokinase in *E. coli* BL21 (DE3) and simultaneously to refold effectively the large amount of the recombinant streptokinase as inclusion bodies overexpressed by *E. coli* BL21 (DE3) under the control of the promoter T7. Only both objectives were gained; then the recombinant *E. coli* overproducing SK as inclusion bodies can become a potential strain for industrial SK production.

2. Materials and Methods

2.1. Chemicals and Reagents. DNA cloning kit, RNase A, restriction enzymes (*Bam*HI, *Not*I, and *Eco*RI), T4-ligase, and Proteinase K were purchased from Fermentas (Thermo Fisher Scientific Inc., Waltham, USA). The DNA Extraction Kit was from Qiagen (Venlo, Netherlands). Protein Extraction Kit and ProBond resin were supplied by Invitrogen Corp. (Carlsbad, CA, USA). Human plasminogen from MP Biomedicals (Santa Ana, USA); SK, N (p-tosyl) gly-pro-lys-4-nitro anilide acetate salt (AAS), SDS from Sigma Aldrich Co. (St. Luis, USA); Plasminogen, Tween 20 and Tween 80 from BioBasic Inc. (NY, USA); Triton X-100 and EDTA from Merck (Darmstadt, Germany). All other reagents were of analytical grade unless otherwise stated.

2.2. Plasmids, Bacterial Strains, and Culture Conditions. The bacterial strain *Streptococcus pyogenes* DT7 (GQ247718) isolated from a patient at the Army Hospital No. 103 (Hanoi, Vietnam) was used as the source of the streptokinase (*sk*) gene. *Escherichia coli* DH5α (F^-, ø80d*lacZ*ΔM15, Δ(*lacZYA-argF*) U169, *deo*R, *rec*A1, *end*A1, *hsdR*17(rK^-, mK^+), *pho*A, *sup*E44, λ–, *thi*-1, *gyr*A96, *rel*A1) and the vector pJET1.2/blunt (Fermentas, Thermo Fisher Scientific Inc., Waltham, USA) were used for DNA manipulations and amplification. *Escherichia coli* BL21 (DE3) cells (F^-*ompT gal dcm lon hsd*S_B ($r_B{}^-m_B{}^-$) λ(*DE3* [*lacI lacUV5-T7 gene 1 ind1 sam7 nin5*]) and pET22b+ vector (Novagen, Merck KGaA, Darmstadt, Germany) were used for expression of SK. LB medium (Luria-Bertani) containing 1% (w/v) bacto tryptone; 0.5% (w/v) yeast extract; 1% (w/v) NaCl; pH 7–7.5 was used for cultivation of *E. coli* DH5α and BL21 (DE3). LB agar contained additionally 2% (w/v) agar and 100 μg ampicillin/mL.

2.3. DNA Manipulations. Genomic and plasmid DNA isolation was carried out by methods which have been previously described [15]. DNA fragments and PCR products were excised from a 0.8% agarose gel and purified by a gel extraction kit (Qiagen, Venlo, The Netherlands) according to the manufacturer's instructions. DNA sequencing was performed on an ABI PRISM 3100 Avant Genetic Analyzer (Applied Biosystems Inc., Foster City, USA). *E. coli* DH5α and BL21 were transformed using heat shock method that has been previously described [15].

2.4. DNA Amplification and Plasmid Construction. The putative sk-coding DNA fragment was amplified from *S. pyogenes* DT7 genomic DNA by PCR with *Taq* DNA polymerase. Based on the nucleotide sequence of the *sk* gene from *S. pyogenes* strain (GenBank: Z48617), 3 oligonucleotides, mSKF GGC GGATCC CATATG ATTGCTGGACCTG, and SKF: GCC CAT GGG CAA AAA TTA CTT AT and SKR GCC TCG AGT TTG TCB TTA GGG TT were designed as primers for introduction of the underlined *Bam*HI and *Xho*I restriction sites, respectively. The PCR mixture contained 2.5 μL 10x PCR buffer; 2 μL of 2.5 mM dNTP; 2.5 μL of 25 mM $MgCl_2$; 0.5 μL genomic DNA (50–100 ng); 0.25 μL 5 unit *Taq* polymerase, and 1 μL each primer (10 pmol), supplemented with 15.25 μL distillated water to a final volume of 25 μL. The thermocycler conditions were as follows: 95°C/4′; 30 cycles of (95°C/30″, 52°C/45″, 72°C/45″); 72°C/10′. The PCR products amplified from the genomic DNA with the primer pair SKF and SKR were inserted into the cloning vector pJET1.2/blunt, resulting in pJSK. DNA sequencing was performed on ABI PRISM 3100 Avant Genetic Analyzer. Sequence alignments were constructed and analyzed using the program MegAlign DNAStar. It was followed by ligation of the *BamHI-Xho*I digested PCR products (with the primer pair mSKF and SKR) with pET22b+ linearized by the same enzymes, resulting in pESK under the control of the T7-promoter induced by isopropyl-β-D-thiogalactopyranoside (IPTG) and possessing the ampicillin marker. The streptokinase rSKhis encoded by the plasmid pESK contains the mature streptokinase fused with the 6x histidine-tag and no native leader sequence.

2.5. rSK Expression. The transformant *E. coli* BL21/pESK was cultivated overnight in 5 mL of LB medium containing 5 μL of 100 mg/mL ampicillin at 37°C on an orbital shaker at 200 rpm. Overnight culture (2 mL) was inoculated in a 1-liter Erlenmeyer flask containing 200 mL of LB broth and 200 μL of 100 mg/mL ampicillin. The culture was grown at 37°C with agitation at 200 rpm and until an optical density (OD) at 600 nm reached 0.6 (for approximately 2.5 h); then 200 μL of 100 mM IPTG was added. The culture was continuously incubated at 37°C with agitation at 200 rpm for 3–6 h induction. Cells were harvested by centrifugation at 6000 rpm for 10 min at 4°C. Wet weight cells were used for protein purification.

2.6. Purification of Streptokinase. The fusion form rSKhis carrying a C-terminal 6xHis tag was expressed in *E. coli* BL21. To purify rSK, 100 mg wet weight cells from a 120 mL culture in LB medium were harvested by centrifugation and suspended in 10 mL of guanidine lysis buffer containing 6 M guanidine hydrochloride, 20 mM sodium phosphate, 500 mM NaCl, and pH 7.8. The cell suspension was sonificated (three bursts of 1 min each at 1 min interval). After 30–60 min incubation in ice with slight shaking, the cell lysate was centrifuged at 13000 rpm and 4°C for 25 min to remove cell debris.

A volume of 8 mL cell lysate was applied to a Ni-NTA column (Invitrogen Corp., Carlsbad, USA) containing 2 mL resin which was equilibrated with denaturing binding buffer and incubated for 45 min at room temperature with gentle hand shaking for several times. The column was washed with 4 times of 8 mL denaturing wash buffer. The bound protein was eluated with 8 mL of denaturing eluation buffer. Then 6 mL of the enzyme extract was applied to a Bio-gel column (2,6 × 6 cm) with elution of 50 mM Tris-HCl buffer (pH 8) at a flow rate of 25 mL/h and then washed with the same buffer.

2.7. Streptokinase Renaturation. The pool of purified SK fragments were renaturated using 50 mM phosphate buffer pH 7 supplemented with 10% (w/v) glycerol and different detergents (0.5% (w/v) Triton X-100, 1% (w/v) Tween 20, 1.5% (w/v) Tween 80) [11]. Diluted cell lysate (1 : 200) and purified rSK (1 : 100) in renaturation buffer were incubated at 37°C for 1 h and 4°C for 6 h. The residual activity was then determined as described below.

2.8. Streptokinase Assay. To estimate the activity of the purified rSK, 10 μL purified protein solution was added to 10 μL of 50 mM Tris buffer pH 7.5 containing 0.05 unit of human plasminogen and incubated at 37°C for 30 min. The color reaction was developed by the addition of 40 μL of 1 mM AAS solution and incubated at 37°C for 15 min. The reaction was stopped by the addition of 10 μL of 0.4 N acetic acid. The absorbance was read at 405 nm against a blank containing human plasminogen, Tris buffer, and AAS but without rSK solution. The activity was estimated using standard SK (Sigma Aldrich Co., St. Luis, USA). One unit (U) of rSK was defined as one unit of standard SK, which liquefies a standard clot of fibrinogen, plasminogen, and thrombin at 37°C and pH 7.5 for 10 min.

2.9. Protein Electrophoresis and Quantification. The homogeneity and molecular mass of the streptokinase were determined by 12.5% SDS polyacrylamide gel electrophoresis [16] with Biometra equipment (Göttingen, Germany). Proteins were visualized by staining with Coomassie Brilliant Blue R-250 or with 0.1% (w/v) of silver nitrate. Protein concentrations were measured by Bradford assay with the bovine serum albumin as standard [17].

2.10. MALDI-TOF Mass Spectrometry. The rSK was identified by MALDI-TOF mass spectrometry as previously described [18]. The predicted protein band on SDS-PAGE was cut out and the target protein was digested by trypsin treatment into small peptide fragments. The mixture of peptides was analyzed on nano-LC liquid chromatography and ionized by the ESI (electrospray ionization). The mass spectra were obtained by QSTAR XL mass spectrometer (Applied Biosystems, MDS SCIEX, Canada) with a nano-ESI ion source. Protein fragments were identified by the Mascot v1.8 Search Software from the database (NCBInr, SwissProt). Peptide fragments showing ion scores above 42 were identified uniquely or high-similarly with $P < 0.05$.

2.11. Biochemical Characterization of rSK. The pH and temperature optimum of rSK were determined by measuring the activity as described above using 100 mM potassium phosphate buffer (pH 5.5–7.5) and 100 mM Tris-HCl buffer (pH 7.5–10) at 37°C, and in the temperature range of 4 to 60°C using 100 mM potassium phosphate buffer, pH 7.5, respectively.

For the determination of temperature and pH stability, the purified rSK, 0.1 μg for each reaction, was preincubated in 100 mM potassium phosphate buffer pH 7 at different temperatures 4–60°C for 0–96 h, and pH range from 4 to 9.5 (pH 4-5, 100 mM potassium acetate buffer; pH 5.5–7.5, 100 mM potassium phosphate buffer; and pH 7.5–9.5, 100 mM Tris-HCl) at 37°C for 0–48 h, respectively. The residual activity was then determined.

Effect of surfactants on the activity of rSK was check by mixture of 0.4 unit purified rSK and substrate and supplemented with either Triton X-100, Tween 20, or Tween 80, each at a final concentration of 0.5, 1.0, 1.5, and 2.0% (w/v) in appropriate buffer pH 7 and incubated at 37°C for 60 min. The residual activity of rSK was determined as described above.

The effect of additives on the activity of the purified rSK was investigated by incubating the mixture of 0.4 unit of the purified rSK and either of Ag^{+}, Ca^{2+}, Co^{2+}, Cu^{2+}, Fe^{2+}, K^{+}, Mn^{2+}, Ni^{2+}, Zn^{2+}, or EDTA, at a final concentration of 1, 3, and 5 mM. The reaction mixtures were incubated at 28°C for 60 min. The residual activity of rSK was then measured as shown above. All measurements were carried out in triplicate with the resulting values being the mean of the cumulative data obtained.

3. Results and Discussion

3.1. Gene Cloning and Analysis. The recombinant plasmid pTSK with inserted *sk* gene was sequenced and aligned with sequences from GenBank using DNAstar. Nucleotide sequence of *sk* gene from *S. pyogenes* DT7 exhibited 84.4% to 99.6% identities with sequences from *Streptococcus pyogenes* groups of A, C, and G strains in GenBank (CP000262, CP000261, M19347, AM903378, and AY234136). The putative amino acid sequence of the gene *sk* showed 77.9 to 99.3% identities with the corresponding amino acid sequences from the abovementioned *Streptococcus pyogenes* strains. The sequence was deposited in the GenBank with an accession number of ACG50170.

3.2. Expression and Purification of SK. The DNA fragment (1245 bps) encoding the mature streptokinase (SK) truncated 26 N-terminal amino acids from *S. pyogenes* DT7 was inserted into pET22b+ vector at the *Bam*HI and *Xho*I sites resulting in the recombinant plasmid pESK. The transformant *E. coli* BL21/pESK was grown in LB medium for the SK production. After IPTG induction, the cells were collected and used for purification and renaturation. The expression level of rSK as inclusion bodies by *E. coli* BL21/pESK was 60% of the total proteins (Figure 1(a), lane 1) using Dolphin 1D software. This level was as high as that (65%) reported by

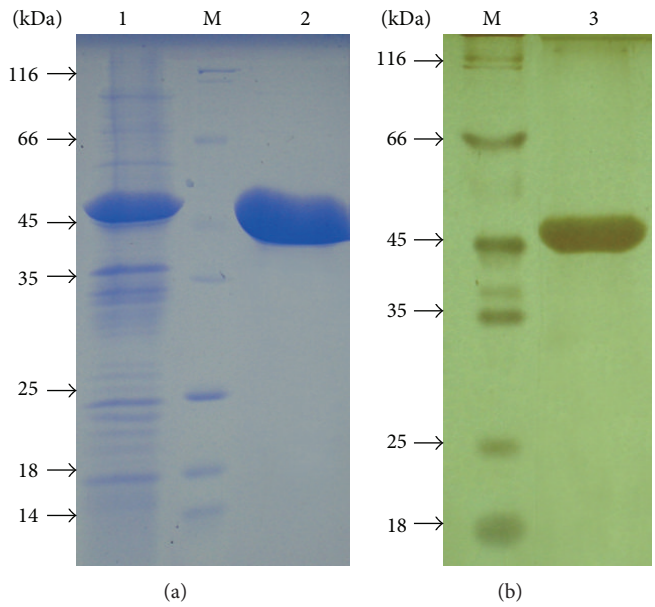

Figure 1: SDS-PAGE of the purified rSK by ProBond Resin. Lane 1, *E. coli* BL21/pESK cell lysate; Lane 2, purified rSK stained by using Coomassie Brilliant Blue R250; Lane 3, purified rSK stained by using silver nitrate; Lane M, molecular standards indicated in kDa.

Table 1: Effect of surfactant, glycerol, and temperature on the renaturation of cell lysate *E. coli*/pESK.

Parameter	SK activity (U/mL)		
	at 37°C for 1 h	at 37°C for 1 h + 10% glycerol	at 4°C for 6 h + 10% glycerol
0.5% Triton X-100	643.4 ± 3.6	5574.0 ± 36.2	7591.3 ± 45.2
1% Tween 20	657.6 ± 5.7	4592.8 ± 27.1	6587.7 ± 27.1
1.5% Tween 80	691.6 ± 6.6	5226.8 ± 50.6	6578.7 ± 63.3
No surfactant	182.1 ± 1.8	184.3 ± 3.6	189.4 ± 3.6

Table 2: The renaturation of purified rRSK.

Fraction number	rSK activity (U/mg)		
	at 37°C for 1 h	at 4°C for 6 h + 0.5% Triton X-100 and 10% glycerol	at 37°C for 1 h + 0.5% Triton X-100 and 10% glycerol
1	69.1 ± 1.0	1622.4 ± 29.3	2519.0 ± 15.7
2	360.5 ± 4.8	10312.5 ± 55.2	11264.2 ± 27.6
3	199.9 ± 1.4	2039.3 ± 21.1	3862.5 ± 15.2
4	55.3 ± −0.3	1516.9 ± 18.9	1907.6 ± 11.8

Zhang et al. (1999) [19] and more than two to four times as high as those (25%) reported by [20], (20%) by [21], and 15% by [22].

3.3. Renaturation of Streptokinase. The cell lysate was renatured by using various surfactants including Triton X-100, Tween 20, and Tween 80 each or in combination with glycerol. Triton X-100 was known as detergent to dissolves and refolding aggregated protein. In absence of surfactants, rSK exhibited the same activity (182–189 U/mL) with or without glycerol (Table 1). The addition of surfactants increased the rSK activity obviously to 3.5–3.8 folds without glycerol, but steeply to 25.2–30.6-folds in combination with glycerol at 37°C for 60 min, even to 36.1–41.7 folds at 4°C for 6 h. At lower temperature (4°C), the enzyme activity was recovered better than at higher temperature (37°C), increased by 26–43%. The combination of glycerol at the concentration of 10% (w/v) and Triton X-100 at the concentration of 0.5% (w/v) recovered the highest activity of rSK and reached 7,591 U/mL at 4°C (Table 1). The renaturation of the purified rSK with 10% glycerol containing 0.5% Triton X-100 at 4°C for 6 h and at 37°C for 1 h recovered the enzyme activity of 28.6 and 36.5 folds, respectively (Table 2), corresponding to the specific activity of 10,312.5, and 11,264.2 U/mg protein. The reason the renaturation efficiency in this study was much higher than that reported by Cherish Babu et al. (2008). At the same conditions for treatment, the enzyme activity was recovered with only 9.7 folds in comparison to control [11].

Table 3: Purification steps of the streptokinase from *E. coli*/pESK.

Total proteins	Purified proteins	Specific activity (U/mg) of		Yield (%)	Purification factor
		supernatant of cell lysate	purified rSK		
90375 mg	21789 mg	4568	10336	52%	2.26

3.4. Purification of Recombinant SK. rSK from *S. pyogenes* DT7 overexpressed by *E. coli* BL21/pESK cells was purified through affinity chromatography column of Ni^{2+}-ProBond resin to the homogeneity on SDS-PAGE with a molecular mass of approximately 47 kDa (Figure 1, lane 2). The purified rSak gained a specific activity of 10,336 U/mg proteins with a purification factor of 2.56 and a yield of 52% (Table 3). The solution containing rSK protein was loaded onto Biogel P-100 packed column for fractionating and obtained with a purity of 95.7% and specific activity of 11,558 U/mg (Figure 1, lane 3).

3.5. Identification of Recombinant SK. The single protein on SDS-PAGE (Figure 1, lane 3) was cut out from the gel and used for LC-ESI-MS/MS analysis of mass spectrum database by using Mascot v1.8 program. The total score of SK identification was 203 to 509 and matched peptides were 29 to 39 fragments. Four peptide fragments of the purified enzyme identified by MALDI-TOF mass spectrometry agreed with those of the streptokinase found in GenBank gi|153807, streptokinase (*S. pyogenes*) VNVNYEVSFVSETGDLDFTPLLR (position 158–180) (Figure 2(a)), NQYHLTTLAVGDSLSSQELAAIAQFILSK (position 181–209) (Figure 2(b)), TNNTDLISEKYYVLK (position 263–278) (Figure 2(c)), NLDFRDLYDPR (position 320–330) (Figure 2(d)), corresponding to a monoisotopic mass of 2613.3, 3117.63, 1799.93, and 1422.69 Da and to m/z ion scores of 102, 111, 73, and 51, respectively. Whereas the peptide fragments showing ion scores above 42 were identified uniquely or highly similarly to $P < 0.05$. These peptides of the recombinant streptokinase expressed by *E. coli*/pESK showed 100% identity with the corresponding fragments of the putative streptokinase protein from *S. pyogenes* (gi|153807) (Figure 2(e)).

3.6. Temperature and pH Optimum. The temperature and pH optimum for the reaction of SK-plasmin were observed at 37°C and pH 7 (Figures 3(a) and 3(b)). The enzyme showed over 80% activity at the temperature range from 25 to 45°C and pH 6.7–7.5 (for 100 mM potassium phosphate buffer) and pH 8.5–10 (for Tris-HCl buffer) in comparison with the optimum activity. The temperature optimum for the SK-plasmin reaction was in agreement with that from other reports. Rajagopalan et al. (1987) reported that the reactions of α2-macroglobulin (α2M) with plasmin or streptokinase-plasmin (ogen) (SkP1) was markedly temperature-dependent and initial rates of reaction at 0 and 24°C were only 3 and 40% of the rate of 37°C, respectively [23]. Mumme et al. (1993) reported that the highest fibrinolysis activity with streptokinase was obtained at 40°C, with lower activities having been recorded at both higher and lower temperatures [24]. The optimum temperature and pH of streptokinase from β-haemolytic streptococci were 27–37°C and 7 [25]. Another thrombolytic agent, closely related to the streptokinase, staphylokinase (Sak) from *Staphylococcus aureus* exhibited the same profile. The native Sak from *S. aureus* V8 showed the pH optimum at pH 7.5 and 8.5 [26]. The temperature and pH optimum for Sak from *S. aureus* QT08 expressed in *E. coli* and *P. pastoris* were observed at 30–37°C, pH 7, and pH 9 [27] and pH 7,5, and pH 8.5 [28], respectively.

Why the streptokinases and staphylokinases shared a common property that the optimum temperature was not more than 40°C and pH optimum exhibited 2 peaks? because the fibrinolytic activity of streptokinase originates in its ability to activate blood plasminogen to plasmin, the enzyme that degrades fibrin cloth through its specific lysine binding site [29]. The temperature optimum for the human plasmin was at 37°C [30] and the optimal pH value for the human plasmin and that for SK or Sak were significantly different.

3.7. Temperature and pH Stability. The streptokinase from *S. pyogenes* DT7 was stable up to 37°C and retained more than 80% of its initial activity after incubation for 9 h and more than 50% after incubation for 96 h (Figure 4(a)). The enzyme exhibited more stability at pH 7 than at pH 9 and retained more than 73% of its initial activity after incubation at pH 7 for 24 h, whereas it retained only more than 65% of its initial activity after incubation at pH 9 for 8 h (Figure 4(b)). K. Vesterberg and O. Vesterberg (1972) also reported that the concentrated material containing Sak from *S. aureus* V8 was stable at refrigerator temperature over a pH range of 3.0–8.5. Sak from *S. aureus* QT08 expressed in *E. coli* and *P. pastoris* was stable at a temperature range from 25°C to 50°C, and at a pH range from 7 to 9 after incubation for 2 h with a residual activity of more than 70% [26, 28]. The results depicted in Figure 4(b) indicating that there were two sharp peak, one at pH 7.0 and the other one at pH 9.0 with the activity of 100% and 98%, respectively. The experiments of the optimal pH value for the high level activity of rSK were rather complicated since two reactions happened continuously in the same reaction mixture: at first, the activation reaction of plasminogen to plasmin was activated by rSK, and second, the digestion process of AAS was catalyzed by plasmin. The optimal pH value for human plasmin and that for SK was significantly different; therefore, this could cause the appearance of second peak activity. The data depicted in Figure 4(b) showing that the second peak activity at pH value of 9,0 might therefore be due to optimal pH for the plasmin activity in Tris-HCl buffer. Similarly, these observations were also reported by K. Vesterberg and O. Vesterberg (1972) in which staphylokinase was a plasminogen activator.

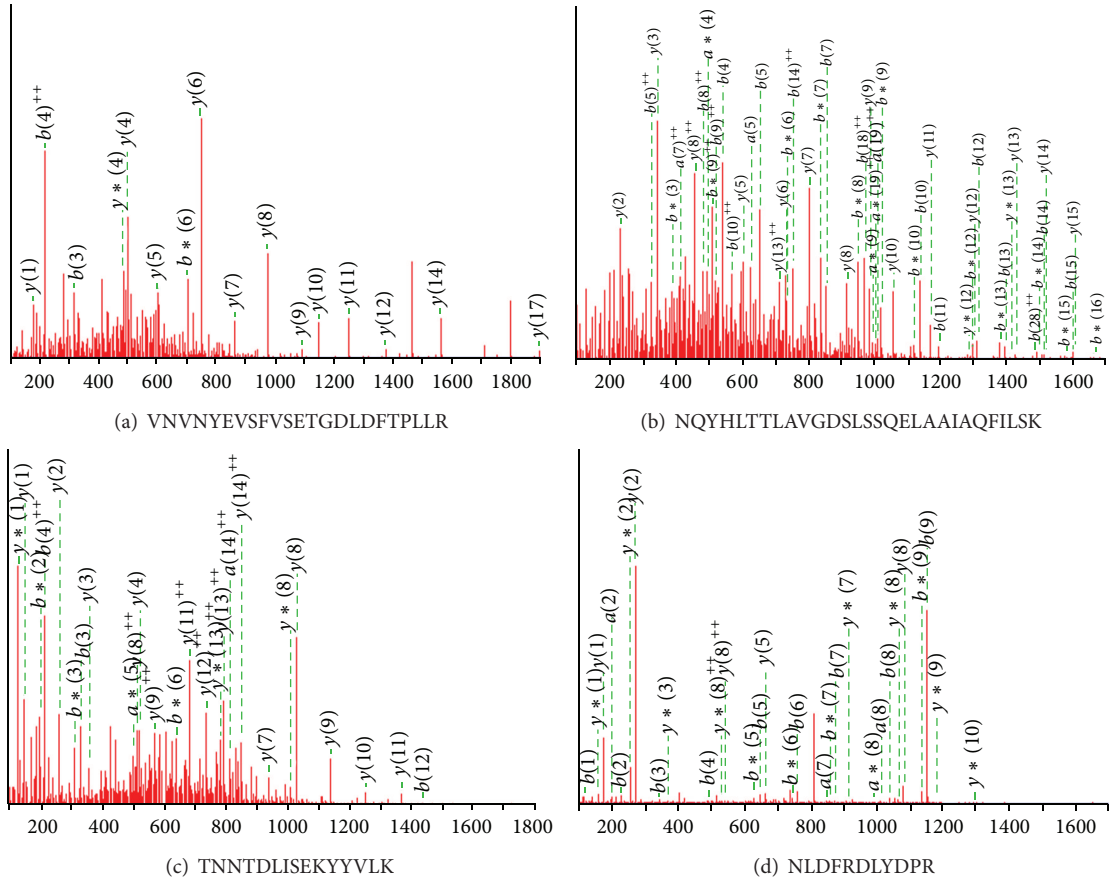

(e)

```
         10         20         30         40         50         60         70         80         90        100
1   IAGYEWLLDRPSVNNSQLVVSVAGTVEGTNQEISLKFFEIDLTSRPAHGGKTEQGLSPKSKPFATDKGAMSHKLEKADLLKAIQEQLIANVHSNDGYFEV  GI153807a
1   ----------------------------------------------------------------------------------------------------  4 peptides
1   IAGPEWLLDRPSVNNSQLVVSVAGTVEGTNQEISLKFFEIDLTSGPAQGGKTEQGLSPKSKPFATNKGAMPHKLEKADLLKAIQEQLIANVHSNDGYFEV  ACG50170a

       110        120        130        140        150        160        170        180        190        200
101 IDFASDATITDRNGKVYFADKDDSVTLPTQPVQEFLLSGHVRVKPYQPKAVHNSAERVNVNYEVSFVSETGDLDFTPLLRNQYHLTTLAVGDSLSSQELA  GI153807a
1   ----------------------------------------------------VNVNYEVSFVSETGDLDFTPLLRNQYHLTTLAVGDSLSSQELA  4 peptides
101 IDFASDATITDRNGKVYFADRDDSVTLPTQPVQEFLLSGHVRVRPYQPKAVHNSAERVNVNYEVSFVSETGDLDFTPLLRNQYHLTTLAVGDSLSSQELA  ACG50170a

       210        220        230        240        250        260        270        280        290        300
201 AIAQFILSKKHPDYIITKRDSSIVTHDNDIFRTILPMDQEFTYHIKDREQAYKANSKTGIEEKTNNTDLISEKYYVLKKGEKPYDPFDRSHLKLFTINYV  GI153807a
44  AIAQFILS------------------------------------------------------KTNNTDLISEKYYVLK--------------------  4 peptides
201 AIAQFILSKKYPDYIITKRDSSIVTHDNDIFRTILPMDQEFTYHIKDREQAYKANSKTGIVEKTNNTDLISEKYYVLKKGEKPYDPFDRSHLKLFTINYV  ACG50170a

       310        320        330        340        350        360        370        380        390        400
301 DVNTNKLLKSEQLLTASERNLDFRDLYDPRDKAKLLYNNLDAFGIMDYTLTGKVEDNHDDTNRIITVYMGKRPEGENASYHLAYDKDRYTEEEREVYSYL  GI153807a
68  --------------------NLDFRDLYDPR                                                                      4 peptides
301 DVNTNELLKSEQLLTASERNLDFRDLYDPRDKAKLLYNNLDAFGIMDYTLTGKVEDNHNDTNRIITVYMGKRPEGENASYHLAYDKDRYTEEEREVYSYL  ACG50170a

       410
401 RYTGTPIPDNPKDK                                                                                        GI153807a
78                                                                                                          4 peptides
401 RYTGTPIPDNPKDK                                                                                        ACG50170a
```

Figure 2: Monoisotopic mass of three neutral identified peptides. (a) VNVNYEVSFVSETGDLDFTPLLR position 158–180 (a); (b) NQYHLTTLAVGDSLSSQELAAIAQFILSK position 181–208; (c) TNNTDLISEKYYVLK position 263–279; (d) NLDFRDLYDPR position 320–330 found in gi: 153807, streptokinase from *Streptococcus pyogenes* (GenBank, AAA26973) corresponding to ion scores of 102, 111, 73, and 51 with $P < 0.05$, respectively. (e) Alignment of four neutral identified peptides (4 peptides) with streptokinase from *Streptococcus pyogenes* AAA26973 (gi153807) and rSK from *S. pyogenes* DT07 (ACG50170).

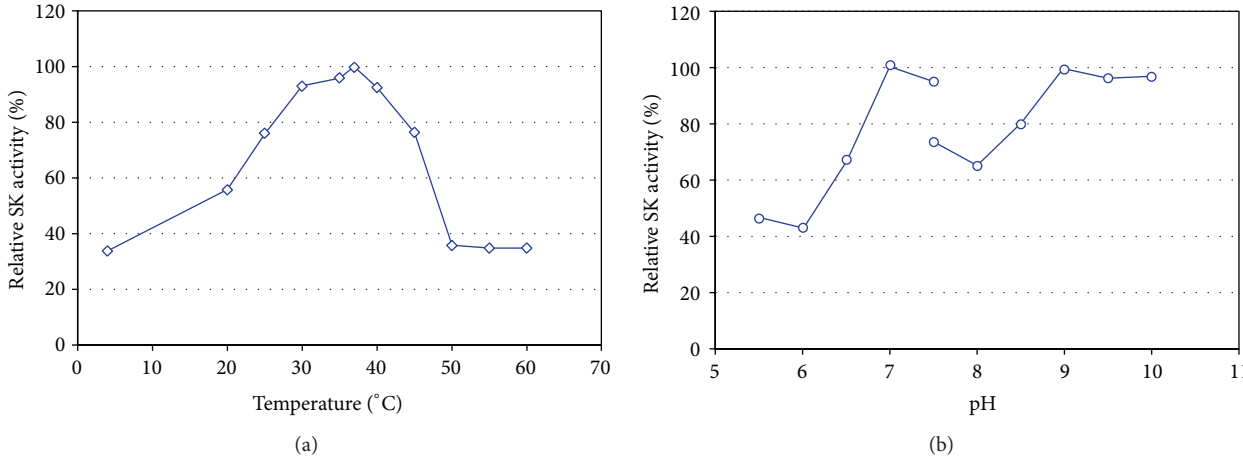

Figure 3: Temperature (a) and pH (b) optimum of rSK from *S. pyogenes* DT07.

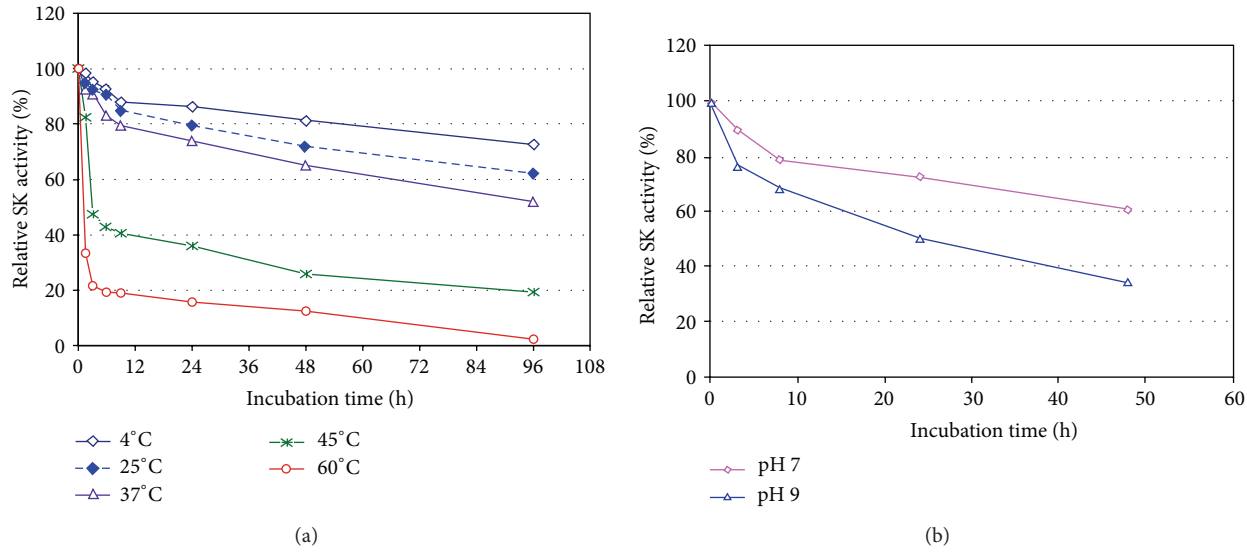

Figure 4: Temperature (a) and pH (b) stability of rSK from *S. pyogenes* DT07.

3.8. Effect of Surfactants. The addition of either Tween 80, Tween 20, or Triton X-100 at the final concentration of 0.5–2% (w/v) in reaction mixture showed an activation of the streptokinase from *S. pyogenes* DT07 up to 150% of its original activity. The enzyme activity increased up to 154% after incubation for 24 h but deeply decreased to 18% after longer incubation for 48 h (Table 4). Similarly, Cherish Babu et al. (2008) reported that rSK was treated with guanidine and then supplemented with Triton X-100 that enhanced the activity of rSK.

3.9. Effect of Metal Ions and EDTA. In the present study, effect of various additives on the purified rSK activity was investigated. The addition of EDTA and metal ions showed a clear effect on the streptokinase activity. EDTA, Mn^{2+}, and K^{+} inhibited the enzyme partially whereas Ag^{+}, Ca^{2+}, and Co^{2+} exhibited a strong inhibition. But the metal ions Cu^{2+}, Fe^{2+}, Ni^{2+}, and Zn^{2+} at a final concentration of 1 mM completely inhibited the streptokinase (Table 5). In previous studies, it was also observed that the addition of Zn^{2+} and Cu^{2+} almost completely inhibited the activity of the recombinant staphylokinase from *Staphylococcus aureus* QT08 [27] and the native staphylokinase from *S. aureus* V8 [31], another thrombolytic agent, closely related to the streptokinase. Why the streptokinases and staphylokinases shared a common property that addition of Zn^{2+} and Cu^{2+} resulted in almost completely inhibition of activities? Because the plasmin completely lost its activity when it was incubated with Zn^{2+} and Cu^{2+} [32, 33].

4. Conclusion

SK is a promising blood-clot dissolving agent for the treatment of patients suffering from a heart attack. It would be desirable to produce high yield of protein with high activity for thrombolytic therapy. In the present study, a *sk* gene from

Table 4: Effect of surfactants on streptokinase activity.

Detergent	Residual activity (%) at the concentration (%)			
	0.5	1.0	1.5	2.0
Tween 20	137.5 ± 2.6	138.3 ± 1.8	135.0 ± 2.3	136.5 ± 2.6
Tween 80	119.1 ± 2.8	125.9 ± 2.6	142.2 ± 1.5	115.4 ± 2.2
Triton X-100	150.3 ± 1.9	140.6 ± 3.6	143.6 ± 0.9	126.6 ± 2.0
	Relative activity (%) after incubation for (h)			
	0	8	24	48
Tween 20	117.6 ± 1.5	149.2 ± 1.3	154.7 ± 1.2	21.9 ± 0.2
Tween 80	121.9 ± 1.9	151.9 ± 0.7	154.4 ± 1.1	27.6 ± 0.2
Triton X-100	119.3 ± 1.6	162.6 ± 1.3	15.4 ± 0.1	18.1 ± 0.2

Table 5: Effect of metal ions on streptokinase activity.

Additive	Residual activity (%) at the concentration (mM)		
	1	3	5
$AgNO_2$	16.1 ± 0.1	n.d.	n.d.
$CaCl_2$	14.5 ± 0.2	n.d.	n.d.
$CoCl_2$	15.6 ± 0.1	n.d.	n.d.
EDTA	50.4 ± 0.2	70.5 ± 0.3	88.2 ± 0.4
KCl	18.5 ± 0.1	25.2 ± 0.2	59.6 ± 0.5
$MnSO_4$	40.5 ± 0.4	54.2 ± 0.3	68.4 ± 0.5

Streptococcus pyogenes DT7 was overexpressed in *E. coli* with a level of 60% of total proteins which is highest yield of any rSK expressed in *E. coli* till date. A simple renaturation system dramatically covered the rSK activity with 41 folds, which was not reported before. Overproduction of rSK in *E. coli* in combination with a simple and highly effective renaturation made the recombinant *E. coli* become a potential strain for industrial SK production.

Conflict of Interests

The authors declare that there is no conflict of interests regarding the publication of this paper.

Acknowledgments

This study was supported by the Ministry of Science and Technology with the project KC10.28/06-10 "Production of Recombinant Streptokinase and Tissue Plasminogen Activator Used for Therapy" and Vietnam Academy of Science and Technology (2008).

References

[1] R. N. Vellanki, R. Potumarthi, and L. N. Mangamoori, "Constitutive expression and optimization of nutrients for streptokinase production by *Pichia pastoris* using statistical methods," *Applied Biochemistry and Biotechnology*, vol. 158, no. 1, pp. 25–40, 2009.

[2] V. Kunadian and C. M. Gibson, "Thrombolytics and myocardial infarction," *Cardiovascular Therapeutics*, vol. 30, no. 2, pp. e81–e88, 2012.

[3] C. Klessen and H. Malke, "Expression of the streptokinase gene from *Streptococcus equisimilis* in *Bacillus subtilis*," *Journal of Basic Microbiology*, vol. 26, no. 2, pp. 75–81, 1986.

[4] H. Malke, D. Gerlach, W. Kohler, and J. J. Ferretti, "Expression of a streptokinase gene from *Streptococcus equisimilis* in *Streptococcus sanguis*," *Molecular and General Genetics*, vol. 196, no. 2, pp. 360–363, 1984.

[5] E. Pimienta, J. C. Ayala, C. Rodríguez et al., "Recombinant production of *Streptococcus equisimilis* streptokinase by *Streptomyces lividans*," *Microbial Cell Factories*, vol. 6, article 20, 2007.

[6] M.-R. Kim, Y.-H. Choeng, W.-J. Chi, D.-K. Kang, and S.-K. Hong, "Heterologous production of streptokinase in secretory form in *Streptomyces lividans* and in nonsecretory form in *Escherichia coli*," *Journal of Microbiology and Biotechnology*, vol. 20, no. 1, pp. 132–137, 2010.

[7] R. Kumar and J. Singh, "Expression and secretion of a prokaryotic protein streptokinase without glycosylation and degradation in *Schizosaccharomyces pombe*," *Yeast*, vol. 21, no. 16, pp. 1343–1358, 2004.

[8] J. Pratap and K. L. Dikshit, "Effect of signal peptide changes on the extracellular processing of streptokinase from *Echerichia coli*: requirement for secondary structure at the cleavage junction," *Molecular and General Genetics*, vol. 258, no. 4, pp. 326–333, 1998.

[9] K. Sriraman and G. Jayaraman, "Enhancement of recombinant streptokinase production in *Lactococcus lactis* by suppression of acid tolerance response," *Applied Microbiology and Biotechnology*, vol. 72, no. 6, pp. 1202–1209, 2006.

[10] H. Malke and J. J. Ferretti, "Streptokinase: cloning, expression, and excretion by *Escherichia coli*," *Proceedings of the National Academy of Sciences of the United States of America*, vol. 81, no. 11, pp. 3557–3561, 1984.

[11] P. V. Cherish Babu, V. K. Srinivas, V. Krishna Mohan, and E. Krishna, "Renaturation, purification and characterization of

streptokinase expressed as inclusion body in recombinant *E. coli*," *Journal of Chromatography B: Analytical Technologies in the Biomedical and Life Sciences*, vol. 861, no. 2, pp. 218–226, 2008.

[12] J. Pratap, G. Rajamohan, and K. L. Dikshit, "Characteristics of glycosylated streptokinase secreted from *Pichia pastoris*: enhanced resistance of SK to proteolysis by glycosylation," *Applied Microbiology and Biotechnology*, vol. 53, no. 4, pp. 469–475, 2000.

[13] F. Baneyx, "Recombinant protein expression in *Escherichia coli*," *Current Opinion in Biotechnology*, vol. 10, no. 5, pp. 411–421, 1999.

[14] B. Balagurunathan and G. Jayaraman, "Theoretical and experimental investigation of chaperone effects on soluble recombinant proteins in *Escherichia coli*: effect of free DnaK level on temperature-induced recombinant streptokinase production," *Systems and Synthetic Biology*, vol. 2, no. 1-2, pp. 27–48, 2008.

[15] D. T. Quyen, T. T. Dao, and S. L. T. Nguyen, "A novel esterase from *Ralstonia sp*. M1: gene cloning, sequencing, high-level expression and characterization," *Protein Expression and Purification*, vol. 51, no. 2, pp. 133–140, 2007.

[16] U. K. Laemmli, "Cleavage of structural proteins during the assembly of the head of bacteriophage T4," *Nature*, vol. 227, no. 5259, pp. 680–685, 1970.

[17] M. M. Bradford, "A rapid and sensitive method for the quantitation of microgram quantities of protein utilizing the principle of protein dye binding," *Analytical Biochemistry*, vol. 72, no. 1-2, pp. 248–254, 1976.

[18] T. T. H. Vu, D. T. Quyen, T. T. Dao, and S. L. T. Nguyen, "Cloning, high-level expression, purification, and properties of a novel endo-β-1,4-mannanase from *Bacillus subtilis* G1 in *Pichia pastoris*," *Journal of Microbiology and Biotechnology*, vol. 22, no. 3, pp. 331–338, 2012.

[19] X.-W. Zhang, T. Sun, X.-N. Huang, X. Liu, D.-X. Gu, and Z.-Q. Tang, "Recombinant streptokinase production by fed-batch cultivation of *Escherichia coli*," *Enzyme and Microbial Technology*, vol. 24, no. 10, pp. 647–650, 1999.

[20] N. Pérez, E. Urrutia, J. Camino et al., "Hydrophobic interaction chromatography applied to purification of recombinant streptokinase," *Minerva Biotecnologica*, vol. 10, no. 4, pp. 174–177, 1998.

[21] B. Balagurunathan, N. S. Ramchandra, and G. Jayaraman, "Enhancement of stability of recombinant streptokinase by intracellular expression and single step purification by hydrophobic interaction chromatography," *Biochemical Engineering Journal*, vol. 39, no. 1, pp. 84–90, 2008.

[22] E. Pupo, B. A. Baghbaderani, V. Lugo, J. Fernández, R. Páez, and I. Torréns, "Two streptokinase genes are expressed with different solubility in *Escherichia coli* W3110," *Biotechnology Letters*, vol. 21, no. 12, pp. 1119–1123, 1999.

[23] S. Rajagopalan, S. L. Gonias, and S. V. Pizzo, "The temperature-dependent reaction between alpha 2-macroglobulin and streptokinase-plasmin(ogen) complex," *The Journal of Biological Chemistry*, vol. 262, no. 8, pp. 3660–3664, 1987.

[24] A. Mumme, M. Kemen, H.-H. Homann, and V. Zumtobel, "Temperature-dependent fibrinolysis with streptokinase," *Deutsche Medizinische Wochenschrift*, vol. 118, no. 44, pp. 1594–1596, 1993.

[25] R. Dubey, J. Kumar, D. Agrawala, T. Char, and P. Pusp, "Isolation, production, purification, assay and characterization of fibrinolytic enzymes (Nattokinase, Streptokinase and Urokinase) from bacterial sources," *African Journal of Biotechnology*, vol. 10, no. 8, pp. 1408–1420, 2011.

[26] K. Vesterberg and O. Vesterberg, "Studies of staphylokinase," *Journal of Medical Microbiology*, vol. 5, no. 4, pp. 441–450, 1972.

[27] T. H. T. Nguyen and D. T. Quyen, "Cloning, high-level expression, purification and characterization of a staphylokinase variant SakφC from *Staphylococcus aureus* QT08 in *Escherichia coli* BL21," *African Journal of Biotechnology*, vol. 6, pp. 2129–2136, 2012.

[28] T. H. T. Nguyen and D. T. Quyen, "High-level expression, purification and properties of a fully active even glycosylated staphylokinase variant SakφC from *Staphylococcus aureus* QT08 in *Pichia pastoris*," *African Journal of Microbiology Research*, vol. 11, pp. 5995–6003, 2012.

[29] P. Rodriguez, P. Fuentes, M. Barro et al., "Structural domains of streptokinase involved in the interaction with plasminogen," *European Journal of Biochemistry*, vol. 229, no. 1, pp. 83–90, 1995.

[30] H. Lu, C. Soria, E. M. Cramer et al., "Temperature dependence of plasmin-induced activation or inhibition of human platelets," *Blood*, vol. 77, no. 5, pp. 996–1005, 1991.

[31] K. Vesterberg and O. Vesterberg, "Studies of staphylokinase," *Journal of Medical Microbiology*, vol. 5, no. 4, pp. 441–450, 1972.

[32] L. I. Sokolovskaya, A. Y. Slominskii, and G. L. Volkov, "Induction of catalytic activity of plasminogen by monoclonal antibody IV-Ic in the presence of divalent metal cations and α2-antiplasmin," *Biochemistry*, vol. 71, no. 6, pp. 627–633, 2006.

[33] P. Nowak and A. Zgirski, "Effects of metal ions on activity of plasmin," *Biological Trace Element Research*, vol. 93, no. 1-3, pp. 87–94, 2003.

Hindawi Publishing Corporation
BioMed Research International
Volume 2014, Article ID 614038, 8 pages
http://dx.doi.org/10.1155/2014/614038

Research Article

Fungal Laccases Degradation of Endocrine Disrupting Compounds

Gemma Macellaro, Cinzia Pezzella, Paola Cicatiello, Giovanni Sannia, and Alessandra Piscitelli

Department of Chemical Sciences, University of Naples "Federico II", Complesso Universitario Monte S. Angelo, Via Cinthia 4, 80126 Naples, Italy

Correspondence should be addressed to Alessandra Piscitelli; apiscite@unina.it

Received 13 January 2014; Revised 12 March 2014; Accepted 31 March 2014; Published 15 April 2014

Academic Editor: Sofiane Ghorbel

Over the past decades, water pollution by trace organic compounds (ng/L) has become one of the key environmental issues in developed countries. This is the case of the emerging contaminants called endocrine disrupting compounds (EDCs). EDCs are a new class of environmental pollutants able to mimic or antagonize the effects of endogenous hormones, and are recently drawing scientific and public attention. Their widespread presence in the environment solicits the need of their removal from the contaminated sites. One promising approach to face this challenge consists in the use of enzymatic systems able to react with these molecules. Among the possible enzymes, oxidative enzymes are attracting increasing attention because of their versatility, the possibility to produce them on large scale, and to modify their properties. In this study five different EDCs were treated with four different fungal laccases, also in the presence of both synthetic and natural mediators. Mediators significantly increased the efficiency of the enzymatic treatment, promoting the degradation of substrates recalcitrant to laccase oxidation. The laccase showing the best performances was chosen to further investigate its oxidative capabilities against micropollutant mixtures. Improvement of enzyme performances in nonylphenol degradation rate was achieved through immobilization on glass beads.

1. Introduction

In the last years assessment and conservation of environmental quality have represented an interesting field of technologic applications. The main problem in industrialized states is represented by a constant and continuous pollution of soil, water-bearing stratum, surface water, and air. This is due to the introduction, in the environment, of toxic and dangerous contaminants for many organisms, including humans. In this context endocrine disrupting chemicals (EDCs) play a significant role. EDCs have been found to disturb the endogenous hormone pathway and interrupt the function of hormone receptors via estrogens-mimicking chemicals, resulting in the alteration of physiological functions, such as reproduction and development of different species, including humans [1]. EDCs are found in many products derived from cosmetic industries and working environment [2]. Many natural chemicals (e.g., phytoestrogens, including genistein and coumestrol), found in human and animal food, can also act as endocrine disruptors [2, 3].

Between 2000 and 2006 the European Commission has contracted diverse studies on the identification and evaluation of this class of substances, and a list of substances potentially endocrine disruptor has been drawn up [4]. Efficient and applicable techniques for removing EDCs in wastewater treatment processes remain a challenge of high environmental and public health significance [5]. One promising approach consists in the use of enzymatic systems able to degrade EDCs into nontoxic or easy to remove products [6]. The promise of phenol oxidases (laccases and tyrosinases) and peroxidases for the elimination of EDCs from aqueous solutions has been established over the last few years and is attracting an increasing attention [7, 8]. Nonetheless, the application of enzymes in continuous systems such as

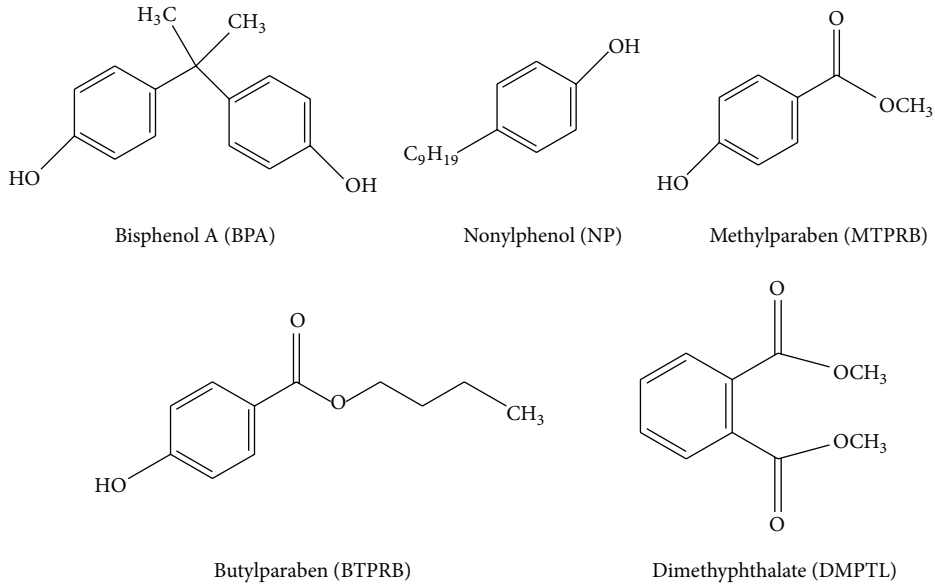

Figure 1: Chemical structure of endocrine disrupting substances used in this study.

wastewater treatment plants remains a challenge as it is limited by their non-reusability, the instability of their structures, and their sensitivity to harsh process conditions. Many of these undesirable limitations may be overcome by the use of immobilized enzyme. In the immobilized form, enzymes are more robust and more resistant to environmental changes allowing easy recovery and multiple reuses [8].

As a fact, examples referring to treatment of EDCs molecules [9–11], as well as of contaminated synthetic water and municipal wastewater [12], with different fungal peroxidases, laccases, and tyrosinases are present in the recent literature. In all reported cases, estrogenic activities were completely removed. Recent efforts have been focused on the immobilization of biocatalysts in order to tackle this major limitation and to facilitate their possible reuse [8].

Laccases (p-diphenol-dioxygen oxidoreductases; EC 1.10.3.2) are blue multicopper oxidases, catalysing the oxidation of a broad range of xenobiotics concomitantly with the reduction of molecular oxygen to water. This renders them very attractive compared to other enzymatic systems because no additional/expensive cosubstrate or cofactor is required apart from oxygen. These enzymes usually contain four copper ions distributed in three active sites, which are involved in the electron transfer from the substrate (T1 active site) towards oxygen (T2/T3 active sites) [13].

In this project, among various chemical classes, the EDCs bisphenol A (BPA), nonylphenol (NP), methylparaben (MTPRB), butylparaben (BTPRB), and dimethylphthalate (DMPTL) (Figure 1) have been selected, based on information about their toxicity, the amount discharged per year, and their commercial availability. BPA is a high production volume chemical used as an intermediate in the fabrication of polycarbonate plastic and epoxy resins [14]. Due to its daily use, high concentrations of BPA are observed in wastewater and in wastewater sludge (0.004–1.36 mg kg^{-1}). NP is a mixture of para-, ortho-, and metaisomers; the most prevalent of them is para-NP. It is a viscous, colourless liquid and it is subjected to ethoxylation to give alkylphenol ethoxylates [15]. This compound is very toxic and recalcitrant; thus it shows a high potential to bioconcentrate [16]. Parabensare esters of parahydroxybenzoic acid, widely used as preservatives in food, pharmaceutical, and cosmetic industries to prevent bacterial growth [17, 18]. Phthalates are a group of persistent, high production volume chemicals, used for a variety of products, including personal care products (e.g., perfumes, lotions, and cosmetics), varnish, medical devices, pharmaceuticals, solvents, additives, and insect repellents [19].

Four different fungal laccases were used in this study to set up EDCs enzymatic treatment, also in the presence of both synthetic and natural mediators. Three out of four selected enzymes were high redox potential laccases from *Pleurotus ostreatus*: POXC [20, 21], POXA1b [21, 22] heterologously expressed in the filamentous fungus *Aspergillus niger* [23], 1H6C, a POXA1b variant obtained through random mutagenesis [24] and produced in *A. niger* [23]. Finally, a commercial laccase, the Novoprime Base 268 (Novozymes), was also used for enzymatic treatment. Moreover, considering that in the natural environment pollutant mixtures are common, this study also evaluated the effect of the best performing enzyme, both free and immobilized, towards the presence of pollutants mixtures.

2. Materials and Methods

2.1. Organism and Culture Conditions. The *P. ostreatus* (Jacq.: Fr.) Kummer (type: Florida) (ATCC number MYA-2306) fungus was maintained through periodic transfer at 4°C on potato dextrose yeast extract (PDY) 24 g/L potato dextrose; 5 g/L yeast extract. Growth was carried out at 28°C in the

dark by preinoculating 300 mL of PDY in 500 mL shaken flasks with 6 agar plugs of mycelium grown on solid state on Petri dishes (11 mm diameter). 50 mL of a 5-day-old culture was transferred in 1 L flasks containing 450 mL of PDY broth. Cultures were incubated in the dark at 28°C under agitation (150 rpm).

A. niger D15#26 strain [25] was grown in liquid medium (300 mL) containing 70 mM $NaNO_3$, 7 mM KCl, 200 mM Na_2HPO_4, 2 mM $MgSO_4{\cdot}7H_2O$, 5% (w/v) glucose, 2 g/L casamino acids, and 5 g/L yeast extract. pH was daily adjusted to 5.0 by adding 1 M citric acid [23].

2.2. Enzymes. Laccase POXC [20] was purified from *P. ostreatus* with slight modifications in the purification protocol. After 10 days of culture, the medium was collected and filtered through gauze. 1 mM of the serine protease inhibitor, phenylmethanesulfonyl fluoride (PMSF), was added to the supernatant. Secreted proteins were precipitated from the filtered medium by addition of $(NH_4)_2SO_4$ up to 80% saturation and loaded on Phenyl Sepharose High Performance 35/100 (GE Healthcare, Milan, Italy). POXC was eluted with a linear gradient of decreasing $(NH_4)_2SO_4$ concentration from 1 M to 0 M. Fractions corresponding to POXC were pooled, equilibrated in buffer 50 mM sodium phosphate (NaP) pH 6.5, and loaded onto a DEAE Sepharose Fast Flow column (GE Healthcare, Milan, Italy) with a linear gradient from 0 M to 0.5 M NaCl, and fractions corresponding to POXC were pooled and desalted.

POXA1b and 1H6C were heterologously expressed and purified from *A. niger*, as previously described [23].

Laccase Novoprime Base 268 (Novozymes) was dissolved in 50 mM NaP pH 6.5.

2.3. Assay of Enzymatic Activity. Laccase activity was assayed at 25°C by monitoring the oxidation of 2,2′-azino-bis(3-ethylbenzothiazoline-6-sulphonic acid) (ABTS) at 420 nm ($\varepsilon_{420} = 36 \times 10^3\ M^{-1}\,cm^{-1}$). The assay mixture contained 2 mM ABTS in 100 mM sodium citrate buffer, pH 3.0.

Immobilized enzyme activity was assayed incubating 10 mg of glass beads in 1 mL of 2 mM ABTS in 100 mM sodium citrate buffer (pH 3.0). The activity was determined by measuring the absorbance at 420 nm every 30″ following the reaction for 2 min. Enzymatic units were expressed as U/g.

2.4. Laccase Immobilization on Glass Beads. Glass beads type S (0.4–0.6 mm diameter) were supplied by Silibeads (Sigmund Lindner GmbH, Germany). Beads were pretreated with 1.2 M HNO_3 at 60°C for 4 hours, extensively washed with water, and then dried at 60°C. Carrier derivatization was performed as follows: 5 g of dry pretreated beads was mixed with 10% APTES (γ-aminopropyltriethoxysilane, Sigma-Aldrich) in 50 mL distilled water and incubated at 80°C for 2 h under constant mixing. The suspension was then washed thoroughly with 50 mM NaP buffer pH 6.5 and treated with 2.5% glutaraldehyde for 1 h at room temperature. The activated beads were extensively washed with the overcited buffer and finally incubated for 1 h with a solution of laccase mixture in 50 mM NaP buffer, pH 6.5 at room temperature. Residual active glutaraldehyde was inactivated by 1 h incubation with 100 mM glycine at room temperature. Immobilization yield (Y) was defined as the ratio between laccase activity assayed on the solid biocatalyst and total activity available in the liquid solution at the beginning of the immobilization processes. A yield of 83% was obtained following this procedure.

2.5. EDCs Enzymatic Degradation. 1 mM stock solution of each EDC (Sigma-Aldrich, Milan, Italy) was prepared in hot water. To improve the solubility of NP and DMPTL in hot water, methanol (0.4% v/v) and Tween 80 (0.1% w/v) were added, respectively. 100 μM of each EDC was incubated for 1 h at 25°C in a reaction mixture containing 1.5 U/mL of purified laccase in 50 mM sodium citrate buffer, pH 5.0; total reaction volume was set to 4 mL. Amounts of EDC were quantified every 30 minutes (t_0, $t_{30'}$, $t_{60'}$) by reverse-phase HPLC. Enzymatic reaction was stopped by adding 50 μL of hydrochloric acid (HCl) to 500 μL of reaction mixture and centrifuging at 15, 100 g for 15 min at room temperature. 100 μL of the supernatant was analysed by HPLC. Degradation of EDCs mixture was performed in the same condition, using a final concentration of 25 μM of each EDC, but for DMPTL. Thus, the final concentration of EDCs mixture was of 100 μM. Control reactions were always performed in the same conditions without enzyme addition. Mediators used were ABTS, dissolved in sodium citrate buffer 50 mM, pH 5.0, and acetosyringone (AS), dissolved in hot sodium citrate buffer, 50 mM, pH 5.0. Concentrations used for both mediators were 20 μM and 200 μM.

Degradation of EDCs mixture by means of immobilized enzyme was performed in the same conditions, using an amount of beads corresponding to 6 U total in the presence of 20 μM AS.

2.6. High-Performance Liquid Chromatography. All EDCs were quantitatively analysed using a C18 column (Grace Vydac, Hesperia, CA, USA) on an HPLC instrument (Agilent Technologies, Italy). The fractions were eluted by using a linear gradient of water-acetonitrile (A solvent 0.1% trifluoroacetic acid in Milli-Q (MQ) water; B solvent 0.07% trifluoroacetic acid, 5% MQ water in acetonitrile) at a flow rate of 1 mL/min. The gradient program for BPA analysis was 0–3 min (acetonitrile 30%), 3–9 min (acetonitrile 30–90%), 9–12 min (acetonitrile 90%), 12-13 min (acetonitrile 90–30%), and 13–15 min (acetonitrile 30%). The eluted sample was monitored by UV absorbance at 227 nm. The retention time for BPA was 6.9 min under these conditions. As regards NP, the applied gradient was 0–3 min (acetonitrile 20%), 3–9 min (acetonitrile 20–90%), 9–12 min (acetonitrile 90%), 12-13 min (acetonitrile 90–20%), and 13–15 min (acetonitrile 20%). The detection wavelength was 277 nm. The retention time for NP was 14.5 min under these conditions. The gradient program for parabens analyses was 0–7 min (acetonitrile 30–70%), 7-8 min (acetonitrile 70–90%), 8–11 min (acetonitrile 90%), 11-12 min (acetonitrile 90–30%), and 12–14 min (acetonitrile 30%). The detection wavelength was 254 nm. Under these

conditions the retention times for MTPRB and BTPRB were 5.8 min and 8.8 min, respectively. As regards DMPTL, the applied gradient was the same used for parabens, while the detection wavelength was 274 nm. The retention time for DMPTL was 6.8 min under these conditions.

As far as the EDCs mixtures are concerned, each molecule was analysed with its optimised program.

The peak area on the chromatogram was used to calculate the remaining amount of EDC as a percentage of the initial value.

3. Results and Discussion

3.1. Endocrine Disruptors Degradation by Enzymes. Enzymatic degradation of EDC bisphenol A (BPA), nonylphenol (NP), methylparaben (MTPRB), butylparaben (BTPRB), and dimethylphthalate (DMPTL) was tested in solution at pH 5.0 in the presence of the different selected laccases. Among the EDC molecules, only BPA was degraded by enzymes in the absence of any mediator within the time of incubation analysed (Figure 2). After 1 hour of incubation Novoprime Base 268 was able to degrade 60% of BPA, whereas POXC degradation rate was slower than that obtained by Novoprime 268, reaching 30% of BPA degradation after both 30 minutes and 1 h incubation. Both POXA1b and 1H6C were less efficient, with the latter being more able to degrade BPA, probably thanks to its higher redox potential [23]. The rate of BPA degradation was comparable with that obtained for other laccases in similar conditions. A careful comparison of results present in the recent scientific literature reveals that different strategies have been used to obtain BPA removal, along with different time of reaction and concentration of both enzyme and substrate. Gassara and coworkers [26] reported a rate of BPA degradation of 13% after 2 hours of incubation in the presence of 0.05 U/mL of a laccase from *Phanerochaete chrysosporium*. A purified laccase from *Grifola frondosa* was able to degrade 15% BPA (0.65 mM) in 1 hour [27], whereas a purified laccase from *Phlebia tremellosa* [28] removed around 65% of BPA estrogenic activity after 3 h incubation with 50 U of enzymatic activity. Interesting results were obtained using a purified laccase by *Trametes villosa*, able to totally degrade 2.2 mM BPA after 3 h incubation [29].

3.2. EDCs Degradation by Enzymes in the Presence of Mediators. With the aim to enhance laccase efficiencies towards selected EDCs, two different mediators, a synthetic and a natural one, were added to the reaction mix. The selected mediators were ABTS, the first acknowledged laccase mediator [30], and the natural mediator AS, an eco-friendly, easily and economically available mediator [31].

As it is shown in Figure 3(a), the presence of both mediators enhances laccase performances towards BPA but for Novoprime 268 and ABTS mediator is more effective than AS with all the tested laccases. As a fact, in the presence of ABTS, POXC was able to almost fully degrade BPA (95%) after 1 hour reaction. It is also possible to note that in the presence of both mediators POXA1b and 1H6C showed the same efficiency. Unexpectedly, the presence of mediators did not influence or even decreased Novoprime base 268 efficiency. A similar effect has also been observed for a *Coriolopsis polyzona* laccase towards NP using 1-hydroxybenzotriazole (HBT) as mediator [10].

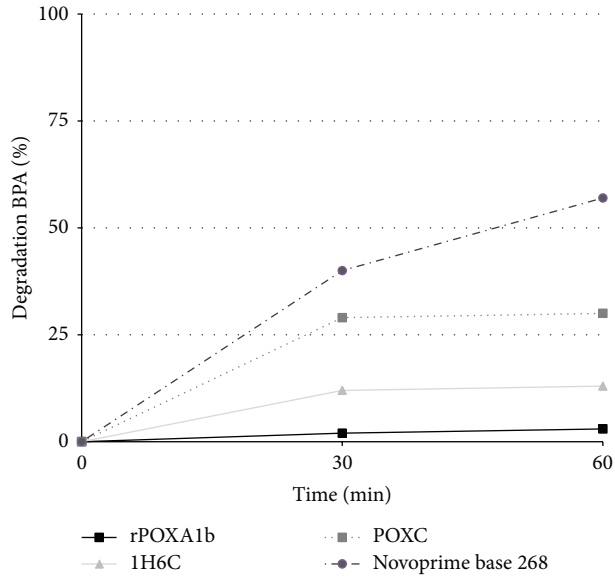

Figure 2: Percentage degradation (%) of BPA by fungal laccases. Reaction conditions: 100 μM BPA, pH 5.0 (50 mM sodium citrate buffer), 25°C, and 1.5 U/mL laccase, with a reaction time of 1 h. All results are averages from two replicate experiments and the standard deviation is less than 10%.

Also when considering nonylphenol, the presence of both mediators enhances laccase performances, with ABTS being more effective than AS with all tested laccases (Figure 3(b)). In this case, POXC and Novoprime base 268 showed almost the same degradation rate both in the presence of ABTS and AS. On the other hand, POXA1b and 1H6C showed an opposite behaviour. As a fact, in the presence of ABTS, 1H6C was more effective than POXA1b, whereas in the presence of AS, POXA1b proved to be more efficient than its variant. This result seems to indicate that no simple rule regarding redox potential or affinity can be easily drawn, as the whole reaction mechanism is quite complex. The obtained results seem promising if carefully compared with other systems. Indeed, a laccase from the white rot fungus *C. polyzona* was able to eliminate 50% BPA and 66% NP in the presence of 10 μM ABTS as mediator [10]. When the synthetic mediator HBT (200 μM) was used to improve laccase degradation, an enhanced degradation of almost 1.3-fold for both substrates was observed, reaching a degradation of 95% and 80% for BPA and NP, respectively [32].

When the mediator concentration was increased up to 200 μM, AS was revealed to be the best mediator, since all enzymes were able to also degrade methylparaben and butylparaben after 1 h incubation (Table 1). Also in this case, POXC showed the best performances, being able to degrade in 30 minutes 50% and 60% of methyl and butylparaben, respectively (degradation did not improve after 1 h incubation). Among parabens, butylparaben was more susceptible

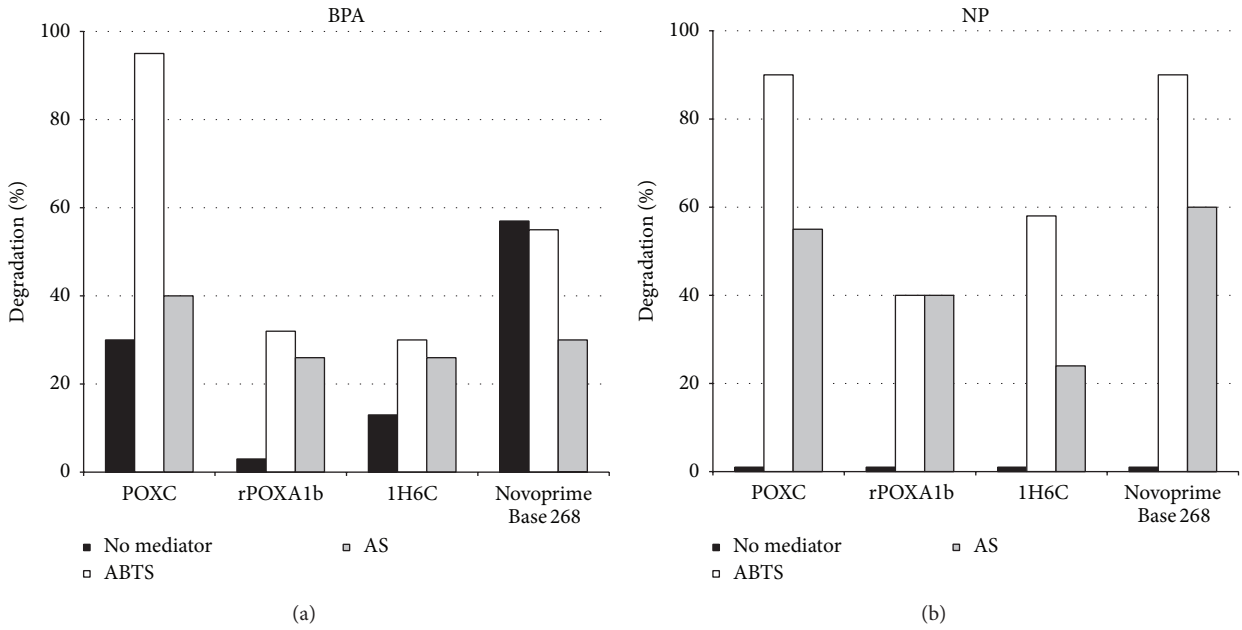

Figure 3: Effect of absence of mediator, 20 μM of ABTS, or AS on the removal of EDCs after a 1 h treatment at pH 5.0 and at a temperature of 25°C with 1.5 U/mL of laccases. (a) BPA; (b) NP. All results are averages from two replicate experiments and the standard deviation is less than 10%.

Table 1: Degradation of MTPRB and BTPRB in the presence of 200 μM of ABTS, or AS after a 1 h treatment at pH 5.0 25°C with 1.5 U/mL of laccases. All results are averages from two replicate experiments and the standard deviation is less than 10%.

Enzymes	MTPRB (% degradation)		BTPRB (% degradation)	
	ABTS	AS	ABTS	AS
POXC	—	50	15	60
rPOXA1b	—	35	—	40
1H6C	5	7	7	8
Novoprime Base 268	—	40	—	50

to laccase degradation in the presence of mediators than methylparaben. In the scientific literature are present only few reports regarding paraben degradation by laccases. Mizuno and coworkers [33] demonstrated that both iso-butylparaben and n-butylparaben were almost completely removed (95%) after 2 h of treatment and completely disappeared after 4 h of treatment with 0.5 U/mL of laccase activity in the presence of 2 mM HBT. The only substrate recalcitrant to laccase oxidation in all the tested conditions was dimethylphthalate.

3.3. Degradation of EDCs Mixture by Free and Immobilized POXC. POXC, the best performing enzyme, was chosen for further degradation analyses against a mixture of the selected EDCs in a total final concentration of 100 μM. The analyses were conducted in the presence of four out of five substrates. As a fact, DMPTL was not used, considering its recalcitrance to laccase degradation under all the tested conditions. It is worth to note that in the absence of any mediator POXC is able to degrade almost 40% BPA and 80% NP after 1 h incubation, whereas methyl and butylparaben were not degraded (Figure 4). As far as BPA is concerned, a slower degradation rate was observed when BPA concentration was lowered if compared with the degradation observed with high BPA concentration. When mediator was added to the reaction, the efficiency was greatly enhanced, and full disappearance of BPA was observed in the presence of AS. On the other hand, POXC is able to efficiently degrade NP at low concentration also in the absence of mediators, and no increase is observed when mediators are added to the reaction mix. Thus, it may be hypothesized that the enzyme shows a higher affinity towards NP than towards BPA. Parabens at low concentration were not oxidised in the presence of both mediators.

When immobilized POXC was used towards EDCs mix in the presence of AS, NP degradation improved with respect to the free enzyme, reaching the same extent of degradation (80%) within only 15 min, and no further increase was observed. On the other hand, a slightly lower BPA removal (80%) was observed using the immobilized enzyme with respect to the free one. Parabens were not degraded, following the same trend already observed for the soluble counterpart. Control reactions were carried out using the silanized and derivatized carrier (without enzyme) against the mix of EDCs and no adsorption on the carrier was observed. Laccase immobilized on glass beads maintained significant activity during storage at 4°C in 50 mM phosphate buffer pH 6.5. After one month of storage, the retained laccase activity was 100%.

In order to assess reusability of the immobilized laccase against mixture of EDCs, six successive cycles of batch degradation were performed. After six cycles, there was a 20%

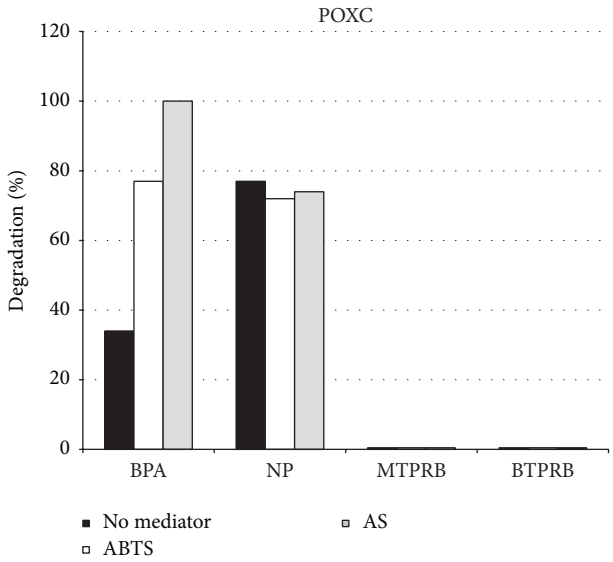

Figure 4: Effect of absence of mediator, 20 μM of ABTS, or AS on the removal of EDCs mixtures by POXC. Reaction conditions: 25 μM of each molecule, pH 5.0 (50 mM sodium citrate buffer), 25°C, and 1.5 U/mL laccase, with a reaction time of 1 h. All results are averages from two replicate experiments and the standard deviation is less than 10%.

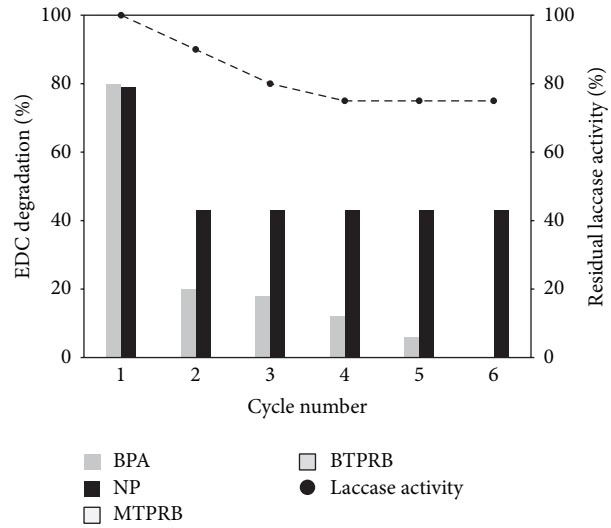

Figure 5: Percentage degradation (%) of BPA and NP by immobilized POXC. Reaction conditions: 6 U_{TOT} versus 25 μM each EDC, pH 5.0 (50 mM sodium citrate buffer), 25°C, and in the presence of 20 μM AS with a reaction time of 1 h. Residual laccase activity is reported as filled black circle. All results are averages from two replicate experiments and the standard deviation is less than 10%.

drop in laccase activity (Figure 5). As far as EDC removal is concerned, a gradual loss of BPA degradation during six cycles was observed. On the other hand, NP degradation was decreased up to 40% after the first cycle, but no further drop was observed during the following 5 cycles.

4. Conclusions

The growing attention accorded to the removal of EDCs from environmental matrices makes oxidative enzymes an attractive candidate in the bioremediation arsenal. Four different laccases were chosen for their interesting characteristics and tested towards EDC molecules. The obtained results have shown that all laccases are able to oxidize different EDCs. In particular, BPA is the only substrate oxidized under all conditions tested. Furthermore, to improve laccase capabilities, mediators were added to reaction mixtures. Among the chosen laccases, POXC was the enzyme with the highest bioremediation capacity under all conditions analysed. Its performance was increased in the presence of both mediators. Interesting results were obtained in the presence of the natural mediator acetosyringone. When used at high concentration, this natural mediator enhanced the bioremediation capacity of POXC determining a rate degradation of 50% of both parabens in 30 minutes. Thus, results herein obtained confirm laccase capabilities [33] to degrade this kind of substrates, very poorly investigated till now. Furthermore, oxidative capabilities of POXC were also studied in the presence of EDCs mixtures. Removal rates were different in micropollutant mixtures if compared with removal rates obtained treating individually the different molecules with alternating results towards BPA and NP, respectively. Improvement of enzyme performances in NP removal was achieved through immobilization on glass beads.

These results highlight the influence on the enzymatic degradation efficiency of the ratio between xenobiotic concentration and enzyme affinity. Thus, a challenge still open to face EDCs degradation is the discovery/tailoring enzymes capable of degrading the target compounds with an affinity constant of the same order of magnitude with respect to the actual concentrations of the EDCs in the environment. As a fact, since EDCs concentration in real wastewater is very low (ng/L), enzymes displaying a very high efficiency (high turnover together with high affinity) towards this molecule are excellent candidates to efficiently achieve their removal.

Conflict of Interests

The authors declare that there is no conflict of interests regarding the publication of this paper.

Acknowledgment

This work was supported by grants from the Italian MIUR (Ministero dell'Università e della Ricerca Scientifica Progetti di Rilevante Interesse Nazionale) PRIN 2009STNWX3.

References

[1] T. T. Schug, A. Janesick, B. Blumberg, and J. J. Heindel, "Endocrine disrupting chemicals and disease susceptibility," *Journal of Steroid Biochemistry and Molecular Biology*, vol. 127, no. 3–5, pp. 204–215, 2011.

[2] S. Combalbert and G. Hernandez-Raquet, "Occurrence, fate, and biodegradation of estrogens in sewage and manure," *Applied Microbiology and Biotechnology*, vol. 86, no. 6, pp. 1671–1692, 2010.

[3] E. Diamanti-Kandarakis, J.-P. Bourguignon, L. C. Giudice et al., "Endocrine-disrupting chemicals: an Endocrine Society scientific statement," *Endocrine Reviews*, vol. 30, no. 4, pp. 293–342, 2009.

[4] European Union, "Commission staff working document. An implementation of the community strategy for endocrine disrupters—a range of substances suspected of interfering with the hormone systems of humans and wildlife," no. 1372, Belgium, Brussels, 2004.

[5] Z.-H. Liu, Y. Kanjo, and S. Mizutani, "Removal mechanisms for endocrine disrupting compounds (EDCs) in wastewater treatment—physical means, biodegradation, and chemical advanced oxidation: a review," *Science of the Total Environment*, vol. 407, no. 2, pp. 731–748, 2009.

[6] P. Galliker, G. Hommes, D. Schlosser, P. F.-X. Corvini, and P. Shahgaldian, "Laccase-modified silica nanoparticles efficiently catalyze the transformation of phenolic compounds," *Journal of Colloid and Interface Science*, vol. 349, no. 1, pp. 98–105, 2010.

[7] H. Cabana, J. P. Jones, and S. N. Agathos, "Elimination of endocrine disrupting chemicals using white rot fungi and their lignin modifying enzymes: a review," *Engineering in Life Sciences*, vol. 7, no. 5, pp. 429–456, 2007.

[8] S. Yang, F. I. Hai, L. D. Nghiem et al., "Understanding the factors controlling the removal of trace organic contaminants by white-rot fungi and their lignin modifying enzymes: a critical review," *Bioresource Technology*, vol. 141, pp. 97–108, 2013.

[9] Y.-J. Kim and J. A. Nicell, "Impact of reaction conditions on the laccase-catalyzed conversion of bisphenol A," *Bioresource Technology*, vol. 97, no. 12, pp. 1431–1442, 2006.

[10] H. Cabana, J.-L. H. Jiwan, R. Rozenberg et al., "Elimination of endocrine disrupting chemicals nonylphenol and bisphenol A and personal care product ingredient triclosan using enzyme preparation from the white rot fungus *Coriolopsis polyzona*," *Chemosphere*, vol. 67, no. 4, pp. 770–778, 2007.

[11] C. Nicolucci, S. Rossi, C. Menale et al., "Biodegradation of bisphenols with immobilized laccase or tyrosinase on polyacrylonitrile beads," *Biodegradation*, vol. 22, no. 3, pp. 673–683, 2011.

[12] M. Auriol, Y. Filali-Meknassi, R. D. Tyagi, and C. D. Adams, "Laccase-catalyzed conversion of natural and synthetic hormones from a municipal wastewater," *Water Research*, vol. 41, no. 15, pp. 3281–3288, 2007.

[13] P. Giardina, V. Faraco, C. Pezzella, A. Piscitelli, S. Vanhulle, and G. Sannia, "Laccases: a never-ending story," *Cellular and Molecular Life Sciences*, vol. 67, no. 3, pp. 369–385, 2010.

[14] D. P. Mohapatra, S. K. Brar, R. D. Tyagi, and R. Y. Surampalli, "Parameter optimization of ferro-sonication pre-treatment process for degradation of bisphenol A and biodegradation from wastewater sludge using response surface model," *Journal of Hazardous Materials*, vol. 189, no. 1-2, pp. 100–107, 2011.

[15] X. Jie, L. Jian Mei, F. Zheng, L. Gong, B. Zhang, and J. Yu, "Neurotoxic effects of nonylphenol: a review," *The Central European Journal of Medicine*, vol. 125, no. 3-4, pp. 61–70, 2013.

[16] Commission Directive 2002/8/EC of 6 February 2002 amending Directives 72/168/EEC and 72/180/EEC concerning the characteristics and minimum conditions for examining vegetable and agricultural varieties respectively.

[17] M. G. Soni, G. A. Burdock, S. L. Taylor, and N. A. Greenberg, "Safety assessment of propyl paraben: a review of the published literature," *Food and Chemical Toxicology*, vol. 39, no. 6, pp. 513–532, 2001.

[18] P. W. Harvey and P. Darbre, "Endocrine disrupters and human health: could oestrogenic chemicals in body care cosmetics adversely affect breast cancer incidence in women? A review of evidence and call for further research," *Journal of Applied Toxicology*, vol. 24, no. 3, pp. 167–176, 2004.

[19] M. J. Tsai, P. L. Kuo, and Y. C. Ko, "The association between phthalate exposure and asthma," *Kaohsiung Journal of Medical Sciences*, vol. 28, no. 7, pp. 28–36, 2012.

[20] G. Palmieri, P. Giardina, L. Marzullo et al., "Stability and activity of a phenol oxidase from the ligninolytic fungus *Pleurotus ostreatus*," *Applied Microbiology and Biotechnology*, vol. 39, no. 4-5, pp. 632–636, 1993.

[21] A. M. Garzillo, M. C. Colao, V. Buonocore et al., "Structural and kinetic characterization of native laccases from *Pleurotus ostreatus*, *Rigidoporus lignosus*, and *Trametes trogii*," *Journal of Protein Chemistry*, vol. 20, no. 3, pp. 191–201, 2001.

[22] P. Giardina, G. Palmieri, A. Scaloni et al., "Protein and gene structure of a blue laccase from *Pleurotus ostreatus*," *Biochemical Journal*, vol. 341, no. 3, pp. 655–663, 1999.

[23] G. Macellaro, M. C. Baratto, A. Piscitelli et al., "Effective mutations in a high redox potential laccase from *Pleurotus ostreatus*," *Applied Microbiology and Biotechnology*, 2014.

[24] A. Miele, P. Giardina, E. Notomista, A. Piscitelli, G. Sannia, and V. Faraco, "A semi-rational approach to engineering laccase enzymes," *Molecular Biotechnology*, vol. 46, no. 2, pp. 149–156, 2010.

[25] C. L. Gordon, V. Khalaj, A. F. J. Ram et al., "Glucoamylase: green fluorescent protein fusions to monitor protein secretion in *Aspergillus niger*," *Microbiology*, vol. 146, no. 2, pp. 415–426, 2000.

[26] F. Gassara, S. K. Brar, M. Verma, and R. D. Tyagi, "Bisphenol A degradation in water by ligninolytic enzymes," *Chemosphere*, vol. 92, no. 10, pp. 1356–1360, 2013.

[27] T. Nitheranont, A. Watanabe, T. Suzuki, T. Katayama, and Y. Asada, "Decolorization of synthetic dyes and biodegradation of bisphenol a by laccase from the edible mushroom, *Grifola frondosa*," *Bioscience, Biotechnology and Biochemistry*, vol. 75, no. 9, pp. 1845–1847, 2011.

[28] Y. Kim, S. Yeo, M. K. Kim, and H. T. Choi, "Removal of estrogenic activity from endocrine-disrupting chemicals by purified laccase of *Phlebia tremellosa*," *FEMS Microbiology Letters*, vol. 284, no. 2, pp. 172–175, 2008.

[29] T. Fukuda, H. Uchida, Y. Takashima, T. Uwajima, T. Kawabata, and M. Suzuki, "Degradation of bisphenol A by purified laccase from *Trametes villosa*," *Biochemical and Biophysical Research Communications*, vol. 284, no. 3, pp. 704–706, 2001.

[30] R. Bourbonnais and M. G. Paice, "Oxidation of non-phenolic substrates. An expended role for laccase in lignin biodegradation," *FEBS Letters*, vol. 267, no. 1, pp. 99–102, 1990.

[31] A. I. Cañas and S. Camarero, "Laccases and their natural mediators: biotechnological tools for sustainable eco-friendly processes," *Biotechnology Advances*, vol. 28, no. 6, pp. 694–705, 2010.

[32] Y. Tsutsumi, T. Haneda, and T. Nishida, "Removal of estrogenic activities of bisphenol A and nonylphenol by oxidative enzymes

from lignin-degrading basidiomycetes," *Chemosphere*, vol. 42, no. 3, pp. 271–276, 2001.

[33] H. Mizuno, H. Hirai, S. Kawai, and T. Nishida, "Removal of estrogenic activity of iso-butylparaben and n-butylparaben by laccase in the presence of 1-hydroxybenzotriazole," *Biodegradation*, vol. 20, no. 4, pp. 533–539, 2009.

Hindawi Publishing Corporation
BioMed Research International
Volume 2014, Article ID 345980, 8 pages
http://dx.doi.org/10.1155/2014/345980

Research Article

Streptomyces flavogriseus HS1: Isolation and Characterization of Extracellular Proteases and Their Compatibility with Laundry Detergents

Sofiane Ghorbel, Maher Kammoun, Hala Soltana, Moncef Nasri, and Noomen Hmidet

Laboratoire de Génie Enzymatique et de Microbiologie, Ecole Nationale d'Ingénieurs de Sfax, BP 1173, 3038 Sfax, Tunisia

Correspondence should be addressed to Sofiane Ghorbel; so_fian@hotmail.com

Received 13 January 2014; Revised 22 February 2014; Accepted 5 March 2014; Published 6 April 2014

Academic Editor: Neelu Nawani

The present study describes the isolation of a new protease producing *Streptomyces* strain HS1 and the biochemical characterization of the secreted proteases. By sequencing of its noted 16S rDNA, HS1 strain was found to have a 100% identity with *Streptomyces flavogriseus*. The highest protease production was found using FermII media. In these conditions maximum protease production (99 U/mL) was obtained after 96 h incubation at 30°C and 150 rpm. HS1 strain produced at least five proteases as revealed by zymogram technique. The enzyme preparation exhibited activity over a broad range of pH (5–11) and temperature (25–70°C). Optimum activity was observed at a pH of 7.0 and a temperature of 50°C. Proteolytic activity was significantly unaffected by Ca^{2+} and Mg^{2+}. EDTA and PMSF highly decreased the original activity. The crude extracellular proteases showed high stability when used as a detergent additive. These properties offer an interesting potential for enzymatic hydrolysis at the industrial level.

1. Introduction

Actinomycetes, a Gram-positive filamentous bacteria, can degrade various macromolecules in soil [1]. Among actinomycetes, *Streptomyces* species are the most industrially useful because of their capacity of producing numerous secondary metabolites, particularly antibiotics. Similarly, these bacteria offer a second industrial interesting use by producing large amounts of proteolytic enzymes, with different substrate specificities [2]. The investigation of proteases does not take place only in scientific fields such as protein chemistry and protein engineering, but also in other industrial uses including cleaning detergents, leather, and food additives. Such a wide use of proteases in the industrial field shows their importance especially that they represent around 60% of the total enzyme market [3]. Unlike proteases from other bacteria which have been extensively characterized, proteases from actinomycetes did not receive a similar attention [4]. Still, their ability to produce a variety of enzymes may be an attractive phenomenon of these prokaryotes.

The composition of the protease complexes secreted by *Streptomyces* is determined by the taxonomic position of the producers [5–8]. The potential use of *Streptomyces* for producing proteases is justified by their ability to release the proteins into extracellular media. Such a capability is generally regarded as safe (GRAS) with food and drug administration. *Streptomyces* spp. that produce proteases include *S. clavuligerus, S. griseus, S. rimouses, S. thermoviolaceus*, and *S. thermovulgaris* [7]. Some of these proteases, like the serine proteases of *Streptomyces griseus* [8, 9] and *Streptomyces fradiae* [10], have been characterized structurally and enzymatically. There have also been many descriptions of isolation and partial characterization of alkaline protease activities from other members of the genus *Streptomyces* like *Streptomyces clavuligerus*, *Streptomyces gulbargensis*, *Streptomyces viridifaceins*, and *Streptomyces* sp. [11–13].

Present study describes the isolation of a multiple protease producing *Streptomyces flavogriseus* HS1 strain, isolated from a Tunisian soil. We report the biochemical characterization of the crude enzyme for evaluation of its biotechnological potential as detergent additive.

2. Material and Methods

2.1. Isolation of the Actinomycete Strain. The isolation of the Actinomycete strains from a soil sample was done by serial

dilution plate technique on ISP4 agar media containing (g/L) starch 10, casein 0.3, KNO_3 2, NaCl 2, K_2HPO_4 2, $MgSO_4 \cdot 7H_2O$ 0.05, $CaCO_3$ 0.02, $FeSO_4 \cdot 7H_2O$ 0.01, and 15 agar [14].

2.2. Identification of HS1 Strain. The 16S rRNA gene of the HS1 strain was amplified by PCR using the following primers: F (forward), 5′-CCGAATTCGTCGACAACAGAGTTTGATCCTGGCTCAG-3′ and R (reverse), 5′-CCCGGGATCCAAGCTTAAGGAGGTGATCCAGCC-3′. The PCR mixture contained 30 pmol of primers, 20 pmol of each deoxynucleoside triphosphate, polymerisation buffer, and 5 U Taq polymerase. The PCR program involved 35 cycles of denaturing at 94°C for 1 min, primer annealing at 55°C for 1 min, and extension at 72°C for 90 s. The sequencing was performed three times using the DNA sequencer ABI PRISM 3100/3100-Avant Genetic Analyser (CA, USA). 16S rDNA sequence was searched for similarities to known sequences in the GenBank database (National Center for Biotechnology Information, National Library of Medicine) using the BLAST search program. The sequence was aligned with those of the reference strains using ClustalW [15]. A phylogenetic tree was constructed by the neighbour-joining method [16].

2.3. Determination of Protease Activity. Measuring of the protease activity was done as described by Kembhavi et al. [17], using casein as substrate 1% (w/v) in 100 mM Tris-HCl buffer, pH 7.0. The mixture was incubated for 15 min at 50°C and the reaction was stopped by addition of 0.5 mL 20% (w/v) TCA (trichloroacetic acid). The mixture was left at room temperature for 10 minutes and then centrifuged at 10000 g for 15 minutes to remove the precipitate. The absorbance of the soluble TCA peptides was recorded at 280 nm. One unit of protease activity was defined as the amount of enzyme required to liberate 1 μg of tyrosine per minute under the experimental conditions used. All measurements were carried out in triplicate.

2.4. Protease Production. The proteolytic isolates were cultured in three different liquid medium: FermII media: (g/L) dextrin 20, tryptone 10, KH_2PO_4 1.0, K_2HPO_4 3.4, $MgSO_4 \cdot 7H_2O$ 0.3, $FeSO_4 \cdot 7H_2O$ 0.01, $ZnCl_2$ 0.1, $CuSO_4 \cdot 7H_2O$ 0.01, $MgCl_2 \cdot 4H_2O$ 0.003, $CaCl_2$ 0.01, NaCl 0.03, pH 7.0 [18], gelatin containing media: (g/L): gelatin, 10; peptone, 5; yeast extract, 5; NaCl, 50; and pH 9, and liquid ISP4 media [14].

A 1 mL spore suspension (10^4 to 10^6 spores/mL) was added to a 250 mL Erlenmeyer flask containing 100 mL of liquid media [14], and the flasks were incubated at 30°C and 150 rpm for 96 h. The culture medium was centrifuged at 5000 rpm to remove mycelia and medium debris, and the supernatant was used as a crude enzyme preparation.

2.5. Characterization of Proteases. Zymography was performed on NativePAGE according to the method of Garcia-Carreno et al. [19]. After electrophoresis, the gel was submerged in 1% (w/v) casein in 100 mM glycine-NaOH buffer, pH 7.0, and incubated at 50°C for 20 min. After washing, the gel was stained with Coomassie Brilliant Blue R-250 and destained with 5% ethanol-7.5% acetic acid. A clear zone appeared on the blue background of the gel which indicated the presence of protease activity.

2.6. Effect of Temperature and pH on Protease Activity and Stability. To investigate the temperature effect, the protease assay was performed at different temperatures between 20 and 80°C, using casein as substrate for 10 min at pH 7.0. For thermal stability, the enzyme was incubated at different temperatures for 60 min. Aliquots were withdrawn at the designed time intervals to test the remaining activity. The residual activity was assayed at pH 7.0 and 50°C for 10 min. The nonheated enzyme was considered as control (100% activity).

Protease activity was assayed over the pH range 5.0–12.0 at 50°C for 10 min, using casein as a substrate. The effect of pH on enzyme stability was evaluated by measuring the residual enzyme activity after incubation at various pH for 60 min at 25°C. The following buffer systems were used: 100 mM glycine-HCl, pH 4.0 and 5.0; 100 mM sodium acetate, pH 6.0; 100 mM phosphate-buffer, pH 7.0; 100 mM Tris-HCl, pH 8.0; 100 mM glycine-NaOH, pH 9.0 and 10; and 100 mM $Na_2HPO_4 \cdot NaOH$, pH 12.0.

2.7. Effect of Metal Ions and Other Chemicals on Protease Activity and Stability. The effects of different monovalent (Na^+ or K^+) or divalent (Fe^{2+}, Mn^{2+}, Zn^{2+}, Cu^{2+}, Ba^{2+}, Mg^{2+}, or Hg^{2+}) metal ions, at a concentration of 5 mM, on protease activity were investigated by adding them to the reaction mixture. The activity in the absence of any additives was taken as 100%.

The effects of enzyme inhibitors on protease activity were studied using PMSF and EDTA. The crude enzyme was preincubated with each inhibitor for 30 min at 25°C, and then the remaining enzyme activity was estimated using casein as a substrate. The activity in the absence of inhibitors was taken as 100%. The effects of some surfactants (Triton X-100, Tween 80, and SDS) and oxidizing agents (sodium perborate) on enzyme stability were studied by preincubating the crude enzyme for 1 h at 25°C. The residual activity was measured at pH 7.0 and 50°C. The activity of the enzyme without any additive was taken as 100%.

2.8. Detergent Compatibility. The compatibility of the HS1 extracellular proteases with commercial laundry detergents was studied using Ariel (Procter and Gamble, Switzerland), Newdet (Sodet, Tunisia), and Dixan (Henkel, Spain) as solid detergents. The endogenous proteases contained in these detergents were inactivated by heating the diluted detergents for 1 h at 65°C prior to the addition of the enzyme preparation. The extracellular proteases of *Streptomyces flavogriseus* HS1 were incubated with different diluted detergents (1/100) for 1 h at 30°C, 40°C, and 50°C and then the remaining activities were determined under the standard assay conditions. The enzyme activity of a control, without detergent, incubated under similar conditions, was taken as 100%.

2.9. Statistical Analysis. Statistical analyses were performed with Statgraphics ver. 5.1, professional edition (Manugistics

Table 1: Effect of various culture media on the production of extracellular proteases from *Streptomyces flavogriseus* HS1.

Medium	Proteolytic activity (U/mL)
FermII	98
Gelatin based medium	4.7
ISP4	51.8

The activity of the proteases was determined at 50°C and pH 7.0 after 96 h of culture.

Corp., USA) using ANOVA analysis. Differences were considered significant at $P < 0.05$. Results represent the means of at least two determination carried out in duplicate. The difference between values did not exceed 5%.

3. Results and Discussion

3.1. Isolation of the Actinomycete Strain. Samples were taken from an organic rich soil in Sfax city (Tunisia). Isolation of the actinomycete strains was obtained after 96 h of incubation at 30°C. One isolate was selected for further studies because of its important extracellular proteases secretion and named HS1 strain (Figure 1). HS1 strain was confirmed as belonging to the genus *Streptomyces* since it possessed nonfragmented substrate mycelia, aerial hyphae, and smooth spores organized in straight chains. Analysis of the 16S rRNA gene sequence of this strain showed a high similarity (100%) with *Streptomyces flavogriseus* (Figure 2).

Streptomyces flavogriseus was well known to produce several enzymes such as cellulose, xylanase, and glucose isomerase [19–21], but no data was found describing extracellular proteases.

3.2. Protease Production. Three liquid culture media optimized for the production of extracellular proteases in *Streptomyces* were tested, among them are FermII [18], ISP4 [14], and gelatin based media (this study). In the light of this experiment, FermII was found to be the best medium for the production of *Streptomyces flavogriseus* HS1 extracellular proteases (Table 1). The fermentation time course for protease production by *Streptomyces flavogriseus* HS1 (data not shown) indicates that the maximum protease activity (99 U/mL) was obtained after 96 h of cultivation, when cells were in the stationary phase, and its production was not growth associated. Similar results were obtained by Gibb and Strohl [22], who observed that the maximum protease production by *Streptomyces peucetius* occurred after 100 h of cultivation at the stationary phase growth. This period was shorter than that of the well-studied *Streptomyces* (e.g., *Streptomyces moderatus* required 120 h of cultivation for maximum protease production [6]). However, Dastager et al. [13] showed that the protease activity measured in the cell-free supernatant fluid of *Streptomyces gulbargensis* sp. Nov. was maximum (121.8 U/mL) after 48 h of growth.

3.3. Zymogram. To give more information about the diversity of extracellular proteases secreted by HS1 strain, zymogram analysis was done as described in the "Material and Methods" section. As shown in Figure 3, proteolytic activity profiles of cell-free enzymatic preparation of *Streptomyces flavogriseus* HS1 showed at least five major proteases. This is a common feature for the streptomycetes [6, 23]. However, the nature and characteristics of the enzymes of protease complex derived from streptomycetes have not been widely studied [6]. All the thermophilic bacterial extracellular proteases so far reported are, interestingly, serine or neutral metalloproteases [24].

Figure 1: Plate assay showing the zone of proteolytic activity by protease-producing *Streptomyces flavogriseus* HS1 strain.

3.4. Effect of the pH on Activity and Stability of Streptomyces flavogriseus HS1 Extracellular Proteases. The pH profile of protease activity from *Streptomyces flavogriseus* HS1 is shown in Figure 4(a). The crude enzyme was highly active between pH 6.0 and 8.0, having an optimum around pH 7.0. The relative activities at pH 6.0 and 8.0 were about 65 to 75%. Similar results were described for several *Streptomyces* strains in the literature with optimum pH range being between 6.0 and 12.0 [25]. The optimum pH activity of *Streptomyces flavogriseus* proteases was similar to that from other *Streptomyces* species, such as *Streptomyces griseus* pronase [26]. Therefore, this activity was lower than that of other *Streptomyces* described proteases, showing maximum activity at pH 8.0 like *Streptomyces* sp. DP2 [27] and *Streptomyces* sp. CN902 [28]. The pH stability test showed that the crude proteases were highly stable over a broad pH range, maintaining more than 70% of its original activity between pH 5.0 and 9.0 (Figure 4(b)).

3.5. Effect of Temperature on the Activity and Stability of Streptomyces flavogriseus HS1 Extracellular Proteases. The temperature profile of protease activity from *Streptomyces flavogriseus* HS1 is presented in Figure 5(a). The HS1 crude extract was active at temperatures from 30 to 70°C and had an optimum at 50°C, while activity decreased rapidly above 70°C. The relative activities at 40 and 60°C were about 63%

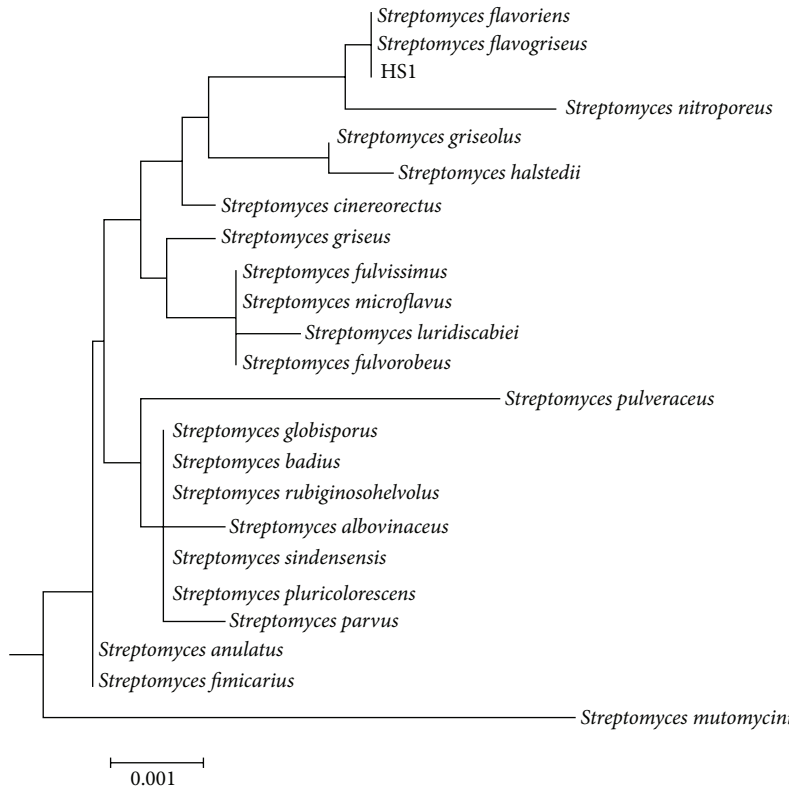

Figure 2: Dendrogram showing the relationships between *Streptomyces flavogriseus* HS1 and other *Streptomyces* species. Topology was inferred using the neighbour-joining method.

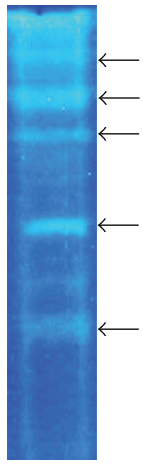

Figure 3: Zymography analysis of *Streptomyces flavogriseus* HS1 crude extracellular proteases.

and 60%, respectively. Several actinomycete thermophilic proteases, with high activity at 70°C, have been reported for *Thermoactinomyces vulgaris* and *Nocardiopsis dassonvillei*, *S. corchorusii* [23], *S. megasporus* [29], *S. thermovulgaris* [4], and *S. thermoviolaceus* [7]. Above 60°C, protease activity from *Streptomyces flavogriseus* HS1 rapidly fell, as shown for proteases of *Streptomyces* spp. and other bacteria.

The thermal stability profile of the crude enzyme showed a high stability at temperatures below 40°C but was inactivated at higher temperatures (Figure 5(b)). After 45 min of incubation at 60°C, 78% of the initial activity was lost. *Streptomyces flavogriseus* HS1 proteases were stable at 40 and 50°C after 1 h incubation. At low temperatures (−20 and 4°C), the crude enzyme preparation retained 75% of its activity after 2 months. El-Raheem et al. [23] observed that for alkaline proteases from a strain of *S. corchorusii*, activity did not decrease after storage at −20°C for one year, at pH values between 4.0 and 12.0, and repeated freezing and thawing.

3.6. Effects of Metal Ions. The effects of some metal ions, at a concentration of 5 mM, on the activity of *Streptomyces flavogriseus* HS1 crude enzyme were studied at pH 7.0 and 50°C by the addition of the respective cations to the reaction mixture (Table 2). The Ca^{2+}, Mg^{2+}, and Na^{+} were shown to have no effect on the protease activity. The latter was slightly affected by Ba^{2+} and K^{+} and it retains about 79.1% and 66.6% of its activity, respectively. The Hg^{2+}, Cu^{2+}, and Zn^{2+} greatly affected the enzymatic activity till the total inhibition. Reduction in protease activity of *Streptomyces* spp. has been previously observed [30, 31], especially for Cu^{2+}, probably as a result of the denaturing action of copper [31] and the chelating effect of EDTA. Proteases from *Streptomyces* spp. and *N. dassonvillei* were also stimulated by Mg^{2+}, Mn^{2+}, Ca^{2+}, and Zn^{2+} [30], whereas cation-requiring proteases

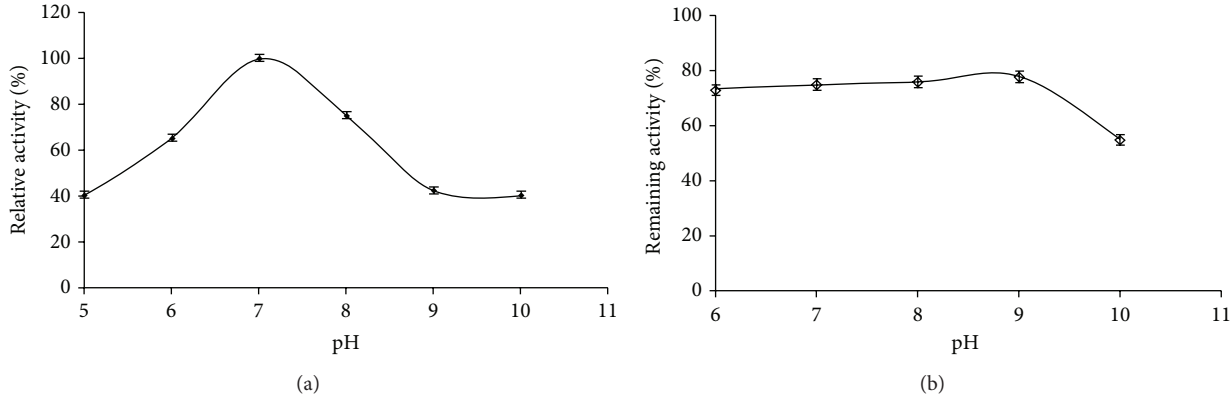

Figure 4: Effect of pH on activity (a) and stability (b) of the crude protease from *Streptomyces flavogriseus* HS1. The protease activity was assayed in the pH range of 5.0–12.0 using buffers of different pH values at 50°C. The maximum activity obtained from pH 7.0 was considered as 100% activity. The pH stability of the *Streptomyces flavogriseus* HS1 crude enzyme was assayed in the rage of 5.0–12.0 and determined by incubating the crude protease in different buffers for 1 h at 25°C and the residual activity was determined at pH 7.0 and 50°C. The proteolytic activity before incubation was taken as 100%.

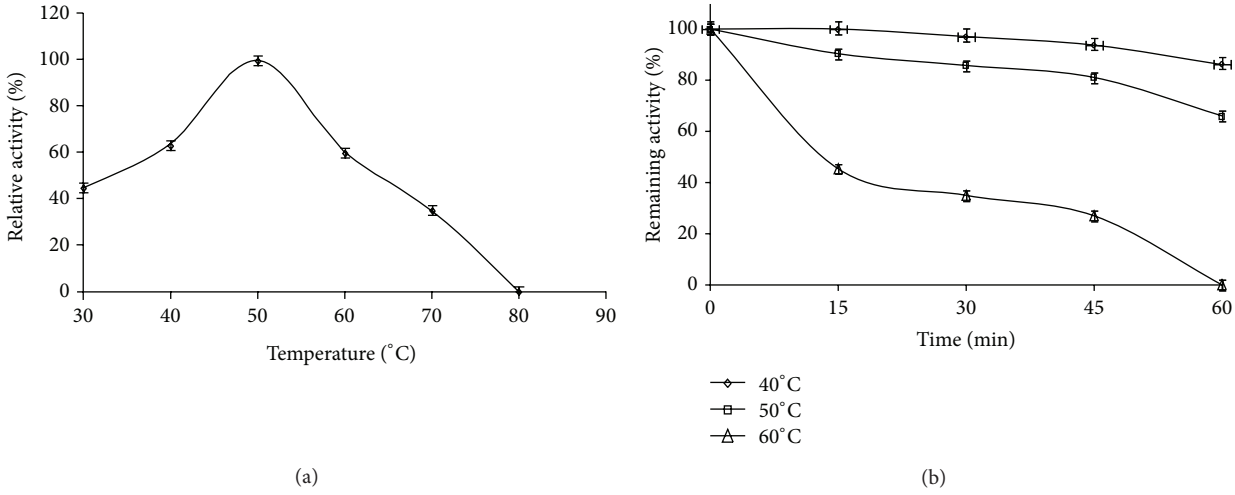

Figure 5: Effect of temperature on activity (a) and stability (b) of the crude protease from *Streptomyces flavogriseus* HS1. The temperature profile was determined by assaying protease activity at temperatures between 30 and 80°C. The activity of the crude enzyme at 50°C was taken as 100%. The temperature stability was determined by incubating *Streptomyces flavogriseus* HS1 crude enzyme at temperatures from 40 to 60°C for 1 h. The residual proteolytic activity was determined at regular intervals under standard assay conditions. The original activity before preincubation was taken as 100%.

from streptomycetes have also been reported [32]. However, *Streptomyces* sp. 594 protease stability was enhanced only by Ca^{2+} and Ba^{2+} [33]. It was shown that the Ca^{2+} ions are important for catalysis. James et al. [7] suggested that most probably they stabilize the protein through specific or nonspecific binding sites and may also allow for additional bonding within the enzyme molecule, preventing unfolding at higher temperatures, as has been demonstrated for protease from thermophilic bacteria, mainly thermolysin.

3.7. Effects of Enzyme Inhibitors on Protease Activity. Proteases can be classified by their sensitivity to various inhibitors [34]. In order to confirm the nature of the extracellular proteases, the effects of different enzyme inhibitors, such as chelating agent and a specific group of reagents, on the protease activity were investigated (Table 3). The crude proteolytic preparation was strongly inhibited by the serine protease inhibitor (PMSF) indicating that the HS1 crude extract contained serine proteases. In addition, the enzymatic extract was also inhibited by the chelating agent EDTA (5 mM), with 77% of its original activity being lost, indicating the importance of ions in enzyme stabilization. These findings are in line with several earlier reports showing that active structure of serine proteases contains Ca^{2+} binding site(s) and the removal of Ca^{2+} from the strong binding site is associated with a significant reduction in thermal stability [35]. From this result, HS1 can contain serine metalloproteases since the crude enzyme is strongly inhibited by both PMSF and EDTA.

Table 2: Effect of various metal ions (5 mM) on the activity of crude enzyme from *Streptomyces flavogriseus* HS1.

Ions (5 mM)	None	Ca^{2+}	Mg^{2+}	Fe^{2+}	Mn^{2+}	Cu^{2+}	Ba^{2+}	Hg^{2+}	Na^{+}	K^{+}
Relative activity (%)	100	100	100	71	100	0	79	0	100	67

The activity of the proteases was determined by incubating the enzyme in the presence of various metal ions for 10 min at 50°C and pH 7.0.

Table 3: Effect of various enzyme inhibitors (5 mM) on the activity of extracellular proteases from *Streptomyces flavogriseus* HS1.

Inhibitors	Remaining activity (%)
None	100
PMSF	5
EDTA	23

The secreted proteases from *Streptomyces flavogriseus* HS1 were preincubated with various enzyme inhibitors for 30 min at room temperature and the remaining activity was determined at pH 7.0 and 50°C. Crude protease activity measured in the absence of any inhibitor was taken as 100%.

Table 4: Stability of the *Streptomyces flavogriseus* HS1 extracellular proteases in the presence of various surfactants and oxidizing agents.

Detergents	Concentrations (%)	Remaining activity (%)
Triton X-100	1%	61.4
	5%	40.5
Tween 80	1%	71.4
	5%	40.5
Tween 20	1%	70.2
	5%	37.8
SDS	0.1%	18.9
	0.5%	0
Sodium perborate	0.1%	64.1
	1%	39.8
H_2O_2	0.1%	61.4
	0.5%	58.7

The crude extracellular proteases were incubated with different surfactants and oxidizing agents for 1 h at 25°C and the remaining activity was measured under standard conditions. The activity is expressed as a percentage of the activity level in the absence of additives.

3.8. Effects of Oxidizing Agents and Surfactants on Protease Stability. In order to be effective during washing, a good detergent protease must be compatible and stable with all commonly used detergent compounds such as surfactants, oxidizing agents, and other additives, which might be present in the detergent formulation [29, 30]. HS1 protease extract was preincubated 60 min at 25°C in the presence of SDS, Tween 20 and 80, and Triton X-100 and the residual activities were assayed at pH 7.0 and 50°C (Table 4). Interestingly, the *Streptomyces flavogriseus* HS1 proteases were less stable against the strong anionic surfactant (SDS) and retained only 19% of its activity in the presence of 0.1% (w/v) SDS. However, HS1 protease activity was little influenced by oxidizing agents and retained 64.1% and 39.8% of its activity after incubation for 1 h at 25°C in the presence of 0.1% and 1% sodium perborate, respectively (Table 4). The stability of the enzyme in the presence of oxidizing agents is a very important characteristic for its eventual use in detergent formulations.

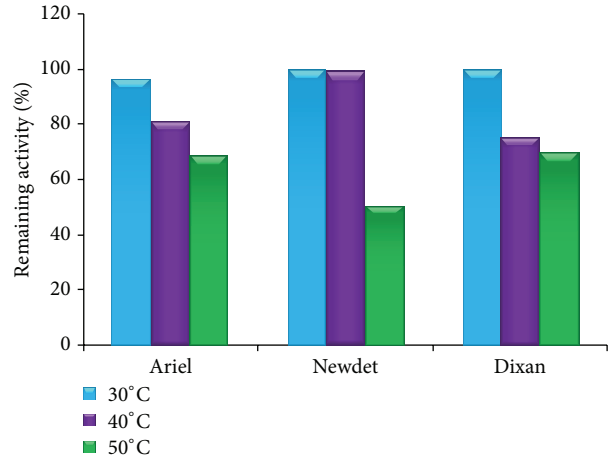

Figure 6: Stability of crude protease from *Streptomyces flavogriseus* HS1 in the presence of various commercial solid detergents. The enzyme at 100 U/mL was incubated 1 h at 30°C, 40°C, and 50°C in the presence of solid detergents. The remaining activities were determined at pH 7.0 and 50°C using casein as a substrate. Enzyme activity of control sample without any detergent, incubated under the similar conditions, was taken as 100%.

Important commercial detergent proteases like Subtilisin Carlsberg, Subtilisin BPN′, Alcalase, Esparase, and Savirase are stable in the presence of various detergent components. However, most are unstable in the presence of oxidant agents, such as hydrogen peroxide [36].

3.9. Stability of the Streptomyces flavogriseus HS1 Proteases with Commercial Solid Detergents. The high activity and stability of the *Streptomyces flavogriseus* HS1 proteases in the pH range 5.0–10.0 and their relative stability towards surfactants and oxidizing agents are very useful for its eventual application as a detergent additive. To check the compatibility of the proteases with solid detergents, the crude enzyme was preincubated in the presence of various commercial laundry solid detergents for 1 h at different temperatures (30, 40, and 50°C) (Figure 6). The data showed that the proteases were stable in Ariel and Dixan, retaining 70% of their activity at 50°C. The obtained results clearly indicated that the performance of enzymes in detergents depends on number of factors, including the detergents compounds since the proteolytic stability of HS1 proteases varied with each laundry tested detergent.

Singh et al. [37] reported that the alkaline protease from *Bacillus* sp. SSR1 retained 37% of its initial activity after 1 h incubation at 40°C in the presence of Ariel at a concentration of 5 mg/mL. Alkaline protease from *Conidiobolus coronatus* retained only 16% activity in Revel, 11.4% activity in Ariel,

and 6.6% activity in Wheel at 50°C, in the presence of 25 mM $CaCl_2$ [38].

4. Conclusion

This work describes the isolation of an actinomycete strain identified as *Streptomyces flavogriseus* HS1, which produces at least five proteases as described by zymogram technique. Crude protease was shown to have optimum activity at pH 7 and 50°C. The crude enzyme has a good stability toward the oxidizing agents and was found to be useful as a detergent additive.

Conflict of Interests

The authors declare that there is no conflict of interests regarding the publication of this paper.

Acknowledgment

This work was funded by the Ministry of Higher Education and Scientific Research, Tunisia.

References

[1] H. Tsujibo, K. Miyamoto, T. Hasegawa, and Y. Inamori, "Purification and characterization of two types of alkaline serine proteases produced by an alkalophilic actinomycete," *Journal of Applied Bacteriology*, vol. 69, no. 4, pp. 520–529, 1990.

[2] W. Peczynska-Czoch, "Actinomycete enzymes," in *Actinomycetes in Biotechnology*, pp. 219–283, Academic Press, London, 1988.

[3] M. B. Rao, A. M. Tanksale, M. S. Ghatge, and V. V. Deshpande, "Molecular and biotechnological aspects of microbial proteases," *Microbiology and Molecular Biology Reviews*, vol. 62, no. 3, pp. 597–635, 1998.

[4] K. H. Yeoman and C. Edwards, "Protease production by *Streptomyces thermovulgaris* grown on rapemeal-derived media," *Journal of Applied Bacteriology*, vol. 77, no. 3, pp. 264–270, 1994.

[5] M. Pokorny, L. Vitale, V. Turk, M. Renko, and J. Žuvanić, "*Streptomyces rimosus* extracellular proteases-1. Characterization and evaluation of various crude preparations," *European Journal of Applied Microbiology and Biotechnology*, vol. 8, no. 1-2, pp. 81–90, 1979.

[6] S. Chandrasekaran and S. C. Dhar, "Multiple proteases from Streptomyces moderatus. II. Physicochemical and enzymatic properties of the extracellular proteases," *Archives of Biochemistry and Biophysics*, vol. 257, no. 2, pp. 402–408, 1987.

[7] P. D. A. James, M. Iqbal, C. Edwards, and P. G. G. Miller, "Extracellular protease activity in antibiotic-producing Streptomyces thermoviolaceus," *Current Microbiology*, vol. 22, no. 6, pp. 377–382, 1991.

[8] T. Muro, T. Murakami, Y. Tominaga, T. Tokuyama, and S. Okada, "Purification and some properties of protease I having transfer action from Streptomyces griseus var. alcalophilus," *Agricultural and Biological Chemistry*, vol. 55, no. 2, pp. 307–314, 1991.

[9] V. K. Antonov, *Chemistry of Proteolysis*, Springer, New York, NY, USA, 1993.

[10] K. Kitadokoro, H. Tsuzuki, E. Nakamura, T. Sato, and H. Teraoka, "Purification, characterization, primary structure, crystallization and preliminary crystallographic study of a serine proteinase from Streptomyces fradiae ATCC 14544," *European Journal of Biochemistry*, vol. 220, no. 1, pp. 55–61, 1994.

[11] J. Thumar and S. P. Singh, "Two-step purification of a highly thermostable alkaline protease from salt-tolerant alkaliphilic Streptomyces clavuligerus strain Mit-1," *Journal of Chromatography B: Analytical Technologies in the Biomedical and Life Sciences*, vol. 854, no. 1-2, pp. 198–203, 2007.

[12] A. S. Rana, I. S. Rana, and L. Yadav, "Alkaline proteases from Streptomyces viridifaceins and its application with detergents," *Advanced Biotechnology*, vol. 10, no. 4, pp. 10–14, 2010.

[13] S. G. Dastager, A. Dayanand, W.-J. Li et al., "Proteolytic activity from an alkali-thermotolerant Streptomyces gulbargensis sp. nov," *Current Microbiology*, vol. 57, no. 6, pp. 638–642, 2008.

[14] M. K. Kharel, M. D. Shepherd, S. E. Nybo, M. L. Smith, M. A. Bosserman, and J. Rohr, "Isolation of Streptomyces species from soil," *Current Protocols in Microbiology*, no. 19, Article ID 10E.4, 2010.

[15] J. D. Thompson, D. G. Higgins, and T. J. Gibson, "CLUSTAL W: improving the sensitivity of progressive multiple sequence alignment through sequence weighting, position-specific gap penalties and weight matrix choice," *Nucleic Acids Research*, vol. 22, no. 22, pp. 4673–4680, 1994.

[16] N. Saitou and M. Nei, "The neighbor-joining method: a new method for reconstructing phylogenetic trees," *Molecular Biology and Evolution*, vol. 4, no. 4, pp. 406–425, 1987.

[17] A. A. Kembhavi, A. Kulkarni, and A. Pant, "Salt-tolerant and thermostable alkaline protease from Bacillus subtilis NCIM No. 64," *Applied Biochemistry and Biotechnology*, vol. 38, no. 1-2, pp. 83–92, 1993.

[18] W.-J. Chi, J.-H. Song, E. A. Oh et al., "Medium optimization and application of affinity column chromatography for trypsin production from recombinant Streptomyces griseus," *Journal of Microbiology and Biotechnology*, vol. 19, no. 10, pp. 1191–1196, 2009.

[19] F. L. Garcia-Carreno, L. E. Dimes, and N. F. Haard, "Substrate-gel electrophoresis for composition and molecular weight of proteinases or proteinaceous proteinase inhibitors," *Analytical Biochemistry*, vol. 214, no. 1, pp. 65–69, 1993.

[20] W. P. Chen, A. W. Anderson, and Y. W. Han, "Extraction of glucose isomerase from Streptomyces flavogriseus," *Applied and Environmental Microbiology*, vol. 37, no. 4, pp. 785–787, 1979.

[21] R. Srivastava, S. S. Ali, and B. S. Srivastava, "Cloning of xylanase gene of Streptomyces flavogriseus in Escherichia coli and bacteriophage λ-induced lysis for the release of cloned enzyme," *FEMS Microbiology Letters*, vol. 78, no. 2-3, pp. 201–205, 1991.

[22] G. D. Gibb and W. R. Strohl, "Physiological regulation of protease activity in Streptomyces peucetius," *Canadian Journal of Microbiology*, vol. 34, no. 2, pp. 187–190, 1988.

[23] A. El-Raheem, R. El-Shanshoury, M. A. El-Sayed, R. H. Sammour, and W. A. El-Shouny, "Purification and partial characterization of two extracellular alkaline proteases from *Streptomyces corchorusii* ST36," *Canadian Journal of Microbiology*, vol. 41, no. 1, pp. 99–104, 1995.

[24] D. Cowan, R. Daniel, and H. Morgan, "Thermophilic proteases: properties and potential applications," *Trends in Biotechnology*, vol. 3, no. 3, pp. 68–72, 1985.

[25] P. Sampath, C. Subramanian, and G. Chandrakasan, "Extracellular proteases from streptomyces spp. G157: purification and

characterization," *Biotechnology and Applied Biochemistry*, vol. 26, no. 2, pp. 85–90, 1997.

[26] M. Trop and Y. Birk, "The specificity of proteinases from Streptomyces griseus (pronase)," *Biochemical Journal*, vol. 116, no. 1, pp. 19–25, 1970.

[27] B. K. Bajaj and P. Sharma, "An alkali-thermotolerant extracellular protease from a newly isolated Streptomyces sp. DP2," *New Biotechnology*, vol. 28, no. 6, pp. 725–732, 2011.

[28] H. Lazim, H. Mankai, N. Slama, I. Barkallah, and F. Limam, "Production and optimization of thermophilic alkaline protease in solid-state fermentation by Streptomyces sp. CN902," *Journal of Industrial Microbiology and Biotechnology*, vol. 36, no. 4, pp. 531–537, 2009.

[29] D. Patke and S. Dey, "Proteolytic activity from a thermophilic Streptomyces megasporus strain SDP4," *Letters in Applied Microbiology*, vol. 26, no. 3, pp. 171–174, 1998.

[30] W. Aretz, K. P. Koller, and G. Riess, "Proteolytic enzymes from recombinant Streptomyces lividans TK24," *FEMS Microbiology Letters*, vol. 65, no. 1-2, pp. 31–35, 1989.

[31] N. S. Demina and S. V. Lysenko, "Exoproteases of *Streptomyces lavendulae*," *Microbiology*, vol. 64, no. 4, pp. 385–387, 1995.

[32] V. Bascarán, C. Hardisson, and A. F. Braña, "Regulation of extracellular protease production in Streptomyces clavuligerus," *Applied Microbiology and Biotechnology*, vol. 34, no. 2, pp. 208–213, 1990.

[33] L. A. I. de Azeredo, M. B. de Lima, R. R. R. Coelho, and D. M. G. Freire, "A low-cost fermentation medium for thermophilic protease production by Streptomyces sp. 594 using feather meal and corn steep liquor," *Current Microbiology*, vol. 53, no. 4, pp. 335–339, 2006.

[34] M. J. North, "Comparative biochemistry of the proteinases of eucaryotic microorganisms," *Microbiological Reviews*, vol. 46, no. 3, pp. 308–340, 1982.

[35] R. Oberoi, Q. K. Beg, S. Puri, R. K. Saxena, and R. Gupta, "Characterization and wash performance analysis of an SDS-stable alkaline protease from a Bacillus sp," *World Journal of Microbiology and Biotechnology*, vol. 17, no. 5, pp. 493–497, 2001.

[36] R. Gupta, K. Gupta, R. K. Saxena, and S. Khan, "Bleach-stable, alkaline protease from *Bacillus sp*," *Biotechnology Letters*, vol. 21, no. 2, pp. 135–138, 1999.

[37] J. Singh, N. Batra, and R. C. Sobti, "Serine alkaline protease from a newly isolated Bacillus sp. SSR1," *Process Biochemistry*, vol. 36, no. 8-9, pp. 781–785, 2001.

[38] S. H. Bhosale, M. B. Rao, V. V. Deshpande, and M. C. Srinivasan, "Thermostability of high-activity alkaline protease from Conidiobolus coronatus (NCL 86.8.20)," *Enzyme and Microbial Technology*, vol. 17, no. 2, pp. 136–139, 1995.

Hindawi Publishing Corporation
BioMed Research International
Volume 2014, Article ID 438787, 7 pages
http://dx.doi.org/10.1155/2014/438787

Research Article

A Noncellulosomal Mannanase26E Contains a CBM59 in *Clostridium cellulovorans*

Kosuke Yamamoto[1] and Yutaka Tamaru[1,2,3]

[1] *Department of Life Sciences, Graduate School of Bioresources, Mie University, 1577 Kurimamachiya, Tsu, Mie 514-8507, Japan*
[2] *Graduate School of Bioresources, Department of Bioinfomatics, Mie University Life Science Research Center, Mie University, 1577 Kurimamachiya, Tsu, Mie 514-8507, Japan*
[3] *Laboratory of Applied Biotechnology, Mie University Industrial Technology Innovation Institute, Mie University, 1577 Kurimamachiya, Tsu, Mie 514-8507, Japan*

Correspondence should be addressed to Yutaka Tamaru; ytamaru@bio.mie-u.ac.jp

Received 12 December 2013; Accepted 18 February 2014; Published 27 March 2014

Academic Editor: Sofiane Ghorbel

A multicomponent enzyme-complex prevents efficient degradation of the plant cell wall for biorefinery. In this study, the method of identifying glycoside hydrolases (GHs) to degrade hemicelluloses was demonstrated. The competence of *C. cellulovorans*, which changes to be suitable for degradation of each carbon source, was used for the method. *C. cellulovorans* was cultivated into locust bean gum (LBG) that is composed of galactomannan. The proteins produced by *C. cellulovorans* were separated into either fractions binding to crystalline cellulose or not. Proteins obtained from each fraction were further separated by SDS-PAGE and were stained with Coomassie Brilliant Blue and were detected for mannanase activity. The proteins having the enzymatic activity for LBG were cut out and were identified by mass spectrometry. As a result, four protein bands were classified into glycosyl hydrolase family 26 (GH26) mannanases. One of the identified mannanases, Man26E, contains a carbohydrate-binding module (CBM) family 59, which binds to xylan, mannan, and Avicel. Although mannose and galactose are the same as a hexose, the expression patterns of the proteins from *C. cellulovorans* were quite different. More interestingly, zymogram for mannanase activity showed that Man26E was detected in only LBG medium.

1. Introduction

The plant cell wall is composed of cellulose, hemicelluloses, and lignin. The formation of plant cell wall prevents a biomass saccharification for biorefinery [1]. Since hemicellulose was composed of various sugar chains such as glucose, xylose, galactose, mannose, and arabinose, the degradation of plant cell wall needed various and different kinds of enzymes [2]. β-mannanase mainly produces mannose to degrade galactomannan or glucomannan. Galactomannan, which is a main component in locust bean gum (LBG), is composed of β-(1-4)-D-mannopyranoside chain attached with α-D-galactose (Figure 1).

C. cellulovorans, which is an anaerobic mesophile [3], has an ability to degrade plant-biomass directly to produce a multienzyme complex called the "cellulosome" [4–8]. Genomic analysis revealed that this organism not only has 17 cellulosomal cellulases and 10 cellulosomal hemicellulases, but it also has 63 noncellulosomal enzymes related to polysaccharides degradation [9, 10]. In addition, members of cellulosomal subunits are changed to suitable and target substrates [11–14]. Thus, the method of functional protein evaluation is the best way to identify the enzymes for degrading each carbohydrate substrates. In this study, we identified several mannanases from *C. cellulovorans* for degrading LBG using functional protein evaluation and genomic data. In addition, we report that one of the identified mannanase 26E (Man26E) contains a carbohydrate-binding module (CBM) family 59.

2. Materials and Methods

2.1. Bacterial Strains and Media. The proteins used in proteomic and comparative analyses were produced by *C. cellulovorans* 743B. This organismwas grown under strictly anaerobic conditions at 37°C in medium containing 0.5%

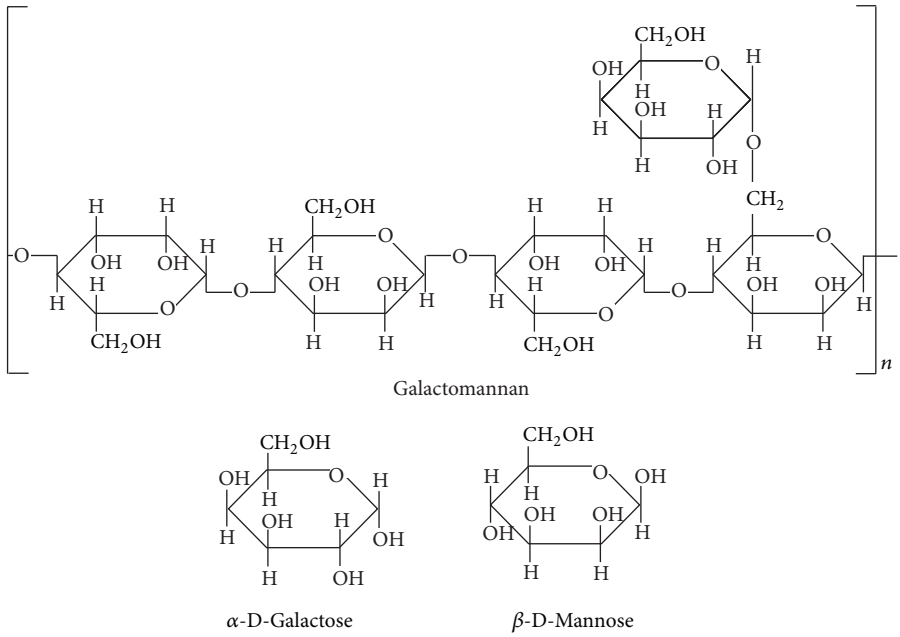

Figure 1: Structural formulas for galactomannan and component sugars. Galactomannan is a polysaccharide consisting of a mannose backbone with galactose side chains: the ratio of mannose : galactose is 4 : 1.

(w/v) glucose, mannose, galactose, or LBG as a carbon source [3].

2.2. Alignment of Amino Acid Sequences and Phylogenetic Trees. The databases used for sequencing data are as follows: NCBI (http://www.ncbi.nlm.nih.gov/), GenomeNet (http://www.genome.jp/), and CAZy (http://www.cazy.org/). The Clustal program [15] was used to carry out alignments of amino acid sequences.

2.3. Protein Production and Purification. The culture supernatants in *C. cellulovorans* were centrifuged and the supernatant was collected. The proteins in the supernatant were precipitated by dissolving ammonium sulfate and the precipitate was dissolved in 50 mM acetate buffer (pH 6.0). The solution was dialyzed at 4°C for three hours. This solution was used as a total protein fraction. Crystalline cellulose (Avicel) was added to a 1-mL aliquot and incubated at 4°C for 1 hour. The mixture was centrifuged and the supernatant was used as a nonbound fraction. The pellets binding to Avicel were washed twice by the same buffer at 4°C and were centrifuged. After the supernatant was removed, the pellets binding to Avicel were washed by distilled water at 25°C. The supernatant was used as a bound fraction. The concentration of proteins was determined with bovine serum albumin as a standard using protein assay kit (BIO-RAD).

2.4. Zymogram. The zymogram for mannanase activity was performed with 7.5% (w/v) polyacrylamide gel containing 0.07% (w/v) LBG. After SDS-PAGE was performed, the gels were soaked into 25% isopropanol at room temperature for 6 h. The gels were washed for 20 min with 50 mM acetate buffer (pH 6.0) and were incubated at 37°C for 1 hour in the same buffer. Next, the gels were stained with 0.2% (w/v) Congo red solution for 20 min. The stained gels were destained by 1 M NaCl several times until white halos emerge.

2.5. Functional Protein Evaluation. The purified proteins were separated by SDS-PAGE and were stained by Coomassie brilliant blue (CBB) and for mannanase activity. The selected 5 bands, which were observed by mannanase activity with zymogram, were cut out. The pieces of gels containing protein(s) were alkylated and digested by trypsin (Figure 2). The digested products by typsin were separated to 119 aliquots by nano-LC and the aliquots were analyzed by mass spectrums (MS). The proteins containing the aliquots were identified to compare amino acid sequences. The resulted analysis was performed with genomic data using Mascot software (MATRIX SCIENCE).

3. Results and Discussion

3.1. Comparison of Man26E and Other GH Family 26 Mannanases in C. cellulovorans. According to *C. cellulovorans* genomic data, schematic models of GH family 26 mannanases are shown in Figure 2. Four GH26 mannanases (Man26A, Man26C, Man26D, and ManB) were identified into cellulosomal enzymes that have a dockerin domain at the C-terminus. In contrast, Man26E and Man26F were classified into noncellulosomal enzymes. The alignment of the catalytic domains among GH26 mannanases is shown in Figure 3(a). Based on amino acid sequences of the catalytic domains among them, phylogenetic trees of GH26 mannanases in *C. cellulovorans* are shown in Figure 3(b). Man26A, Man26C and Man5B [3] have carbohydrate-binding module 6 (CBM6)

Table 1: Identified mannanases by functional protein evaluation.

Band name	Accession number	GH family number	CBM family number	Dockerin	Name
LBGB1	YP_003845544.1	26	6	+	Man26A
LBGB1	YP_003844553.1	5	11	+	Man5B
LBGB3	YP_003844078.1	26	6	+	ManB
LBGB4	YP_003845549.1	26	59	−	Man26E
LBGN1	YP_003845549.1	26	59	−	Man26E

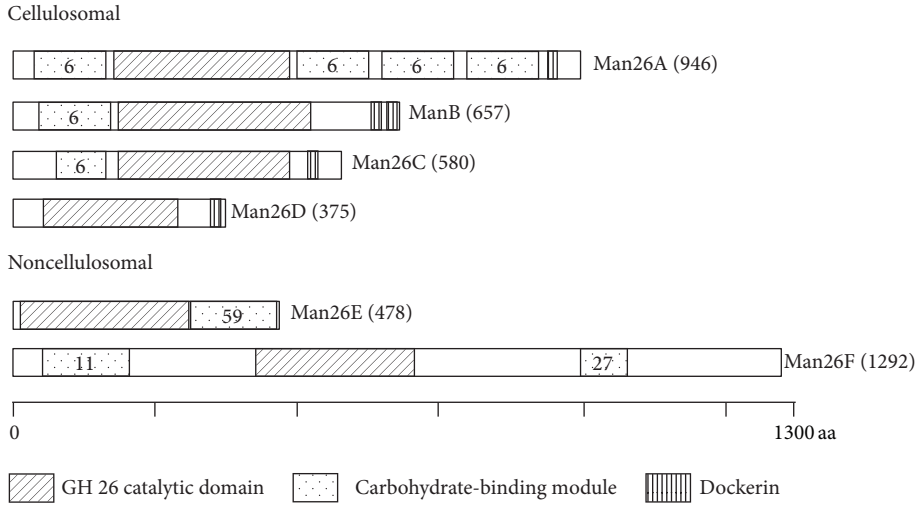

Figure 2: Schematic models for *C. cellulovorans* GH family 26 mannanases. Numbers in the model indicate CBM family number. Protein names are represented on the right side of the model. A length of amino acid sequence is in parentheses.

that were reported for binding amorphous cellulose and β-1,4-xylan. On the other hand, Man26F has a CBM11 binding of β-1,4-glucan and β-1,3-1,4-mixed linked glucans and a part of CBM27 binding to mannan, respectively. Putative catalytic base [16, 17], which is Glu-166 in Man26E, was conserved in all GH26 mannanases in *C. cellulovorans* (Figure 3(a)). Interestingly, phylogenetic tree indicated that Man26A, Man5B, and Man26C were closely located, while Man26D, Man26E, or Man26F was far from each other (Figure 3(b)). These results suggested that three genes encoding: Man26A, Man5B, and Man26C were close to each other because there enzymes are cellulosomal enzymes. Moreover, it is possible that the genes encoding Man26D, Man26E, and Man26F might be obtained from other organisms except *Clostridia*.

3.2. Functional Protein Evaluation and Induced Expression of Man26E Caused by the Difference of Carbon Source. Table 1 shows the identified mannanases by functional protein evaluation. The protein bands that are represented to LBGB1 and LBGB3 contained Man26A and ManB [18], respectively (Figure 4), while LBGB4 and LBGN1 contained Man26E. On the other hand, LBGB1 contained Eng5B (accession number: YP_003842513.1.) which belongs to GH5. More interestingly, all these enzymes except Eng5B in the LBG media had a GH26 region.

C. cellulovorans can be grown on glucose, mannose, galactose, or LBG. The proteins from the culture supernatants were subjected to SDS-PAGE. There was no difference of bands in all fractions between glucose and mannose as a hexose (Figure 5(a)). On the other hand, several different bands appeared between galactose and LBG in comparison with glucose and mannose. In particular, only few bands having mannanase activity were detected with galactose (Figure 5(b)). More interestingly, although LBG is comprised of mannose and galactose, Man26E band appeared in only LBG in all fractions.

3.3. Man26E Contains a CBM59. Amino acid sequence analysis indicated Man26E has a CBM59 at its C-terminal region (Figure 6). The homologies between 163 amino acid sequence of CBM59 in Man26E and the other amino acid sequences were, for example, as follows: 53% with mannan endo-1,4-beta-mannosidase A and B from *Paenibacillus mucilaginosus* 3016; 52% with glycoside hydrolase families 5 and 6 from *Paenibacillus polymyxa* SC2; 51% with mannanase from *Bacillus circulans*; 48% with beta-mannanase precursor from *Bacillus* sp. N16-5; 48% with mannanase from *Bacillus* sp. JAMB-602; 41% with xylanase from uncultured bacterium. Phylogenetic tree showed that there were no *Clostridia* possessing a CBM59 except for *C. cellulovorans* (Figure 7). All of 15 organisms (containing uncharacterized organisms) having a CBM59 were bacteria and firmicutes outside of *Herpetosiphon aurantiacus*, which is classified into chloroflexi. Interestingly, CBM59 of *C. cellulovorans* was most close to *H. aurantiacus* CBM59 between the evolutionary relationships (Figure 7). The xylanase ManF-X10

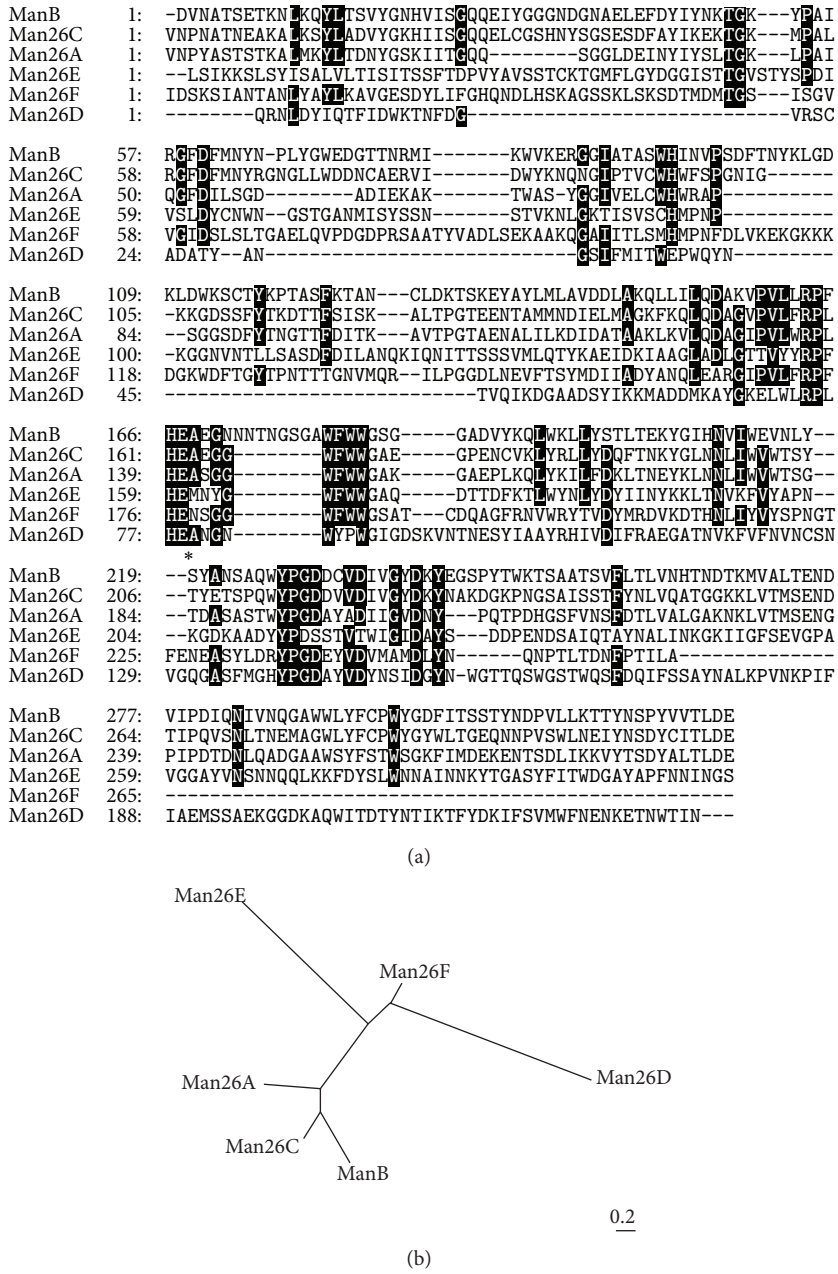

Figure 3: Alignment of catalytic domain of *C. cellulovorans* GH family 26 mannanases (a) and phylogenetic tree based on amino acid sequences of GH family 26 mannanases (b). An amino acid followed by an asterisk indicates the putative catalytic base. Phylogenetic tree was constructed by the neighbour-joining (NJ) method. Bar: 0.2 expected amino acid substitutions per site.

from uncultured bacterium sharing 41% identity with the C-terminal region of Man26E was demonstrated to bind ivory nut mannan, oat spelt xylan and Avicel [19]. However, it is suggested that the Avicel-bound activity of Man26E showed only nonbound fractions (Figures 4 and 5(b)). Furthermore, although Man26A, Man5B, and ManB were detected with an Avicel-bound fraction, Man26E was identified into a nonbound fraction (Figure 4 and Table 1). Putative aromatic residues of binding to the carbohydrate substrates were conserved in three-fourths of aromatic residues between ManF-X10 and Man26E (Figure 6). These results indicated that the affinity of CBM59 in Man26E to polysaccharides such as cellulose and hemicelluloses was weakened by deletion of aromatic amino acids.

Since CBM59 in Man26E binds to LBG and Avicel, Man26E could play a role on degradation of mannan attached to cellulose in the plant cell wall. These results in this study were strongly supported by previous studies that a high-synergistic effect was generated between the cellulosome and noncellulosomal enzymes [20]. For example, it is known that

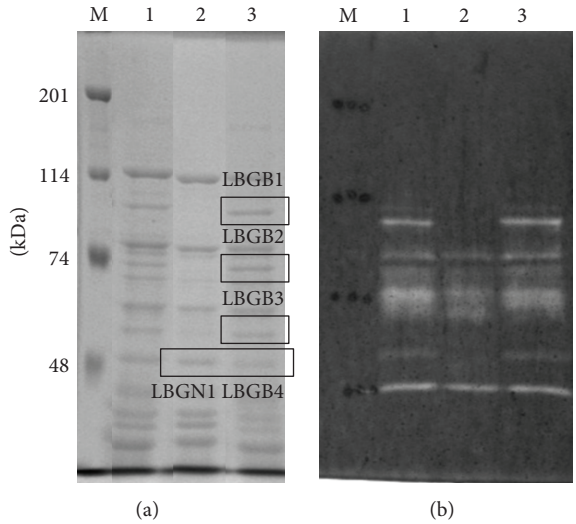

Figure 4: SDS-PAGE analysis (a) zymogram (b) of the proteins from *C. cellulovorans* grown on LBG. The protein bands in a square were cut out for functional protein evaluation. SDS-PAGE was performed with a 7.5% polyacrylamide gel. Zymogram was carried out with a 7.5% polyacrylamide gel containing 0.07% LBG. Lane M, protein molecular mass standards (molecular masses shown in the left); lane 1, total protein fraction; lane 2, Avicel-nonbound fraction; lane 3, Avicel-bound fraction.

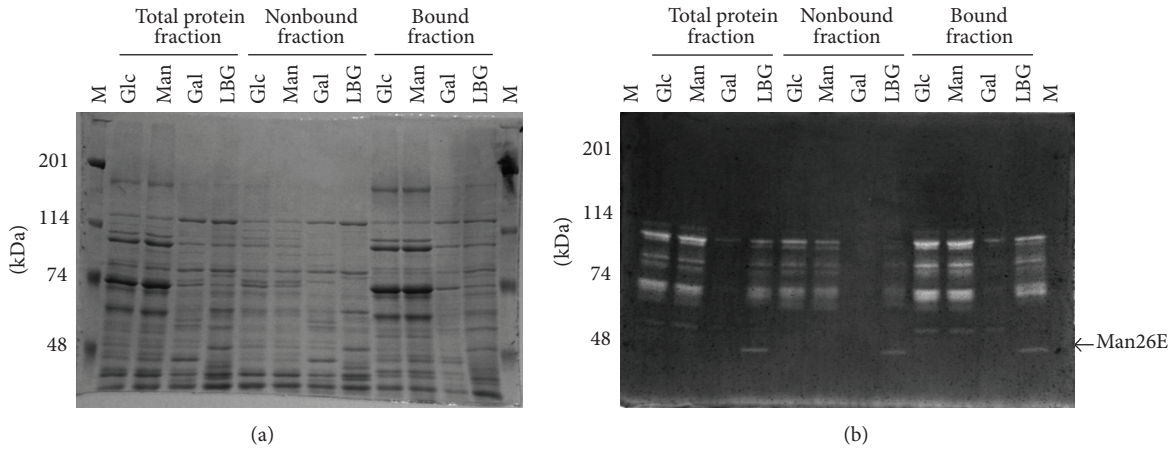

Figure 5: SDS-PAGE analysis of total, nonbound and bound fractions obtained from cells grown on different carbon sources. After electrophoreses, the gels were stained by Coomassie brilliant blue (a) and were detected for mannanase activity (b). M, protein molecular mass standard (molecular masses shown at the left); Glc, D-glucose; Man, D-mannose; Gal, D-galactose; LBG, Locust bean gum.

```
Man26E CBM      1:LLFTKSDSSATSSALT-K-YN-FENSNQGWVGNTNVIGPWSVNEWSDKGSYSLKGNITLS  57
ManF-X10 CBM    1:------GSTGGGGGTITSAYADFESGTEGWIGSNIVGGPWSTTAWSSKNTHSLQVDVAMS  54

Man26E CBM     58:SGTKYYLYNPISDNYSGYKTLKARVKVASWGNLGSGLTAKLYVKTGNSYTWYDGGSVIVN  117
ManF-X10 CBM   55:PNSQHTVSKIVNANFSAHTKLKATVHGSEWGGYGSGLGVKLFVKHGNAYTFTDSGWATIS  114
                                                  *      **
Man26E CBM     118:TSSTTLTLNLANIINTSQIKEVGVEFIGGSNSSGTSAIYVDNITLE-              163
ManF-X10 CBM   115:KSGTIDLTLDLTTVNAADIREYGIQFIDASNSSGQASVYVDNVYLSN               161
```

Figure 6: Alignment of CBMs in Man26E from *C. cellulovorans* and ManF-X10 from uncultured bacteria.**:** Aromatic amino acids that are estimated to bind carbohydrate substrates are marked with an asterisk.

the main scaffolding protein CbpA in the *C. cellulovorans* cellulosome binds to crystalline cellulose. Therefore, it is assumed that Man26E should be close to the cellulosome and could contribute to degrade the plant cell wall such as LBG with synergistic activity.

4. Conclusions

Man26E, which was one of the identified mannanases from the culture supernatant of *C. cellulovorans* by functional protein evaluation, was expressed only in LBG consisting

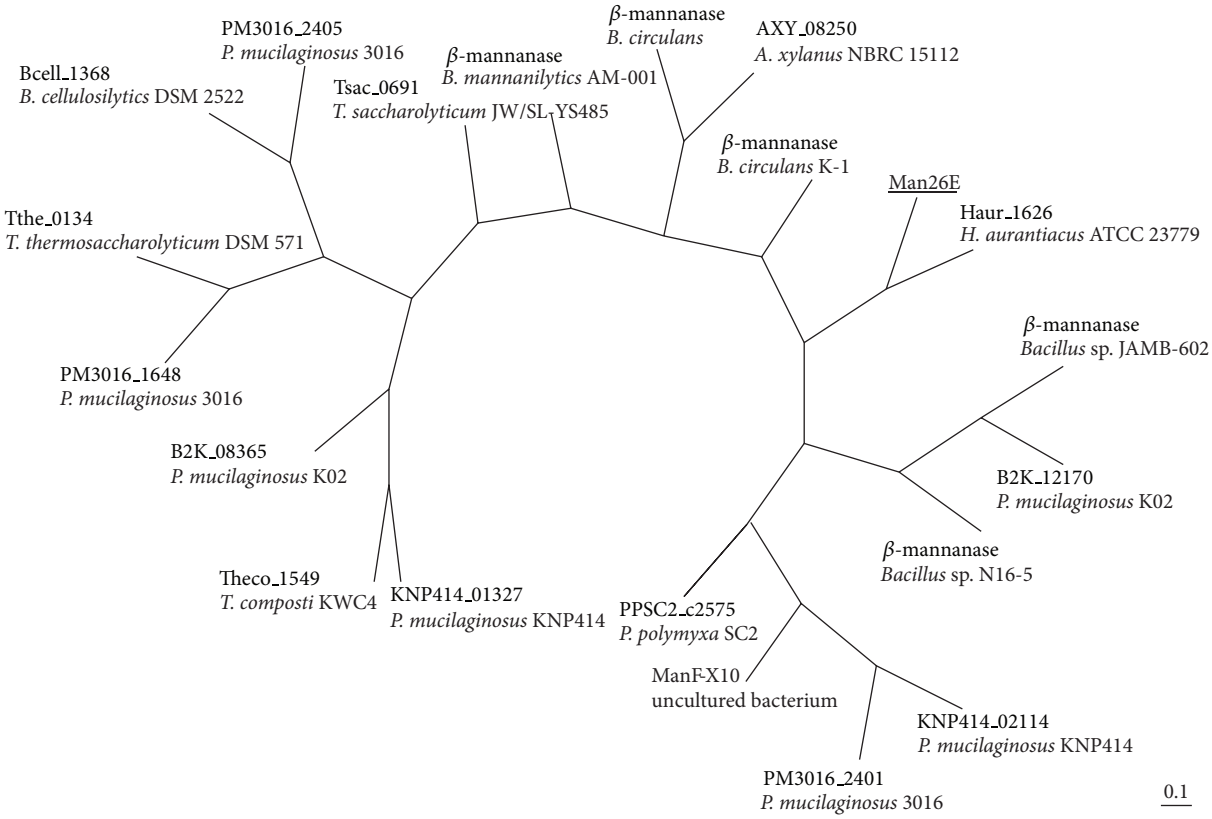

Figure 7: Phylogenetic trees based on amino acid sequences of CBM family 59. The tree was constructed by the neighbour-joining (NJ) method. Abbreviated generic name was described as follows: *Amphibacillus xylanus* NBRC 15112, *Bacillus cellulosilyticus* DSM 2522, *Bacillus circulans*, *Bacillus circulans* K-1, *Bacillus mannanilyticus, Herpetosiphon aurantiacus* ATCC, *Paenibacillus mucilaginosus* 3016, *Paenibacillus mucilaginosus* K02, *Paenibacillus mucilaginosus* KNP414, *Paenibacillus polymyxa* SC2, *Thermoanaerobacterium saccharolyticum* JW/SL-YS485, *Thermoanaerobacterium thermosaccharolyticum* DSM 571, and *Thermobacillus composti* KWC4. Bar: 0.1 expected amino acid substitutions per site.

of mannose and galactose, whereas it was not induced into glucose, mannose, or galactose. The alignment of CBM59 in Man26E revealed that aromatic amino acids were highly conserved and estimated to bind carbohydrate substrates. This is the first report that Man26E in *C. cellulovorans* contains a CBM59 which has never been found in *Clostridia*.

Conflict of Interests

The authors declare that there is no conflict of interests regarding the publication of this paper.

Acknowledgments

This research was in part supported by Japan Society for Bioscience, Biotechnology, and Agrochemistry and the Sumitomo Foundation for Environmental Research.

References

[1] L. R. Lynd, P. J. Weimer, W. H. van Zyl, and I. S. Pretorius, "Microbial cellulose utilization: fundamentals and biotechnology," *Microbiology and Molecular Biology Reviews*, vol. 66, no. 3, pp. 506–577, 2002.

[2] L. R. Lynd, C. E. Wyman, and T. U. Gerngross, "Biocommodity engineering," *Biotechnology Progress*, vol. 15, no. 5, pp. 777–793, 1999.

[3] R. Sleat, R. A. Mah, and R. Robinson, "Isolation and characterization of an anaerobic, cellulolytic bacterium, *Clostridium cellulovorans* sp. nov," *Applied and Environmental Microbiology*, vol. 48, no. 1, pp. 88–93, 1984.

[4] R. H. Doi, M. Goldstein, S. Hashida, J.-S. Park, and M. Takagi, "The *Clostridium cellulovorans* cellulosome," *Critical Reviews in Microbiology*, vol. 20, no. 2, pp. 87–93, 1994.

[5] R. H. Doi and Y. Tamaru, "The *Clostridium cellulovorans* cellulosome: an enzyme complex with plant cell wall degrading activity," *Chemical Records*, vol. 1, no. 1, pp. 24–32, 2001.

[6] M. A. Goldstein, M. Takagi, S. Hashida, O. Shoseyov, R. H. Doi, and I. H. Segel, "Characterization of the cellulose-binding domain of the *Clostridium cellulovorans* cellulose-binding protein A," *Journal of Bacteriology*, vol. 175, no. 18, pp. 5762–5768, 1993.

[7] O. Shoseyov, M. Takagi, M. A. Goldstein, and R. H. Doi, "Primary sequence analysis of *Clostridium cellulovorans* cellulose binding protein A," *Proceedings of the National Academy of Sciences of the United States of America*, vol. 89, no. 8, pp. 3483–3487, 1992.

[8] M. Takagi, S. Hashida, M. A. Goldstein, and R. H. Doi, "The hydrophobic repeated domain of the *Clostridium cellulovorans*

cellulose-binding protein (CbpA) has specific interactions with endoglucanases," *Journal of Bacteriology*, vol. 175, no. 21, pp. 7119–7122, 1993.

[9] Y. Tamaru, H. Miyake, K. Kuroda et al., "Genome sequence of the cellulosome-producing mesophilic organism *Clostridium cellulovorans* 743B," *Journal of Bacteriology*, vol. 192, no. 3, pp. 901–902, 2010.

[10] Y. Tamaru, H. Miyake, K. Kuroda et al., "Comparison of the mesophilic cellulosome-producing *Clostridium cellulovorans* genome with other cellulosome-related clostridial genomes," *Microbial Biotechnology*, vol. 4, no. 1, pp. 64–73, 2011.

[11] S. O. Han, H. Yukawa, M. Inui, and R. H. Doi, "Effect of carbon source on the cellulosomal subpopulations of *Clostridium cellulovorans*," *Microbiology*, vol. 151, no. 5, pp. 1491–1497, 2005.

[12] S. O. Han, H. Yukawa, M. Inui, and R. H. Doi, "Regulation of expression of cellulosomal cellulase and hemicellulase genes in *Clostridium cellulovorans*," *Journal of Bacteriology*, vol. 185, no. 20, pp. 6067–6075, 2003.

[13] H. Morisaka, K. Matsui, Y. Tatsukami et al., "Profile of native cellulosomal proteins of *Clostridium cellulovorans* adapted to various carbon sources," *AMB Express*, vol. 2, article 37, 2012.

[14] Y. Tamaru, S. Ui, K. Murashima et al., "Formation of protoplasts from cultured tobacco cells and Arabidopsis thaliana by the action of cellulosomes and pectate lyase from *Clostridium cellulovorans*," *Applied and Environmental Microbiology*, vol. 68, no. 5, pp. 2614–2618, 2002.

[15] M. A. Larkin, G. Blackshields, N. P. Brown et al., "Clustal W and Clustal X version 2.0," *Bioinformatics*, vol. 23, no. 21, pp. 2947–2948, 2007.

[16] D. N. Bolam, N. Hughes, R. Virden et al., "Mannanase A from *Pseudomonas fluorescens* ssp. cellulosa is a retaining glycosyl hydrolase in which E212 and E320 are the putative catalytic residues," *Biochemistry*, vol. 35, no. 50, pp. 16195–16204, 1996.

[17] K. L. Braithwaite, G. W. Black, G. P. Hazlewood, B. R. S. Ali, and H. J. Gilbert, "A non-modular endo-β-1,4-mannanase from *Pseudomonas fluorescens* subspecies cellulose," *Biochemical Journal*, vol. 305, no. 3, pp. 1005–1010, 1995.

[18] S. D. Jeon, K. O. Yu, S. W. Kim, and S. O. Han, "A celluloytic complex from *Clostridium cellulovorans* consisting of mannanase B and endoglucanase e has synergistic effects on galactomannan degradation," *Applied Microbiology and Biotechnology*, vol. 90, no. 2, pp. 565–572, 2011.

[19] R. Li, R. Kibblewhite, W. J. Orts, and C. C. Lee, "Molecular cloning and characterization of multidomain xylanase from manure library," *World Journal of Microbiology and Biotechnology*, vol. 25, no. 11, pp. 2071–2078, 2009.

[20] A. Kosugi, T. Arai, and R. H. Doi, "Degradation of cellulosome-produced cello-oligosaccharides by an extracellular non-cellulosomal β-glucan glucohydrolase, BglA, from *Clostridium cellulovorans*," *Biochemical and Biophysical Research Communications*, vol. 349, no. 1, pp. 20–23, 2006.

Hindawi Publishing Corporation
BioMed Research International
Volume 2014, Article ID 684506, 11 pages
http://dx.doi.org/10.1155/2014/684506

Review Article

From Structure to Catalysis: Recent Developments in the Biotechnological Applications of Lipases

Cristiane D. Anobom, Anderson S. Pinheiro, Rafael A. De-Andrade, Erika C. G. Aguieiras, Guilherme C. Andrade, Marcelo V. Moura, Rodrigo V. Almeida, and Denise M. Freire

Departamento de Bioquímica, Universidade Federal do Rio de Janeiro, Avenida Athos da Silveira Ramos, 21941-909 Rio de Janeiro, RJ, Brazil

Correspondence should be addressed to Cristiane D. Anobom; anobom@iq.ufrj.br and Denise M. Freire; freire@iq.ufrj.br

Received 12 December 2013; Accepted 17 February 2014; Published 24 March 2014

Academic Editor: Noomen Hmidet

Microbial lipases are highly appreciated as biocatalysts due to their peculiar characteristics such as the ability to utilize a wide range of substrates, high activity and stability in organic solvents, and regio- and/or enantioselectivity. These enzymes are currently being applied in a variety of biotechnological processes, including detergent preparation, cosmetics and paper production, food processing, biodiesel and biopolymer synthesis, and the biocatalytic resolution of pharmaceutical derivatives, esters, and amino acids. However, in certain segments of industry, the use of lipases is still limited by their high cost. Thus, there is a great interest in obtaining low-cost, highly active, and stable lipases that can be applied in several different industrial branches. Currently, the design of specific enzymes for each type of process has been used as an important tool to address the limitations of natural enzymes. Nowadays, it is possible to "order" a "customized" enzyme that has ideal properties for the development of the desired bioprocess. This review aims to compile recent advances in the biotechnological application of lipases focusing on various methods of enzyme improvement, such as protein engineering (directed evolution and rational design), as well as the use of structural data for rational modification of lipases in order to create higher active and selective biocatalysts.

1. Introduction

Lipases (triacylglycerol acyl hydrolases, E.C. 3.1.1.3) are enzymes that catalyze the hydrolysis of fats and oils with release of free fatty acids, diglycerides, monoglycerides, and glycerol. Furthermore, in organic media, these enzymes also catalyze synthetic reactions including esterification, acidolysis, alcoholysis, and interesterifications [1, 2]. Lipases may act under mild conditions, are highly stable in organic solvents, show broad substrate specificity, and usually show high regio- and/or stereoselectivity in catalysis. This versatility makes lipases one of the most widely used group of biocatalysts for biotechnological processes [3–5]. Lipases find applications in food modification, detergent formulation, cosmetic, pharmaceutical, leather, textile, and paper industries, biodiesel and biopolymer production, or pretreatment of lipid-rich wastewaters [1, 6]. These enzymes are found in many species of animals, plants, bacteria, and fungi. Moreover, microbial lipases are the most appealing ones mainly because of their applied properties, such as versatility and ease of mass production [5, 6].

2. Biotechnological Applications of Lipases

2.1. Hydrolysis of Oils and Fats: Detergents, Pulp and Paste, and Leather. The most commercially important field for lipase application is their incorporation to detergents, which are used mainly in industrial laundry and household dishwashers to remove fat-containing stains [3]. The detergent lipases mostly used are the ones from *Thermomyces* sp., expressed in recombinant strains of *Aspergillus oryzae* (Lipolase, Novozymes), as well as from *Pseudomonas* spp. (Lumafast and Lipomax, Gist-Brocades). The requirements for lipase application in detergent industries may include high broad substrate specificity, activity and stability at alkaline pH and

temperatures above 40°C, and compatibility with different components in a detergent, including metal ions, surfactants, oxidants, and proteases [5, 7, 8]. Another application of these enzymes is in the removal of "pitch" (hydrophobic components of wood, namely, triglycerides and waxes) from pulp produced in the paper industry. This enzymatic pitch control method has been used in large scale since early 1990s [3, 5]. Lipases can also be used to remove fats and grease from skins and hides. This process generates a higher-quality product (more uniform colour and a cleaner appearance) when compared to leather that is manufactured by traditional methods [5].

2.2. Pretreatment of Lipid-Rich Wastewaters. Wastewaters from dairies, slaughterhouses, and fish-processing contain high levels of fats and proteins with low biodegradability that may cause serious environmental damage if not properly treated [9, 10]. An enzymatic hydrolytic step before further biological treatment can reduce the particles diameter, increasing their surface area and favoring organic matter assimilation by the microbial consortium [11]. Thus, the application of lipases in wastewater treatment may improve biological degradation of fatty wastewaters, thereby accelerating this process [10]. Nevertheless, this added pretreatment procedure becomes economically unfeasible if there are high costs associated with the commercial enzymatic preparations. Therefore, the development of low-cost enzyme preparations becomes essential.

2.3. Food Processing and Improving Quality. In dairy industry, microbial lipases have been used in selective hydrolysis of fat triglycerides to release free fatty acids, which are used to develop flavored products, such as cheese, butter, margarine, milk chocolate, and sweets [3]. Certain microbial lipases are highly regio- and fatty acid-specific and thus are commonly used for the production of new oils and fats through interesterification reactions [1]. These reactions are used to produce high added value products, such as cocoa butter equivalents, human milk fat substitutes, pharmaceutically important polyunsaturated fatty acids (PUFAs), rich/low calorie lipids, and "designers fats" or "structured lipids." Enzymatic transesterification can also be used to modify the properties of triacylglycerol mixtures and produce fats with optimum melting characteristics and free of trans fatty acids, targeting commercial applications for food industries. Sellami et al. investigated the production of a trans-free fat, for margarine formulation, by enzymatic transesterification of palm stearin and palm olein blends. The margarine prepared with transesterified fat showed similar spreadability to that of a commercial product [12]. The major attractions for lipase utilization are energy saving and the decrease of lipid degradation due to high temperatures [5, 13].

2.4. Synthesis of Fine Chemicals (Therapeutics, Agrochemicals, Flavors and Fragrances, Emulsifiers, and Cosmetics). Stereospecificity is especially important for the synthesis of bioactive molecules, as chirality is a key factor in the efficacy of many drugs and usually only one of the enantiomeric forms manifests bioactivity. In this context, the use of lipases to synthesize the chiral building blocks for the production of pharmaceuticals, agrochemicals, and pesticides with high enantiomeric purity has become widespread. These biocatalysts offer several advantages over traditional chemical routes, such as practicality, high efficiency, selectivity, easy separation from the unreacted substrates, and mild reaction conditions [5, 14–16]. It is important to highlight that lipase cost does not restrict the production of added value products, such as pharmaceuticals. The kinetic resolution of (R,S)-1,2-isopropylidene glycerol ester derivatives (solketal) catalyzed by different lipases was investigated by Machado et al. [14]. Solketal is an important chiral synthon in the synthesis of diglycerides, glyceryl phosphates, tetraoxaspiroundecanes, and many biologically active compounds, such as glycerolphospholipids, β-blockers, prostaglandins, and leucotrienes. *Pseudomonas* sp. lipase (Amano AK) was proven to be the most effective in promoting the resolution of (R,S)-IPG esters yielding 22% of (R)-IPG octanoate (99% ee) in 48 h at 30°C. Cunha et al. studied the enzymatic kinetic resolution of (±)-1,2-O-Isopropylidene-3,6-di-O-benzyl-myo-inositol (precursor of chiral myo-inositol derivatives (inositol phosphates and their analogs)) by Novozym 435. The use of vinyl acetate as acylating agent has increased the yield to over 49%, while maintaining a very high ee (>99%) [17]. Similar results were obtained by Manoel et al. [18] in the kinetic resolution of DL-1,3,6-tri-O-benzyl-myo-inositol by *Pseudomonas* spp. lipases (PS-C, PS-IM) and Novozym 435, where the O-acylated L enantiomorph was obtained in up to >99% ee with conversions up to >49% [18]. In another work, Manoel et al. investigated the biocatalytic continuous flow process in a packed-bed reactor (PBR) for the kinetic resolution of (±)-1,3,6-tri-O-benzyl-myo-inositol ((±)-1) by alcoholysis using Novozym 435 [15]. Excellent conversions and enantiomeric ratios (50% conversion and eep >99%) were attained in short reaction time (3 min of residence time) using TBME (*tert*-butyl-methyl-ether) as solvent and vinyl acetate as acetylating agent. The lipase remained stable over a longer period of time (9-cycle experiment). Lipases are currently being used by many pharmaceutical companies world-wide for the preparation of optically active intermediates on a kilogram scale [5]. Despite the large number of publications in this field, the number of industrial enantioselective processes based on lipase catalysis is still limited.

Organic esters from short-chain fatty acids are amongst the most important natural fragrances and flavors. Examples of these esters include anthranilic acid alkyl esters (which possess sweet and orange odor with a pungent taste), butyl butyrate, isoamyl acetate (banana flavor), ethyl valerate (green apple flavor), and butyl acetate (pineapple flavor) [19]. The use of lipases leads to better quality products suitable to fragrance and flavor industry [20].

Monoacylglycerols (MAGs) are nonionic surfactants and constitute the main category of emulsifiers used in pharmaceutical and cosmetic formulations as well as prepared foods [19]. Lipases can be used to overcome the drawbacks (dark color, thermal degradation, and burnt taste) of the chemical glycerolysis that is carried out at high temperatures

(220–250°C) employing alkaline catalysts and high pressures [6]. The enzymatic synthesis of MAGs can be performed by selective hydrolysis using 1,3-regiospecific lipases, glycerolysis of fats or oils, and esterification of fatty esters with glycerol. da Silva et al. reported the synthesis of monocaprin by direct esterification of glycerol with capric acid catalyzed by a commercial immobilized lipase (Lipozyme IM 20) [21]. The composition of the final product met the requirements established by the World Health Organization food emulsifiers (61.3% monocaprin, 19.9% dicaprin, and 18.8% capric acid).

Tyrosyl lipophilic derivatives are antioxidants with application in food, cosmetic, and pharmaceutical industries. Aissa et al. studied the synthesis of tyrosyl fatty acid esters by direct esterification of tyrosol with different fatty acids (from C2 to C18:1) using Novozyme 435 as biocatalyst. Tyrosyl esters derivatives TyC8, TyC10, and TyC12 exhibited antibacterial and antileishmanial activities [22].

2.5. Production of Biofuels and Biolubricants. Biodiesel has attracted considerable interest in recent years as an alternative and renewable energy source. Nowadays, particular attention has been drawn to the use of lipases as biocatalysts for biodiesel synthesis. These enzymes may substitute conventional alkaline processes that generate undesirable byproducts, render the separation of the catalyst from glycerol difficult, produce highly alkaline waste, and use high-quality raw materials [23, 24]. Lipases can catalyze both the transesterification of triacylglycerols and the esterification of free fatty acids to yield monoalkyl-esters. They perform their catalytic activity with oils from different origins, including waste oils with a high acidity and water content. Furthermore, the enzymatic process enables easy separation from the byproduct, glycerol [25, 26]. The enzymatic biodiesel production has been carried out by several research groups using both extracellular and intracellular lipases as well as raw materials from different sources (animal fat, vegetable oil, used cooking oil, and acid waste from vegetable oils production) [24, 27–30]. These reports show good results with conversion ranges above 90%. However, enzyme's high cost remains a barrier for enzymatic production of biodiesel [23]. Efforts have been focused on the development of low-cost enzyme preparations and more stable and active biocatalysts, in order to improve conversion yields in a shorter period of time and to recycle the enzyme for as much batches as possible [13].

Biolubricants are another group of great industrial interest in which lipases can be used as biocatalysts. The patent EP 2657324 A1 [31] describes an enzymatic process for production of biolubricant from methyl ricinoleate (biodiesel from castor oil) and/or from a mixture of methyl oleate and linoleate (biodiesel from *Jatropha* oil) by transesterification with trimethylolpropane. Conversions of 80% to 99% of the ester (castor oil and *Jatropha* oil biodiesel) were achieved and the product showed good properties of viscosity, viscosity index (VI), pour point, and oxidation stability. Aguieiras et al. have investigated biolubricant synthesis from oleic acid and methyl ricinoleate using immobilized commercial lipases [32]. Novozym 435 showed the best performance and the synthesized product exhibited good values of pour point, viscosity, and viscosity index.

2.6. Production of Biodegradable Polymers. Another field for lipases application is the synthesis of useful and biodegradable biopolymers like polyesters, produced from renewable natural resources [33]. Lipase-catalyzed polymerization reactions are classified into two major polymerization modes: ring-opening polymerization [34] and polycondensation. The latter may include polycondensation of dicarboxylic acids or their derivatives with diols and polycondensation of oxyacids or their esters [33]. This polymerization approach has been successfully employed by several works through a range of strategies. *Rhizomucor miehei* lipase was used in the polymerization of bis(2,2,2-trifluoroethyl) sebacate and aliphatic diols [33, 34]. Mahapatro et al. have studied the polymerization of 12-hydroxydodecanoic acid catalyzed by Novozym 435 and obtained conversion of 91% in oligomers of high molecular weight [35]. Polyesters of ricinoleic acid with 72% of conversion were synthesized by Bódalo et al. using immobilized lipase from *Candida rugosa* [36]. These results indicate the applicability of lipases for polymerization reactions through different pathways.

Taking into account the wide range of applications and the importance of lipases in biotechnology, many efforts have been directed toward the understanding of how these enzymes work at the molecular and atomic level. Since the BRIDGE-T lipase project (1990–1994) until today, numerous three-dimensional structures of lipases from several different organisms have been reported, shedding light onto the mechanism used by these enzymes during catalysis.

3. Structural Features of Lipases

Despite their low primary sequence identity, lipases display a very similar fold. Other enzymes, such as esterases, proteases, dehalogenases, epoxide hydrolases, and peroxidases, exhibit similar structural features and, altogether, they constitute the $\alpha\beta$ hydrolase family [37]. The $\alpha\beta$ hydrolase fold is characterized by the presence of a central β-sheet containing eight parallel β-strands, with the exception of $\beta 2$, which is antiparallel with respect to the others. The central β-sheet has a left-handed superhelical twist, generating a 90° angle between the first and the last strands. Strands $\beta 3$ to $\beta 8$ are connected by a bundle of helices: helices A and F pack against the concave side of the central β-sheet, while helices B, C, D, and E pack against the convex side [38, 39]. The active site of $\alpha\beta$ hydrolases consists of a highly conserved catalytic triad: one nucleophilic residue (serine, cysteine, or aspartic acid), one catalytic acidic residue (aspartic or glutamic acid), and one histidine residue. In lipases, the nucleophile has always been characterized as a serine residue [39–41].

3.1. Active Site. The nucleophilic residue is located in a highly conserved pentapeptide Sm-X-Nu-X-Sm, where Sm—small residue, usually a glycine, which may occasionally be substituted by alanine, valine, serine, or threonine; X—any residue; Nu—nucleophilic residue. This pentapeptide

forms a very sharp γ turn between strand β5 and α-helix C named the "nucleophilic elbow." The conformation of this strand-loop-helix motif causes the nucleophilic residue to adopt energetically unfavorable backbone dihedral angles that impose steric constraints on vicinal residues [37, 39, 42]. The "nucleophilic elbow" is the most conserved structural feature of the $\alpha\beta$ hydrolase fold [38]. In a typical $\alpha\beta$ hydrolase fold, the catalytic acid is situated in a reverse loop located after strand β7, interacting with the catalytic histidine through a hydrogen bond. However, in some enzymes, the catalytic acid can be found after strand β6 [37, 42]. Lipases are the only example of $\alpha\beta$ hydrolases that possess a glutamic acid in the catalytic triad [43]. Histidine is the only residue of the catalytic triad that is absolutely conserved. This residue is located in a loop positioned after strand β8. The shape and length of this loop may differ considerably among various members of this family [37, 42].

3.2. Enzyme Mechanism. Substrate hydrolysis starts when the oxygen atom of the catalytic serine attacks the carbon atom of the ester linkage carbonyl group, generating a tetrahedral intermediate that makes hydrogen bonds with backbone nitrogen atoms in the "oxyanion hole." This stabilizes the negatively charged transition state that occurs during hydrolysis. An alcohol is released, leaving the acyl-lipase complex behind, which is ultimately hydrolyzed releasing free fatty acid and regenerating the enzyme [3, 37, 43, 44]. Petersen et al. mapped the electrostatic surface of several lipases and esterases, showing that the active site of these enzymes is negatively charged in their optimal pH range (pH 6–10) [45]. Thus, after the ester cleavage, the ionized carboxylic acid is immediately expelled from the active site due to electrostatic repulsion between its negatively charged carboxyl group and the negative electrostatic potential of the active site, in the so-called "electrostatic catapult" mechanism.

3.3. The Lid Domain. Many lipases exhibit a mobile subdomain called lid, which controls the access of substrate molecules to the catalytic center. Crystallographic structures have shown that this domain is able to adopt two distinct conformations: the closed and the opened states. In the closed state, the active site is not accessible to solvent and, as a consequence, enzyme's surface is mainly hydrophilic rendering the lipase inactive. In the opened state, the active site becomes accessible revealing a large hydrophobic surface that makes the enzyme functional [41, 46]. The activation mechanism through which the movement of the lid operates is still poorly understood. Depending on the structural architecture of the lid, several transition mechanisms have been proposed. In lipases with a lid consisting of only one propeller, the transition has been suggested to be a fast rigid body motion. In contrast, in lipases with a more complex lid, such as *Candida rugosa* lipase, the secondary structure of the lid changes during the opening process and, hence, a partial refolding is expected, which can be a bottleneck to the enzyme kinetics [47]. The conformational rearrangement for lid opening is related to the phenomenon of interfacial activation [41]. Some lipases exhibit a significant increase in their enzymatic activity when the substrate concentration exceeds the solubility limit, that is, when the substrate is a hydrophobic interface [39, 48].

Characterization of large conformational transitions at the atomic level in real time through biophysical experimental methods remains a challenge [49]. X-ray techniques provide essential information about the static conformational states but offer a poor dynamic view [41]. NMR spectroscopy is not widely used due to limitations of the technique for high molecular weight proteins, which is the case for many lipases, and only a few lipases as cutinase and *Pseudomonas mendocina* lipase have been structurally characterized by solution NMR [46]. Thus, in an attempt to predict and understand the conformational changes of macromolecular systems, other tools as molecular dynamics simulation have gained considerable attention. A series of molecular dynamics (MD) studies have been performed in order to gain information on conformational changes of the lid domain and the role played by the environment (solvent, pH, and temperature) and by the dynamic properties of various lipases. However, few studies have investigated all aspects of the transitions between open and closed conformations and the molecular details of this important feature of lipase function remain unknown [41].

3.4. What Have We Learned from the Three-Dimensional Structures of Lipases? Through the past few decades, many studies have been conducted on the three-dimensional structure of lipases. X-ray crystallography has been the most used technique to thoroughly describe enzyme's catalytic activity and high selectivity, as well as to reveal the structural basis for interfacial activation.

The first crystal structures of lipases from the fungi *Rhizomucor miehei* [50, 51] and *Geotrichum candidum* [52] were solved in 1990 and 1991, respectively. In 1993, the first crystal structure of a bacterial lipase, from *Pseudomonas glumae* [53], was determined. The structure of this bacterial lipase from the I.2 family revealed for the first time the identity of the catalytic triad and the presence of a lid that controls substrate access to the active site. Although its acidic group was not necessary for lipase function, another aspartate located at position 241 was discovered to be essential for enzyme activity; this residue is capable of binding a calcium ion that is responsible for maintaining protein's stability [53]. Further studies have demonstrated that bacterial lipases from the I.5 family, which also contain a single calcium binding site, exhibit similar characteristics [54].

In 1993, another fungal lipase structure was resolved. The *Candida rugosa* lipase (CRL) structure has allowed a comparison with its homolog from *Geotrichum candidum* and new insights on interfacial activation were unraveled. In contrast to the crystal structure of *Geotrichum candidum* lipase, which has its active site inaccessible from the solvent and covered by loops, CRL has three loops in the vicinity of the active site and its interfacial activation is associated with conformational modifications involving those loops [55]. In 1994, another conformation corresponding to the closed state of this enzyme was crystallized, and only one single loop

that occluded the active site in the inactive state was found to be involved in structural rearrangement. In the open form, a large hydrophobic surface area around the active site is exposed and a 9% increase in the total hydrophobic surface of the enzyme is observed [56].

The first crystallographic study of lipase B from *Candida antarctica*, the most widely used fungal lipase in biotechnological processes, was presented in 1994 [57]. CalB contains only seven β-strands and thus deviates from the traditional α/β-hydrolase fold. In addition, the conserved pentapeptide GxSxG located around the catalytic serine is different from most lipases in CalB, with the first glycine being replaced by a threonine residue (TWSQG). The crystal structure showed a quite narrow and deep channel that culminates in an open active site that contains an oxyanion hole. The shape of this channel is probably responsible for the high stereospecificity of the enzyme. A putative lid was also identified based on the mobility of α-helix 5 [57]. In contrast, lipase A from *Candida antarctica*, CalA, had its structure solved only fourteen years later revealing a much larger lid composed of 92 residues [58]. Molecular dynamics simulations of CalB in explicit organic solvents (methanol chloroform (CL3), isopentane (ISO), toluene (TOL), and cyclohexane (CHE)) showed a 10% decrease in the hydrophilic and a 1% increase in the hydrophobic surface area of the protein. The dynamics of CalB proved to be largely dependent on the dielectric constant of the solvent, showing high flexibility in water and low flexibility in organic solvents. A significant increase in the number of water molecules bound to the enzyme's surface was observed, decreasing the dielectric constant and spanning the water network [59].

It was only in 1997, seven years after the determination of the first crystal structure of *Rhizomucor miehei* lipase (Rml), that molecular dynamics simulations on free and dialkyl phosphate-bound Rml were performed. This study revealed that hydrophobic residues are exposed while polar residues are buried during the activation process, which is caused by a displacement of the active site helix. Helices showed to be relatively rigid and motions were mostly observed in loop regions, mainly in loops Gly35-Lys50 and Thr57-Asn63 [60]. Further studies using Rml complexed with a substrate (ester) or a product (fatty acid) in the presence of a lipid aggregate have demonstrated that the active site lid opens wider in the presence of a lipid patch consisting of substrate molecules than in an aqueous environment [61].

In the early 2000s, the first crystal structure of a bacterial lipase from the I.1 family was solved. *Pseudomonas aeruginosa* PAO1 lipase showed a variant of the α/β hydrolase fold without the first two β-strands and one α-helix (αE). A stabilizing intramolecular disulfide bridge is formed between Cys183 and Cys235 due to helix αE absence. The active site loop containing the catalytic histidine is stabilized by the coordination of a calcium ion. Three pockets that accommodate the sn-1, sn-2, and sn-3 fatty acid chains were observed. The size of the acyl pocket and its interactions with the substrate, specifically with the sn-2 fatty acid chain, are the predominant determinants of the enzyme's regio- and enantio-preference [62].

In 2001, an example of one of the few lipases that do not exhibit interfacial activation in oil-water interfaces was crystallized. LipA from *Bacillus subtilis* (I.4 family of bacterial lipases) showed a compact minimal α/β-hydrolase fold with a six-stranded parallel β-sheet surrounded by five α-helices. No lid domain was observed and the catalytic serine was solvent exposed [63].

Tyndall et al. resolved the first crystallographic structure of a lipase from a thermophilic organism. *Bacillus stearothermophilus* P1 (BSP) lipase shared less than 20% amino acid sequence identity with any other previously crystallized lipase [64]. Its structure contains significant insertions in the canonical α/β hydrolase fold and a zinc binding site that may be important for thermal stability. In addition, BSP lipase has significantly more salt bridges and α-helical content, as well as proline and aromatic residues than any other previously analyzed lipase.

In the past decade, several structural studies have been performed on members of the I.3 lipase family. This unique bacterial lipase family contains two lids covering the active site and is characterized by the presence of three calcium binding sites [54, 65]. The Ca1 site is required for the full opening of the active site by anchoring lid1, the most common lipase lid. Ca2 and Ca3 sites are responsible for stabilizing the enzyme structure, while Ca2 is also required for enzyme full activation. In order to clarify the role of lid2, *Pseudomonas* sp. lipase MIS38 (PML) was used as a model and a lid2 deletion mutant (DL2-PML) was constructed. The crystal structures showed that mutant and native proteins required calcium for lipase activity, suggesting that the enzyme only exhibits activity when lid1 is fully open. The comparison of DL2-PML models in a closed and open conformation with the crystal structures of PML suggests that the hydrophobic surface area provided by lid1 and lid2 in an open conformation is considerably decreased by lid2 deletion. This study proposed that this hydrophobic surface area is necessary to hold firmly the micellar substrates in the active site and, therefore, lid2 is essential for interfacial activation of PML [65]. Previous studies had shown the importance of lid2 for the full activation of PML. Molecular dynamics simulations of PML in the open conformation showed that lid2 closes first, while lid1 stays opened, in the absence of micelles. Similarly, in the absence of Ca^{2+} and in the presence of octane or trilaurin micelles, molecular dynamics simulations of PML in the closed conformation showed that lid1 opens, while lid2 remains closed. These results suggest that Ca1 is necessary not only for fully opened conformation of lid1 but also for the initiation of subsequent opening of lid2 [66].

Recently, the thermoalkalophilic lipase from *Geobacillus zalihae* (T1 lipase from the I.5 family) had its crystal structure in its closed conformation resolved. Based on the structural analysis of lipases from the I.5 family, it was proposed that the lid domain includes helices α6 and α7 connected by a loop. The activation process is governed by interfacial activation coupled with a temperature-switch activation, as the large structural rearrangement of the lid domain was only observed in the water-octane interface caused by the interaction between the hydrophobic residues of the lid with the octane solvent [67].

Another recent work used a computer-aided software to study the predicted structure and function of the psychrophilic lipase AMS8 (from the psychrophilic *Pseudomonas* sp. obtained in the Antarctic soil). MD simulations were performed at different temperatures for the analysis of structural flexibility and stability. The results showed that the enzyme is most stable at 0°C and 5°C. The N-terminal catalytic domain is more stable than the C-terminal noncatalytic domain, even though the noncatalytic domain displays higher flexibility [68].

Lipases are remarkable biocatalysts used in a variety of bioprocesses. However, in some fields, the industrial application of lipases is still restricted by their high costs. This motivates researches worldwide to find novel strategies to create enzymatic preparations with a more cost-effective profile. Structural information plays an important role in designing lipases for specific purposes. Recent progress in protein engineering and structure-based rational design has led to the customization of lipases for different bioprocesses.

4. Tailor-Made Lipases: The Importance of the Structural Knowledge

Traditionally, the use of enzymes for biocatalysis, in particular lipases, began by employing proteins from millions of years of evolution to accelerate chemical reactions, often different from those they have evolved to do. In this "conventional paradigm," the desired application is frequently different from the natural function of the enzyme. The development of the processes was thus limited by the characteristics of the biocatalyst (i.e., catalytic activity, stability, and enantioselectivity) [69, 70].

Over the past two decades, the advent of techniques such as X-ray crystallography, NMR spectroscopy, and site-specific mutagenesis allowed a better understanding of protein sequence, structure, and function relationships. Because most enzymes from nature do not meet the requirements for a large-scale application, aspects such as chemo-, regio-, and stereoselectivity need to be enhanced in order to establish the process [70–72].

In the "ideal biocatalyst paradigm," the catalytic characteristics of a target enzyme are often designed by protein engineering, thus building the biocatalyst for a specific optimized process [69]. The paradigm shift brings the focus from the process to the catalyst, which is tailor-made for the desired application.

Protein engineering techniques generally use two different approaches: directed evolution and rational design. The first approach consists in making a series of random mutations in the gene that codes for the target protein, creating a library of transformants that will then be screened for a specific property [70, 73]. There are various techniques to obtain the core steps of directed evolution—mutation, recombination, and screening or selection. The most used are error-prone PCR, which maximize the error rate of DNA polymerase during the PCR reaction [74, 75] and DNA shuffling, which consists in digesting a gene with endonucleases creating a pool of random DNA fragments that can be reassembled into a full-length gene. The DNA fragments anneal with each other based on homology and when fragments from one copy of a gene anneal with those of another copy, recombination occurs causing a template switch [76–78]. The main bottleneck in this approach is the infrastructure necessary to work with a large library of variants (10^3–10^{10}), often requiring high-throughput methods and powerful tools to evaluate the catalysts [73].

The second approach, rational design, preselects promising target sites to make specific changes in the catalyst based on information from protein sequence, structure, and function. This approach may greatly reduce the need for large libraries, focusing on smaller, higher quality ones in order to minimize the screening/selection process [69, 73, 79]. Researchers often look for regions of interest that can be important to the specific target characteristic. Well-conserved function domains, active sites, and key structure points are the focus of the technique. For many enzymes it may be sufficient just to target regions near (10–30 amino acids) the active sites of the proteins in order to obtain significant results in the desired phenotype [73, 80, 81].

However, despite recent advances in this field, engineering an arbitrary protein remains a daunting challenge, because the rules defining the relations among protein sequence, structure, and function are still not entirely understood [82]. To overcome this problem, many hybrid approaches have been used, such as circular permutation, iterative saturation mutagenesis (ISM), combinatorial active-site saturation testing (CASTing), cassette mutagenesis, restricted libraries, and structure-guided consensus [79, 83, 84].

Current literature has many examples of protein engineering using lipases. As multifunctional as these catalysts are, there are examples of directed evolution and rational design towards many characteristics. Table 1 encompasses successful cases of lipases improvement between 2007 and 2013.

Candida antarctica Lipase B (CalB) is a well-known lipase used for many industrial purposes. Its versatility has led to various paths of optimization throughout the past decade. Lutz and Patrick reported several of these changes made over CalB structure in a comprehensive review [85]. *Pseudomonas aeruginosa* Lipase A is another well-studied lipase, which had its enantiomeric ratio (E) towards 2-methyldecanoic acid increased from 1.1 to 581 through a series of sequential combined approaches, such as error-prone PCR and ISM [86].

Liebeton et al. used directed evolution to enhance the enantioselectivity of the extracellular lipase from *Pseudomonas aeruginosa* (PAL) [90]. Successive rounds of random mutagenesis by ep-PCR and saturation mutagenesis resulted in increased enantioselectivity from $E = 1.1$ for the wild-type enzyme to $E = 25.8$. This mutant (94G12) showed 5 substitutions (S149G, S155F, V47G, V55G, and S164G) with higher conformational flexibility by accumulation of glycine residues, resulting in modifications of interactions between important structures involved in the catalytic site and oxyanion hole.

Table 1: Examples of lipase improvement using protein engineering (from 2007 to 2013).

Enzyme	Protein engineering approach	Substrate	Optimization	Reference
Lipase B from *Candida antarctica* (CalB)	Circular permutation	2-(3-Fluoro-4-phenyl-phenyl)propionic acid and others	E_{wt} $(R) = 25$ E_{ep} $(R) = 40$	Qian et al. [87]
Rhizomucor miehei lipase	Site-directed mutagenesis	*p*-Nitrophenyl caprylate	5-fold more thermal stability at 60°C	Han et al. [88]
Bacillus pumilus lipase	DNA shuffling	*p*-Nitrophenyl palmitate	8-fold specific activity 9-fold half life	Akbulut et al. [78]
Rhizopus chinensis lipase	Error-prone PCR/DNA shuffling	*p*-Nitrophenyl palmitate	20°C enhancement in thermal stability	Yu et al. [77]
Lipase A from *Pseudomonas aeruginosa* (PAL)	ISM	2-Methyldecanoic acid p-nitrophenyl ester and other derivatives	E_{wt} $(S) = 1.1$ E_{ep} $(S) = 594$	Reetz et al. [89]
Lipase from *Yarrowia lipolytica* (Lip2p)	Rational design	2-Bromo-phenylacetic acid ethyl ester and 2-bromo-o-tolylacetic acid ethyl ester	E_{wt} $(S) = 5.5$ E_{ep} $(S) = 59$ and E_{wt} $(S) = 27$ E_{ep} $(S) = 111$	Bordes et al. [75]
Lipase A from *Candida antarctica* (CalA)	CASTing	2-Phenyl propanoicacid p-nitrophenylester	E_{wt} $(S) = 20$ E_{ep} $(R) = 276$	Engström et al. [74]

Altering optimum pH by structural modifications has been shown by Neves-Petersen et al. using the triglyceride lipase/cutinase from *Fusarium solani pisi* [86]. Previous studies suggested that this enzyme operates through the electrostatic catapult model. Knowing that catalytic Asp175 and Glu44 are key residues involved in this mechanism, mutations E44A (charge removal), E44 K (charge reversal), and T45P were proposed in order to pinpoint the role of these electrostatic changes. Thr45, a neighbouring residue, was mutated with the aim of shifting the spatial location of Glu44. Typically, the substitution of Glu44 pushes the onset of the active site negative potential towards a more alkaline condition, increasing pH optima.

Structural studies and modeling of CalB allowed a great range of experiments to improve its selectivity and thermal stability. Mutation S74A showed a higher enantioselectivity toward 1-chloro-2-octanol. Replacement of a threonine near the active site by valine causes the loss of lipase activity, which is restored when 2-hydroxy-propanoate is used as a substrate. This mutant also presents improved enantioselectivity [40]. Mutants 23G5 (V210I and A281E) and 195F1 (derived from 23G5 with one additional mutation, V221D) showed over a 20-fold increase in half-life at 70°C in comparison to the wild-type CalB, by decreasing mutants propensity to aggregate in the unfolded state. Mutations V221D and A281E are critical for lipase stability, while V210I had only a marginal effect. The mutants catalytic efficiencies against p-nitrophenyl butyrate and 6,8-diuoro-4-methylumbelliferyl octanoate were higher than that for wild-type CalB [91].

NMR analyses of *Pseudomonas mendocina* lipase and its F180P/S205G mutant indicated virtually identical structures with notable differences in local dynamics. These substitutions resulted in a mutant with higher activity and stability for use in washing powders, for instance. While both protein cores are very rigid and widely protected from H/D exchange, specific mutations can stabilize the helices α1, α4, and α5 and destabilize the hydrogen bond network of the β-sheet β7–β9 [92].

Kamal et al. obtained a mutant with twelve stabilizing mutations (A15S, F17S, A20E, N89Y, G111D, L114P, A132D, M134E, M137P, I157 M, S163P, and N166Y) named 6B by performing multiple rounds of directed evolution and mutation by recombination on the lipase A of *Bacillus subtilis* [93]. Eleven of these mutations are involved in better anchoring of loops or increasing their rigidity through substitution of any amino acid by a proline. More importantly, three of the stabilizing mutations (A132D, M134E, and I157 M) are adjacent to two residues of the catalytic triad (D133 and H156), causing increased rigidity of the active site. Interestingly, this increased stiffness resulted in a higher activity. Lipase 6B showed a melting temperature of 22°C and a thermodynamic stability of 3.7 kcal/mol higher than the wild-type protein.

More recently, two mutants (D311E and K344R) of T1 lipase isolated from *Geobacillus zalihae* were constructed to introduce an additional ion pair at the inter- and the intraloop, respectively. The stability of the wild-type and mutant lipases was studied using circular dichroism. The T_m for wild-type lipase and mutants D311E and K344R were

approximately 68.52°C, 70.59°C, and 68.54°C, respectively. Analysis of D311E lipase crystal structure revealed an additional ion pair around E311 that may regulate the stability of this mutant at high temperatures [94].

In conclusion, enzyme engineering is a full blossoming field with many interesting works and a myriad of possibilities. Coupling directed evolution with structure-based rational design appears to bring lipase catalysis closer to the "ideal biocatalyst paradigm," enabling the production of more active, selective, and stable catalysts.

Conflict of Interests

The authors declare that they have no conflict of interests regarding the publication of this paper.

References

[1] R. Sharma, Y. Chisti, and U. C. Banerjee, "Production, purification, characterization, and applications of lipases," *Biotechnology Advances*, vol. 19, no. 8, pp. 627–662, 2001.

[2] A. M. P. Koskinen and A. M. Klibanov, *Enzymatic Reactions in Organic Media*, Blackie Academic and Professional Publisher, 1st edition, 1996.

[3] K. Jaeger and M. T. Reetz, "Microbial lipases form versatile tools for biotechnology," *Trends in Biotechnology*, vol. 16, no. 9, pp. 396–403, 1998.

[4] M. Kapoor and M. N. Gupta, "Lipase promiscuity and its biochemical applications," *Process Biochemistry*, vol. 47, no. 4, pp. 555–569, 2012.

[5] F. Hasan, A. A. Shah, and A. Hameed, "Industrial applications of microbial lipases," *Enzyme and Microbial Technology*, vol. 39, no. 2, pp. 235–251, 2006.

[6] H. Horchani, I. Aissa, S. Ouertani, Z. Zarai, Y. Gargouri, and A. Sayari, "Staphylococcal lipases: biotechnological applications," *Journal of Molecular Catalysis B: Enzymatic*, vol. 76, pp. 125–132, 2012.

[7] R. Liu, X. Jiang, H. Mou, H. Guan, H. Hwang, and X. Li, "A novel low-temperature resistant alkaline lipase from a soda lake fungus strain *Fusarium solani* N4-2 for detergent formulation," *Biochemical Engineering Journal*, vol. 46, no. 3, pp. 265–270, 2009.

[8] S. Grbavčić, D. Bezbradica, L. Izrael-Živković et al., "Production of lipase and protease from an indigenous *Pseudomonas aeruginosa* strain and their evaluation as detergent additives: compatibility study with detergent ingredients and washing performance," *Bioresource Technology*, vol. 102, no. 24, pp. 11226–11233, 2011.

[9] D. R. Rosa, I. C. S. Duarte, N. K. Saavedra et al., "Performance and molecular evaluation of an anaerobic system with suspended biomass for treating wastewater with high fat content after enzymatic hydrolysis," *Bioresource Technology*, vol. 100, no. 24, pp. 6170–6176, 2009.

[10] M. C. Cammarota and D. M. G. Freire, "A review on hydrolytic enzymes in the treatment of wastewater with high oil and grease content," *Bioresource Technology*, vol. 97, no. 17, pp. 2195–2210, 2006.

[11] A. B. G. Valladão, M. C. Cammarota, and D. M. G. Freire, "Performance of an anaerobic reactor treating poultry abattoir wastewater with high fat content after enzymatic hydrolysis," *Environmental Engineering Science*, vol. 28, no. 4, pp. 299–307, 2011.

[12] M. Sellami, H. Ghamgui, F. Frikha, Y. Gargouri, and N. Miled, "Enzymatic transesterification of palm stearin and olein blends to produce zero-trans margarine fat," *BMC Biotechnology*, vol. 12, article 48, 8 pages, 2012.

[13] R. Fernandez-Lafuente, "Lipase from *Thermomyces lanuginosus*: uses and prospects as an industrial biocatalyst," *Journal of Molecular Catalysis B: Enzymatic*, vol. 62, no. 3-4, pp. 197–212, 2010.

[14] A. C. O. Machado, A. A. T. da Silva, C. P. Borges, A. B. C. Simas, and D. M. G. Freire, "Kinetic resolution of (R,S)-1,2-isopropylidene glycerol (solketal) ester derivatives by lipases," *Journal of Molecular Catalysis B: Enzymatic*, vol. 69, no. 1-2, pp. 42–46, 2011.

[15] E. A. Manoel, K. C. Pais, M. C. Flores et al., "Kinetic resolution of a precursor for myo-inositol phosphates under continuous flow conditions," *Journal of Molecular Catalysis B: Enzymatic*, vol. 87, pp. 139–143, 2013.

[16] K. Jaeger and T. Eggert, "Lipases for biotechnology," *Current Opinion in Biotechnology*, vol. 13, no. 4, pp. 390–397, 2002.

[17] A. G. Cunha, A. A. T. da Silva, A. J. R. da Silva et al., "Efficient kinetic resolution of (±)-1,2-O-isopropylidene-3,6-di-O-benzyl-myo-inositol with the lipase B of *Candida antarctica*," *Tetrahedron Asymmetry*, vol. 21, no. 24, pp. 2899–2903, 2010.

[18] E. A. Manoel, K. C. Pais, A. G. Cunha, M. A. Z. Coelho, D. M. G. Freire, and A. B. C. Simas, "On the kinetic resolution of sterically hindered myo-inositol derivatives in organic media by lipases," *Tetrahedron Asymmetry*, vol. 23, no. 1, pp. 47–52, 2012.

[19] A. A. Mendes, P. C. Oliveira, and H. F. de Castro, "Properties and biotechnological applications of porcine pancreatic lipase," *Journal of Molecular Catalysis B: Enzymatic*, vol. 78, pp. 119–134, 2012.

[20] R. C. Rodrigues and R. Fernandez-Lafuente, "Lipase from *Rhizomucor miehei* as an industrial biocatalyst in chemical process," *Journal of Molecular Catalysis B: Enzymatic*, vol. 64, no. 1-2, pp. 1–22, 2010.

[21] M. A. M. da Silva, V. C. Medeiros, M. A. P. Langone, and D. M. G. Freire, "Synthesis of monocaprin catalyzed by lipase," *Applied Biochemistry and Biotechnology A: Enzyme Engineering and Biotechnology*, vol. 105–108, no. 1–3, pp. 757–768, 2003.

[22] I. Aissa, R. Sghair, M. Bouaziz, D. Laouini, S. Sayadi, and Y. Gargouri, "Synthesis of lipophilic tyrosyl esters derivatives and assessment of their antimicrobial and antileishmania activities," *Lipids in Health and Disease*, vol. 11, article 13, 8 pages, 2012.

[23] A. Gog, M. Roman, M. Toşa, C. Paizs, and F. D. Irimie, "Biodiesel production using enzymatic transesterification: current state and perspectives," *Renewable Energy*, vol. 39, no. 1, pp. 10–16, 2012.

[24] J. S. de Sousa, E. D. Cavalcanti-Oliveira, D. A. G. Aranda, and D. M. G. Freire, "Application of lipase from the physic nut (*Jatropha curcas* L.) to a new hybrid (enzyme/chemical) hydroesterification process for biodiesel production," *Journal of Molecular Catalysis B: Enzymatic*, vol. 65, no. 1–4, pp. 133–137, 2010.

[25] A. Robles-Medina, P. A. González-Moreno, L. Esteban-Cerdán, and E. Molina-Grima, "Biocatalysis: towards ever greener biodiesel production," *Biotechnology Advances*, vol. 27, no. 4, pp. 398–408, 2009.

[26] L. Fjerbaek, K. V. Christensen, and B. Norddahl, "A review of the current state of biodiesel production using enzymatic

transesterification," *Biotechnology and Bioengineering*, vol. 102, no. 5, pp. 1298–1315, 2009.

[27] Y. Shimada, Y. Watanabe, T. Samukawa et al., "Conversion of vegetable oil to biodiesel using immobilized *Candida antarctica* lipase," *Journal of the American Oil Chemists' Society*, vol. 76, no. 7, pp. 789–793, 1999.

[28] K. Ban, M. Kaieda, T. Matsumoto, A. Kondo, and H. Fukuda, "Whole cell biocatalyst for biodiesel fuel production utilizing *Rhizopus oryzae* cells immobilized within biomass support particles," *Biochemical Engineering Journal*, vol. 8, no. 1, pp. 39–43, 2001.

[29] Ö. Köse, M. Tüter, and H. A. Aksoy, "Immobilized *Candida antarctica* lipase-catalyzed alcoholysis of cotton seed oil in a solvent-free medium," *Bioresource Technology*, vol. 83, no. 2, pp. 125–129, 2002.

[30] I. N. S. Corrêa, S. L. Souza, M. Catran et al., "Enzymatic biodiesel synthesis using a byproduct obtained from palm oil refining," *Enzyme Research*, vol. 2011, Article ID 814507, 8 pages, 2011.

[31] J. A. da Silva, D. M. G. Freire, A. Habert, and V. Soares, "Process for the production of bio-lubricant from methyl biodiesel and bio-lubricant obtained by said process," EP 2657324 A1, 2013.

[32] E. C. G. Aguieiras, C. O. Veloso, J. V. Bevilaqua et al., "Estolides synthesis catalyzed by immobilized lipases," *Enzyme Research*, vol. 2011, Article ID 432746, 7 pages, 2011.

[33] J. Kadokawa and S. Kobayashi, "Polymer synthesis by enzymatic catalysis," *Current Opinion in Chemical Biology*, vol. 14, no. 2, pp. 145–153, 2010.

[34] H. Uyama and S. Kobayashi, "Enzymatic ring-opening polymerization of lactones catalyzed by lipase," *Chemistry Letters*, vol. 22, pp. 11497–11150, 1993.

[35] A. Mahapatro, A. Kumar, and R. A. Gross, "Mild, solvent-free ω-hydroxy acid polycondensations catalyzed by *Candida antarctica* lipase B," *Biomacromolecules*, vol. 5, no. 1, pp. 62–68, 2004.

[36] A. Bódalo, J. Bastida, M. F. Máximo, M. C. Montiel, M. Gómez, and M. D. Murcia, "Production of ricinoleic acid estolide with free and immobilized lipase from *Candida rugosa*," *Biochemical Engineering Journal*, vol. 39, no. 3, pp. 450–456, 2008.

[37] M. Nardini and B. W. Dijkstra, "α/β hydrolase fold enzymes: the family keeps growing," *Current Opinion in Structural Biology*, vol. 9, no. 6, pp. 732–737, 1999.

[38] J. D. Schrag and M. Cygler, "Lipases and α/β hydrolase fold," *Methods in Enzymology*, vol. 284, pp. 85–107, 1997.

[39] K.-E. Jaeger, B. W. Dijkstra, and M. T. Reetz, "Bacterial biocatalysts: molecular biology, three-dimensional structures, and biotechnological applications of lipases," *Annual Review of Microbiology*, vol. 53, pp. 315–351, 1999.

[40] U. T. Bornscheuer, "Microbial carboxyl esterases: classification, properties and application in biocatalysis," *FEMS Microbiology Reviews*, vol. 26, no. 1, pp. 73–81, 2002.

[41] F. Bordes, S. Barbe, P. Escalier et al., "Exploring the conformational states and rearrangements of *Yarrowia lipolytica* lipase," *Biophysical Journal*, vol. 99, no. 7, pp. 2225–2234, 2010.

[42] D. L. Ollis, E. Cheah, M. Cygler et al., "The α/β hydrolase fold," *Protein Engineering*, vol. 5, no. 3, pp. 197–211, 1992.

[43] P. Heikinheimo, A. Goldman, C. Jeffries, and D. L. Ollis, "Of barn owls and bankers: a lush variety of α/β hydrolases," *Structure*, vol. 7, no. 6, pp. R141–R146, 1999.

[44] R. Gupta, N. Gupta, and P. Rathi, "Bacterial lipases: an overview of production, purification and biochemical properties," *Applied Microbiology and Biotechnology*, vol. 64, no. 6, pp. 763–781, 2004.

[45] M. T. N. Petersen, P. Fojan, and S. B. Petersen, "How do lipases and esterases work: the electrostatic contribution," *Journal of Biotechnology*, vol. 85, no. 2, pp. 115–147, 2001.

[46] S. Ranaldi, V. Belle, M. Woudstra et al., "Amplitude of pancreatic lipase lid opening in solution and identification of spin label conformational subensembles by combining continuous wave and pulsed EPR spectroscopy and molecular dynamics," *Biochemistry*, vol. 49, no. 10, pp. 2140–2149, 2010.

[47] S. Rehm, P. Trodler, and J. Pleiss, "Solvent-induced lid opening in lipases: a molecular dynamics study," *Protein Science*, vol. 19, no. 11, pp. 2122–2130, 2010.

[48] L. Sarda and P. Desnuelle, "Action de la lipase pancréatique sur les esters en émulsion," *Biochimica et Biophysica Acta*, vol. 30, no. 3, pp. 513–521, 1958.

[49] K. Henzler-Wildman and D. Kern, "Dynamic personalities of proteins," *Nature*, vol. 450, no. 7172, pp. 964–972, 2007.

[50] L. Brady, A. M. Brzozowski, Z. S. Derewenda et al., "A serine protease triad forms the catalytic centre of a triacylglycerol lipase," *Nature*, vol. 343, no. 6260, pp. 767–770, 1990.

[51] Z. S. Derewenda, U. Derewenda, and G. G. Dodson, "The crystal and molecular structure of the *Rhizomucor miehei* triacylglyceride lipase at 1.9 Å resolution," *Journal of Molecular Biology*, vol. 227, no. 3, pp. 818–839, 1992.

[52] J. D. Schrag, Y. Li, S. Wu, and M. Cygler, "Ser-His-Glu triad forms the catalytic site of the lipase from *Geotrichum candidum*," *Nature*, vol. 351, no. 6329, pp. 761–764, 1991.

[53] M. E. M. Noble, A. Cleasby, L. N. Johnson, M. R. Egmondb, and L. G. J. Frenkenb, "The crystal structure of triacylglycerol lipase from *Pseudomonas glumae* reveals a partially redundant catalytic aspartate," *Annual Reviews in Microbiology*, vol. 53, pp. 315–351, 1999.

[54] K. Kuwahara, C. Angkawidjaja, H. Matsumura, Y. Koga, K. Takano, and S. Kanaya, "Importance of the Ca^{2+}-binding sites in the N-catalytic domain of a family I.3 lipase for activity and stability," *Protein Engineering, Design and Selection*, vol. 21, no. 12, pp. 737–744, 2008.

[55] P. Grochulski, Y. Li, J. D. Schrag et al., "Insights into interfacial activation from an open structure of *Candida rugosa* lipase," *The Journal of Biological Chemistry*, vol. 268, no. 17, pp. 12843–12847, 1993.

[56] P. Grochulski, Y. Li, J. D. Schrag, and M. Cygler, "Two conformational states of *Candida rugosa* lipase," *Protein Science*, vol. 3, no. 1, pp. 82–91, 1994.

[57] J. Uppenberg, M. T. Hansen, S. Patkar, and T. A. Jones, "The sequence, crystal structure determination and refinement of two crystal forms of lipase B from *Candida antarctica*," *Structure*, vol. 2, no. 4, pp. 293–308, 1994.

[58] D. J. Ericsson, A. Kasrayan, P. Johansson et al., "X-ray structure of *Candida antarctica* lipase A shows a novel lid structure and a likely mode of interfacial activation," *Journal of Molecular Biology*, vol. 376, no. 1, pp. 109–119, 2008.

[59] P. Trodler and J. Pleiss, "Modeling structure and flexibility of *Candida antarctica* lipase B in organic solvents," *BMC Structural Biology*, vol. 8, article 9, 2008.

[60] G. H. Peters, D. M. F. van Aalten, A. Svendsen, and R. P. Bywater, "Essential dynamics of lipase binding sites: the effect of inhibitors of different chain length," *Biophysical Journal*, vol. 74, pp. 1251–1262, 1998.

[61] G. H. Peters and R. P. Bywater, "Influence of a lipid interface on protein dynamics in a fungal lipase," *Biophysical Journal*, vol. 81, no. 6, pp. 3052–3065, 2001.

[62] M. Nardini, D. A. Lang, K. Liebeton, K. Jaeger, and B. W. Dijkstra, "Crystal structure of *Pseudomonas aeruginosa* lipase in the open conformation. The prototype for family I.1 of bacterial lipases," *The Journal of Biological Chemistry*, vol. 275, no. 40, pp. 31219–31225, 2000.

[63] G. van Pouderoyen, T. Eggert, K. Jaeger, and B. W. Dijkstra, "The crystal structure of *Bacillus subtilis* lipase: a minimal α/β hydrolase fold enzyme," *Journal of Molecular Biology*, vol. 309, no. 1, pp. 215–226, 2001.

[64] J. D. A. Tyndall, S. Sinchaikul, L. A. Fothergill-Gilmore, P. Taylor, and M. D. Walkinshaw, "Crystal structure of a thermostable lipase from *Bacillus stearothermophilus* P1," *Journal of Molecular Biology*, vol. 323, no. 5, pp. 859–869, 2002.

[65] M. Cheng, C. Angkawidjaja, Y. Koga, and S. Kanaya, "Requirement of lid2 for interfacial activation of a family I. 3 lipase with unique two lid structures," *FEBS Journal*, vol. 279, pp. 3727–3737, 2012.

[66] C. Angkawidjaja, H. Matsumura, Y. Koga, K. Takano, and S. Kanaya, "X-ray crystallographic and MD simulation studies on the mechanism of interfacial activation of a family I.3 lipase with two lids," *Journal of Molecular Biology*, vol. 400, no. 1, pp. 82–95, 2010.

[67] M. Z. A. Rahman, A. B. Salleh, R. N. Z. R. A. Rahman, M. B. A. Rahman, M. Basri, and T. C. Leow, "Unlocking the mystery behind the activation phenomenon of T1 lipase: a molecular dynamics simulations approach," *Protein Science*, vol. 21, pp. 1210–1221, 2012.

[68] M. S. M. Ali, S. F. M. Fuzi, M. Ganasen, R. N. Z. R. A. Rahman, M. Basri, and A. B. Salleh, "Structural adaptation of cold-active RTX lipase from *Pseudomonas* sp. strain AMS8 revealed via homology and molecular dynamics simulation approaches," *BioMed Research International*, vol. 2013, Article ID 925373, 9 pages, 2013.

[69] S. Lutz, "Beyond directed evolution-semi-rational protein engineering and design," *Current Opinion in Biotechnology*, vol. 21, no. 6, pp. 734–743, 2010.

[70] U. T. Bornscheuer, G. W. Huisman, R. J. Kazlauskas, S. Lutz, J. C. Moore, and K. Robins, "Engineering the third wave of biocatalysis," *Nature*, vol. 485, pp. 185–194, 2012.

[71] S. G. Burton, D. A. Cowan, and J. M. Woodley, "The search for the ideal biocatalyst," *Nature Biotechnology*, vol. 20, no. 1, pp. 37–45, 2002.

[72] S. Luetz, L. Giver, and J. Lalonde, "Engineered enzymes for chemical production," *Biotechnology and Bioengineering*, vol. 101, no. 4, pp. 647–653, 2008.

[73] N. J. Turner, "Directed evolution drives the next generation of biocatalysts," *Nature Chemical Biology*, vol. 5, no. 8, pp. 567–573, 2009.

[74] K. Engström, J. Nyhlén, A. G. Sandström, and J.-E. Baäckvall, "Directed evolution of an enantioselective lipase with broad substrate scope for hydrolysis of alpha-substituted esters," *Journal of the American Chemical Society*, vol. 132, pp. 7038–7042, 2010.

[75] F. Bordes, L. Tarquis, J. Nicaud, and A. Marty, "Isolation of a thermostable variant of Lip2 lipase from *Yarrowia lipolytica* by directed evolution and deeper insight into the denaturation mechanisms involved," *Journal of Biotechnology*, vol. 156, no. 2, pp. 117–124, 2011.

[76] W. P. C. Stemmer, "DNA shuffling by random fragmentation and reassembly: In vitro recombination for molecular evolution," *Proceedings of the National Academy of Sciences of the United States of America*, vol. 91, no. 22, pp. 10747–10751, 1994.

[77] X. Yu, R. Wang, M. Zhang, Y. Xu, and R. Xiao, "Enhanced thermostability of a *Rhizopus chinensis* lipase by in vivo recombination in *Pichia pastoris*," *Microbial Cell Factories*, vol. 11, pp. 102–113, 2012.

[78] N. Akbulut, M. T. Öztürk, T. Pijning, S. I. Öztürk, and F. Gümüsel, "Improved activity and thermostability of *Bacillus pumilus* lipase by directed evolution," *Journal of Biotechnology*, vol. 164, pp. 123–129, 2013.

[79] A. S. Bommarius and M. F. Paye, "Stabilizing biocatalysts," *Chemical Society Reviews*, vol. 42, no. 15, pp. 6534–6565, 2013.

[80] K. L. Morley and R. J. Kazlauskas, "Improving enzyme properties: when are closer mutations better?" *Trends in Biotechnology*, vol. 23, no. 5, pp. 231–237, 2005.

[81] S. Park, K. L. Morley, G. P. Horsman, M. Holmquist, K. Hult, and R. J. Kazlauskas, "Focusing mutations into the *P. fluorescens* esterase binding site increases enantioselectivity more effectively than distant mutations," *Chemistry and Biology*, vol. 12, no. 1, pp. 45–54, 2005.

[82] S. Park and J. Cochran, *Protein Engineering and Design*, CRC Press, 2009.

[83] D. Böttcher and U. T. Bornscheuer, "Protein engineering of microbial enzymes," *Current Opinion in Microbiology*, vol. 13, no. 3, pp. 274–282, 2010.

[84] G. A. Strohmeier, H. Pichler, O. May, and M. Gruber-Khadjawi, "Application of designed enzymes in organic synthesis," *Chemical Reviews*, vol. 111, no. 7, pp. 4141–4164, 2011.

[85] S. Lutz and W. M. Patrick, "Novel methods for directed evolution of enzymes: quality, not quantity," *Current Opinion in Biotechnology*, vol. 15, no. 4, pp. 291–297, 2004.

[86] M. T. Neves-Petersen, E. I. Petersen, P. Fojan, M. Noronha, R. G. Madsen, and S. B. Petersen, "Engineering the pH-optimum of a triglyceride lipase: from predictions based on electrostatic computations to experimental results," *Journal of Biotechnology*, vol. 87, no. 3, pp. 225–254, 2001.

[87] Z. Qian, C. J. Fields, and S. Lutz, "Investigating the structural and functional consequences of circular permutation on lipase B from *Candida antarctica*," *ChemBioChem*, vol. 8, no. 16, pp. 1989–1996, 2007.

[88] Z. Han, S. Han, S. Zheng, and Y. Lin, "Enhancing thermostability of a *Rhizomucor miehei* lipase by engineering a disulfide bond and displaying on the yeast cell surface," *Applied Microbiology and Biotechnology*, vol. 85, no. 1, pp. 117–126, 2009.

[89] M. T. Reetz, S. Prasad, J. D. Carballeira, Y. Gumulya, and M. Bocola, "Iterative saturation mutagenesis accelerates laboratory evolution of enzyme stereoselectivity: rigorous comparison with traditional methods," *Journal of the American Chemical Society*, vol. 132, no. 26, pp. 9144–9152, 2010.

[90] K. Liebeton, A. Zonta, K. Schimossek et al., "Directed evolution of an enantioselective lipase," *Chemistry and Biology*, vol. 7, no. 9, pp. 709–718, 2000.

[91] N. Zhang, W. Suen, W. Windsor, L. Xiao, V. Madison, and A. Zaks, "Improving tolerance of *Candida antarctica* lipase B towards irreversible thermal inactivation through directed evolution," *Protein Engineering*, vol. 16, no. 8, pp. 599–605, 2003.

[92] N. Sibille, A. Favier, A. I. Azuaga et al., "Comparative NMR study on the impact of point mutations on protein stability of *Pseudomonas mendocina* lipase," *Protein Science*, vol. 15, no. 8, pp. 1915–1927, 2006.

[93] M. Z. Kamal, S. Ahmad, T. R. Molugu et al., "In vitro evolved non-aggregating and thermostable lipase: structural and thermodynamic investigation," *Journal of Molecular Biology*, vol. 413, no. 3, pp. 726–741, 2011.

[94] R. Ruslan, R. N. Z. R. A. Rahman, T. C. Leow, M. S. M. Ali, M. Basri, and A. B. Salleh, "Improvement of thermal stability via outer-loop ion pair interaction of mutated T1 lipase from *Geobacillus zalihae* strain T1," *International Journal of Molecular Sciences*, vol. 13, no. 1, pp. 943–960, 2012.